

UNIVERSITY OF LEICESTER

Novel NMDA Receptor splice variants

Thesis submitted for the degree of
Doctor of Philosophy at the University of Leicester

By

António Miguel de Jesus Domingues

Faculty of Medicine and Biological Sciences

September 2009

Abstract

Novel NMDA receptor splice variants

António Miguel de Jesus Domingues

Injury to white matter oligodendrocytes is central to several important disorders including cerebral palsy, stroke and multiple sclerosis. Dr. Fern's group and others have recently shown that NMDA receptors are present on oligodendrocyte processes and mediate injury of these myelinating processes. The pharmacological profile of NMDA receptors present in white matter is quite unique. NMDA receptors are composed of the subunits NR1, NR2A-D and NR3A-B that assemble to form a heterotetrameric complex. Importantly, the subunit composition determines the properties of the receptor complex. Two possibilities were proposed to explain the unusual profile of NMDA receptor-mediated currents in white matter: (1) novel splice variants are expressed in glia and/or (2) the major NMDA receptor complex present is composed of an uncharacterized NMDA receptor subunit stoichiometry. In this PhD project I explored these two hypotheses. NR1, NR2C and NR3A, which are thought to be the major components of NMDA receptors in oligodendrocytes, were cloned from the myelinating rat optic nerve. In addition, all known NMDA receptor subunits were cloned from the neonate rat brain. This analysis revealed that only a subset of NR1 splice variants, those lacking exon 5, is expressed in white matter. I have also cloned NR3B and identified several putative novel splice variants of this subunit in both the optic nerve and the brain. Novel splice variants of NR2B-D were also cloned. Four of these novel NR3B variant were characterized by single cell Ca^{2+} imaging revealing that the novel variants form function receptors. Furthermore, NR3 subunits influence NMDA receptor glutamate sensitivity and Mg^{2+} in an NR2-dependent manner. The results here presented reveal a previous uncharacterized wealth of NMDA receptor splice variants which modify NMDA receptor physiology.

“A testing and a questioning hath been all my travelling - and verily, one must also learn to answer such questioning!”

Thus spoke Zarathustra, Friedrich Nietzsche (1883)

Acknowledgments

I would first like to thank Dr. Bob Fern for giving me the opportunity to undertake this project. His advice, patience and enthusiasm were invaluable throughout the project. I would also like to thank Dr. Mike Salter for introducing me to the wonderful world of molecular biology and its pitfalls. His advice was very important for the successful completion of the project. I am also indebted to a friend, Dr. Alyona Minina, for her tips on improving reverse transcription.

Table of contents

Abstract	ii
Acknowledgments	iv
List of figures	x
List of tables	xii
List of abbreviations.....	xiii
Chapter I.....	1
Introduction	1
I.1 Foreword	1
I.2 Glutamate receptor classification	1
I.2.1 Metabotropic glutamate receptors.....	2
I.2.2 Non-NMDA ionotropic glutamate receptors.....	3
I.3 NMDA receptors	5
I.3.1 Molecular arrangement of NMDA receptor complexes.....	6
I.3.2 NMDA receptor structural domains.....	7
I.4 Alternative splicing mechanisms	9
I.4.1 Splicing and RNA editing of AMPA/kainate receptors	10
I.4.2 NR1 splice variants	12
I.5 Oligodendrocytes and Myelination.....	14
I.5.1 The optic nerve.....	15
I.5.2 Ischaemic damage to oligodendrocytes.....	15
I.5.3 White matter NMDA receptors.....	18
I.5.4 NMDA receptors may have particular membrane distribution in glial cells	19
I.5.5 Glutamate availability in neuron-glia connections.....	20
I.5.6 Stoichiometry of white matter NMDA receptors.....	21
I.5.7 Physiological role of NMDA receptors in Glia	22
I.6 OBJECTIVES.....	23
Chapter II.....	24
Materials and Methods	24
II.1 Animals and tissue dissection	25
II.1.1 Method.....	27

II.2 RNA extraction.....	27
II.2.1 RNA extraction from the optic nerve - method	28
II.2.2 RNA extraction from the brain - method	29
II.3 Reverse transcriptase-polymerase chain reaction (RT-PCR)	29
II.3.1 RT.....	30
II.3.2 PCR	31
II.3.3 Expression of receptors - method	32
II.3.4 Full-length cDNA amplification - method.....	34
II.3.5 Cloning of PCR products - method	37
II. 4 Creation of error-free clones	37
II.5 Construction of fluorescently tagged subunits.....	40
II.6 Cell culture and transfection	45
II.6.1 Cell culture method.....	46
II.6.2 Transfection protocol.....	46
II.7 Imaging	47
II.7.1 Ca ²⁺ and Na ²⁺ imaging - method.....	47
II.8 Ca ²⁺ calibration.....	50
II.8.1 Ca ²⁺ calibration - method	50
II.9 Bioinformatics tools	51
II.9.1 DNA sequence assembly	52
II.10 Statistical analysis	52
Chapter III	53
NR1 expression in the Optic Nerve.....	53
III.1 Introduction.....	54
III.1.1 The homomeric NR1	54
III.1.2 NR1 splice variants.....	55
III.1.3 Regional and developmental expression of NR1 splice variants	58
III.1.4 NR1 splice variants modify channel physiology.....	60
III.1.5 NR1 splice variant subcellular localization and trafficking.....	61
III.1.6 Neuronal activity and NR1 splicing	62
III.2 Results	64
III.3 Discussion	69
Chapter IV	71

Cloning and molecular characterization of novel NR2 splice variants	71
IV.1 Introduction.....	72
IV.1.1 NR2 expression and sub-cellular localization.....	73
IV.1.2 Triheteromeric NMDA receptors.....	73
IV.1.3 Synaptic vs extrasynaptic location of NMDA receptors.....	74
IV.1.4 Studies with gene knockout animals	75
IV.1.5 NR2 subunits splice variants	77
IV.1.5.1 NR2B	77
IV.1.5.2 NR2C	78
IV.1.5.3 NR2D	79
IV.2 Results	81
IV.2.1 NR2A cloning.....	83
IV.2.2 NR2B novel splice variants.....	83
IV.2.3 NR2B _{Δ635} recombinant expression	86
IV.2.4 NR2C.....	86
IV.2.5 NR2D	89
IV.3 Discussion.....	95
IV.3.1 Strategical and practical considerations	95
IV.3.2 Novel NR2B splice variants.....	97
IV.3.3 NR2C splice variants.....	100
IV.3.4 NR2D splice variants: artefacts or overlooked?	101
Chapter V.....	104
Cloning and molecular characterization of novel NR3 splice variants	104
V.1 Introduction.....	105
V.1.1 Molecular properties of NR3 subunits.....	105
V.1.2 NR3A splice variants	106
V.1.3 NR3 expression.....	107
V.1.3.1 NR3A	107
V.1.3.2 NR3A splice variants expression	107
V.1.3.3 NR3B	108
V.2 Results.....	109
V.2.1 NR3A and NR3B expression	109
V.2.1.1 NR3A cloning.....	110

V.2.1.2 NR3B cloning reveals a wealth of novel splice variants	110
V.2.1.3 Predicted structure of NR3B splice variants	116
V.2.1.4 Addendum to annotated NR3B mRNA sequence	121
V.3 Discussion	126
V.3.1 NR3 expression in white matter	126
V.3.2 Novel NR3B splice variants.....	127
V.3.2.1 Structural and functional consequences of NR3B splicing.....	127
V.3.2.2 Translation of splice variants	128
V.3.2.3 Unspliced NR3B splice variants.....	130
V.3.3 <i>Grin3B</i> polymorphic nature may be the cause of extensive alternative splicing.....	133
Chapter VI	135
Physiology of NR3 subunits.....	135
VI.1 Introduction.....	136
VI.1.1 NR3 modulatory properties	136
VI.1.2 NR3 assembly and tracking	137
VI.1.3 NR3 (extra-)synaptic localization.....	138
VI.1.4 Knockout mice and the neuroprotective role of NR3 subunits.....	139
VI.2 Results	141
VI.2.1 NR3 subunits modulate glutamate potency	144
VI.2.1.1 NR3A and NR3B.....	144
VI.2.1.2 NR3B splice variants.....	144
VI.2.2 NR3 modulation of glutamate-induced $[Ca^{2+}]_i$ rises	148
VI.2.2.1 NR3A and NR3B.....	148
VI.2.2.2 NR3B splice variants.....	151
VI.2.3 Mg^{2+} sensitivity	155
VI.2.3.1 NR3 modulation of Mg^{2+} -block	155
VI.2.4 NR1/NR3 glycine receptors	159
VI.3 Discussion.....	164
VI.3.1 Dominant-negative function of NR3s	164
VI.3.1.1 NR3A	164
VI.3.1.2 NR3B	164
VI.3.2 Relief Mg block is not a common feature of NR3 receptors	165
VI.3.3 Comparison with previous reports	166

VI.3.4 Novel splice variants properties	167
VI.3.5 NR1/NR3 glycine receptor.....	169
Chapter VII	171
Concluding remarks	171
VII.1 Is NR1/NR2C/NR3A the “oligodendrocytic NMDA receptor”?	173
VII.2 NR3B splice variants.....	175
VII.2.1 Expression in white and grey matter	175
VII.2.2 Future research on NR3B splice variants	176
Bibliography.....	179

List of figures

Figure I-1: Classification of glutamate receptors	4
Figure I-2: General structural features of ionotropic glutamate receptors.....	8
Figure I-3: Alternative splicing events.....	11
Figure I-4: Alternative splicing and RNA editing of AMPA receptor subunits.....	13
Figure I-5: Oligodendrocytes and Schwann cells extend processes to myelinate axons	17
Figure II-1: Outline of the experimental procedure for amplification and cloning of NMDA receptors.....	26
Figure II-2: Relative location of primers used for amplification of full-length NMDA receptor subunits cDNA and sequencing of clones.....	36
Figure II-3: Procedure to eliminate nucleotide mutations from clones.....	39
Figure II-4: Construction of fluorescently labelled NMDA receptor subunits	42
Figure II-5: NMDA receptor expression in triple transfected hek293 cells.....	48
Figure II-6: Plot of Ca^{2+} standards versus 340/380 background corrected ratios	51
Equation I: formula used to calculate $[Ca^{2+}]_i$ at any given time point	51
Figure III-1: Alternative splicing of NMDA receptor subunit NR1	57
Figure III-2: NR1 expression in the neonatal rat optic nerve and brain	65
Figure III-3: Amplification of full-length NR1 cDNA from the optic nerve.....	66
Figure III-4: NR1 variants containing exon 5 are absent from the neonatal optic nerve.....	68
Figure IV-1: Expression of NR2 subunits in the neonatal rat optic nerve and brain	82
Figure IV-2: Amplification of full-length NR2 subunit cDNA.....	84
Figure IV-3: Gene organization of <i>Grin2b</i> and new NR2B splice variants.....	85
Figure IV-4: Glutamate stimulation of NR1/NR2B $_{\Delta 635}$ does not produce $[Ca^{2+}]_i$ rises.....	87
Figure IV-5: Gene organization of <i>Grin2c</i> and of a new NR2C splice variant.....	88
Figure IV-6: Gene organization of <i>Grin2d</i> and of a newly identified NR2D splice variant ...	90

Figure IV-7: Sequence alignment of mouse, rat and human NR2D-1 and NR2D-2 splice sites	91
Figure IV-8: Amino acid sequence alignment of NR2D splice variants.....	92
Figure V-1: Both NR3 subunits are expressed in the neonatal rat optic nerve.....	112
Figure V-2: Amplification of full-length NR3 cDNA from the RON.....	113
Figure V-3: Gene organization of <i>Grin3b</i> and NR3B splice variants predicted to be targeted for mRNA degradation pathways	118
Figure V-4: NR3B splice variants that retain coding sequences for important NMDA receptor domains	119
Figure V-5: Sequence alignment the splice junction of canonical NR3B, NR3B _{Δ24} and NR3B _{Δ45}	122
Figure V-6: Alignment of NR3B variants predicted polypeptide sequences	124
Figure V-7: Transmembrane domain prediction of NR3B and NR3B _{Δ600}	125
Figure VI-1: Representative traces of glutamate-evoked [Ca ²⁺] _i in Hek293 cells transfected with NMDA receptors	143
Figure VI-2: Glutamate dose-response curves of NMDA receptors.....	146
Figure VI-3: Estimates of glutamate potency (pEC ₅₀) for NMDA receptors	147
Figure VI-4: Quantification of transfected cells and responsive cells after stimulation with glutamate	150
Figure VI-5: NR3A and NR3B subunits change Ca ²⁺ influx through NMDA receptors in a NR2-dependent fashion	154
Figure VI-6: Effect of NR3B splice variants on [Ca ²⁺] _i rises mediated by NMDA receptors	157
Figure VI-7: Sensitivity of NR1/NR2A to Mg ²⁺ block in the presence of NR3 subunits.....	160
Figure VI-8: Sensitivity of NR1/NR2B to Mg ²⁺ block in the presence of NR3 subunits.....	161
Figure VI-9: Sensitivity of NR1/NR2C to Mg ²⁺ block in the presence of NR3 subunits. ...	162
Figure VI-10: Representative traces of glutamate and/or glycine-evoked [Na ²⁺] _i rises in Hek293cells transfected with NMDA receptors	163

List of tables

Table II-1: List of PCR primers used for expression studies.....	33
Table II-2: List of PCR primers used for the detection of NR1 and NR3A splice variants....	34
Table II-3: List of PCR cycle conditions used for full-length cDNA amplification.	35
Table II-4: List of PCR primers used for full-length cDNA amplification	35
Table II-5: list of restriction enzymes used to replace erroneous sequences in cloned cDNA.	38
Table II-6: Properties of fluorescents proteins used to tag NMDA receptor subunits.....	40
Table II-7: List of primers used for amplification of clones inserted in <i>pGEM-T</i>	43
Table II-8: Filter sets and monochromator illumination (excitation wavelength) used to detect Fura-2, ECFP, EYFP and mCherry.....	49
Table III-1: Commonly used nomenclature for NR1 alternative splicing variants	58
Table IV-1: Splice site analyses of <i>Grin2D</i>	93
Table IV-2 - Molecular properties of rat NR2 subunits mRNA.....	96
Table IV-3: Splice site analyses for <i>Grin2B</i>	98
Table V-1: NR3B splice variants	115
Table V-2: Splice site analyses of <i>Grin3B</i>	120
Table V-3: Sizes of rat NMDA receptors genes	131
Table V-4: <i>Grin3B</i> intron-exon organization	133
Table VI-1: Summary of NR3 effects on glutamate potency of NMDA receptors.....	145
Table VI-2: NR3 subunits modulate glutamate-induced $[Ca^{2+}]_i$ raise of NR1/NR2 receptors	152
Table VI-3: Modulation of NR1/NR2 Mg^{2+} -block by NR3 subunits.....	158

List of abbreviations

[Ca ²⁺] _i	Intracellular Ca ²⁺ concentration
ALS	Amyotrophic lateral sclerosis
AMPA	α -amino-3-hydroxy-5-methyl-4-isoxazolepropionate
apo	Apolipoprotein
BDNF	Brain-derived neurotrophic factor
CaMK	Ca ²⁺ /calmodulin-dependent protein kinase
CDS	Coding sequence
CIP	Calf Intestinal Alkaline Phosphatase
CNS	Central nervous system
CREB	cAMP response element binding
dNTPs	Deoxynucleotides
DRG	Dorsal root ganglia
EC50	Half maximal effective concentration
ER	Endoplasmic reticulum
ESPCs	Excitatory postsynaptic current
Hek293	Human Embryonic kidney cells
kd	Dissociation constant
LTD	Long-term depression
LTP	Long-term potentiation
MAGUK	Membrane-associated guanylate kinase
NMD	Non-sense mediated decay
NMDA	<i>N</i> -methyl-D-aspartate
pEC50	negative logarithm of the EC50
PBS	Phosphate-Buffered Saline
PCR	Polymerase Chain Reaction
PKA	Protein kinase A

PKC	Protein kinase C
PNS	Peripheral nervous system
PSD-95	Postsynaptic density-95
PTC	Premature termination codon
PVL	Periventricular leukomalacia
RNase H	Hybrid-dependent exoribonuclease
RT	Reverse Transcription
RT-PCR	Reverse transcriptase-polymerase chain reaction
RUST	Regulated Unproductive Splicing and Translation
SAP102	Synapse-associated proteins 102
SNc	<i>Substantia nigra</i>
UTR	Untranslated region

Chapter I

Introduction

I.1 Foreword

L-Glutamate is the major excitatory neurotransmitter in the mammalian central nervous system (CNS), acting through both ligand gated ion channels (ionotropic receptors) and G-protein coupled (metabotropic) receptors (figure I-1) (Hollmann & Heinemann, 1994; Nakanishi, 1992). Ionotropic receptors are further subdivided into three classes on the basis of their pharmacology: α -amino-3-hydroxy-5-methyl-4-isoxazolepropionate (AMPA), kainate and *N*-methyl-D-aspartate (NMDA) receptor channels. Activation of these receptors is responsible for basal excitatory synaptic transmission and forms of synaptic plasticity such as long-term potentiation (LTP) and long-term depression (LTD), which are thought to underlie learning and memory (Riedel *et al*, 2003).

Glutamate also has a dark side; by excessively stimulating its receptors, particularly ionotropic receptors, glutamate can cause cell death in a process known as excitotoxicity (Doble, 1999). Ionotropic glutamate receptors are permeable to Ca^{2+} and overactivation in pathological condition can lead to an excessive entry of Ca^{2+} in cells, unbalancing ionic homeostasis and ultimately leading to cell death (Doble, 1999). This pathological mechanism is thought to be central in a variety of conditions such as Alzheimer disease, Huntington disease and ischaemic injury. My PhD project will focus on a particular class of ionotropic glutamate receptors, NMDA receptors. In this thesis introduction I will briefly refer to glutamate receptor classification, but only the NMDA receptor literature will be reviewed thoroughly in this and subsequent chapters. Some insight into oligodendrocyte biology and injury mechanisms will also be given.

I.2 Glutamate receptor classification

Before the advent of molecular biology in the late 1980's, glutamate receptors were identified and studied using pharmacological and biochemical tools (Monaghan *et al*, 1989;

Nakanishi, 1992). Application of kainate and NMDA elicited different responses in neuronal populations, providing the first evidence for the existence of at least two glutamate receptor classes (McCulloch *et al*, 1974). Glutamate receptors were subsequently divided into three main classes of ionotropic glutamate receptor receptors (figure I-1), AMPA receptors, kainate receptors, and NMDA receptors, each named after their selective agonists (Monaghan *et al*, 1989). Since few pharmacological agents distinguish between AMPA and kainate receptors, they are often referred to as 'non-NMDA' receptors. The first compelling evidence for the existence of metabotropic glutamate receptors came from a study in 1985 (Sladeczek *et al*, 1985), where the authors showed that glutamate provoked inositol phosphate formation directly, rather than indirectly by the evoked release and subsequent actions of adenosine or acetylcholine.

With the cloning of glutamate receptors, initiated with GluR1, molecular data was gathered on this superfamily of receptors and their classification was established (Hollmann & Heinemann, 1994; Hollmann *et al*, 1989; Nakanishi, 1992). Consistent with the previous division of classes based on pharmacological and biochemical evidence, two major families were recognised (figure I-1): those that mediate fast synaptic responses by opening ion channels (ionotropic glutamate receptor), and those that cause slower synaptic effects, associated with biochemical changes (metabotropic receptor).

1.2.1 Metabotropic glutamate receptors

Based on their amino acid sequence homology, pharmacological profile and second messenger coupling, metabotropic glutamate receptors fall into 3 groups (figure I-1). mGlu1 and mGlu5 (group I) are linked to phospholipase C activation causing an increase in inositol triphosphate concentration and Ca²⁺ immobilization. Group II (mGlu2 and mGlu3) and III (mGlu4, 6, 7 and 8) receptors inhibit adenylyl cyclase activity, resulting in a fall in intracellular cAMP concentration. Physiologically, group I receptors are usually associated

with excitatory synaptic responses whereas group II and III with depression of synaptic responses, via inhibition of glutamate release (reviewed in (Riedel *et al*, 2003)).

1.2.2 Non-NMDA ionotropic glutamate receptors

AMPA receptors are either homomeric or heteromeric oligomers composed of GluR1-4 subunits and mediate rapid postsynaptic glutamatergic neurotransmission (Keinanen *et al*, 1990). Differences in the functional properties of native AMPA receptors are a consequence of different assemblies of these subunits. Both homomeric and heteromeric receptors have high affinity for AMPA and low affinity for kainate. Despite this relatively low affinity for AMPA receptors, kainate is a strong activator of AMPA receptors (reviewed in (Bettler & Mulle, 1995) and (Ozawa *et al*, 1998)).

Kainate receptors are composed of 5 subunits: GluR5-7 and KA1-2. Kainate receptors contribute to excitatory postsynaptic currents in many regions of the central nervous system. Presynaptic kainate receptors modulate transmitter release at both excitatory and inhibitory synapses (Huettnner, 2003). The subunits GluR5-7 have a moderate degree of homology (35-40%) to the AMPA receptor subunits and are components of high affinity kainate receptors. GluR5 and GluR6 form homomeric channels activated by kainate. GluR7, KA1, and KA2, fail to form channels when each protein is expressed alone, but contribute to heteromeric assemblies of functional kainate receptors when expressed with GluR5 and GluR6. The co-expression of GluR5-7 with KA1 and KA2 in different combinations, leads to the formation of channels with unique properties that resemble neuronal kainate receptors. These receptors have a high affinity for domoic acid and kainate, lower affinity for glutamate, and low affinity for AMPA (Bettler *et al*, 1990; Egebjerg *et al*, 1991; Herb *et al*, 1992; Lomeli *et al*, 1992; Sommer *et al*, 1992; Werner *et al*, 1991).

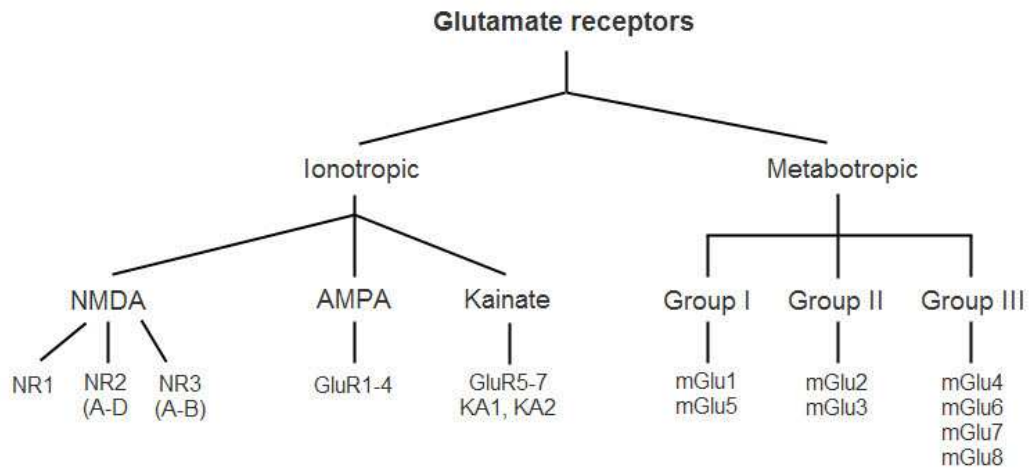


Figure I-1: Classification of glutamate receptors

Glutamate receptors are divided in 2 major families separated by their modes of action: through ligand gated ion channels (ionotropic receptors) or coupled to G-protein (metabotropic receptors). Further division arises from activation by selective agonists (AMPA, kainate, NMDA), second messenger coupling (Group I-III) and molecular properties (Watkins & Jane, 2006).

I.3 NMDA receptors

NMDA receptors mediate excitatory neurotransmission in the CNS. One distinctive feature of NMDA receptors, as compared to AMPA/kainate receptors, is the requirement for the binding of a co-agonist, glycine, simultaneously with glutamate for channel opening. There are other unique features of NMDA receptors: (1) at resting potentials the receptor channel remains blocked by Mg^{2+} and ions flow through the receptor only when the cell membrane is depolarized; (2) high permeability to Ca^{2+} ; and (3) slow gating kinetics, meaning that NMDA receptor-mediated neurotransmission occurs slowly and lasts for a prolonged period (Lester *et al*, 1990; MacDermott *et al*, 1986; Mayer & Westbrook, 1987; Mayer *et al*, 1984). Further physiological complexity of NMDA receptor regulation is added by modulatory agents such as polyamines, protons, redox agents and Zn^{2+} (reviewed in (Dingledine *et al*, 1999)).

Because of these properties, the NMDA receptor serves as a molecular apparatus that can detect coincident presynaptic activity and postsynaptic depolarization at the synapse, and inject the postsynaptic cell with a sufficient amount of the second messenger ion Ca^{2+} . This can initiate plastic changes that strengthen synaptic connections (Riedel *et al*, 2003). But high Ca^{2+} permeability, low desensitization and high affinity for glutamate, make NMDA receptors pivotal player excitotoxicity (Doble, 1999; Waxman & Lynch, 2005). Prolonged glutamate stimulation can overactivate NMDA receptors, leading to sustained increases in $[Ca^{2+}]_i$, ultimately leading to cell death (Doble, 1999; Waxman & Lynch, 2005).

The first NMDA receptor subunit to be identified was NR1 almost immediately followed by the cloning of NR2A-D (Ikeda *et al*, 1992; Ishii *et al*, 1993; Kutsuwada *et al*, 1992; Meguro *et al*, 1992; Monyer *et al*, 1992; Moriyoshi *et al*, 1991). A few years later the modulatory subunits NR3A-B were also identified (Chatterton *et al*, 2002; Ciabarra *et al*, 1995; Matsuda *et al*, 2002; Nishi *et al*, 2001; Sucher *et al*, 1995). NR1, NR2 or NR3 subunits do not form homomeric functional NMDA receptors. However, coexpression of NR1 with

any NR2 generates fully functional channels (Ikeda *et al*, 1992; Ishii *et al*, 1993; Kutsuwada *et al*, 1992; Meguro *et al*, 1992; Monyer *et al*, 1992; Moriyoshi *et al*, 1991). NR3 subunits need to be assembled with both NR1 and NR2 to form functional glutamate receptors (Ciabarra *et al*, 1995; Matsuda *et al*, 2003; Nishi *et al*, 2001; Perez-Otano *et al*, 2001; Schuler *et al*, 2008; Sucher *et al*, 1995).

Recombinant expression of various NR1/NR2 subunits produces receptors with distinctive biophysical and pharmacological features. These include: (1) single-channel conductance; (2) strength of Mg^{2+} block; (3) sensitivity of modulation by glycine, reducing agents, polyamines and phosphorylation; (4) desensitization; and (5) affinities for specific agonists and antagonists (Buller *et al*, 1994; Ishii *et al*, 1993; Kohr *et al*, 1994; Kutsuwada *et al*, 1992; Lynch *et al*, 1994; Monyer *et al*, 1994; Monyer *et al*, 1992; Moriyoshi *et al*, 1991; Stern *et al*, 1992; Sullivan *et al*, 1994; Wafford *et al*, 1993; Williams *et al*, 1994; Yamazaki *et al*, 1992). When expressed with NR1 and NR2 subunits, NR3A and NR3B act in a dominant-interfering manner, reducing the Ca^{2+} permeability of glutamate-induced currents in cells expressing NR1 and NR2A (Ciabarra *et al*, 1995; Matsuda *et al*, 2002; Nishi *et al*, 2001; Sasaki *et al*, 2002a).

1.3.1 Molecular arrangement of NMDA receptor complexes

Although not yet definitive, evidence is mounting that supports a tetrameric arrangement of NMDA receptors incorporating two NR1 and two NR2 subunits of the same or different subtypes (Dingledine *et al*, 1999; Laube *et al*, 1998; Luo *et al*, 1997; Schuler *et al*, 2008). In cells expressing NR3 subunits, it is likely that this subunit co-assembles with NR1 and NR2 to form ternary NR1/NR2/NR3 tetrameric complexes (Perez-Otano *et al*, 2001; Sasaki *et al*, 2002a; Schuler *et al*, 2008). It has been proposed that in receptors containing NR1, NR2 and NR3 subunits, one NR3 subunit substitutes for one of the NR2 subunits (Kew & Kemp, 2005; Schuler *et al*, 2008).

The existence of triheteromeric NMDA receptors has been known for over ten years, yet their functional properties only recently have been elucidated (Chazot & Stephenson, 1997; Hatton & Paoletti, 2005; Luo *et al.*, 1997; Sheng *et al.*, 1994). The interesting aspect about these receptors is that they have hybrid properties of the subunits that compose them. NMDA receptors formed by co-assembly of NR1, NR2A and NR2B retain sensitivity for submicromolar concentrations of Zn^{2+} , a typical feature of NR2A-containing receptors, and ifenprodil (NR2B-selective antagonist). Nevertheless, ifenprodil inhibition is not as effective in NR1/NR2A/NR2B as in NR1/NR2B (Hatton & Paoletti, 2005). Deactivation time of NR1/NR2A/NR3B is also intermediate between those recorded for diheteromeric receptors (Vicini *et al.*, 1998).

1.3.2 NMDA receptor structural domains

All NMDA receptors subunits share a common membrane topology (figure I-2) characterized by a large extracellular N-terminus, a membrane region comprising three transmembrane segments (M1, 3 and 4), plus a re-entrant pore loop (M2), an extracellular loop between M3 and M4 (L3), and a cytoplasmic C-terminus which varies in size depending upon the subunit. The N-terminal region plays an important role in subunit assembly (Meddows *et al.*, 2001). In NR2A and NR2B, this region also contains binding sites for allosteric inhibitors such as Zn^{2+} and ifenprodil. The pre-TM1 region and the TM3–TM4 loop form the agonist binding site (Furukawa *et al.*, 2005; Yao & Mayer, 2006). Activation of NMDA receptors requires the simultaneous binding of two co-agonists: glutamate and glycine (or D-serine). The NR1 and NR3 agonist binding domains bind glycine whereas NR2 agonist binding domains bind glutamate (Furukawa *et al.*, 2005; Yao & Mayer, 2006). The C-terminal region provides multiple sites of interaction with numerous intracellular proteins and is least homologous among different subunits (Dingledine *et al.*, 1999; Mayer, 2006; Ryan *et al.*, 2008; Salter & Kalia, 2004; Sheng, 2001).

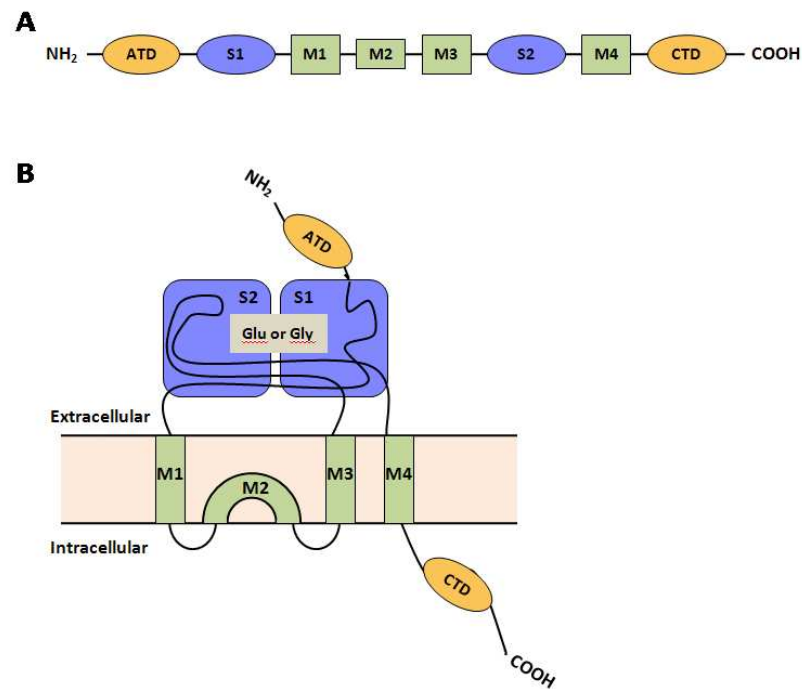


Figure I-2: General structural features of ionotropic glutamate receptors

(a) A glutamate receptor subunit containing four hydrophobic domains (M1–M4) which lie in the cell membrane. Two other domains, one N-terminal to M1 (S1) and the other between M3 and M4 (S2), form the ligand-binding pocket of the receptor. NMDA receptor proteins have an unusually long C-terminal domain (CTD) that contains numerous sites of phosphorylation and protein–protein interaction. NMDA receptor domains are organized tri-dimensionally in the cell membrane (b). M1, M3 and M4 span the membrane, whereas M2 forms a pore loop coming in and out of the membrane on its cytoplasmic side. Domains are not drawn to scale (Wollmuth & Sobolevsky, 2004).

I.4 Alternative splicing mechanisms

Molecular modifications such as splicing or RNA editing can alter glutamate receptor properties (Lomeli *et al*, 1994; Sommer *et al*, 1990). Alternative splicing is the mechanism by which certain gene sequences are differentially included in the final mRNA. Metazoan genes are not a long, uninterrupted stretch of coding nucleotides. Indeed it is quite the opposite: almost all human protein-coding genes contain introns (non-coding gene regions) that are removed in the nucleus by RNA splicing during pre-mRNA processing (Human Genome Sequencing, 2004). The average human protein-coding gene contains approximately 9 exons (coding regions) with a mean size of 145 nt, interrupted by introns whose average length is 3365 nt. After pre-mRNA processing the average mRNA exported into the cytosol consists of a 1340 nt coding sequence, a 1070 nt untranslated regions (UTRs) and a poly(A) tail (Lander *et al*, 2001). This shows that more than 90% of the pre-mRNA is removed as introns, and only about 10% of the average pre-mRNA is joined as exonic sequences by pre-mRNA splicing (Tazi *et al*, 2009).

Most exons are constitutive, meaning that they are always included in the final mRNA (Black, 2003). Regulated or alternatively spliced exons are sometimes included and sometimes excluded from the mRNA. These exons can also be termed “cassette” exons. To generate multiple transcripts from one gene, the splicing machinery can alter exon inclusion in many ways (figure I-3). The most common are the alternative inclusion of cassette exon or the retention of an intron (Black, 2003; Matlin *et al*, 2005). When a gene has multiple cassette exons, these can be mutually exclusive - the final mRNAs includes only one. Exon size can also be changed by the use of alternative splice sites. Alternative splicing is not exclusive to the coding regions of the mRNA. Some genes contain multiple promoters (5' end of the mRNA) and polyadenylation sites that can be alternatively included in a given mRNA. Typically, the use of alternative promoters is a mechanism for transcriptional control (Black, 2003; Matlin *et al*, 2005). Adding to complexity of alternative splicing patterns, some or all the above mentioned mechanism can occur in a given gene (Bharadwaj & Kolodkin, 2006; Chen *et al*,

2006). The regulation of alternative splicing is complex, since predicted sequences that identify inclusion/exclusion of an exon are highly degenerate and occur at high frequency in the genome (Blencowe, 2006; Matlin *et al*, 2005). Furthermore, exceptions to the “rules” of splicing exist in abundance (Hiller & Platzer, 2008; Szafranski *et al*, 2007; Yu *et al*, 2008).

Alternative splicing is a key regulator of gene expression as it generates numerous transcripts from a single protein-coding gene. Alternative splicing explains why the human genome has about 30,000 protein encoding genes but produces approximately 90,000 proteins (Human Genome Sequencing, 2004). This process is more widely used than previously thought and was recently estimated to affect more than 90% of human protein-coding genes (Kampa *et al*, 2004; Tazi *et al*, 2009). Alternative splicing is responsible for many biologically relevant processes including mammalian synaptic transmission (Ben-Dov *et al*, 2008). The CNS appears to be a “hotspot” for regulated alternative splicing events (Grabowski, 1998). It was recently uncovered that 28% of the human genes are differentially alternatively spliced in developing brain regions, underlying the importance of alternative splicing for brain development (Johnson *et al*, 2009).

1.4.1 Splicing and RNA editing of AMPA/kainate receptors

Each of the GluR1–4 subunits exists in two different forms, “flip” and “flop”, created by alternative splicing of a 115-base pair (bp) region before the M4 coding sequence (figure I-4). Receptors that contain the flop forms of GluR1–4 proteins desensitize more rapidly to glutamate-induced activation and do not have the characteristic low conductance, non-desensitizing state of the receptor channels found in those that contain the flip form of the proteins (Sommer *et al*, 1990). Kainate receptor subunits GluR6 and GluR7 have two splice variants that differ in their C-termini. When expressed as homomeric receptors in Hek293 cells, GluR7a receptors gave rise to 5- to 10-fold larger currents than GluR7b (Gregor *et al*, 1993; Schiffer *et al*, 1997).

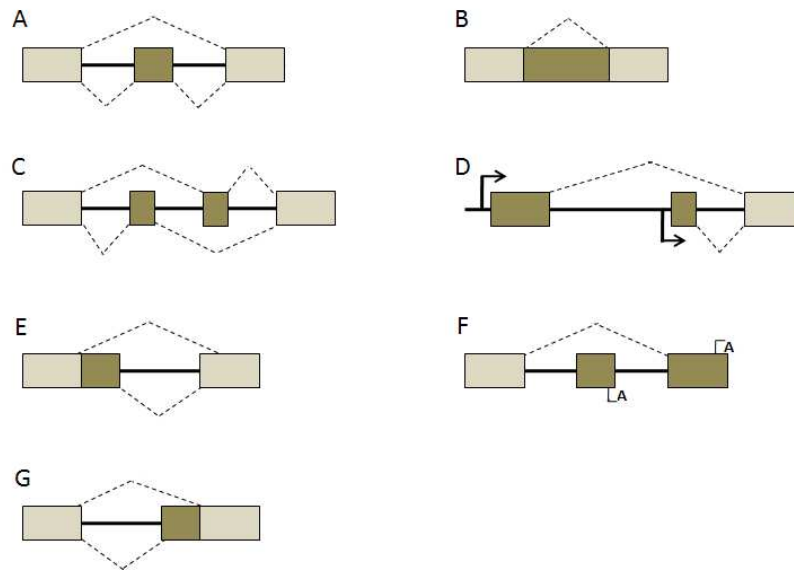


Figure I-3: Alternative splicing events

Alternative splicing can alter an mRNA molecule in many ways: (A) Cassette exon inclusion/exclusion in the mRNA; (B) intron retention; (C) Mutually exclusive insertion of two or more exons; (D) alternative splicing of alternative promoters which may influence transcription or splicing in the coding regions; (E and G) Use of alternative 5' and 3' splice sites in exons generating shorter or longer exons; and/or (F) alternative usage of 3'-end processing sites (Matlin *et al.*, 2005).

AMPA and kainate receptors are also post-transcriptionally modified by RNA editing which leads to single amino acid exchanges (figure I-4) (Rueter *et al*, 1995). In this process, selected adenosines in an mRNA are deaminated to inosines by dsRNA adenosine desaminases. Inosine is recognized as guanosine by the translation machinery, resulting in a *de facto* change of the amino acid codon (Hoopengardner, 2006). Under-editing of the GluR2 Q/R site greatly increases the Ca²⁺ permeability of AMPA receptors and has been implicated in the aetiology of amyotrophic lateral sclerosis (ALS) (Burnashev *et al*, 1992; Hume *et al*, 1991; Kwak & Kawahara, 2005; Verdoorn *et al*, 1991). Genetically engineered mice that cannot edit GluR2 Q/R site developed seizures and die by 3 weeks of age, revealing the importance of RNA editing to the normal functioning brain (Brusa *et al*, 1995).

1.4.2 NR1 splice variants

NR1 exists as 8 different splice variants due to alternative splicing of exon 5 (N1) and exons 21 and 22 (C1 and C2) (chapter III and figure III-1 for more details). NR1 splice variants strongly influence NMDA receptor properties. For example, the pH sensitivity of NMDA receptors is determined by the presence of exon 5 (in the amino terminus). At physiological pH, splice variants that include exon 5 are fully active, whereas those that lack exon 5 are partially blocked (Durand *et al*, 1993; Hollmann *et al*, 1993; Sugihara *et al*, 1992; Traynelis *et al*, 1998; Traynelis *et al*, 1995). It has also been shown that splicing of exon 5 can influence the deactivation properties of NMDA receptors (Rumbaugh *et al*, 2000). NR1 splicing can also affect intracellular trafficking, localization and the anchoring of signalling pathways to the receptor complex (Ehlers *et al*, 1998; Feliciello *et al*, 1999; Standley *et al*, 2000). The molecular and physiological features of NR1 splice variants are described in detail in chapter III of this thesis.

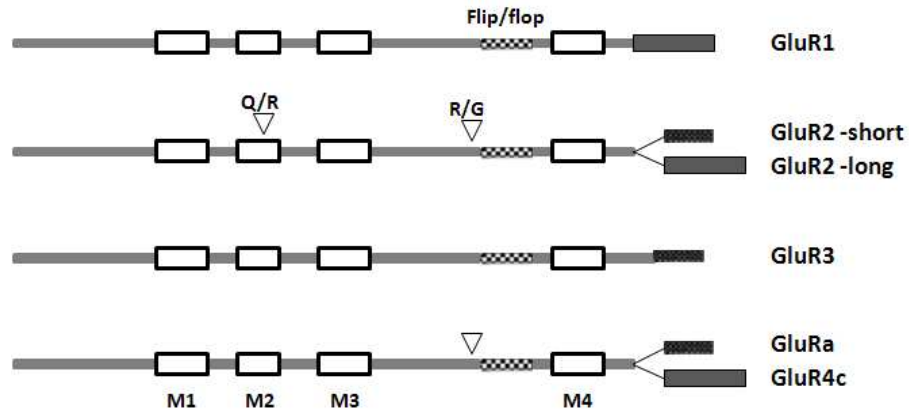


Figure I-4: Alternative splicing and RNA editing of AMPA receptor subunits

All AMPA receptor subunits undergo splicing before the M4 domain, resulting in flip/flop splice variants. The C-terminal of these receptors can exist in two forms: short and long. Membrane domains are shown as boxes M1-4 and editing sites also indicated (Q/R, R/G) (Dingledine *et al.*, 1999).

I.5 Oligodendrocytes and Myelination

The human nervous system contains about 300 billion cells, which can be classified into thousands of different types. The two principal and distinct classes are nerve cells (neurons) and neuroglial cells, also called neuroglia or simply glia. Glial cells form the bulk of cells in the nervous system, comprising over 90% of the total. Glial cell types include astrocytes, microglia, Schwann cells, oligodendroglia and satellite cells. Classical studies attributed a secondary role to glial cells as support cells for neurons, providing nutrition, maintaining homeostasis and forming myelin to wrap axons (Kettenmann & Ransom, 1995). More recent studies have shown that oligodendroglia and astrocytes can participate actively in neurotransmission (Bergles *et al*, 2000; Fields, 2008; Hamilton *et al*, 2008; Karadottir *et al*, 2008; Lalo *et al*, 2006).

Oligodendrocytes (from Greek: oligo, meaning 'few', dendro meaning 'branch', and kytos which denotes 'cell'), or oligodendroglia (Greek: oligos, "little, few"; dendron, "den- drite"; glia, "glue") make up for the majority of cells in mature white matter. Oligodendrocytes extend processes that enwrap internodal segments of axons to form the myelin sheath (myelination), an electrically insulating phospholipid layer that facilitates the fast conduction of nerve impulses. Oligodendrocytes are also important for the formation of nodes of Ranvier, the sites of action potential propagation in axons, and maintaining axonal integrity (Baumann & Pham-Dinh, 2001; Dewar *et al*, 2003). During rodent nervous system development, myelinogenesis starts around 4 days after birth and within a few days large amounts of plasma membranes are synthesized by oligodendrocytes and Schwann cells, in the CNS and peripheral nervous system (PNS) respectively, to enwrap axons (figure I-4) (Frank *et al*, 1999). In contrast with Schwann cells that myelinate a single axon, one oligodendrocyte can myelinate the internodes of up to 40 axons (figure I-4), thus damage to a single oligodendrocyte can potentially alter the function of several axons (Baumann & Pham-Dinh, 2001).

1.5.1 The optic nerve

One of the best characterized white matter tracts is the optic nerve, which lacks neuronal cell bodies and synapses. The optic nerve is composed of the axons of retinal ganglion cells and the glial cells that support them: oligodendrocytes, NG2 cells, astrocytes and microglia (Butt *et al*, 2004). The axons are aligned in a parallel fashion in the nerve and oligodendrocytes surround these axons extending process and insulating them. Astrocytes lie along the axis of the nerve in regularly spaced intervals and extend processes into the nodes of Ranvier (figure 6). NG2 cells and microglia are also found throughout the optic nerve. Each oligodendrocyte in the rodent optic nerve can extended process to insulate 5-30 axons (Butt *et al*, 2004). During post-natal development, oligodendrocytes in the optic nerve are generated from rapidly dividing precursor cells (OPCs). Oligodendroglial cells can be identified as early as in P2 and differentiation continues up to post natal day 45. The highest rate of myelination appears to occur between P7 and P21 during which time oligodendrocyte processes increase in length by about 10 times (Butt & Ransom, 1993; Foster *et al*, 1982; Skoff, 1990). By the end of myelination, oligodendrocyte somata typically lie in interfascicular rows of approximately four or five cells along the longitudinal axis of the nerve and outnumber astrocytes by approximately 2:1 (Burne *et al*, 1996).

1.5.2 Ischaemic damage to oligodendrocytes

Ischaemic damage to developing oligodendroglia is the pathogenic mechanism responsible for periventricular leukomalacia (PVL), which is the major form of brain injury in the premature infant. PVL is the leading cause of neurological disability in survivors of premature birth and results in the chronic spastic motor deficits of cerebral palsy as well as cognitive impairment (Volpe, 2001). During human brain development, there is a window of vulnerability when hypoxia-ischaemia and other insults damage the premature cerebral white matter to produce focal cystic necrotic lesions and related disturbances of myelination (Kinney & Back, 1998). This vulnerability appears to be due to increased sensitivity of oligodendrocyte

progenitors to ischaemic injury (Back & Volpe, 1997). Several studies have shown that oligodendrocyte vulnerability to oxidative damage and hypoxia-ischaemia is dependent on the differentiation stage of these cells and immature oligodendrocytes are more sensitive to injury (Back *et al*, 1998; Back *et al*, 2002; Fern & Muller, 2000). The traditional view is that neurons are the cell type most susceptible to an ischaemic insult. However, over recent years data has shown that gray and white matter oligodendrocytes are as vulnerable as neurons to ischaemia *in vivo* (Dewar *et al*, 2003; Goldberg & Ransom, 2003). For instance, after transient global ischaemia in the rat, oligodendrocytes exhibited greater vulnerability than neurons in the cerebral cortex and thalamus (Petito *et al*, 1998). Furthermore, immature oligodendrocytes are particularly sensitive to ischaemia (Fern & Muller, 2000; Goldberg & Choi, 1993; Lyons & Kettenmann, 1998; Pantoni *et al*, 1996).

Oligodendrocyte sensitivity to ischaemia is related to the presence of glutamate receptors (Fern & Muller, 2000; Matute *et al*, 2002; Matute *et al*, 1997; McDonald *et al*, 1998). Oligodendrocytes are highly vulnerable to overactivation of glutamate receptors (Fern & Muller, 2000; Karadottir *et al*, 2005; Matute *et al*, 1997; McDonald *et al*, 1998; Micu *et al*, 2006; Salter & Fern, 2005; Yoshioka *et al*, 1996). This feature led to the proposal that oligodendroglial excitotoxicity might be involved in the pathogenesis of demyelinating diseases, such as PVL, which are characterized by the destruction of myelin, oligodendrocyte cell death and inflammation (Matute *et al*, 1999; Noseworthy, 1999; Pitt *et al*, 2000; Smith *et al*, 2000).

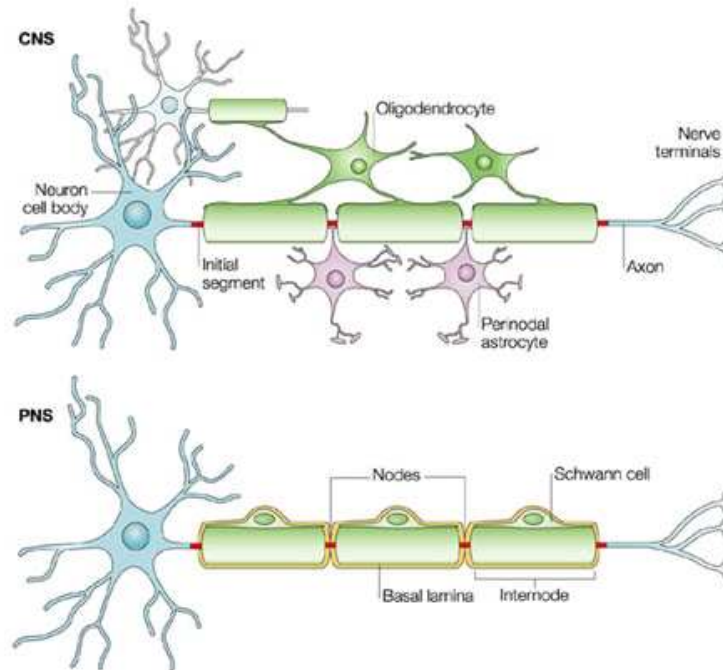


Figure I-5: Oligodendrocytes and Schwann cells extend processes to myelinate axons

Oligodendrocytes or Schwann cells are responsible for myelination of axons in the central (CNS) and peripheral nervous system (PNS). These cells extended their membranes that will form the myelin sheath insulating the axon. Myelin covers the axon leaving exposed axolemma at intervals to form the nodes of Ranvier. Oligodendrocytes can myelinate multiple axons, whereas Schwann cells myelinate a single axon. Adapted with permission from Macmillan Publishers Ltd: Nature Reviews Neuroscience (Poliak & Peles, 2003), copyright (2003).

Cellular Ca^{2+} overload is a key trigger of excitotoxic neuronal and glial death (Choi, 1995; Micu *et al*, 2006; Salter & Fern, 2005; Verkhratsky *et al*, 1998). High concentrations of extracellular glutamate, generated after traumatic or ischaemic CNS injury, results in overstimulation of ionotropic glutamate receptors and an excessive influx of Na^+ and Ca^{2+} . Subsequently, the Na^+ influx can trigger a secondary increase in the intracellular Ca^{2+} concentration through voltage-gated Ca^{2+} channels and reverse operation of the $\text{Na}^+/\text{Ca}^{2+}$ exchanger (Choi, 1995; Verkhratsky & Kettenmann, 1996). In neuronal cultures, glutamate toxicity is mostly prevented by NMDA receptor antagonists, although AMPA/kainate receptors are also relevant to neuronal excitotoxicity (Choi & Rothman, 1990). A major difference between the way glial cells and neurons deal with excessive Ca^{2+} is their ability to buffer excessive Ca^{2+} . In neurons, ionic imbalance can be dealt with, at least partially, by Ca^{2+} -binding-proteins (Nicotera & Lipton, 1999). However, several of these Ca^{2+} -binding proteins are not expressed in oligodendrocytes rendering them more vulnerable to excitotoxic insults (Green & Kroemer, 1998; Matute *et al*, 2001).

1.5.3 White matter NMDA receptors

Since glutamate can act as a potent toxin to CNS cells including oligodendrocytes, and it is an important mechanism underlying white-matter damage, much research has been done in this area (Goldberg & Ransom, 2003; Matute, 2006; Matute *et al*, 2001; Stys, 2004). For a long time the role of NMDA receptors in these processes was overlooked, mainly because of the difficulty in detecting their expression in white matter (Stys & Lipton, 2007). Recently, three reports have provided compelling evidence for the involvement of oligodendrocyte NMDA receptors in glutamate-mediated damage to these cells (Karadottir *et al*, 2005; Micu *et al*, 2006; Salter & Fern, 2005). NMDA receptor mRNA and protein expression was detected as were NMDA evoked inward currents, showing that glial NMDA receptors are functional (Karadottir *et al*, 2005; Micu *et al*, 2006; Salter & Fern, 2005). Importantly, ischaemia lead to

a rapid Ca^{2+} -dependent damage to oligodendrocyte processes and cell bodies, blocked partially by MK-801, an activity-dependent NMDA receptor channel blocker (Salter & Fern, 2005).

A particular feature of neuronal NMDA receptors is their voltage-dependent Mg^{2+} -block (Dingledine *et al*, 1999). Intriguingly, NMDA receptors in precursor, immature and mature oligodendrocytes are less susceptible to Mg^{2+} block than neuronal receptors; indeed, they generate a substantial current even at the cell resting potential (Karadottir *et al*, 2005). As a consequence, NMDA-receptor-mediated responses in oligodendrocytes can occur in the absence of concomitant stimulatory activity by AMPA and kainate receptors, in contrast to the situation in neurons. This property of native NMDA receptors in oligodendrocytes might be conferred by NR3 subunits, which render NMDA receptors in neurons less sensitive to Mg^{2+} block (Sasaki *et al*, 2002a; Tong *et al*, 2008).

1.5.4 NMDA receptors may have particular membrane distribution in glial cells

NMDA receptor mediated currents induced by ischaemia were found in precursor and mature oligodendrocytes (Karadottir *et al*, 2005). Initially NMDA receptors were reported to be present in clusters on oligodendrocyte processes, whereas AMPA and kainate receptors were diffusely located on oligodendrocyte somata (Salter & Fern, 2005). Furthermore, NR1, NR2 and NR3 subunits were found in the myelin sheath at a density similar to that observed in the postsynaptic density of the mossy-fiber–granule-cell synapse (Karadottir *et al*, 2005; Micu *et al*, 2006; Salter & Fern, 2005). Ischaemic conditions raise intracellular Ca^{2+} concentration ($[\text{Ca}^{2+}]_i$) and damage oligodendrocyte processes (Micu *et al*, 2006; Salter & Fern, 2005). Consistent with the preferential NMDA receptor location at the myelin sheet, blocking NMDA receptors during ischaemia prevented $[\text{Ca}^{2+}]_i$ rises and conferred protection against injury to oligodendrocyte process (Micu *et al*, 2006; Salter & Fern, 2005). However, recent evidence shows a more widespread expression of NMDA receptors. In addition to expression in compact myelin, NR1 was also found in regions where oligodendrocyte process membrane ran parallel to the axolemma of small premyelinated axons (Alix & Fern, 2009). Also in

astrocytes, NMDA receptors are localized in distal process, although some expression can be found in the soma (Conti *et al*, 1996).

1.5.5 Glutamate availability in neuron-glia connections

The location of NMDA receptors in oligodendrocytes processes, which are more sensitive to ischaemia, raises questions about the accessibility of glutamate for receptor activation. NMDA receptors located at process are close to axons but away from synapses, where glutamate is abundant (Shigeri *et al*, 2004). One possibility is that glutamate originates from surrounding astrocytes or oligodendrocytes. In ischaemic conditions, there is a reversal of these glutamate transporters releasing glutamate from glia and axons, that would be available to activate NMDA receptors (Fern & Muller, 2000; Li *et al*, 1999). Inhibition of glutamate transporters expressed in astrocytes and oligodendrocytes raises the local glutamate concentration, suggesting glial cells as a source of neurotransmitter (Danbolt, 2001; Karadottir *et al*, 2005; Matute *et al*, 1999). But this is unlikely to explain physiological activation of NMDA receptors that are at the cell process and facing the axolemma.

A recent development in glial biology could provide the explanation for the source of glutamate to activate NMDA receptors in processes: physiological release of neurotransmitter from axons in response to action potentials (Kukley *et al*, 2007). Developing axons in the optic nerve possess the molecular machinery needed for formation and release of glutamate-containing vesicles (Alix *et al*, 2008; Kukley *et al*, 2007; Ziskin *et al*, 2007). Glutamate is released from discrete axonal regions in response to action potentials and this release elicits glutamatergic responses in oligodendrocyte precursor cells (Kukley *et al*, 2007; Ziskin *et al*, 2007). Axons also seem to be the sole repository of vesicular glutamate in developing white matter (Alix *et al*, 2008; Kukley *et al*, 2007; Ziskin *et al*, 2007). Interestingly, axonal glutamate release appears to be an event specific to unmyelinated axons and occurs at random sites in the axolemma, suggesting a role in guidance of oligodendrocytes to the axon, or a signal for oligodendrocyte precursor cells differentiation (Kukley *et al*, 2007; Ziskin *et al*, 2007).

1.5.6 Stoichiometry of white matter NMDA receptors

NMDA receptors expressed in white matter are thought to be composed by NR1, NR2A-NR2C and NR3A subunits (Karadottir *et al*, 2005; Micu *et al*, 2006; Salter & Fern, 2005). This deduced composition is mainly based on the fact that most NMDA currents found in astrocytes and oligodendrocytes are Mg²⁺-insensitive (Hamilton *et al*, 2008; Karadottir *et al*, 2005; Lalo *et al*, 2006). The subunit that confers this property to NMDA receptors is NR3A, which is expressed in oligodendrocytes (Karadottir *et al*, 2005; Micu *et al*, 2006; Nowak *et al*, 1984; Salter & Fern, 2005; Sasaki *et al*, 2002a). However, the role of NR3A in relief of NMDA receptor voltage-dependent Mg²⁺-block is still a matter of debate since different results have been obtained in different systems (Sasaki *et al*, 2002a; Sucher *et al*, 1995; Tong *et al*, 2008). Furthermore, it has been described that in a class of glial cells, NG2-glia, considered to be glial precursor cells, NMDA receptors currents are sensitive to Mg²⁺-block at resting membrane potential (Ziskin *et al*, 2007). This suggests that more than one NMDA receptor population is expressed in white matter and regulated cell or developmental-specific of receptors may exist.

The identity of the NR2 subunits that are present in glial NMDA receptor complexes is also unknown. All NR2 subunits are expressed in white matter and pharmacological analysis shed little light about which subunit form white matter NMDA receptors (Conti *et al*, 1996; Krebs *et al*, 2003; Luque & Richards, 1995; Salter & Fern, 2005; Schipke *et al*, 2001; Von Boyen *et al*, 2006). Ifenprodil, a selective NR2B antagonist, did not affect NMDA receptor currents in mature oligodendrocytes nor did pregnalone sulphate, which potentiates NR2A-B and inhibits NR2C-D receptors. This lead to the suggestion that NMDA receptors expressed in oligodendrocytes have a previously uncharacterized composition, or that novel splice variants are expressed (Karadottir *et al*, 2005; Salter & Fern, 2005). Due to the relative Mg²⁺-insensitive properties of glial NMDA receptors, higher expression of NR3A and NR2C compared to other subunits, and the fact that NR1/NR2C/NR3A have not yet been

characterized it was speculated that this could be “the” glial NMDA receptor (Karadottir *et al*, 2005; Matute, 2006).

1.5.7 Physiological role of NMDA receptors in Glia

The physiological role of NMDA receptors in myelinating white matter is still speculative but might involve axon–glial signalling during myelinogenesis (Kukley *et al*, 2007). Myelin initiation begins with the extension of multiple processes from the somata that make contact with axons. At this point, oligodendroglial processes will either proceed with myelination or retract from the axon (Butt & Ransom, 1993). How this decision is controlled is unclear, but Ca²⁺ influx through activated NMDA receptors could affect cytoskeletal elements within the processes and determine stabilization/retraction.

NMDA receptors could also participate in glia-neuron communication in other ways. It has now been shown that NG2 cells in developing white matter can generate action potentials upon receiving axonal input from neurons (Karadottir *et al*, 2008). The glial “excitatory postsynaptic currents” (ESPCs) are mediated by NMDA and AMPA receptors (Karadottir *et al*, 2008). Moreover, not all NG2 cells generate action potentials, but the population that does is more sensitive to ischaemic damage (Karadottir *et al*, 2008). Consistent with the known role of NMDA receptors in oligodendroglial ischaemic damage, pre-incubation with a NMDA receptors antagonist, AP-5, prevented ischaemic damage of action potential generating cells (Karadottir *et al*, 2005; Karadottir *et al*, 2008; Micu *et al*, 2006; Salter & Fern, 2005).

Regardless of NMDA receptor’s role on developing oligodendrocyte processes and glial-neuron communication, their pathophysiological relevance is high as they confer sensitivity to injury that is likely to have significance for a variety of neurological diseases (Salter & Fern, 2005).

I.6 OBJECTIVES

The properties of NMDA receptors in white matter appear to differ from receptors expressed on neuronal cells. In this PhD project I sought to elucidate the reason why glial NMDA receptors display such peculiar properties. One possibility is that they are composed of an uncommon and as yet uncharacterized subunit arrangement. Another possibility is the presence of new NMDA receptor subunits splice variants. To evaluate both possibilities I have cloned NMDA receptors from the rat optic nerve, expressed these subunits in a recombinant system and characterize their physiological properties. In the next chapters I will describe the results of NMDA receptor cloning, and their molecular properties (chapters III-V), and the physiologic properties of novel splice variants (chapter VI).

Chapter II

Materials and Methods

To determine the molecular composition of NMDA receptors in white matter I choose to amplify and clone the full-length cDNA of transcripts present in this tissue (figure II-1). Methodologically, the starting point were reverse-transcription and PCR protocols used for RT-PCR aimed at detection of short DNA sequences (described in section II.3.3). These protocols proved insufficient for the amplification of longer DNA sequences, since attempts to amplify the entire coding regions of NMDA receptor subunits yielded no PCR products or non-specific short length products. The method was then improved at two steps: (i) reverse-transcription and (ii) PCR (figure II-1). This was an interactive process in which the following aspects were optimized: (i). RNase H⁺ vs RNase H⁻ reverse-transcriptases; (ii) time length of reverse-transcription and amount of enzyme; and (iii) duration and temperature of each PCR step, in particular annealing temperatures and extension times. In sections II.3.1 and II.3.2 the reasons underlining the optimizations are explained in detail.

II.1 Animals and tissue dissection

In humans, the susceptibility to PVL is higher in pregnancy weeks 23-32, a period in which ischaemic events cause damage to oligodendrocyte processes by a mechanism that is thought to involve NMDA receptors (Payam & Andrew, 2002; Salter & Fern, 2005). To probe for NMDA receptor expression and assess the existence of novel splice variants, optic nerves of rats 10-14 days old were used. At this age, the rat optic nerve is initiating the process of myelination, with the first layers of myelin appearing, and corresponds to the developmental stage at which white matter is susceptible to PVL in the human foetus (Back *et al*, 2001; Foster *et al*, 1982).

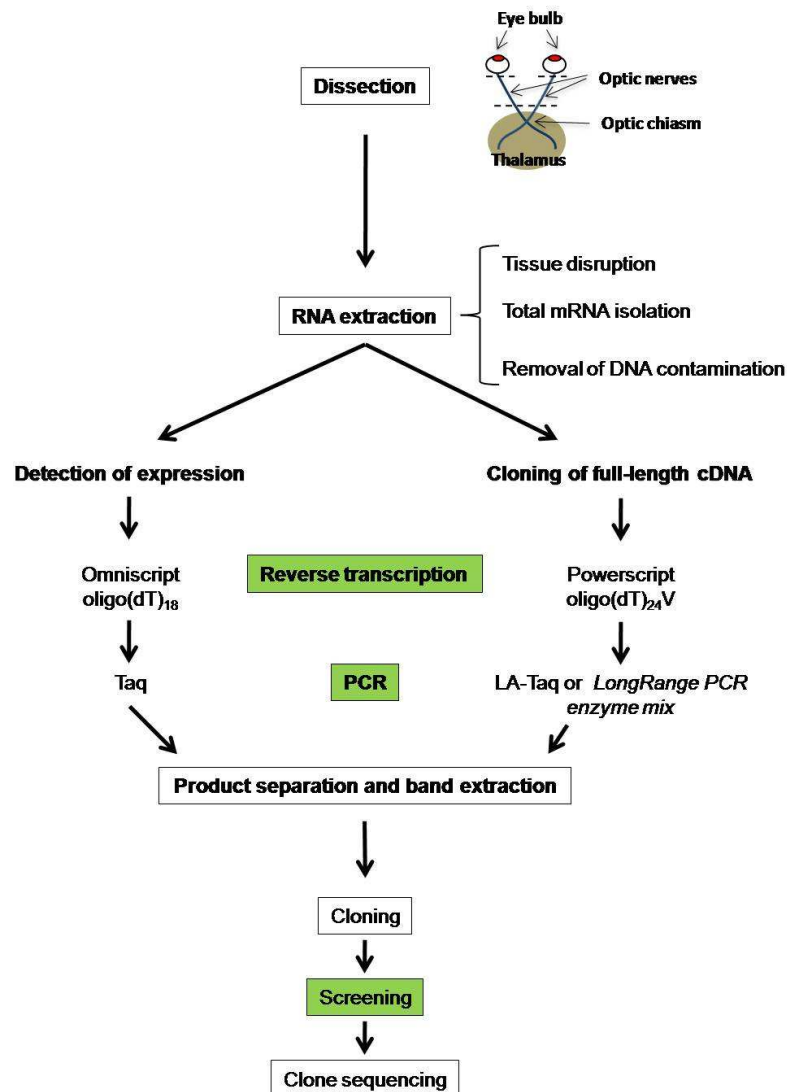


Figure II-1: Outline of the experimental procedure for amplification and cloning of NMDA receptors

Following optic nerve dissection (section II.1.1), total RNA was extracted (section II.2) and reverse-transcribed (section II.3). Depending on the end-application (detection of expression or amplification of full-length sequences), reverse transcription and PCR were performed differently (section II.2). PCR products were separated by electrophoresis, cloned and sequenced (section II.9). Green-shaded boxes represent steps that required optimization.

The optic nerve is a CNS white matter tract and comprises the axons of retinal ganglion cells together with the glia which support them, namely oligodendrocytes, astrocytes and microglia (Butt *et al*, 2004). This structure is the only white matter model that does not contain neuronal cell bodies, and is ideal for the extraction of mRNA that is mostly of glial origin (Butt *et al*, 2004; Salter & Fern, 2005). In addition, there is a wealth of literature available on optic nerve myelination.

II.1.1 Method

P10-14 Lister-hooded rats (male and female) were sacrificed by cervical dislocation in accordance with the regulations of the British Home Office. Optic nerves were then excised between the eye and the optic chiasm, which remained attached to the brain, and placed in Phosphate-Buffered Saline (PBS) composed of (mM): 138 NaCl; Na₂HPO₄; 2.7 KCl; and 1.5 KH₂PO₄. Optic nerves were centrifuged at 12,000 x g for 2 min and PBS was removed by aspiration before proceeding to RNA extraction.

II.2 RNA extraction

Extraction of high quality RNA is a crucial step for successful RT-PCR. RNA is an unstable molecule, having a shorter half-life than DNA, and is more easily degradable by nucleases (RNases). Thus special care must be taken when working with RNA. Although several efficient methods have been developed for the extraction of RNA from different animal tissues, optic nerves have a few peculiarities that make RNA extraction challenging. Each individual optic nerve has a small mass and relatively high content of protein and lipids (it is estimated that myelin is composed of 80% lipids and 20% protein) compared to brain grey matter (O'Brien & Sampson, 1965). A general method to disrupt tissues for RNA extraction is a pestle and mortar. This method has been tried in our lab to extract RNA from optic nerves, but RNA yield was low due to loss of sample tissue during the procedure (Salter MG, personal communication).

To overcome the difficulties of RNA extraction from optic nerve using physical disruption, our lab has optimized an alternative method by combining two commercially available reagents: *MELT-system* (Multi-Enzymatic Liquefaction of Tissue; Ambion) and *Trizol* reagent (Qiagen). *MELT* uses a protein cocktail in an optimized buffer to disrupt tissues and protect RNA by destroying RNases. *Trizol* is a mono-phasic solution of phenol and guanidine isothiocyanate. This reagent maintains the integrity of the RNA and dissolves other cell components. The procedure consists of 3 main steps: 1) Tissue disruption using *MELT* enzymes, present in the kit; 2) Separation of RNA from other cellular components with *Trizol*; 3) Purification of RNA using columns from *RNA RNeasy lipid RNA mini kit* (Qiagen). The method was developed by Michael G. Salter for mice optic nerves and adapted by me to rat (Salter & Fern, 2005).

II.2.1 RNA extraction from the optic nerve - method

For optic nerve tissue disruption, 96 μ l 1X *MELT Buffer* and 4 μ l *MELT Cocktail* (Ambion) were added to 20 optic nerves from Lister-hooded rats aged P10-14 (male and female), prior to shacking for 10-15 min in a vortex. Once no visible fragments remained, 1 ml of *Trizol* reagent (Qiagen) was added to the mixture. After 5 min incubation at room temperature, 200 μ l of chloroform were added prior to incubation at room-temperature for 2-3 min, followed by centrifugation at 12,000 x g for 15 min, 4°C. After centrifuging, the sample separates into an organic phase and an aqueous phase in which the RNA is present. The aqueous phase was carefully decanted and the RNA was column-purified (*RNeasy lipid RNA mini kit, Qiagen*) according to the manufacturer's instructions. Final elution was made with 32 μ l nuclease-free water (Ambion). To remove any contaminating genomic DNA, the RNA samples were treated with *Turbo DNase free kit* (Ambion) using the Rigorous DNase treatment suggested by the manufacturer. The amount of RNA present in the samples was determined by measuring the absorbance at 260 nm in a spectrophotometer. This procedure

routinely yielded 10 µg RNA per 20 optic nerves. RNA was then used as substrate for reverse transcription.

II.2.2 RNA extraction from the brain - method

Whole neonate rat brain (10-14 days old) was dissected and frozen in liquid nitrogen. The tissue was then ground to a fine dust using a pestle and mortar. To avoid RNA degradation, liquid nitrogen was added regularly to the mortar. The ground tissue was immediately transferred to a microtube, 1 mL Trizol added and the protocol proceeded from this point as previously described in this chapter. The amount of RNA extracted from one brain was usually 100 µg.

II.3 Reverse transcriptase-polymerase chain reaction (RT-PCR)

RT-PCR is a technique employed to indirectly amplify RNA sequences. It consists of two sequential steps: Reverse Transcription (RT) and Polymerase Chain Reaction (PCR). In the first step RNA is reverse transcribed in cDNA which is then used as a template and amplified by PCR. I will explain both steps in detail and also the improvements made to achieve full-length amplification of NMDA receptor subunits transcripts.

Amplification of full-length cDNAs present some complications in comparison with RT-PCR to detect transcript expression: 1) the sequences to be amplified are longer, in our case >3Kb; 2) the amplified sequences will be expressed and must not contain mutations leading to amino acid changes; 3) GC rich regions are difficult to amplify and can be circumvented by amplifying other mRNA sequences in short PCR amplification, but have to be amplified if full-length transcripts are to be obtained. In addition, NMDA receptor expression in the optic nerve is relatively low compared to expression in the brain (Salter & Fern, 2005). To overcome these difficulties I have tested several enzymes, DNA polymerases and reverse-

transcriptases, and several aspects of the protocol were optimized. Here I present the most successful protocol for the amplification of full-length NMDA receptor mRNAs.

II.3.1 RT

Reverse transcription is catalyzed by the enzyme reverse transcriptase. Reverse transcriptase performs 3 distinct enzymatic activities: i) an RNA-dependent DNA polymerase; ii) a hybrid-dependent exoribonuclease (RNase H); iii) and a DNA-dependent DNA polymerase. *In vivo*, the combination of these 3 activities allows transcription of the single-stranded RNA genome into double-stranded DNA for retroviral infection. For reverse transcription *in vitro*, only the first two activities are utilized to produce single-stranded cDNA. Reverse transcription is initialized by the annealing of a primer to the RNA and the enzyme then starts adding complementary deoxynucleotides (dNTPs) to form the cDNA. The final product is a RNA:DNA hybrid which needs to be degraded to allow primer binding in the PCR. Reverse transcriptases from the RNase H family (RNase H⁺) possess hybrid-dependent exoribonuclease activity that degrades RNA present in RNA:DNA hybrids and thus improve RT-PCR sensitivity (Polumuri *et al*, 2002). Since cDNA synthesis and RNA template degradation occur in the same conditions, the protocol is also more streamlined. RNase H⁺ enzymes are thus preferable for gene expression detection.

Although RNase H⁺ reverse transcriptases are a better choice for RT-PCR aimed at detection of expression, where only ~100 bp in the transcript 3' end are amplified, these enzymes are less suited for amplification of full-length cDNAs. RNase activity can lead to degradation of RNA:DNA hybrids near the 5' end of the cDNA strands before it is completely formed, thus creating shorter, incomplete cDNAs (Kotewicz *et al*, 1988). Because RNA-dependent DNA polymerase activity of reverse transcriptase is not dependent on concomitant RNase H activity, mutant enzymes that lack RNase activity have been created, and are more suitable for the generation of full-length cDNAs. One of such enzymes is *Powerscript* (Clontech) which has been used in our work.

As previously mentioned primer binding is required for initiation of reverse-transcription. Three different types of primers can be used: a) random primers; b) gene-specific primers; or c) oligo-dT primers that specifically hybridize to the poly-A–tail of mRNAs. In its common form, commercially supplied oligo-dT primers have 18 thymines (oligo(dT)₁₈). This primer will anneal at any position in the A-tail, which may be near the 3' end of the mRNA, or it can also bind to internal poly(A) sequences, generating truncated cDNAs. To increase the yield of full-length cDNA I used an anchored oligo(dT)₂₄V primer, where V represents guanine, cytosine or adenine. The presence of these nucleotides (V) ensures increased binding to the 3' of the mRNA by reducing binding to internal poly(A) sequences and also insertion in the distal end of polyA mRNA tails. The result is an increase in full-length cDNA molecules (Nam *et al*, 2002).

II.3.2 PCR

Polymerase chain reaction (PCR) is a technique used to amplify DNA templates and produce specific DNA fragments *in vitro*. A typical reaction contains the DNA template, a thermostable DNA polymerase, two oligonucleotide primers (forward and reverse), deoxynucleotide triphosphates (dNTPs), reaction buffer and Mg²⁺. To ensure amplification, the reaction is subjected to a series of temperatures for varying amounts of time using a thermal cycler. This series of temperature and time adjustments is referred to as one cycle of amplification. Each PCR cycle theoretically doubles the amount of targeted sequence (amplicon) in the reaction.

The typical PCR cycle has three steps: i) denaturation; ii) annealing; iii) extension. In the first step the temperature is raised to 94°C, or higher, to separate the DNA double helix into single strands. Once the strands are separated they become available for primer binding. In the next step the temperature is lowered so that the primers can form stable associations (anneal) with complementary sequences in the denatured template DNA. The annealing temperature is a particularly important parameter because primer binding is required for the activity of the

DNA polymerase. If the annealing temperature is set too high, the primers will not form bonds with complementary sequences, and no product will be obtained from the PCR. On the other hand, setting the annealing temperature too low may result in primer binding to partially complementary template sequences. This will result in amplification of non-specific sequences.

The synthesis of DNA begins in the amplification step. The temperature is raised for the optimum DNA polymerase reaction temperature (68-72°C) and the enzyme reads the opposing strand sequence and extends the primers by adding paired nucleotides. The duration of each step varies according to the fragment size to be amplified; extension rate of the DNA polymerase; or other properties of the enzyme and/or the cDNA. The number of cycles can also vary depending, for instance, on the number of initial copies of the template cDNA. Variations to the outlined cycle can occur. For instance, if the primers annealing temperature and DNA polymerase extension temperature are similar, the steps can be combined.

DNA polymerases were critically chosen taking in consideration the need for longer extension and higher fidelity than those of Taq. *LA-Taq* DNA polymerase (Takara) is a mixture of DNA polymerases which offers 6.5 times the fidelity of regular Taq and is particularly suited for amplification of long DNA fragments. *LA-Taq* was used for the amplification and cloning of NR1, NR2A, NR2B, NR3A and NR3B. Amplification of NR2C and NR2D revealed itself to be more difficult due to the high GC content of the cDNAs. To overcome this, another DNA polymerase was used: *LongRange PCR enzyme mix* (Qiagen), alongside with the *Q reagent* present in the same kit. This enzyme, in conjunction with *the Q reagent*, is optimized for the amplification of long targets with high GC-content.

II.3.3 Expression of receptors - method

Reverse-transcription was performed on 4 µg of RNA using *Omniscript* (Qiagen) according to the manufacturer's instructions (all quantities were doubled to ensure the correct

concentrations). The reaction was primed with an oligo(dT)₁₈. The generated cDNA was cleaned using *QIAquick PCR Purification Kit* (Qiagen) and eluted in 40 µl. The PCR reaction was prepared mixing 2x *iQ SYBR Green Supermix* (Bio-Rad), 4 µl of the cDNA pool per reaction, 300 nM of the relevant gene-specific primer pairs (both forward and reverse; see table II-1) and nuclease free water to yield a final reaction volume of 40 µl. All primers were tested on whole brain cDNA as a positive control. PCR cycles were the following: 95°C for 45 s, 57°C C for 30 s, 72°C for 45 s, for 40 cycles with a dissociation curve at the end. Intensity of fluorescence was read at the end of each cycle and also during each step of the dissociation curve. PCR reaction products were loaded in a 1% agarose gel and visualized using *SYBR Safe* dye (Invitrogen) and the *Safe Imager* blue light transilluminator system (Invitrogen). All primers were purchased from Sigma Genosys and are listed in table II-1.

Table II-1: List of PCR primers used for expression studies

All primers were designed by me except the primers for actin, which were designed by Dr. Michael Salter.

Primer	Sequence (5'-3')	Sequence accession number	Position
Actin for	TGCTCCTCCTGAGCGCAAGTACTC	NM031144	1071 - 1094
Actin rev	CGGACTCATCGTACTCCTGCTTGC	NM031144	1177 - 1154
NR1 for	GTGTCCCTGTCCATACTCAAGT	NM017010.1	2578 - 2600
NR1 rev	TGAAGACCCCTGCCATGTCTC	NM017010.1	2717 - 2696
NR2A for	AGACCACGCCTCCGATAATC	NM012573.2	4166 - 4185
NR2A rev	GCCTGTGATGGCAATGAGTG	NM012573.2	4273 - 4254
NR2B for	GCTTTCAATGGCTCCAGCAATG	NM12574.1	4734 - 4755
NR2B rev	CTCTCTCTCCCTCACTCAG	NM12574.1	4815 - 4796
NR2C for	GAAGAGGTCAGCAGGAAAC	NM012575.2	4186 - 4205
NR2C rev	AGTCCAGCAGGAACCAAAGC	NM012575.2	4306 - 4287
NR2D for	CGATGGCGTCTGGAATGG	NM022797.1	2281 - 2298
NR2D rev	AGATGAAAACGTGACGGCG	NM022797.1	2540 - 2521
NR3A for	CTCCCTCAATGTAACCTCGG	AF073379.1	3731 - 3749

NR3A rev	GATACTCCTCCAGCTCTGTC	AF073379.1	3852 - 3833
NR3B for	GATCTGCTCCATGACAAGTGG	NM133308.2	2476 - 2496
NR3B rev	TCCTGAGAAGTGGTAGACC	NM133308.2	2574 - 2556

Table II-2: List of PCR primers used for the detection of NR1 and NR3A splice variants

(NR1 primers were designed by Dr. Michel Salter).

Primer	Sequence (5'-3')	Gene accession #	Position
<i>NR1</i>			
ex4	AGTCCAGCGTCTGGTTTGAG	NM_017010.1	705 - 724
ex8	TGATGAGCTGAAGTCCGATG	NM_017010.1	1082 - 1063
ex17	CCCTCAGACAAGTTCATCTA	NM_017010.1	2288 - 2307
3' UTR	TCAGTGGGATGGTACTGCTG	NM_017010.1	3338 - 3319
<i>NR3A</i>			
3444 for	AAGCAGCCACGTTCCAAGAC	AF073379 (NR3A-L)	3444 - 3463
3644 rev	CTGGTTTTGTCCTTCCTCGTC	AF073379 (NR3A-L)	3644 - 3624

II.3.4 Full-length cDNA amplification - method

To create full-length cDNAs of NMDA receptors, reverse transcription was performed using *PowerScript* (Clontech) and mRNA was primed with an oligo(dT)₂₄V primer (SigmaGenosys). Whenever possible, the maximum amount of RNA suggested by the manufacturer protocol was used (10 µg). The reaction was performed with a modification of the suggested protocol (Clontech). All the volumes were doubled and the reaction was performed for 1 h at 42°. At this point an additional 0.5 µl of *PowerScript* were added and the reaction was allowed to continue for another hour. cDNA was purified using *QIAquick PCR Purification Kit* (Qiagen) and the volume corresponding to 1 µg of RNA input was used for the PCR reaction using *LA-Taq* (Takara), according to manufacturer's instructions. PCR cycle conditions varied according to the NMDA receptor subunit amplified and can be found in

table II-2. Primer sequences are listed in table II-3 and the relative location of primers in the cDNA is represented in figure II-2A. PCR reaction products were separated in an 1% agarose gel and visualized using *SYBR Safe* dye (Invitrogen) and the *Safe Imager* blue light transilluminator system (Invitrogen).

Table II-3: List of PCR cycle conditions used for full-length cDNA amplification.

Receptor	Initial denaturation	40 cycles			Final amplification
		Denaturation	Annealing	Amplification	
NR1	95°C 1 min	95°C 30 sec	58°C 30 sec	68°C 8 min	68°C 10 min
NR2B	95°C 1 min	95°C 30 sec	58°C 30 sec	68°C 9 min	68°C 13 min
NR2C	93°C 3 min	93°C 30 sec	64°C 30 sec	68°C 10 min	68°C 15 min
NR2D	93°C 3 min	94°C 30 sec	60°C 30 sec	68°C 10 min	68°C 15 min
NR3A	95°C 1 min	95°C 30 sec	58°C 30 sec	68°C 8 min	68°C 10 min
NR3B	95°C 1 min	95°C 30 sec	63°C 30 sec	68°C 8 min	68°C 10 min

Table II-4: List of PCR primers used for full-length cDNA amplification

Primer	Sequence	Sequence accession number	Position
NR1 for	CAAACACGCTTCAGCACCTC	RNU08267	77 - 96
NR1 rev	AGCAGCAGGACTCATCAGTG	RNU08267	2957 - 2938
NR2B for	CTCTCTCCCTTAATCTGTCCG	NM12574.1	284 - 304
NR2B rev	CTCTCTCTTCCCTCACTCAG	NM12574.1	4815 - 4796
NR2C for	CCCTTCCCTTCTTCTGTTTGTCCATCTACC	NM012575.2	486 - 515
NR2C rev	GCTGCCAGTAACCTCACACTTCTGATTC	NM012575.2	4288 - 4261
NR2D for	TAGCCTCATCCTTGCCTAGTCTGGTG	NM022797	447 - 472
NR2D rev	CAGGTCCGTTTCTGTCTTCCCAAC	NM022797	4830 - 4806
NR3A for	GAGGATGTTAAGCAGAGGAGC	AF073379.1	237 - 257
NR3A rev	GTGTCTCAAGGGCTTCAGAG	AF073379.1	3935 - 3916
NR3B for	CGCACAGCACAGTGGTAACTTC	NM133308.2	47 - 68
NR3B rev	ACAGTGCGGCCTTGTGGTTC	NM133308.2	3105 - 3086

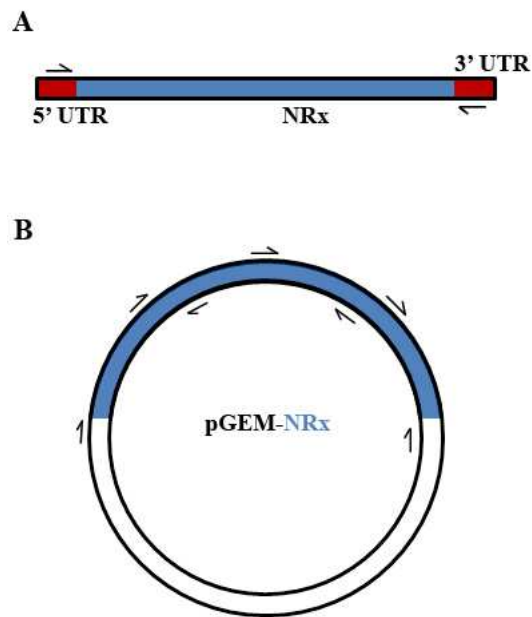


Figure II-2: Relative location of primers used for amplification of full-length NMDA receptor subunits cDNA and sequencing of clones.

(A) For the PCR amplification of NMDA receptor coding sequences forward and reverse primers were designed to anneal at the 5' and 3' UTR of the mRNA and thus include original initiation and termination codons of the subunits. (B) Due to length of the cloned fragments and limitations of sequencing technologies, several primers that generated overlapping sequences were used to sequence the full inserted clone. The figure is merely indicative of the location of annealing and does not represent absolute location or number of primers used, which varied for each clone.

II.3.5 Cloning of PCR products - method

Individual bands resulting from PCR amplification were extracted from the agarose gel, purified with *Gel Extraction kit* (Qiagen) and inserted into the vector *pGEM-T easy* with the *pGEM-T easy* system (Promega) following the manufacturer's instructions. 2 μ L of each ligation reaction were used to transform *Escherichia coli XL1-gold* ultra-competent cells (Stratagene). After transformation, *E. coli* were plated in LB agar (9.14g/L tryptone; 4.57g/L yeast extract; 4.57g/L NaCl, 13.72g/L agar) supplemented with 50 μ g/ml ampicillin and grown overnight at 37°C. Colonies containing inserts were selected using *blue-white screening reagent* (Sigma) and insertion of DNA was further confirmed by PCR screening using the appropriate pair of primers. Several primer pair annealing at different gene regions were used to screen each clone. This generated a pattern of bands for each clone, allowing selection of clones with different patterns corresponding to putative new variants. Routinely 16 clones per gel extracted band were chosen for screening. Individual positive colonies were then grown overnight in LB Broth media (10 g/L enzymatic digest of casein; 5 g/L yeast extract; 5 g/L sodium chloride) containing 50 μ g/ml ampicillin; plasmids were purified using *QIAprep Spin Miniprep Kit* and sent for sequencing at LGC/AGOWA (Germany). Due to the length of cloned fragments several overlapping sequencing reactions were required for each clone, with primers annealing different gene and plasmidic regions (figure II-2B). DNA fragments obtained from the sequencing of each clone were assembled using the software suite Vector NTI Advance 10 (Invitrogen). Fragment assembly is described in section II.9.1.

II. 4 Creation of error-free clones

Despite the use of a high-fidelity DNA polymerase, amplified sequences contained nucleotide mutations that were predicted to alter the final polypeptide chain. These amino acid changes can lead to altered protein physiology and abnormal results. To avoid this, recombinant DNA techniques were used to replace these altered sequences with error-free sequences from other clones. Firstly I created an NR3B clone without errors and then replaced

the spliced regions from the novel variants in this clone. An overview of the protocol is depicted in figure II-3.

NMDA receptor splice variants NR3B $_{\Delta 24}$, NR3B $_{\Delta 45}$, NR3B $_{\Delta 600}$ and NR3B $_{\Delta 1125}$ inserted in vector *pGEM-t* easy were cut using the following reaction: 1 μ g of each plasmid; 3 μ l of 10x restriction buffer; 3 μ l of 1 mg/mL BSA (Bovine serum albumin); 5 U of each restriction enzyme; 5U of CIP (Calf Intestinal Alkaline Phosphatase, New England Biolabs) and nuclease free water to yield a final reaction volume of 30 μ l. The restriction enzymes used are listed in table II-5. After incubating the reaction at 37°C for 1 h, the reaction products were loaded in a 1% agarose gel, to separate the fragments generated in the restriction reaction. Bands corresponding to the fragments of interest were extracted from the gel and purified using the *Gel Extraction kit* (Qiagen).

Table II-5: list of restriction enzymes used to replace erroneous sequences in cloned cDNA

	Restriction enzymes	Supplier
NR2B $_{\Delta 635}$	DraIII/NdeI	Fermentas
NR3B	BamHI/SalI	New England Biolabs /fermentas
NR3B $_{\Delta 24}$	XhoI/BamHI	New England Biolabs
NR3B $_{\Delta 45}$	NheI	Fermentas
NR3B $_{\Delta 600}$	HindIII/ SpeI	New England Biolabs /Roche
NR3B $_{\Delta 1125}$	BamHI/SalI	New England Biolabs /fermentas

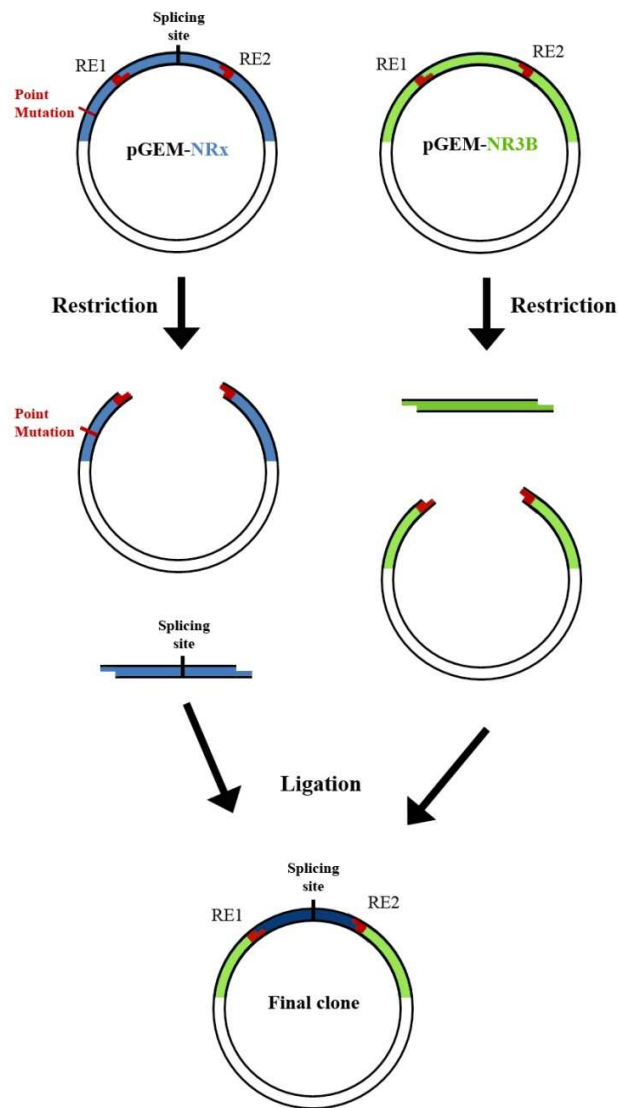


Figure II-3: Procedure to eliminate nucleotide mutations from clones

Cloned cDNA (pGEM-NR_x) contained nucleotide mutations that caused amino acid changes were cut with restriction enzymes that surrounded the splicing site. The same restriction enzymes were used to cut an NR3B clone (pGEM-NR3B) without nucleotide mutations. Mutated sequences were discarded and the splice region was inserted in pGEM-NR3B. The final clone will contain the same splicing site of pGEM-NR_x, but will not code for altered amino acid in the rest of the CDS (coding sequence).

Ligation of fragments was performed using the Rapid DNA Ligation Kit (Fermentas) using a vector:insert ratio of 1:3 (pGEM-NR3B:fragment containing splicing). The ligation reaction mixture contained 50 ng of linearized vector; 3 fold molar excess of DNA insert; 4 μ l Rapid ligation buffer; 4 U T4 DNA ligase and nuclease free water to yield a final reaction volume of 20 μ l. The reaction was performed for 5 min at room temperature. Transformation and identification of positives were done as previously described in section 3.3. Positive clones were sequenced to confirm the correct sequence.

II.5 Construction of fluorescently tagged subunits

To assess the contribution of individual NMDA receptor subunits I needed to identify transfected cells that express specific subunits. Fluorescent tagging of proteins with GFP, GFP derived proteins or other fluorescent proteins is a widely used strategy for visualization of proteins *in vivo*. NMDA receptor subunits have been successfully tagged without altering the channel physiology (Marshall *et al*, 1995). Because the subtypes I wanted to express consisted of NR1/NR2A-C and/or NR1/NR2A-C/NR3A-B, NR1, NR2 and NR3 subunits needed to be tagged with different fluorescent proteins. After analyzing the spectra of fluorescent proteins and available filters, I selected ECFP, EYFP and mCherry (see table II-6 for information on spectra). With that in mind and having already access to NR1 tagged with ECFP and NR2A-B tagged with EYFP (Qiu *et al*, 2005), I tagged NR2C with EYFP and NR3A-B with mCherry. An outline of the strategy is depicted in figure II-4.

Table II-6: Properties of fluorescent proteins used to tag NMDA receptor subunits

	Excitation maximum (nm)	Emission maximum (nm)	Relative brightness of GFP (%)
ECFP	439	476	39
EYFP	514	527	151
mCherry	587	621	47

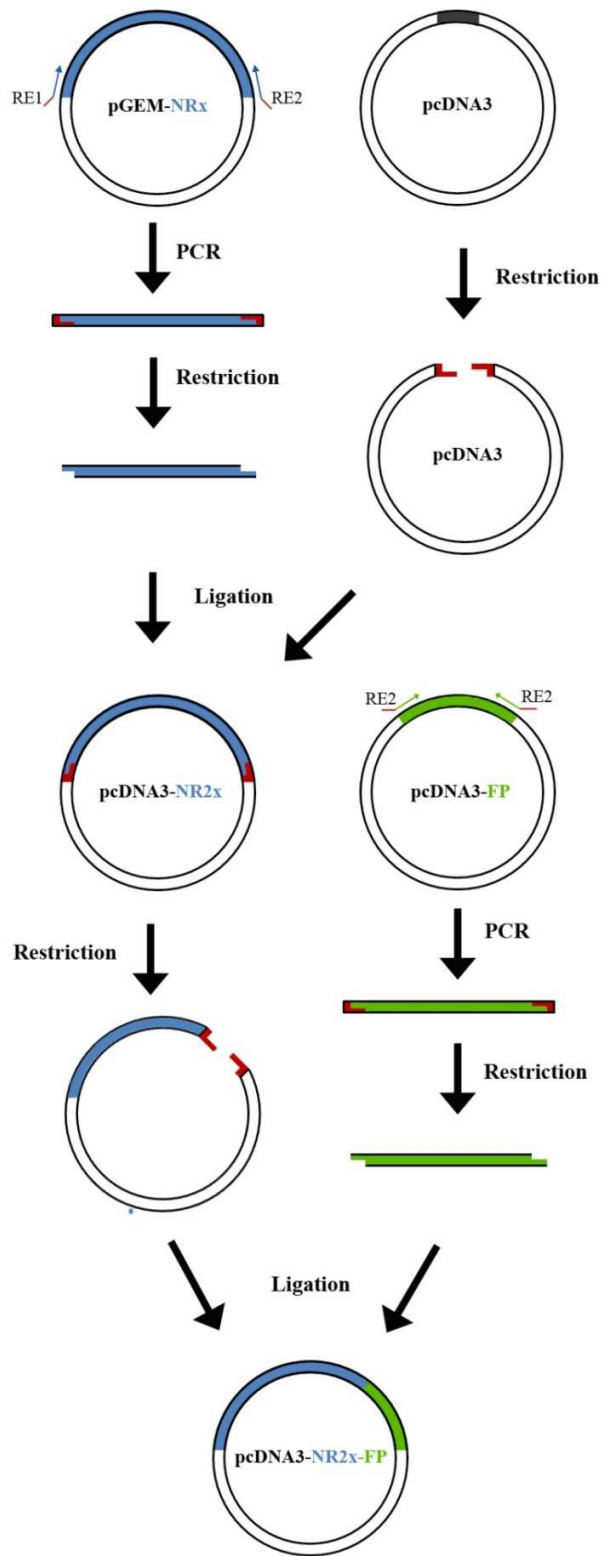


Figure II-4: Construction of fluorescently labelled NMDA receptor subunits

Cloned cDNA in pGEM (pGEM-NRx) was PCR amplified using primers containing different restriction enzyme sites (RE1 and RE2) and inserted in a mammalian expression vector (pcDNA3). The fluorescent protein cDNA was also PCR amplified using primers that contained only RE2. The final construct will be an NMDA receptor subunit fused with a fluorescent protein at its 3' end (pGEM-NRx-FP).

NMDA receptor subunit cDNA, originally cloned in the vector *pGEM-T*, was PCR amplified with *PfuUltra II Fusion HS DNA Polymerase* (Stratagene) with primers containing restriction sites (table II-7). PCR cycles were the following: 94° for 4 min; 94° C for 20 s, 68°C for 3 min 45 s, for 35 cycles; final extension at 68°C for 10 min. PCR products were separated in an 1% agarose gel and visualized using *SYBR Safe* dye (Invitrogen) and the *Safe Imager* blue light transilluminator system (Invitrogen). Bands corresponding to the desired product size were cut from the gel and cleaned using the *Gel Extraction kit* (Qiagen). Extracted bands were cut using the following restriction reaction: 15 µl of each purified PCR product; 3 µl of 10x restriction buffer; 3 µl of 1 mg/mL BSA; 5 U of each restriction enzyme and nuclease free water to yield a final reaction volume of 30 µl. The restriction reactions were then incubated at 37°C during 1 h. The DNA was purified using *QIAquick PCR Purification Kit* (Qiagen). To cut 1 µg of the vector *pcDNA3* (Invitrogen) the restriction reaction was set in the same manner but with the addition of 5 U of CIP (Calf Intestinal Alkaline Phosphatase, New England Biolabs) to avoid vector recircularization. After incubating the reaction at 37°C for 1 h, the products were loaded and separated in a 1% agarose gel, to confirm vector linearization. The band corresponding to the linearized vector was extracted from the gel and purified using the *Gel Extraction kit* (Qiagen). The restrictions enzymes used are listed in table II-7.

Table II-7: List of primers used for amplification of clones inserted in *pGEM-T*

Restriction enzyme cut sites are underlined. Initiation and stop codons are highlighted in bold.

	Primer sequence
<i>NR2C-YFP</i>	
NR2C-EcoRI for	CGGAATTCCTACCTCTCTCTATGCCTGC
NR2C- NotI rev	ATTTGCGGCCGCACTTCTGATTCCAGGCTG
YFP- NotI for	ATTTGCGGCCGCGAGCAAGGGCGAGGAGCTG
YFP-NotI rev	ATTTGCGGCCGCTTACTTGTACAGCTCGTCCATCG
<i>NR3A-mCherry</i>	
NR3A-BamHI for	ATTGGATCCGAGGATGTTAAGCAGAGGAGC

NR3A-NotI rev	ATTTGCGGCCGCGGATTCACAAGTCCGATTTG
mCherry-NotI for	ATTTGCGGCCGCGCGGCCGCGGTGAGCAAGGGCGAGGAGG
mCherry-NotI rev	ATTTGCGGCCGCTTACTTGTACAGCTCGTCCATG
NR3B-mCherry	
NR3B-KpnI for	ATTGGTACCTTCTTTCGGGATGGAGAGTG
NR3B-EcoRI rev	ATGAATTCGCTCTCAGCAGGCCCGCATG
mCherry-EcoRI for	ATGAATTCGCCGCGGTGAGCAAGGGCGAGGAGG
mCherry-EcoRI rev	ATGAATTCCTTACTTGTACAGCTCGTCCATG

Ligation of insert (PCR product) with the vector (pcDNA3) was performed using the *Rapid DNA Ligation Kit* (Fermentas) and using a vector: insert ratio of 1:3. The ligation reaction mixture contained 50 ng of linearized vector; 3 fold molar excess of DNA insert; 4 μ l Rapid ligation buffer; 4 U T4 DNA ligase and nuclease free water to yield a final reaction volume of 20 μ l. The reaction was performed for 5 min at room temperature. Transformation and identification of positives were done as previously. YFP and mCherry cDNA was amplified from pNR2B-YFP and pcDNA3.1/myc/hisA/mCherry plasmids, respectively, using the same procedure described above for NMDA receptor subunit cDNA. The amplicons were then cut with the appropriate enzyme and inserted in the linearized pcDNA3-NR2C or pcDNA3-NR3A-B plasmids. After transformation, positive colonies were tested by PCR for correct insertion of the sequence, and positive clones were sequenced (Agowa/LGC). Error free clones were chosen for expression. To create NR2B $_{\Delta 628}$ -YFP, NR2B-YFP was cut with DraIII and NdeI and replaced with the corresponding fragment from the clone pGEM-NR2B $_{\Delta 628}$.

Fluorescent tags are present at the C-terminus of the subunits NR2C (YFP), NR3A (mCherry) and NR3B (mCherry). NR1-CFP, NR2A-YFP, NR2B-YFP are tagged at the N-terminus (Qiu *et al*, 2005) and are a generous gift from Dr. Luo (Department of Neurobiology, Zhejiang University School of Medicine, Zhejiang, China). Tagging of NMDA

receptors subunits at both N-terminus and C-terminus has been done in the past, and expressed subunits form functional channels (Luo *et al*, 2002; Smothers & Woodward, 2003).

II.6 Cell culture and transfection

Transfection is the term to define non-viral methods of introducing nucleic acids in eukaryotic cells (Bonetta, 2005). DNA is a large molecule that carries a negative charge and thus cannot easily cross mammalian cell membrane. A way to get DNA inside cells is to combine DNA with positively charged carrier molecules, such as such as cationic lipids and polymers. The first compounds to be used for this purpose were DEAE-dextran (McCutchan & Pagano, 1968) and calcium phosphate (Graham & van der Eb, 1973). Although these methods are still used, lipid-based reagents are more efficient, less toxic and easier to use (Dokka *et al*, 2000; Felgner *et al*, 1987). Several advancements have been made in the development of lipid-based reagents, which now combine various lipids and polymers. The mechanism of DNA delivery into the cell appears to be common to these reagents. Liposomal transfection reagents envelop DNA and fuse with the cell, delivering the DNA to the cytoplasm by endocytosis (Hafez *et al*, 2001). I chose to use *Lipofectamine 2000* (Invitrogen), a commercially available formulation with a proprietary composition, which produces relatively high transfection efficiency (Dalby *et al*, 2004).

NMDA receptors subunits were expressed in human embryonic kidney cells (Hek293). Hek293 cells are a cell line created by transformation of human embryonic kidney cells with human adenovirus type 5 DNA (Graham *et al*, 1977). Hek293 cells are a popular choice in cell biology research. They are easy to grow and maintain; easy to transfect using a wide variety of methods; with high transfection efficiency; and faithful translation and processing of proteins (Thomas & Smart, 2005).

II.6.1 Cell culture method

Hek293 (ATCC, CRL-1573) were grown and maintained in high-glucose Dulbecco's modified Eagle's medium (Invitrogen) supplemented with 10% (v/v) foetal bovine serum (Invitrogen) under humidified conditions with 5%CO₂ at 37°C. Cells were grown in 75 cm² tissue culture flask (Nunc) until 80% confluence, before being divided to new flasks or plated in poly-L-lysine coated coverslips to be transfected. Culture media was aspirated and cells were rinsed once with 10 ml PBS. Washing media was aspirated, replaced with 5ml of fresh PBS, and cells returned to the incubator for 5 min. Following this period, cells were detached from the tissue flask by pipetting up and down and 5 ml of DMEM was added. The cell suspension was centrifuged for 3 min at 3.000 rpm, the supernatant discarded and the cell pellet resuspended in 10 ml DMEM. Cells were then diluted 1/10 to new tissue flasks for propagation, or plated at 17.500 cells/cm² in poly-L-lysine coated 15 mm diameter coverslips for transfection.

II.6.2 Transfection protocol

Although the transfection protocol suggests that higher transfection efficiency is achieved at 90% confluence, this has a drawback for single-cell imaging. When grown to high confluence, Hek293 stop forming a monolayer and grow to form several layers, becoming difficult to identify individual transfected cells. For this reason I choose to compromise and cells were transfected at 50–70% confluence. Transfection was performed with lipofectamine 2000, according to the manufacturer's instructions. For co-transfections the plasmid ratio was 1:2 (NR1:NR2) or 1:2:4 (NR1:NR2:NR3) (Yamakura *et al*, 2005). The total amount of plasmidic DNA was 1.6 µg per coverslip. Transfection media was replaced after 4 hours with fresh culture media with 100 µM APV to prevent NMDA receptor mediated excitotoxicity (Anegawa *et al*, 1995). Transfected cells were imaged 24 hours post-transfection.

II.7 Imaging

Fura-2 is a ratiometric fluorescent dye that binds to free intracellular Ca^{2+} (Grynkiewicz *et al.*, 1985). Absorption of Fura-2 changes from 380 nm in Ca^{2+} -free state to 340 nm (Ca^{2+} -saturated). The wavelength of maximum fluorescence emission is relatively independent of Ca^{2+} and is typically detected at 520 nm. The 340/380 ratio is thus directly correlated with the amount of $[\text{Ca}^{2+}]_i$. The use of ratiometric dyes reduces the effects of uneven dye loading, leakage of dye and photobleaching (Morgan, 1993). In addition, examination of the individual 340 and 380 tracings allows easy discrimination between Ca^{2+} changes due to genuine cellular responses, or rises in 340/380 ratio due to technical interference. Fura-2 is bound to an acetoxymethyl ester group (Fura-2/AM) that helps the dye to penetrate cellular membrane. Once fura-2/AM is inside the cell, the ester group is cleaved by intracellular esterases, preventing fura-2 from leaking passively during the experiment. SBFI is a dye that binds to Na^{2+} and behaves in similar fashion to Fura-2 (Negulescu & Machen, 1990).

II.7.1 Ca^{2+} and Na^{2+} imaging - method

Twenty-four hours post-transfection cells were loaded with 5 μM Fura-2 or 5 μM SBFI in modified Ringer's solution (135 mM NaCl, 5.4 mM KCl, 1.8 mM CaCl_2 , 10mM glucose, 5 mM HEPES, pH 7.2, 300 mOsm) supplemented with 1% BSA and 0.025% pluronic acid, for 30 min at 37 °C, and mounted onto an perfusion chamber (Model PH-3, Warner Instrument Corporation, Hamden, USA). The chamber was then placed in the stage of an inverted fluorescent microscope *Eclipse TE200* (Nikon) equipped with a 40x oil immersion objective. Cells were perfused continuously with modified Ringer's solution at a flow rate of 1-2 ml/min using a *valveBank8II* (AutoMate Scientific) system controlled manually. Chamber temperature was maintained at 37°C with a flow-through feedback tubing heater (Warner Instruments) positioned immediately before the perfusion chamber, and a feedback objective heater (Bioptechs) that warmed the objective to 37°C.

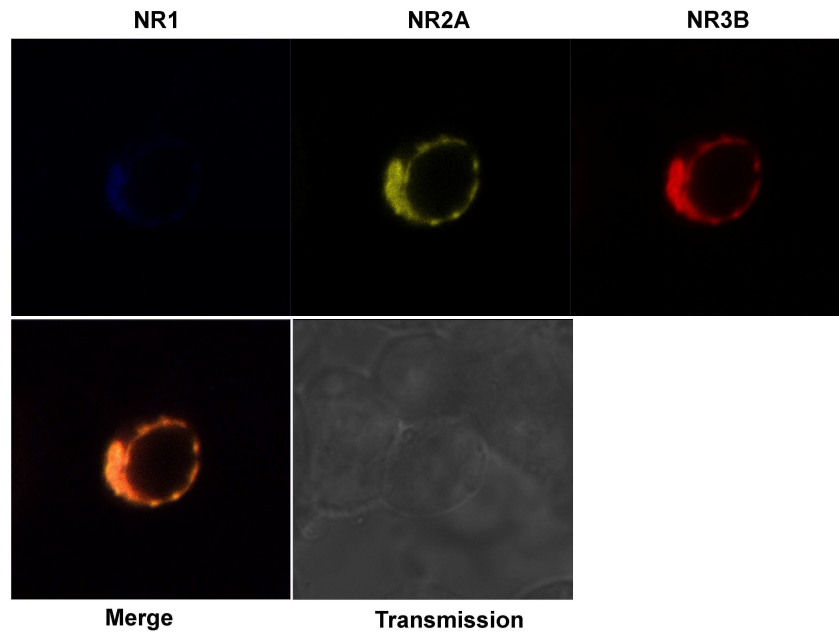


Figure II-5: NMDA receptor expression in triple transfected hek293 cells

Hek293 cells were transfected with NR1-CFP, NR2A-YFP and NR3B-mCherry. 24 hours post-transfection cells were imaged in a Zeiss LSM510 confocal microscope (63x/1.4 objective) showing co-expression of NMDA receptor subunits in triple transfected cells. Transfection with other subunits combinations yielded similar results.

Prior to Ca^{2+} imaging, images for CFP, YFP and mCherry fluorescence were acquired using the appropriate excitation wavelengths and filter sets for each fluorescent protein, listed in table II-8. These images were then used in to select the regions corresponding to transfected cells, and collection of data during experiments. An example of a triple transfected cell is shown on figure II-5.

Table II-8: Filter sets and monochromator illumination (excitation wavelength) used to detect Fura-2, ECFP, EYFP and mCherry

	Excitation wavelength (nm)	Dicrhoic filter (nm)	Emission filter (nm)	Manufacturer
Fura-2	340/10	400DCLP	D510/80m	Chroma
	380/10			
ECFP	430/30	455DCLP	D480/40m	Chroma
EYFP	475/25	505LP	HQ540/50	Nikon/Chroma
mCherry	560/40	Q610LP	HQ640/50m	Chroma

To monitor $[\text{Ca}^{2+}]_i$ changes, cells were illuminated at 340 and 380 nm by a monochromator (Optoscan; Cairn Research), and images were collected at 520 nm using an appropriate filter set (Chroma Technology). Image acquisition was made via a CoolSnap HQ Photometrics video camera (ROPER Scientific, Duluth, GA, USA) controlled by the software Metafluor (v5.01, Universal Imaging Corporation). Image acquisition rate (340/380 pair) was 1 image/sec during the stimulus (and the following minute) and every 10 sec in the wash-out periods. Regions were selected for analysis based on the fluorescence of YFP (NR1/NR2 transfection) or mCherry (NR1/NR2/NR3 transfections). Individual 340 and 380 values were collected for each region that corresponds to an individual cell.

II.8 Ca²⁺ calibration

Data obtained with fura-2 imaging (the 340:380 ratio) although directly correlated with [Ca²⁺]_i levels, does not translate to nominal Ca²⁺ values in a straightforward fashion. The dissociation constant (K_d) of Ca²⁺ indicators varies with the experimental conditions. Calculation of the K_d of fura-2 for Ca²⁺ in our conditions allow us to estimate absolute [Ca²⁺]_i levels. *In situ* Ca²⁺ calibration was performed using the *Fura-2 Calcium Imaging Calibration Kit* (Invitrogen) following the manufacturer's instructions. The method is based on the principle that when the concentrations of Ca²⁺ and EGTA are close to each other, the only free Ca²⁺ available is that which is in equilibrium with EGTA. Thus, the free Ca²⁺ concentration is a function of the dissociation constant (K_d) of CaEGTA. The K_d of an indicator or chelator, defined as the concentration at which it reaches the half-saturation point, varies with ionic strength, pH and temperature (Tsien & Pozzan, 1989).

II.8.1 Ca²⁺ calibration - method

The Fura-2 Ca²⁺ Imaging Calibration kit contains 11 prediluted K₂EGTA/CaEGTA solutions between 0 and 10 mM CaEGTA (0 to 40 μM free Ca²⁺) as well as 50 μM fura-2. A twelfth solution with 10 mM CaEGTA but lacking fura-2 is also provided to monitor background fluorescence. A drop of each solution was put on a coverslip and images were acquired illuminating each separate solution at 340 nm and 380 nm, measuring emission at 520 nm, at 37°C. Data was corrected for background fluorescence, by subtracting the control buffer (without fura-2) values to individual 340 and 380 values. The corrected values were used to calculate the 340/380 ratio and plotted against the corresponding concentration, as shown in figure II-6. [Ca²⁺]_i was then obtained using equation 1, generated from the calibration plot as suggested in the product protocol. Experimental settings used for Fura calibration were kept constant during all experiments presented in this thesis.

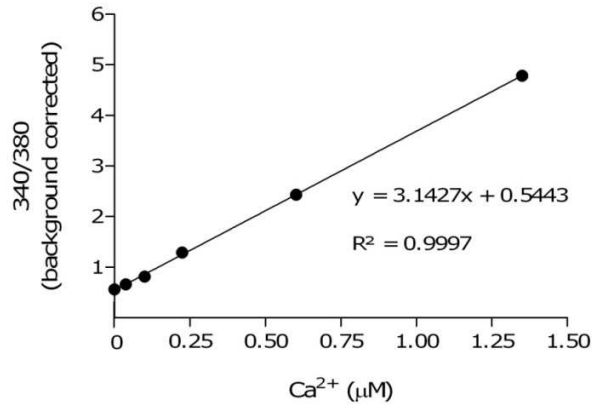


Figure II-6: Plot of Ca²⁺ standards versus 340/380 background corrected ratios

The line represents a linear regression. Trend line equation and the coefficient of correlation (R^2) are also depicted.

$$\text{Equation 1: } [\text{Ca}^{2+}] (\text{nM}) = \left[\left(\frac{340 - 340\text{Back}}{380 - 380\text{Back}} \right) - 0.5443 \right] / 3.1427 * 1000$$

Equation I: formula used to calculate [Ca²⁺]_t at any given time point

Back: background.

II.9 Bioinformatics tools

Most DNA and protein sequence analysis and modification were performed with the components of VectorNTI suite (Invitrogen). Other complementary analysis was performed with the following tools: geecee, GC content analysis; NNSPLICE, EuSplice and NetGene2 to determine splice site strength; Spidey for mRNA-genomic DNA alignment; Genedoc and ClustalW for multiple sequence alignment; PROSITE and NetPhos2.0 for the prediction of putative phosphorylation sites and search of conserved domains/motifs; and transmembrane domains were predicted using TMHMM.

II.9.1 DNA sequence assembly

Sequencing of clones was outsourced to Agowa/LGC and was performed in an ABI 3730xl (Applied Biosystems). Each sequencing run had read length up to 1000 nt, however in most sequencing runs, only up to 900 nt were resolved with enough quality to be used for sequence assembly. As cloned sequences were as much as 4.5 kb in length (table VI-2), more than one sequencing run was needed to cover the entire cloned sequence. Thus several individual primers were used to prime the sequencing reaction in order to obtain overlapping sequences of the entire gene coding sequencing and surrounding vector (figure II-2B). Obtained sequences were assembled using the program *Contig Assembly*, included in the suite *VectorNTI* (Invitrogen), and manually curated when necessary. The manual curation involved correction of ambiguous nucleotides in the sequencing file. This was made taking in account the quality values of chromatogram peaks.

II.10 Statistical analysis

Statistical analysis was performed using the software Prism 5 (Graphpad). Data are presented as mean \pm sem P values are from one-way analysis of variance (ANOVA) and Tukey's post-hoc test. Differences between condition were considered significant at $P < 0.05$. *P < 0.05, **P < 0.01, ***P < 0.001 compared to NR1/NR2, #P < 0.05, ##P < 0.01, ###P < 0.001 compared to NR1/NR2/NR3B.

Chapter III

NR1 expression in the Optic Nerve

III.1 INTRODUCTION

NR1 is the obligatory subunit of NMDA receptors. Its expression is required for neonatal survival and for the formation of functional NMDA receptors (Forrest *et al*, 1994; Li *et al*, 1994). Homozygous NR1 knockout mice (NR1^{-/-}) die 8-15 hours after birth due to respiratory failure (Forrest *et al*, 1994; Li *et al*, 1994). Furthermore, neurons from these animals show no NMDA-inducible increases in intracellular Ca²⁺ or membrane currents. Thus, NR1 expression is fundamental for NMDA receptors function and cannot be replaced by any other subunit.

NR1 was the first NMDA receptor subunit to be identified and cloned (Moriyoshi *et al*, 1991). The NR1 gene (*Grin1*) undergoes alternative splicing of 3 different exons, generating 8 functional variants (figure III-1). Two additional variants have been cloned but are not functional (Anantharam *et al*, 1992; Campusano *et al*, 2005; Durand *et al*, 1992; Hollmann *et al*, 1993; Nakanishi, 1992; Sugihara *et al*, 1992; Yamazaki *et al*, 1992). NR1 expression in *Xenopus* oocytes generates channels with functional properties resembling NMDA receptors. It was thought that NR1 could form homomeric channels (Ishii *et al*, 1993).

III.1.1 The homomeric NR1

The existence of homomeric NR1 receptors has been a matter of debate. Although currents could be recorded following NR1 expression in *Xenopus* oocytes, these currents are at least ten times smaller than those obtained with NR1/NR2 receptors (Ishii *et al*, 1993). Furthermore, NMDA receptors require both glutamate and glycine binding for efficient activation. However, NR1 contains only the binding site for glycine, whereas the glutamate binding site lays in the NR2 subunits (Hirai *et al*, 1996; Laube *et al*, 1997). With the reports that homomeric NR1 receptors fail to form functional channels in any other expression system other than *Xenopus*, the question was raised whether recorded currents in *Xenopus* are not the result of NR1 assembly with endogenously expressed glutamate receptor subunits (Abeliovich

et al, 1993; Lynch *et al*, 1994; Monyer *et al*, 1992; Schmidt *et al*, 2006; Sucher *et al*, 1996; Sydow *et al*, 1996). Recently, homologous NR2 subunits were found in *Xenopus* (*XenNR2A–XenNR2D*) and expression of rat NR1 with *XenNR2B* receptors have identical pharmacology to the proposed NR1 homomeric receptors (Schmidt & Hollmann, 2008). Thus, NMDA receptors are obligatory heteromultimers which require NR1 for the formation of a fully functional channel.

III.1.2 NR1 splice variants

Grin1 has 22 exons spanning over 24 kb of genomic DNA, 3 of which, exons 5, 21 and 22, undergo alternative splicing generating 8 functional variants (figure III-1) (Durand *et al*, 1992; Hollmann *et al*, 1993; Sugihara *et al*, 1992). Using the first NR1 variant to be cloned (NR1-1a) as a reference, the splice variants arise from the insertion of 63 bp (exon 5 or N1 cassette) near the 5' end, and/or 3 possible alternative deletions at the 3' end (Moriyoshi *et al*, 1991). These deletions are a 111 bp deletion (exon 21 or C1 cassette), a 356 bp deletion (exon 22 or C2 cassette) and a 467 bp deletion (concurrent deletion of exons 21 and 22). When exon 22 is spliced out, alone or in combination with exon 21, the original stop codon is removed and an alternative stop codon, previously located in the 3' UTR, is used. This leads to the translation of an extra 66 bp (C2' cassette).

The variants described above have in common the absence of exon 3. This exon encodes for 150 bp followed by a termination codon (Sugihara *et al*, 1992). When present, it expresses a truncated splice variant that appears to be non-functional. Human *Grin1* shares the same intron-exon organization with rat, except for the absence of exon 3. Thus, it is unlikely that this truncated variant is expressed in human (Zimmer *et al*, 1995). A splice variant due to intron 11 retention has also been described. This event results in the appearance of a premature termination codon (PTC) and the mRNA codes for a putative truncated protein of 465 amino acids (Campusano *et al*, 2005). This variant is only expressed in the embryonic brain and in defined brain regions: in the telencephalon, diencephalon, mesencephalon, and

rhombencephalon. Interestingly, inclusion of intron 11 is repressed by Brain-derived neurotrophic factor (BDNF), whereas GluR II activity has the opposite effect (Campusano *et al*, 2005).

The nomenclature used in this thesis for the NR1 splice variants follows that proposed by Hollmann and colleagues (Hollmann *et al*, 1993) and is the most commonly used in the literature (figure III-1). According to this nomenclature, the original NR1 clone (Moriyoshi *et al*, 1991) is termed NR1-1, and the three deletions are named NR1-2, NR1-3, and NR1-4, starting with the shortest deletion to the longest. The presence or absence of exon 5 (also referred to as N1 cassette) is indicated by adding a lowercase letter: “a” denotes splice variants without this insertion (e.g., NR1-1a), and “b” stands for those with the insertion (e.g., NR1-1b). In this way all cDNA clones can be classified into representing either type “a” or type “b” splice variants, independently of the structure of their 3’ends. For other nomenclatures commonly found in the literature, please refer to table III-1.

NR1 splice variants vary considerably in their properties and are differentially localized in the adult and developing animal (Laurie & Seeburg, 1994; Laurie *et al.*, 1995). I will introduce the differences in the expressions patterns of alternative spliced cassettes of NR1 and the physiological features of these variants when expressed with NR2 subunits.

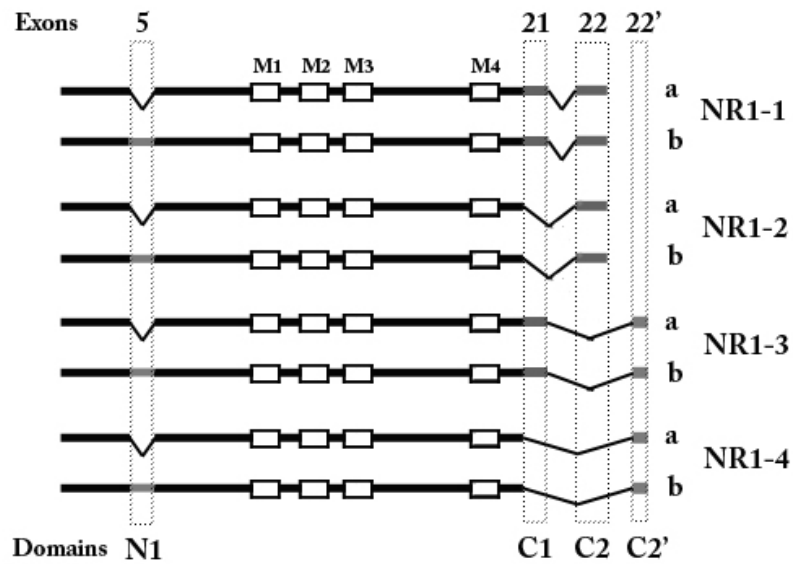


Figure III-1: Alternative splicing of NMDA receptor subunit NR1

A) The different splice variants arise from alternative splicing of the exons 5, 21 and 22, that code for the cassettes N1, C1, C2 and C2' in the protein. Variants not including exon 5 (N1 cassette or domain) are termed “a” and those containing this exon are variants “b”. The variants in the C-terminal are termed NR-1 to NR1-4 based on decreasing mRNA (and amino acid) length. Alternative splicing occurs outside the membrane domains (M1-4), as depicted. See also table III-1 for the common nomenclature used for NR1 splice variants.

Table III-1: Commonly used nomenclature for NR1 alternative splicing variants

The eight splice variants of the NR1 have been named differently by three laboratories: (Hollmann *et al.*, 1993); (Sugihara *et al.*, 1992) and (Durand *et al.*, 1993). Hollman and collaborators choose to term variants not including exon 5 (N1 cassette or domain) as “a” and those containing this exon are variants “b”. The variants in the C-terminal are termed NR-1 to NR1-4 based on decreasing mRNA (and amino acid) length. The first nomenclature attributed a letter to each variant following structural comparison with the first cloned variant, NR1-1a (Sugihara *et al.*, 1992). A third nomenclature (Durand *et al.*, 1993) uses a binary code for the absence, “0”, or presence, “1”, of each alternatively spliced exon.

Exon			Nomenclature		
5	21	22	Hollman <i>et al.</i> , 1993	Sugihara <i>et al.</i> , 1992	Durand <i>et al.</i> , 1993
-	+	+	NR1-1a	NR1A	NR1 ₀₁₁
+	+	+	NR1-1b	NR1B	NR1 ₁₁₁
-	-	+	NR1-2a	NR1C	NR1 ₀₀₁
+	-	+	NR1-2b	NR1F	NR1 ₁₀₁
-	+	-	NR1-3a	NR1D	NR1 ₀₁₀
+	+	-	NR1-3b	NR1H	NR1 ₁₁₀
-	-	-	NR1-4a	NR1E	NR1 ₀₀₀
+	-	-	NR1-4b	NR1G	NR1 ₁₀₀

III.1.3 Regional and developmental expression of NR1 splice variants

NR1 is ubiquitously expressed in the CNS in both grey and white matter. *In situ* hybridization showed that rat NR1 mRNA is expressed throughout the brain with higher levels of expression in hippocampus, hypothalamus and olfactory bulb (Moriyoshi *et al.*, 1991). NR1 expression as been detected as early as embryonic day 14 and is the most prominent subunit during development (Monyer *et al.*, 1994). Staining for NR1 was also found in cervical spinal cord, dorsal root and vestibular ganglia, and in pineal and pituitary glands

(Petralia *et al*, 1994). However, NR1 variants have different expression patterns both regionally and during development.

Expression of the alternative splice forms of the NR1 subunit mRNA has been investigated in the adult rat brain. N-terminal variants without exon 5 and C-terminal variants expressing only exon 22 are present at high levels, and are distributed throughout the brain, except for the inferior colliculus. Variants with exon 5 spliced in and variants without exons 21 and 22 have narrower distribution and are expressed in the parietal cortex, hippocampus CA3, thalamus, inferior colliculus and cerebellar granule cells. In contrast, variants containing both exons 21 and 22 have a complementary distribution being weakly expressed in thalamus and inferior colliculus. Variants containing exon 21 but not exon 22 were not abundant in any structure (Laurie *et al*, 1995; Zhong *et al*, 1995).

The expression of NR1 splice variants is developmentally regulated. In the cerebellum the proportion of NR1 mRNA with exon 5 increases during development and represent approximately 60% of total NR1 mRNA in the cerebellum of adult rats. In the cerebral cortex and hippocampus of neonatal rat, the majority of NR1 variants (85-90% of total NR1 mRNA) has exon 5 spliced out and this proportion does not change in adulthood (Zhong *et al*, 1995). Protein expression of NR1 variants has also been studied in the cerebellum and follows the same pattern as mRNA expression. At P7, exon 5 (N1 cassette) is present in a minority (16%) of NR1 protein and by P42 the majority (78%) of NR1 protein contains this cassette (exon 5). At both developmental stages, less than 10% of the total NR1 protein in the cortex contains the N1 cassette (exon 5) (Prybylowski *et al*, 2000).

There is a developmental increase in C1 cassette (exon 21) inclusion in the total population of NR1 protein in the cerebellum, while this level stays constant in the cortex. The relative inclusion of the C2 cassette (exon 22) decreases during development in both the cortex and cerebellum, while the C2' cassette expression increases. In the cerebellum of young rats (up to P16), the majority of NR1 protein contains the C2 cassette (exon 22). At about P22, a shift in C2 and C2' cassette expression occurs and the percent of total NR1 with the C2'

cassette increases (Prybylowski & Wolfe, 2000). After P28, equal amounts of total NR1 protein contain C2 and C2' cassettes (Prybylowski & Wolfe, 2000).

III.1.4 NR1 splice variants modify channel physiology

Native NMDA receptor channels are inhibited by protons, with an IC₅₀ value close to physiological pH and NR1 splice variants modulate this NMDA receptor property (Tang *et al*, 1990; Traynelis & Cull-Candy, 1990; Vyklicky *et al*, 1990). Protons inhibit heteromeric receptors composed of the NR1 subunit lacking the N1 cassette (exon 5) at physiological pH (IC₅₀=7.2–7.4). Channels comprised of the NR1 subunit with the N1 insert (exon 5) are inhibited by protons with IC₅₀ values of pH 6.6–6.8 (Traynelis *et al*, 1995). Furthermore, this modulatory effect also depends on the NR2 subunits present in the receptor. NMDA receptors composed of NR1/NR2C subunits have low sensitivity to proton inhibition (IC₅₀ 6.2) irrespective of the presence of the N1 insert (Traynelis *et al*, 1995). Thus, exon 5 relieves proton inhibition of NR1/NR2A, NR1/NR2B, NR1/NR2D receptors, but not NR1/NR2C.

Zn²⁺ inhibition of NMDA receptor activity involves both voltage-independent and voltage-dependent components (Williams, 1996). Both NR1/NR2A and NR1/NR2B receptors have comparable voltage-dependent block, but voltage-independent Zn²⁺ inhibition occurs with higher affinity for NR1/NR2A. Inclusion of exon 5 in NR1 increases the IC₅₀ for voltage-independent Zn²⁺ inhibition 3- to 10-fold when expressed as NR1/NR2A or NR1/NR2B receptors. Exon 5 has little effect on Zn²⁺ inhibition of receptors that contain NR2C and NR2D (Chen *et al*, 1997; Paoletti *et al*, 1997; Traynelis *et al*, 1998; Williams, 1996). Interestingly, the same basic amino acid residues within exon 5 that control proton inhibition also appear to control the effects of exon 5 on Zn²⁺ inhibition; this observation has led to the suggestion that Zn²⁺ and proton inhibition may share common structural determinants (Traynelis *et al*, 1998).

Splicing of exon 5 can also influence the deactivation properties of NMDA receptors (Rumbaugh *et al.*, 2000). Unlike NR2A-containing receptors (Vicini *et al.*, 1998), the deactivation time of recombinant NR2B-containing receptors is dependent on whether or not NR1 contains N1. The deactivation rate is roughly four times faster for NR1-1b/NR2B (N1-containing) receptors than for the NR1-1a/NR2B (N1-lacking) receptors. This could be relevant in the context of NMDA receptors EPSC decay that occurs during development, in particular in the thalamus and cerebellum, where exon-5-containing NR1 (NR1-1b) isoforms increase during development (Laurie & Seeburg, 1994). Glycine independent potentiation by polyamines is also controlled in part by exon 5. At saturating concentrations of glycine, polyamines potentiate glycine-independent stimulation of NMDA receptors only when the receptors expressed are formed by NR1 splice variants that lack the N1 insert (NR1a variants) and NR2B (Williams *et al.*, 1994).

III.1.5 NR1 splice variant subcellular localization and trafficking

C-terminal NR1 variants are involved in the regulation of intracellular trafficking, localization and anchoring of signalling pathways to the receptor complex (Ehlers *et al.*, 1998; Feliciello *et al.*, 1999; Standley *et al.*, 2000). NR1 variants with the C1 cassette are retained in the endoplasmic reticulum (ER), allowing assembly with other subunits. This is due to the presence of an ER retention signal in C1. When C2' is also present, the retention signal in C1 is overridden facilitating NR1 surface expression (Ehlers *et al.*, 1995; Scott *et al.*, 2001; Standley *et al.*, 2000). The C2' cassette contains the sequence (tSXV motif) for binding to postsynaptic density (PSD) 95, an NMDA anchoring protein (Kornau *et al.*, 1995), suggesting that interaction with PSD95 may play a role in regulating the surface expression of the receptors (Okabe *et al.*, 1999; Standley *et al.*, 2000). The low cell surface targeting of the C1 variants is also supported by studies showing a strong association between the C1 variants and cytoskeletal neurofilaments (Ehlers *et al.*, 1998).

NR1 splice variants differ in their abilities to form clusters and in their interactions with the family of PSD-95 proteins. NR1-4a (C2' present) coimmunoprecipitates with PSD-95, PSD-93, SAP102, and SAP97, suggesting functional interaction with these proteins. In contrast, NR1-1a (without C2') does not interact directly with any of these members of the PSD-95 protein family (Standley *et al*, 2000). The cytoskeleton proteins yotiao and neurofilament L (Ehlers *et al*, 1998; Lin *et al*, 1998), interact specifically with splice variants of NR1 containing the C1 exon. The functions of yotiao and neurofilament-L in the context of NMDA receptors are unclear. One possibility is that yotiao serves as a connexion between NMDA receptors, protein kinase A (PKA) and protein phosphatase 1 (PP1), facilitating bidirectional NMDA receptor modulation by these enzymes (Westphal *et al*, 1999). Together, this data suggest that NMDA receptor complexes may be selectively targeted to, and stabilized at, postsynaptic locations based on particular splice variants of NR1 present in the complex.

III.1.6 Neuronal activity and NR1 splicing

The link between splicing and synaptic plasticity is particularly interesting for NR1. Not only is NR1 splicing regulated by neuronal activity, but NR1 variants modulate gene expression. In an elegant study by Bradley and colleagues (Bradley *et al*, 2006), NMDA receptor function in NR1^{-/-} neurons was reconstituted with different NR1 constructs. They observed that NMDA-induced gene expression in NR1^{-/-} neurons transfected with NR1-1a is about twice higher than with NR1-2a. The authors also excluded other factors that could explain this difference such as differential association with NR2 subunits, providing evidence that NMDA receptor variants expressing the C1 cassette are important to couple NMDA receptor activity with gene expression.

Inclusion or exclusion of exon 5 is a reversible process sensitive to alterations in Ca²⁺ and pH (Vallano *et al*, 1999). During maturation of granule neurons in the cerebellar cortex, there is an increase in the inclusion of N1 (Nakanishi *et al*, 1992) and this pattern of expression is also observed *in vitro* (Vallano *et al*, 1996). However, when developing granule neurons are

grown in conditions that promote Ca^{2+} influx, inclusion of exon 5 is repressed and the NR1a/NR1b ratio remains unaltered during maturation. When cells are returned to their normal growth conditions, the normal splicing pattern is restored. Exon 5 inclusion is also repressed in low pH conditions (Vallano *et al*, 1999).

Inclusion/exclusion of the C-terminal cassettes is also regulated by neuronal activity. In rat primary cortical cultures, KCl-induced depolarization reduces inclusion of exon 21 (An & Grabowski, 2007). Furthermore, the increased exclusion of exon 21 due to depolarization is dependent on NMDA receptor activity and mediated by Ca^{2+} /calmodulin-dependent protein kinase IV (CaMK IV) (An & Grabowski, 2007; Lee *et al*, 2007). In hippocampal neuronal cultures, decreasing neuronal activity increases the levels of C2' containing receptors (Mu *et al*, 2003). The opposite occurs when neuronal activity is increased: exon 22 inclusion increases and C2' decreases. Furthermore, neuronal activity affects directly the splicing of NR1 mRNA without changing total levels of transcript. Importantly, the increased levels of C2' containing isoforms, were shown to accelerate receptor trafficking to the plasma membrane showing a physiological outcome following changes in splicing patterns (Mu *et al*, 2003).

III.2 RESULTS

It has been previously shown that NMDA receptors mRNA and protein are expressed in white matter oligodendrocytes (Karadottir *et al*, 2005; Micu *et al*, 2006; Salter & Fern, 2005). However these studies did not probe the expression of NR1 variants. Given that important features of NMDA receptor physiology are modulated by splicing, I sought to determine which NR1 variants are expressed in the neonatal rat optic nerve.

Expression of NMDA receptors in P10 optic nerves was detected using real time RT-PCR. Specific primers for each subunit were designed to amplify short-length fragments located at the 3' end of the cDNA (table II-1). The primers for NR1 were designed to anneal in regions outside alternative spliced regions and thus amplify all NR1 variants present in the sample. Brain cDNA from P10 rats was used as a positive control for NMDA receptor expression (figure III-2). As predicted a single band at ~139 bp is observed in gel (figure III-2) confirming that NR1 mRNA is expressed in the optic nerve of rodents (Salter & Fern, 2005).

The NR1 subunit has 8 splice variants that strongly influence NMDA receptor function (Durand *et al*, 1993; Zukin & Bennett, 1995). NR1 is expressed in the neonatal optic nerve, but which variants are present? Full-length NR1 mRNA was amplified from optic nerves using primers designed to bind the 5' UTR and 3' UTR (table II-4) and cloned. Amplification and cloning of NR1 cDNA was relatively easy to achieve due to its high expression and small size, as compared to the other NMDA receptor subunits. Two bands of approximately 4 and 3.5 kb were extracted individually from the gel (figure III-3) and cloned into the vector pGEM-T. Several positive clones were sequenced revealing that four of the NR1 splice variants were cloned: NR1-1A (U08267), NR1-2A (U08262), NR1-3A (U08265) and NR1-4A (U08267) (figure III-1). All these variants have in common the exclusion of exon 5 and all the possible C-terminal variations were identified.

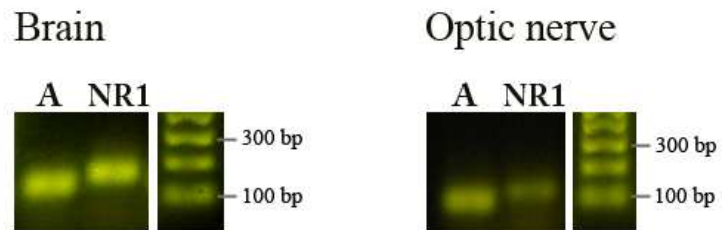


Figure III-2: NR1 expression in the neonatal rat optic nerve and brain

cDNA originating from neonate rat brain and optic nerve mRNA, was PCR amplified using primers that recognized actin (A) used as a PCR control, or all NR1 variants. PCR products were separated in a 1.1% agarose gel, visualized with Sybr Safe dye, and the bands sizes were estimated by comparison with a ladder (1 kb ladder, Invitrogen). Short amplification products were detected at ~100 bp (actin) and ~140 bp (NR1).

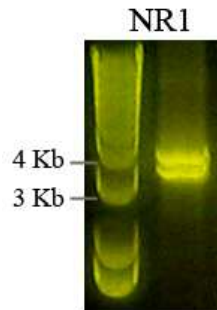


Figure III-3: Amplification of full-length NR1 cDNA from the optic nerve

cDNA originating from neonate rat optic nerve mRNA, was PCR amplified using primers annealing at the 5' and 3' UTR. PCR products were separated in a 1.1% agarose gel, visualized with Sybr Safe dye, and the bands sizes were estimated by comparison with a ladder (1 kb ladder, Invitrogen). Amplification products were detected at ~4 kb and ~3.5 kb.

To confirm the virtual absence of exon 5 in NR1 variants expressed in neonate optic nerve, I amplified NR1 cDNA sequences that span across alternative splicing regions (table II-2). Amplification of the region spanning from exon 4 to exon 8, in brain mRNA, results in two fragments 377 and 440 bp, corresponding to the “a” and “b” NR1 variants, respectively. Both these bands are present when cDNA is amplified from the rat brain (figure III-4). In contrast, amplification from neonatal optic nerve cDNA originated only one product (377 bp) corresponding to variants without exon 5, as expected. This confirms that NR1 alternative splicing is regulated differently in the neonatal rat brain and the optic nerve, and only NR1 variants without exon 5 are expressed the optic nerve.

I also sought to confirm the expression of four possible variants at the 3' end of NR1 transcript due to the presence/absence of exons 21 (C1) and 22 (C2). To identify the C-terminal NR1 variants the cDNA spanning the region between exon 17 and the 3' UTR was amplified (table II-1). The amplification products would have the predicted size of (bp): 1050 (NR1-1a and 1b); 939 (NR1-2a and 2b); 694 (NR3-1a and 3b) or 583 (NR1-4a and 4b) depending of the presence/absence of exons 21/22/22'. However, only two bands of ~1.1 kb and ~580 bp were observed in the optic nerve and brain; possibly correspond to the amplification of NR1-1 and NR1-4. Unfortunately, either due to a poor choice of primers or differences in the relative expression levels of the variants, it was not possible to confirm that all C-terminal variants are expressed (figure III-4). Nonetheless, the independent cloning of the all NR1 variants (without N1), warrants that our cloning results hold true and that the only alternative spliced exon not expressed in the neonate optic nerve is exon 5.

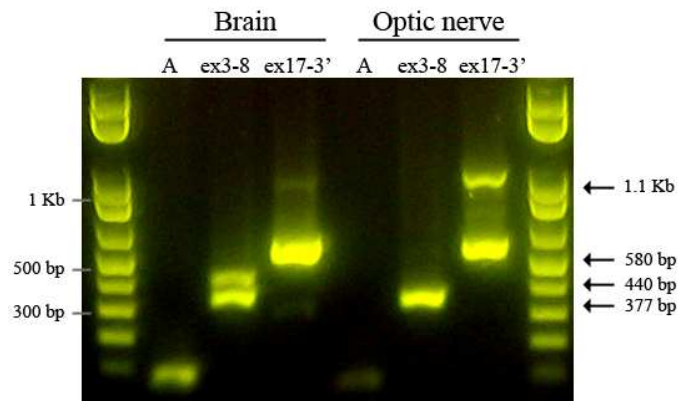


Figure III-4: NR1 variants containing exon 5 are absent from the neonatal optic nerve

cDNA originating from neonate rat brain and optic nerve mRNA, was PCR amplified to detect the expression alternative spliced transcripts of NR1. Exon 5 inclusion/exclusion was probed with a pair of primer flanking this exon (ex4-8). A pair of primers (ex17-3') was used to amplify the region from exon 17 to the 3' UTR in which the C-terminal splicing of NR1 occurs. PCR products were separated in a 1.1% agarose gel, visualized with Sybr Safe dye, and the bands sizes were estimated by comparison with a ladder (1 kb ladder, Invitrogen). A fragment of actin (A) was also amplified for PCR internal control.

III.3 DISCUSSION

Expression of NR1 variants has previously been investigated in glial cells. Rat Müller cells, a type of astrocytes present in the inner vertebrate retina, express predominantly NR1 variants without exon 5 (Lamas *et al*, 2005). These cells also lack variants with C2' which appears to be expressed in retinal neurons. Here I show that neonatal optic nerve glia express all 4 C-terminal NR1 variants, but lack inclusion of exon 5 (N1). It is interesting to notice a trend for the exclusion of exon 5 in NR1 transcripts from glial cells. Lamas and collaborators (2005) also speculate that NR1a/NR2C might be the main NR1 receptor complex in Müller cells consistent with data that suggests that NR2C might also be a major component of NMDA receptors in oligodendrocytes (Karadottir *et al*, 2005; Micu *et al*, 2006; Salter & Fern, 2005).

The significance of NR1 variants in glutamate induced toxicity has been evaluated in transfected CHO cells (Rameau *et al*, 2000). NMDA receptor expression in mammalian cell lines has been extensively used to study NMDA receptor toxicity (reviewed in (Lynch & Guttman, 2002)). Expression of NR1 variants with NR2A elicited cell death but the extent of cell demise differed for each variant: NR1-1a (exon 5 absent and exons 21/22 present) caused more toxicity than NR1-4a/NR2A (exon 5 absent and 22' present). Furthermore, direct comparison between NR1-3a/NR2A and NR1-3b/NR2A showed that inclusion of N1 (exon 5) decreased glutamate induced toxicity. Inclusion of exon 22 was also correlated with increased NMDA toxicity (Rameau *et al*, 2000). It is however unknown whether exon 5 and exon 22 exert their effects on glutamate toxicity by the same mechanism.

Following rat optic nerve crush, a change in NR1 splicing pattern occurs in the retinal ganglion cell layer. Expression of NR1 variants without exon 5 increases 48h after injury, preceding cell death. Exon 21 inclusion followed the same pattern (Kreutz *et al*, 1998). Because these changes in expression occur before cell death, the authors proposed that the increase in exon 5 inclusion reflects splicing response to injury, rather than selective cell death of retinal ganglion cells expression NR1-a variants (Kreutz *et al*, 1998). Furthermore,

reduction of NR1-b by treatment with antisense oligonucleotides increased retinal ganglion cell death after nerve crush. NR1a is also more expressed than NR1-b in the spinal cord. Also, following contusive injury of adult rat spinal cord, NR1 expression increases shortly after injury. In these conditions, no change in expression of the C-terminal cassettes was observed (Prybylowski *et al*, 2001). Taken together, these two studies show that NR1-b variants seem to be crucial for cell survival. Considering that the NR1-b is virtually absent in the neonate white matter, no such mechanism of protection against injury would be present rendering oligodendrocytes more prone to damage.

Exon 5 is responsible for the control of proton and Zn^{2+} inhibition of NMDA receptors. It also controls polyamine potentiation. However, this control is dependent of the NR2 subunit present in the complex. Heteromeric complexes containing NR1-b (containing exon 5) and NR2A/NR2B/NR2D are less sensitive to proton inhibition than heteromers containing NR1-a variants (without exon 5). Interestingly, the presence or absence of exon 5 does not have any effect in NR1/NR2C sensitivity to Zn^{2+} or protons (Traynelis *et al*, 1998; Traynelis *et al*, 1995). This is of particular interest since the NR2C is thought to be the most expressed subunit in oligodendrocytes amongst NR2 subunits (Karadottir *et al*, 2005; Salter & Fern, 2005). It has also been shown that during ischaemia, proton concentration increase in the extracellular spaces, and it has been speculated that this increase in protons inhibit NMDA receptors, thereby minimizing excitotoxic damage (Balestrino & Somjen, 1988; Obrenovitch *et al*, 1990). Since NMDA receptors containing NR2C are less sensitive to proton inhibition (Traynelis *et al*, 1995), drops in pH would not have any protective effect, rendering oligodendrocytes more vulnerable.

Chapter IV

Cloning and molecular characterization of novel NR2 splice variants

IV.1 INTRODUCTION

For the formation of fully functional NMDA receptors channels, the presence of NR2 subunits with NR1 is required. Furthermore, NMDA receptors display different properties depending on which of the four NR2(A-D) subunits are assembled with NR1 (Kutsuwada *et al*, 1992; Moriyoshi *et al*, 1991; Nakanishi, 1992). The receptor properties modulated by NR2 subunits include: (1) single-channel conductance; (2) strength of Mg²⁺ block; (3) sensitivity of modulation by glycine, reducing agents, polyamines and phosphorylation; (4) desensitization; and (5) affinities for specific agonists and antagonists (Buller *et al*, 1994; Ishii *et al*, 1993; Kohr *et al*, 1994; Kutsuwada *et al*, 1992; Lynch *et al*, 1994; Monyer *et al*, 1994; Monyer *et al*, 1992; Moriyoshi *et al*, 1991; Stern *et al*, 1992; Sullivan *et al*, 1994; Wafford *et al*, 1993; Williams *et al*, 1994; Yamazaki *et al*, 1992). Another layer of NMDA receptor physiological diversity comes from splice variants that attribute different functional and pharmacological properties to the receptor complex. Although NR2 splice variants have received less attention than NR1 variants, alternative splicing has been reported for these NMDA receptor subunits. In this chapter I report previously unidentified NR2 splice variants and describe their molecular features.

The four NR2 subunit subtypes (NR2A-D) are generated from four different genes. NR2A-D expression is both developmentally and regionally regulated and correlates with native NMDA receptors physiological properties (Monyer *et al*, 1994). The final polypeptide chain of NR2A–NR2D subunits is composed of 1464, 1482, 1250 and 1323 amino acids, respectively. The amino acid sequence of NR2 subunits is relatively conserved among them, with 55 to 70% sequence homology. Sequence conservation is less between NR1 and NR2 subunits, which share ~18% identity (Hollmann & Heinemann, 1994; Monyer *et al*, 1992; Mori & Mishina, 1995; Nakanishi, 1992). In spite of a substantial divergence in the amino acid sequences of NR2 subunits from NR1, they possess similar structural characteristics (figure I-2).

IV.1.1 NR2 expression and sub-cellular localization

NR2 expression is not homogenous throughout the CNS and the four NR2 transcripts display distinct regional patterns. NR2A mRNA is distributed widely in the brain, but more so in the cerebral cortex, hippocampus and cerebellum. NR2B mRNA is selectively present in the forebrain with high level expression in the cerebral cortex, hippocampus, septum, caudate-putamen and olfactory bulb. NR2C and NR2D mRNA display more restricted regional expression. The NR2C mRNA is expressed predominantly in the granule cell layer of the cerebellum whereas NR2D mRNA is detected mostly in the thalamus and brain stem (Monyer *et al*, 1994).

Expression patterns of NR2 subunits in the brain are regulated developmentally (Monyer *et al*, 1994; Watanabe *et al*, 1994). NR2B and NR2D are expressed prenatally, whereas NR2A and NR2C mRNAs are first detected around birth. As expression of NR2B and NR2D decline, mRNA levels of NR2A and NR2C increase concomitantly. The most prominent developmental change is the switch from NR2B to NR2C expression which occurs in cerebellar granule cells. NR2B mRNAs, which are abundantly expressed in the cerebellar granule cells on embryonic day 7 through the first post natal week, almost disappear by P14 being replaced by NR2C mRNAs (Akazawa *et al*, 1994; Watanabe *et al*, 1994). Protein and mRNA broadly follow the same pattern of expression (Wenzel *et al*, 1997; Wenzel *et al*, 1996).

IV.1.2 Triheteromeric NMDA receptors

Although NR2A and NR2B expression is regulated in opposite directions during development, there is an expression overlap in most brain regions (Monyer *et al*, 1994). These subunits can also coexist in the same functional receptor. Indeed the majority of NMDA receptors present in mature neurons of the forebrain seems to be composed of NR1, NR2A and NR2B subunits (Luo *et al*, 1997). These triheteromeric receptors have hybrid properties of the subunits that compose them. NMDA receptors formed by co-assembly of NR1, NR2A

and NR2B retain sensitivity to submicromolar concentrations of Zn^{2+} , a typical feature of NR2A-containing receptors, and ifenprodil (NR2B-selective antagonist). Nevertheless, ifenprodil inhibition is not as effective in NR1/NR2A/NR2B as in NR1/NR2B (Hatton & Paoletti, 2005). Indirect pharmacological observations suggest the presence of triheteromeric NR1/NR2B/NR2D receptors in P7 *substantia nigra* (SNc) dopaminergic neurons (Brothwell *et al*, 2008; Jones & Gibb, 2005).

IV.1.3 Synaptic vs extrasynaptic location of NMDA receptors

NMDA receptors complexes can be located synaptically or extrasynaptically and receptor subtype subcellular localization changes during development. NR2D subunits form synaptic and extrasynaptic NMDA receptors in SNc dopaminergic neurons and are present in extrasynaptic complexes of cerebellar Golgi cells (Brickley *et al*, 2003; Brothwell *et al*, 2008; Jones & Gibb, 2005; Misra *et al*, 2000). During development, there is a decrease of NR1/NR2B receptors complexes and a proportional increase of triheteromeric NR1/NR2B/NR2D receptors. It is thus possible that NR1/NR2B/NR2D triheteromers form a significant fraction of synaptic NMDA receptors during postnatal development in this brain region (Brothwell *et al*, 2008). In hippocampal neurons, extrasynaptic NMDA receptors are composed predominantly of NR1 and NR2B, whereas synaptic NMDA receptors contain NR2A subunits. NR2A receptors in synapses might be part of diheteromeric receptors with NR1 or form triheteromers with NR1 and NR2B (Tovar & Westbrook, 1999).

The targeting of NMDA receptors to the different synaptic locations appears to be regulated by a number of interacting proteins. The membrane-associated guanylate kinase (MAGUK) family are involved in the targeting of NMDA receptors to the membrane. Synapse-associated proteins 102 (SAP102), a member of the MAGUK family, interacts with NR2B and plays an important role in trafficking and targeting of this subunit to the synapse (Lau *et al*, 1996; Sans *et al*, 2003). Developmentally, expression levels of SAP102 decline whereas levels of other scaffolding proteins, such as postsynaptic density-95 (PSD-95) and

PSD-93, increase concurrently with NR2A expression (Sans *et al*, 2000). With maturity, many NR1/NR2B receptors become extrasynaptic whereas NR1/NR2A/NR2B receptors are incorporated as the major synaptic receptors in the forebrain (Stocca & Vicini, 1998; Tovar & Westbrook, 1999). This suggests that synaptic localization of NMDA receptor subunits depend on the association with members of the MAGUK-related protein family, which anchor NMDA receptors at the synapse through interactions mediated by the C-terminal of NMDA receptors (Kim *et al*, 1996; Müller *et al*, 1996; Niethammer *et al*, 1996).

Following excitotoxic stimulus, extrasynaptic NMDA receptors trigger cell death linked to mitochondrial dysfunction, whereas $[Ca^{2+}]_i$ rises mediated by synaptic NMDA receptors do not result in cell death (Hardingham *et al*, 2002). Furthermore, $[Ca^{2+}]_i$ rises through synaptic NMDA receptors appear to activate an anti-apoptotic pathway that involves increased BDNF gene expression through CEB-signalling (Hardingham *et al*, 2002). In direct opposition, Ca^{2+} entry through extrasynaptic NMDA receptors antagonized nuclear signalling to cAMP response element binding (CREB), blocked BDNF expression, and caused loss of mitochondrial membrane potential leading to cell death (Hardingham *et al*, 2002). Importantly, these effects are not a result of the amount of $[Ca^{2+}]_i$ rises, but of the location of Ca^{2+} entry (Hardingham *et al*, 2002). Thus, it seems that regulation of NMDA receptor location in synapses or extrasynaptic sites has physiological and pathophysiological importance.

IV.1.4 Studies with gene knockout animals

To examine the functional roles of NMDA receptor subunits, NR2A–NR2D genes have been disrupted by gene targeting. Ablation of NMDA receptor subunits causes a variety of morphological and functional defects. Targeted disruption of NR2B results in the early death of the mutant mice (NR2B^{-/-}), demonstrating that NR2B is essential for the survival of newborn mice. Although knockout animal have no gross anatomical abnormalities in the brain, suckling responses are impaired and appear to be the cause of death (Kutsuwada *et al*,

1996). Tactile hairs (whiskers) on the snout of rodents are arranged in an array and collectively form a unique sense organ. This sense organ is connected to the brain via the trigeminal nerve, and in the brainstem trigeminal nuclei whisker-specific neural patterns, termed barrelettes, are formed. The barrelettes are absent in the NR2B^{-/-} mice, indicating that NR2B are involved in the development of neural networks in the CNS (Kutsuwada *et al*, 1996).

NR2D knockout mice (NR2D^{-/-}) grow normally and no obvious histological abnormalities were found in the various brain regions or in the formation of barrelettes. NR2D ablation results in alteration of monoaminergic neuronal systems in the adult hippocampus, due to increased DA and 5-HT metabolism. These changes are not a consequence of altered expression of the other NMDA receptor subunit in the hippocampus, nor to obvious histological abnormalities in any brain region (Ikeda *et al*, 1995; Miyamoto *et al*, 2002). In the elevated plus-maze test and in the light-dark box test, NR2D^{-/-} mice revealed a more exploratory behaviour than wild-type mice (Miyamoto *et al*, 2002) suggesting that NR2D^{-/-} mice may have a reduced susceptibility to stress and/or reduced psychological anxiety.

NR2A and NR2C-ablated mice developed normally and display normal fertility (Ebraldize *et al*, 1996; Sakimura *et al*, 1995). Disruption of the NR2A gene results in a significant reduction of the NMDA receptor channel current and LTP at the hippocampal CA1 synapse. The time required for NR2A^{-/-} to learn how to perform in a hidden-platform task and in the transfer test, are longer than those of wild-types suggesting that NR2A is important for spatial learning (Sakimura *et al*, 1995). The disruption of the NR2C gene results in the disappearance of low-conductance NMDA receptor channels (<37 pS) normally expressed in matured cerebellar granule cells (Ebraldize *et al*, 1996). To generate mice lacking both NR2A and NR2C, NR2A and NR2C mutant mice were mated with each other (Kadotani *et al*, 1996). The NMDA receptor-mediated components in cerebellar granule cells are virtually abolished in mice lacking both NR2A and NR2C. NR2A or NR2C ablation in mice does not affect motor coordination and animals retain the ability to manage simple coordinated tasks such as walking on the ground or staying on the stationary or slowly

running rota-rod. However, NR2A^{-/-}/NR2C^{-/-} mice reveal difficulties in more challenging tasks such as walking on the narrow bar or staying on the quickly running rota-rod (Kadotani *et al*, 1996).

IV.1.5 NR2 subunits splice variants

IV.1.5.1 NR2B

NR2 subunit genes undergo alternative splicing. Five transcripts of the mouse NR2B gene resulting from variation in four noncoding exons of the 5'UTR of the gene (exons 1', 1, 2, 3) have been reported (Tabish & Ticku, 2004). These variants have not been named in the original papers, so I will refer to them using their NCBI accession numbers. Exon 2 is present only in AF033356, that includes all exons (Klein *et al*, 1998; Tabish & Ticku, 2004) and the variant U60210 has exon 2 spliced out (Klein *et al*, 1998; Sasner & Buonanno, 1996). All the remaining three splice variants lack exon 2 completely and exon 1 to different extents: AJ459261 has ~3/4 of exon 1; AJ459262 has ~1/3rd of exon-1; and AJ459263 lacks the entire exon-1 (Tabish & Ticku, 2004).

NR2B variants mRNA is expressed in the mouse brain and show regional distribution. Variants containing exon 2 are expressed at higher levels and variants without exon 2 are preferentially expressed in the striatum and hippocampus (Klein *et al*, 1998). The biological role of these variants may reside in the ability to regulate NR2B gene expression in the cerebellum and cortex during development, and/or translational regulation of NR2B transcripts (Klein *et al*, 1998; Sasner & Buonanno, 1996; Tabish & Ticku, 2004). NR2B exon 2 contains many regulatory sequences including binding sites for the transcriptional factor SP1 and the cyclic AMP-responsive element (CRE) site (Klein *et al*, 1998). Although gene transcription can proceed without exon 2, these genetic elements are involved in regulation of ethanol-induced changes of NR2B expression (Mei & Maharaj, 2005; Rani *et al*, 2005; Sasner & Buonanno, 1996). This indicates a role for exon 2 splicing in ethanol-

responsive regulation of NR2B gene expression. Consistent with this proposition, alcohol consumption and withdrawal modify NR2B expression within striatal and amygdala region of rats (Ilona *et al*, 2009).

IV.1.5.2 NR2C

Various NR2C splice variants have been described for rat, mouse and human. Two NR2C splice variants have been described in the mouse genome, NR2C-L (NM_010350.2) and NR2C-S (BC137849.1) differing in 96 nt due to the use of an alternative acceptor site in the 5' UTR (exon 4). Since no formal name was attributed to the variants in the original paper, I decided to adopt the denominations “NR2C-L” and “NR2C-S” for clarity purposes. Expression of both variants was detected by *in situ* hybridization in the granule cell layer of the adult mouse cerebellum (Suchanek *et al*, 1995).

In rat, 3 splice variants have been identified resulting from intron 11 retention (NR2Cb), intron 10 and 11 retention (NR2Cd) and a 58 nt deletion due to the use of an alternative acceptor site within exon 12 and the donor site of exon 11 (NR2Cc) (Rafiki *et al*, 2000). These splicing events introduce a frameshift in the NR2C mRNA reading frame, leading to the appearance of PTCs after M3 coding region (Rafiki *et al*, 2000). The predicted polypeptide chains would lack the complete ligand-binding domains S2, the membrane domain M4 and the intracellular C-terminus. In cerebellar tissue, and at all stages of development, NR2Ca (prototypical NR2C) is expressed at higher levels than NR2Cb-d which represent only a small proportion of the NR2C mRNAs (Rafiki *et al*, 2000). In the developing cerebellum, NR2Cb expression is higher than that of NR2Cd between P4 and P7. NR2Cd is expressed at relatively high levels when compared with the prototypic NR2C, but only at P0, and the NR2Cb splice variant was barely detectable in the following stages of development. Electrophysiological characterization of recombinant expression of NR2Cb with NR1 showed that this variant does not form a functional channel (Rafiki *et al*, 2000). Thus, rat NR2C splice variants are developmentally regulated but its physiological role is still unknown.

Human NR2C has 4 splice variants generated by deletion of 15 nt (NR2C-2), a 24 nt insertion (NR2C-3) or 51 nt deletion (NR2C-4) compared to the prototypical NR2C (NR2C-1) (Daggett *et al*, 1998). None of the deletions/insertion cause a frameshift. NR2C-2 results from the use of an alternative acceptor site in exon 11, just outside the coding region for M2. NR2C-3 and NR2C-4 occur due to the use of alternative acceptor sites in intron 12 or inside exon 13. Splice sites are the canonical GT-AG, with the exception of NR2C-4 which uses GT-GG. The expression of NR2C-3-4 in the adult human cerebellum is relatively low compared to NR2C-1, possibly less than 10-fold, and thus difficult to detect. When co-expressed with NR1, only NR2C-1 and NR2C-2 produced a response to agonists, with no detectable difference in the current amplitudes, kinetics and agonist-induced $[Ca^{2+}]_i$ rises between the two variants (Daggett *et al*, 1998).

IV.1.5.3 NR2D

Two NR2D splice variants have been cloned from the rat brain (Ishii *et al*, 1993; Monyer *et al*, 1994), NR2D-1 (D13213.1) and NR2D-2 (NM_022797.1). Variants arise from the alternative exclusion of 88 nt inside exon 13, resulting in a frameshift and extended C-terminal (Ishii *et al*, 1993). Recombinant expression of both these variants with NR1 failed to produce functional receptors because high-GC content in the transcriptional start region of the NR2D gene leads to low expression in *Xenopus* oocytes (Ishii *et al*, 1993; Monyer *et al*, 1994). Substitution of the GC-rich sequences by the equivalent NR2A sequences, lead to more efficient expression and since then NR1/NR2D-2 channels have been characterized without resorting to chimeric constructs (Wrighton *et al*, 2008; Wyllie *et al*, 1996). However, NR2D-1 has not been expressed in a recombinant system, and thus its functionality remains to be determined. Expression of NR2D-1 and NR2D-2 was investigated using an RNase protection assay in different regions of the brain and developmental stages, however only NR2D-2 expression was detected suggesting that NR2D-1 is either not expressed or its expression is below the detection limits of the assay (Wenzel *et al*, 1996).

A putative NR2D human variant has also been predicted computationally (AB209292.1 or hsk003001170). This variant results from the use of alternative splice donor in exon 10 and exon 11 acceptor (GT-AG), deleting 51 nt but not altering the mRNA reading frame. The predicted protein sequence would thus have 17 amino acids absent in the ligand-binding domain S2. However, there is no experimental evidence to support the physiological expression of this variant.

IV.2 RESULTS

Expression of NR2 subunits in the mouse optic nerve has been previously established (Salter & Fern, 2005). Here I sought to confirm expression of NR2A-D in the rat optic nerve and clone the full-length cDNA of these subunits. Given the unusual physiological and pharmacological profile of white matter NMDA receptors, I tried to explore the possibility that NR2 subunits expressed in the rat optic nerve possess particular molecular features. Expression of NMDA receptors in P10 optic nerve was detected using real-time RT-PCR. Each PCR reaction resulted in one single product of the expected size: 107 bp, 81 bp, 120 bp and 259 bp corresponding to NR2A, NR2B, NR2C and NR2D, respectively (figure IV-1). PCR products of the same size were detected both using cDNA originated from brain (figure IV-1 left panel) and from optic nerve mRNA (figure IV-1 right panel).

Having established that all NR2 subunits are expressed in the neonatal rat optic nerve I attempted to amplify and clone the full-length cDNA of these subunits (figure IV-2). The goal was to investigate the molecular specificities of white matter NMDA receptors. All NR2 subunits were successfully PCR amplified and cloned from rat brain (figure IV-2 top panel). DNA bands appear to be at higher molecular size than expected possibly due to slower migration of high molecular size bands on the 1.1% agarose gel (figure IV-2 and table IV-4). Amplification products were cloned and sequenced. Despite multiple attempts, the full-length NR2A and NR2D mRNA was not successfully amplified from the optic nerve. Nevertheless, NR2B-C were cloned from this tissue and all NR2 subunits were cloned from the brain (figure IV-2). To detect positive clones containing the expected NR2 subunit, several primer pairs were used to probe the bacterial colonies (clones) by PCR colony screening. The primer pairs were used to probe the bacterial colonies (clones) by PCR colony screening. The primer pairs were chosen to amplify different regions of the mRNA. Using this strategy, I intended not only to choose positive clones, but also to avoid bias against splice variants which lacked the primer binding sites of one primer pair.

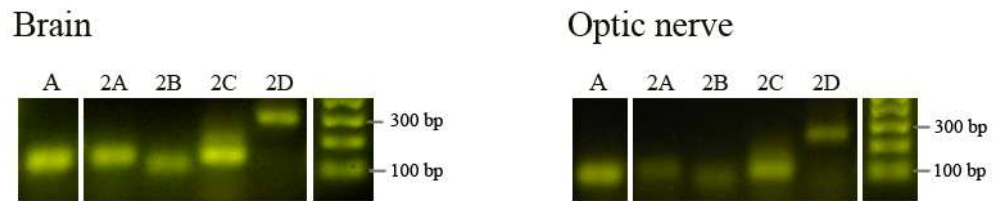


Figure IV-1: Expression of NR2 subunits in the neonatal rat optic nerve and brain

cDNA produced from neonate rat brain (left) and optic nerve mRNA (right), was PCR amplified using primers that for actin (A) or the NR2 subunits: 2A, NR2A; 2B, NR2B; 2C, NR2C; 2D, NR2D. PCR products were separated in a 1.1% agarose gel, visualized with Sybr Safe dye, and the size of PCR products was estimated by comparison with a DNA ladder (1 kb ladder, Invitrogen). Amplification products corresponding to the expected sizes were detected for each subunit.

IV.2.1 NR2A cloning

NR2A was amplified successfully from adult and neonate brain (figure IV-2). PCR products were cloned and sequenced, confirming the identity of clones as NR2A (NM_012573.2). The sequencing of NR2A clones did not reveal novel splice variants. Although several approaches were attempted, NR2A was not cloned from the optic nerve, due to poor PCR amplification of NR2A from optic nerve cDNA.

IV.2.2 NR2B novel splice variants

NR2B was amplified successfully from the brain (P10 and adult) and the P10 optic nerve (figure IV-2). After cloning, several clones were sequenced revealing new NR2B splice variants expressed in NR2B. In figure IV-3 there is a depiction of the three novel NR2B splice variants cloned from the rat optic nerve. NR2B $_{\Delta 635}$ is the result of an intraexonic deletion (+3081 to 3716) within exon 13 using the rare splicing acceptor-donor GC-CT (figure IV-3) (Chong *et al.*, 2004). This deletion creates a premature termination codon in the predicted polypeptide chain. Nonetheless, the sequence coding for the membrane and ligand-binding domains remain intact (figure IV-3). NR2B cl#46 and NR2B cl#26, also cloned from the neonate optic nerve mRNA, share the alternative deletion of exon 10 (figure IV-3) but NR2B cl#46 has a further 30 bp deletion inside exon 2, the first coding exon. The splicing site of this deletion is not a donor-acceptor pair but the short sequence TGAC.

Novel NR2B variants were also identified in the P10 rat brain with drastic deletions (more than 50% of NR2B coding sequence): NR2B cl#61, 3115 deletion; NR2B cl#63, 3019 bp deletion; NR2B cl#67, 2383 bp deletion. If translated, these variants generate polypeptides without the membrane domains or ligand-binding domains of NMDA receptors. Due to this prediction, the clones were not fully sequenced and are not depicted in figure IV-3.

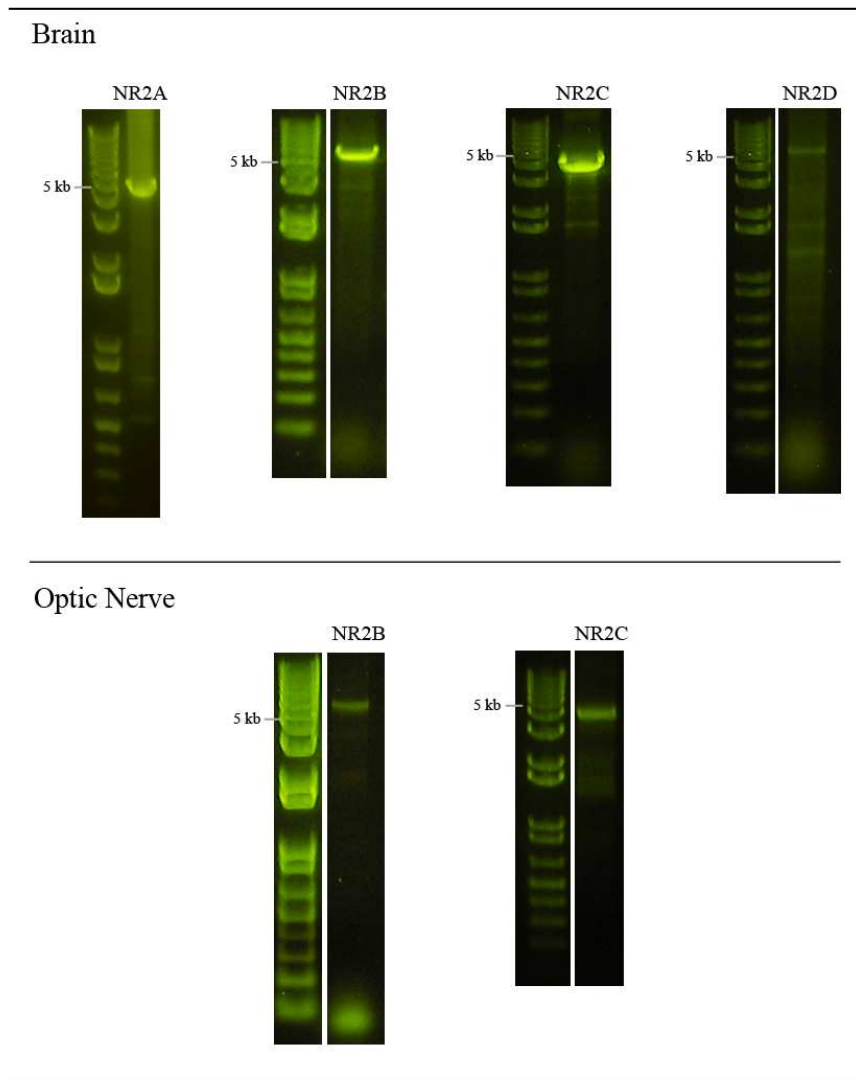


Figure IV-2: Amplification of full-length NR2 subunit cDNA

cDNA originating from neonate rat brain (top) and optic nerve mRNA (bottom), was PCR amplified using primers annealing at the 5' and 3' UTR. PCR products were separated in a 1.1% agarose gel, visualized with Sybr Safe dye, and the bands sizes were estimated by comparison with a DNA ladder (1 kb ladder, Invitrogen). Individual bands were excised from the, cloned into pGEM-T and sequenced.

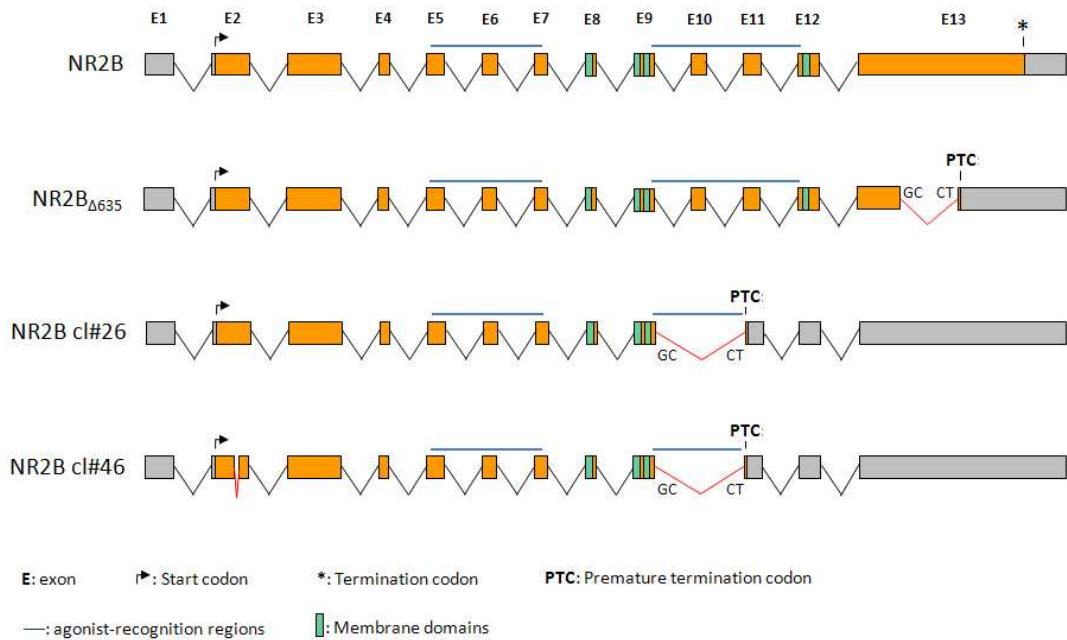


Figure IV-3: Gene organization of *Grin2b* and new NR2B splice variants

Rat NR2B gene (*Grin2b*) has 13 exons and the coding region is represented by orange boxes. Non-coding regions are represented as gray boxes. Introns are excluded (black connecting lines) to give rise to the final mRNA molecule (accession# NM_012574). In the newly identified variants NR2B_{Δ635}, NR2B cl#26 and NR2B cl#46 a different pattern of intron exclusion occurs (red connecting lines) creating premature termination codons. Newly identified variants were cloned from the neonate rat optic nerve. Exons are drawn to scale.

IV.2.3 NR2B_{Δ635} recombinant expression

NR2B_{Δ635} is predicted to maintain the general features needed for functional NMDA receptor subunits (figure IV-3), thus it was chosen to be expressed recombinantly in Hek293 cells. NR2B_{Δ635} was tagged in the N-terminus with YFP and the construct was transfected with NR1-CFP. Twenty-four hours after transfection no cells were detected expressing YFP in NR2B_{Δ635} transfected cells. Expression of full-length NR2B-YFP and NR1-CFP was detected. As I was unable to detect YFP fluorescence in cells transfected with NR2B_{Δ635}-YFP, cells with CFP fluorescence were selected to monitor $[Ca^{2+}]_i$ following stimulation. Cells expressing NR1/NR2B showed $[Ca^{2+}]_i$ rises evoked by glutamate (0.1, 1, 10, 100 and 1000 μ M) and glycine (10 μ M), in Mg²⁺-free solution (figure IV-4). In contrast no $[Ca^{2+}]_i$ rises were observed in cells transfected with NR1/NR2B_{Δ635} following stimulation with glutamate and glycine (figure IV-4). As expected, following stimulation with glutamate and glycine non-transfected Hek293 cells did not show any relevant increase in $[Ca^{2+}]_i$ (figure IV-4, Hek293). Sequencing of the plasmid containing the construct NR2B_{Δ635}-YFP indicated that the construct has YFP in frame with the NR2B_{Δ635} sequence. Thus, the lack of NR2B_{Δ635}-YFP expression, was not due to a technical error and most likely indicates a failure in translation of NR2B_{Δ635} mRNA.

IV.2.4 NR2C

Several of the cloned PCR products corresponded to the published canonical NR2C (M_012575.2) and a novel splice variant, NR2C cl#29, was identified (figure IV-2 and IV-5). NR2C cl#29 was cloned from the optic nerve and is the result of alternative splicing at an acceptor-donor pair GC-TG located internally in exon 7 and extending to exon 15 (+1304 to 3581). The resulting transcript is 2278 bp shorter than the published NR2C (NM_012575). The predicted translation of this transcript generates a protein without the membrane domains or ligand-binding domains of NMDA receptors, as depicted in figure IV-5. Novel splice variants were not found in the rat brain.

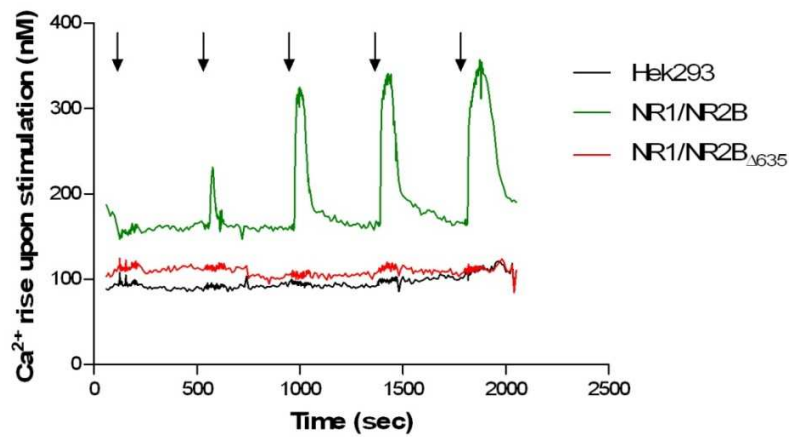


Figure IV-4: Glutamate stimulation of NR1/NR2B_{Δ635} does not produce [Ca²⁺]_i rises

Hek293 cells expressing NMDA receptors were loaded with fura-2 and stimulated for 15 sec with five different glutamate concentrations (0.1; 1; 10; 100 and 1000 μ M), in the presence of 10 μ M Glycine, in Mg²⁺-free solution. Each trace represents recordings from a single representative cell. Arrows indicate the time point of stimulation.

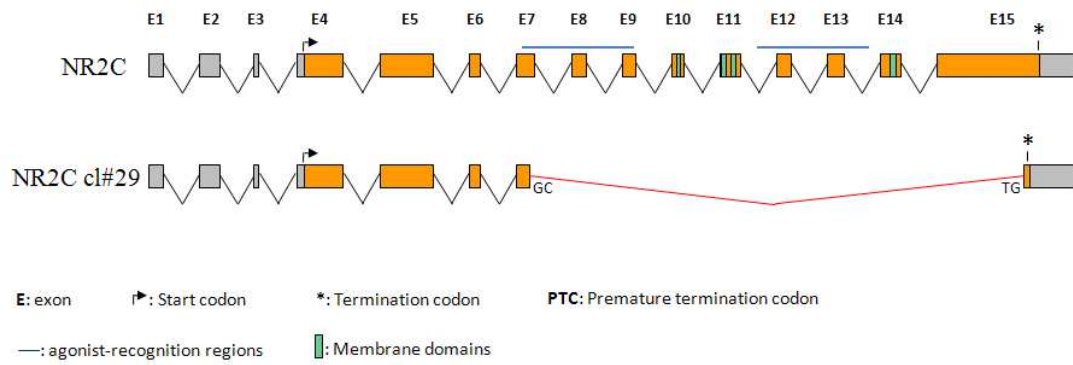


Figure IV-5: Gene organization of *Grin2c* and of a new NR2C splice variant

Rat NR2C gene (*Grin2c*) has 15 exons and the coding region is represented by orange boxes. Non-coding regions are represented as gray boxes. Introns are excluded (black/red connecting lines) to give rise to the final mRNA molecule (accession# NM_012575). In the newly identified variant, NR2C cl#29, a different pattern of intron exclusion occurs (red connecting lines) creating premature termination codons. NR2C cl# was cloned from the neonate rat optic nerve. Exons are drawn to scale.

IV.2.5 NR2D

Full-length NR2D transcripts were amplified and cloned from the rat brain but not from the optic nerve. Amongst the sequenced clones, the canonical NR2D (NM_022797) and 4 novel splice variants were identified (figure IV-6). NR2D cl#50 results from a 49 bp deletion and the splice junction appears to be the repeated sequence TCCCC present at +1371 and +1419 nt in NR2D mRNA. The splice junction of NR2D cl#51 is also a repeated sequence, CGCC, located at nucleotides +2605 and +3752, and the transcript has a deleted sequence of approximately 1147 nt. cl#55 results from 107 bp deleted inside exon 2 at the splice sites GC-CT (+214-320 nt). Of the cloned transcripts, NR2D cl#56 has the most interesting features. It arises from an 18 bp insertion, adding the amino acids LVAPRS to the polypeptide chain, using an alternative consensus acceptor site in exon 6 (table IV-1); and an 886 bp deletion (GC-AC, nt +2927-3812) that alters the transcript reading frame. Due to the frameshift, the canonical NR2D stop codon is not recognized, and instead an alternative stop codon located in the 3' UTR (nt 4151) is used (figure IV-5). NR2D cl#50, cl#51 and cl#69 were cloned from the neonate brain, cl# 55, cl#56 from the adult brain. A clone was also sequenced, albeit not fully, that contains a previously described variation: 82 bp deletion nucleotides located in +3794 to 3875 using splice acceptor-donor pair GC-CC (Ishii *et al*, 1993; Monyer *et al*, 1994).

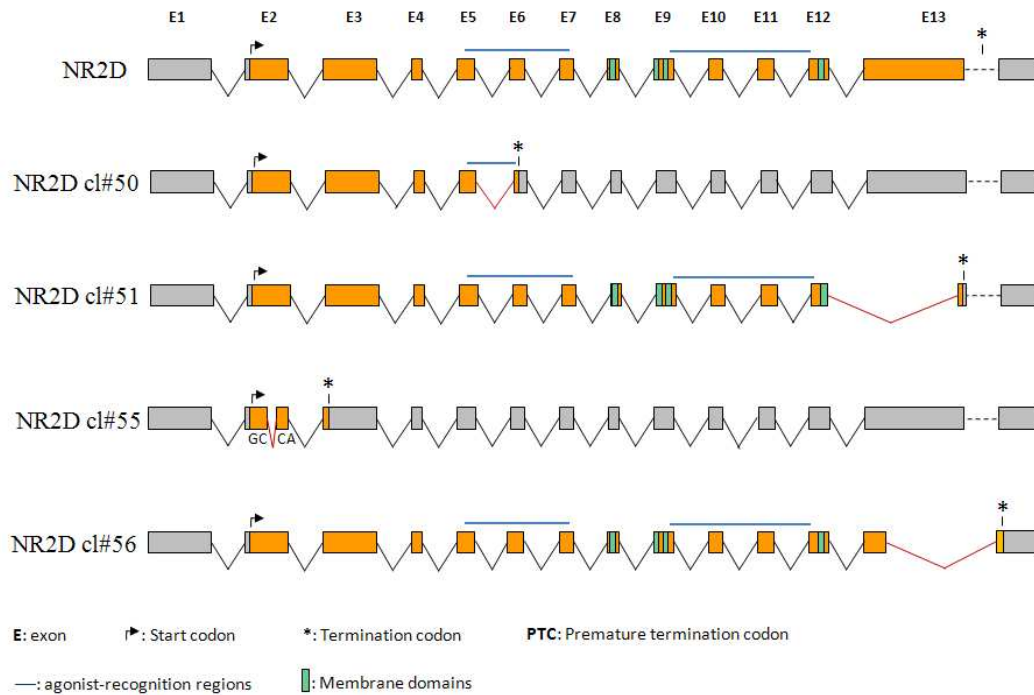


Figure IV-6: Gene organization of *Grin2d* and of a newly identified NR2D splice variant

Rat NR2D gene (*Grin2d*) has 13 exons and the coding region is represented by orange boxes. Non-coding regions are represented as gray boxes. Exon 13 appears discontinued because there is a 100 nt sequence lacking in the database sequence, which is present in the gene product sequence (NR2D mRNA, NM_022797). This is possibly due to incomplete genomic assembly. Introns are excluded (black/red connecting lines) to give rise to the final mRNA molecule (accession# NM_012575). In the newly identified variants, NR2D cl#50, NR2D cl#51, NR2D cl#55, NR2D cl#56, a different pattern of intron exclusion occurs (red connecting lines) creating premature termination codons. NR2D splice variants NR2D cl#50 and cl#51 were cloned from the neonate brain; NR2D cl#55 and NR2D cl#56 were cloned from the adult brain. Exons are drawn to scale.

```

NR2D-1 Rat  GGC GCG CGG GCC GGT GGC TGG GACT TCC CGC CGC CGC CGC CGC ACC TCG CGT TCG CTGG AGG 3814
NR2D-2 Rat  GGC GCG CGG GCC GGT GGC TGG GACT TCC CGC CGC CGC CGC CGC ACC TCG CGT TCG CTGG AGG 4520
NR2D Mouse  GGC GCG CGG CGG GGT GGC TGG GACT TCC CGC CGC CGC CGC CGC ACC TCG CGT TCG CTGG AGG 3895
NR2D Human  GGC GCG CGC CGT TGG GGG CTGG GACT TCC CGC CGC CGC CGC CGC ACC TCG CGT TCG CTGG AGG 3908

NR2D-1 Rat  ACCTGAGCTCC----- 3825
NR2D-2 Rat  ACCTGAGCTCCTGCCCCGCGGGCGGCCCCACGCGCAGGCTCACCGGGCCATCCCGCCACG 4580
NR2D Mouse  ACCTGAGCTCCTGCCCACGGGCGGCCCCACGCGCAGGCTCACCGGGCCCTCGCGCCACG 3955
NR2D Human  ACCTCAGCTCGTGCCCTCGCGCCGCCCTGCGCGCAGGCTTACCGGGCCCTCCCGCCACG 3968

NR2D-1 Rat  -----CGCCCTGCCACCGCATCGCACCGGA 3852
NR2D-2 Rat  CGCGCCGCTGCCCGCACGCTGCGCACTGGGGGCCGCCCTGCCACCGCATCGCACCGGA 4640
NR2D Mouse  CGCGCCGCTGTCCGCACGCTGCGCATTGGGGGCCGCCCTGCCACCGCATCTCACCGGA 4015
NR2D Human  CTCGCAGGTGTCCGCACGCCGCGCACTGGGGGCCGCCCTGCCACAGCTTCCACCGGA 4028

NR2D-1 Rat  GACACCGGGGCGGGGACCTGGGCACACGCAGGGGCTCTGCGCAATTCTCCAGCCTGGAGT 3912
NR2D-2 Rat  GACACCGGGGCGGGGACCTGGGCACACGCAGGGGCTCTGCGCAATTCTCCAGCCTGGAGT 4700
NR2D Mouse  GACACCGGGGCGGGGACCTGGGCACACGCAGGGGCTCTGCGCAATTCTCCAGCCTGGAGT 4075
NR2D Human  GACACCGGGGCGGGGACCTGGGCACCCGAGGGGCTCGGCGCAATTCTCTAGCCTCGAGT 4088

```

Figure IV-7: Sequence alignment of mouse, rat and human NR2D-1 and NR2D-2 splice sites

Previously reported NR2D splice variants arise from an intraexonic deletion in exon 13. Despite the prediction that NR2D-1 is an artefact, conservation of splice sites (red squares)) across species suggest otherwise (Monyer *et al*, 1994). Regions where splicing occurs are delimited by red boxes. Traces represent non-homologous regions. Alignment was made using ClustalW2 (<http://www.ebi.ac.uk/Tools/clustalw2/index.html>).

```

                *           460           *           480
NR2D-1 : IVEPADPISGTCIRDSVPCRSQLNRTHS-----PPPDAPRPEK : 478
NR2D-2 : IVEPADPISGTCIRDSVPCRSQLNRTHS-----PPPDAPRPEK : 478
c1#56  : IVEPADPISGTCIRDSVPCRSQLNRTHSLVAPRSEPPPDAPRPEK : 484

                *           980           *           1000           *
NR2D-1 : GPIEPQGLGLGEARAAPRGAAGRPLSPPTTQPPQKPPPSYFAIV : 1006
NR2D-2 : GPIEPQGLGLGEARAAPRGAAGRPLSPPTTQPPQKPPPSYFAIV : 1006
c1#56  : GPIEPQGLGLGEARAGSPGHPATRAAARTLRTGGRPE----- : 1004

                1240           *           1260           *
NR2D-1 : SHRAPAAAAPHHHRHRAAGGWDFPPPAPTSTRSLEDLS----- : 1263
NR2D-2 : SHRAPAAAAPHHHRHRAAGGWDFPPPAPTSTRSLEDLSFF----- : 1265
c1#56  : ----- : -

                1460           *           1480           *
NR2D-1 : ---SRPCPPHRTGDTGAGTWAHAGALRISPAPSPRYDAAPAPT : 1304
NR2D-2 : ----- : -
c1#56  : ---CPPHRTGDTGAGTWAHAGALRISPAPSPRYDAAPAPT : 1042

                1500           *           1520           *           1540
NR2D-1 : TPAAPSVSAGHGPRGRAKWTGPSWVGKDRNGPGRTPPGAASCAP : 1348
NR2D-2 : ----- : -
c1#56  : TPAAPSVSAGHGPRGRAKWTGPSWVGKDRNGPGRTPPGAASCAP : 1086

                *           1560           *           1580
NR2D-1 : TPFALGEL----- : 1356
NR2D-2 : ----- : -
c1#56  : TPFALGEL----- : 1094

```

Figure IV-8: Amino acid sequence alignment of NR2D splice variants

Previously reported NR2D splice variants NR2D-1 and NR2D-2, differ in their C-terminus. NR2D cl#56 shares the 3' splice junction with the NR2D-1 and have homologous C-terminal sequences. Regions where splicing occurs are delimited by red boxes. Traces represent non-homologous regions. Alignment was made using ClustalW2 (<http://www.ebi.ac.uk/Tools/clustalw2/index.html>).

Table IV-1: Splice site analyses of *Grin2D*

Analysis of splice site strength performed with the tool NNSPLICE. *Grin2D* which codes for NR2D transcripts has 13 exons. Exon 6 has two acceptor sites, **6** and **6'** of similar strength, that are used alternatively to create a novel splice variant (figure IV-6 NR2D #50). Splice site are bolded and exonic sequences are underlined.

Splice junction (intron)	Donor 5' splice site	Acceptor 5' splice site	Donor site score	Acceptor site score
1	AAG GT <u>AAGG</u>	CCCGTCCACGCA AGA	1.00	0.02
2	AAG GT <u>GCGC</u>	CCCTGTTCCCAC AGG	0.98	0.93
3	CAG GT <u>GATT</u>	TTTCTCCTGGGC AGG	0.44	0.93
4	GT GGT <u>GAGT</u>	TGTTTTTTTGCCA AGG	0.97	0.93
5	CAG GT <u>GACA</u>	GTCGCTCCCCGC AGC	0.74	0.57
6	GAG GT <u>AAGA</u>	TCGATCCACCCC AGG	1.00	0.84
6' (cl #56)		CCAACCCCTTCA AGC		0.67
7	TCG GT <u>GAGC</u>	TCCCATGTCCCC AGA	0.97	0.96
8	AAC GT <u>GAGT</u>	CTGGTTCCCCAC AGG	0.99	0.92
9	AAG GT <u>GTGT</u>	CGCTTCCATTC AGT	0.94	0.95
10	AGG GT <u>CAGC</u>	GTCCCTGTCCAC AGG	0.09	0.57
11	ACG GT <u>GCGG</u>	GACTCCATCCTC AGA	0.10	0.85
12	AGG GT <u>AGGA</u>	CCCATCCCTCAC AGG	0.72	

Prediction of the resulting polypeptide chains of the novel NR2D variants shows that in NR2D cl#50 and NR2D cl#55 the deletions lead to a frameshift with the appearance of premature stop codons soon after the splice junction (figure IV-5). As a result these proteins would either contain about half of the one ligand-binding domain, or no domains (figure IV-5). The deletion occurring on NR2D cl#56 also causes a frameshift and the use of an alternative termination codon inside the 3'UTR. Interestingly, this is the same termination codon used in NR2D-1 (figure IV-7). Before the termination codon, 113 amino acids

different from NR2D are generated, 92 of which are similar to NR2D-1 C-terminal as depicted on figure IV-7. The ligand-binding and membrane domains are still coded for but the use of an alternative splice acceptor in exon 7 adds 6 new amino acids in the ligand-binding domain in NR2D cl#56 (figure IV-6 and IV-7).

IV.3 DISCUSSION

IV.3.1 Strategical and practical considerations

Determining the molecular features of white matter NR2 subunits was the main goal of this part of the project. Currently, detection of alternative splicing is either based on EST comparisons or on a combination of computational predictions and comparisons of gene homologous in human and rodents (Cawley & Pachter, 2003; Coward *et al*, 2002; Dror *et al*, 2005; Modrek *et al*, 2001; Wang & Marín, 2006). Using this computational data, probes are then created to search putative splice variants in cDNA libraries. This strategy presents some drawbacks. A general problem is identifying alternative splices with current gene finding programs. Software usually search for optimal exons, splice sites, and gene structure assuming that alternative splice sites are usually weaker than constitutive sites. However, this is not always the case and different programs may give different results for the predicted *strength* of a splice site (Wang & Marín, 2006). Existing databases and bioinformatics tools focusing on splicing also have a bias against non-consensus splice sites and non-canonical splicing. Considering these shortcomings of previous approaches, in this study I choose to clone full-length transcripts expressed in native tissue and then characterizes their molecular nature.

Cloning NMDA receptors from the optic nerve proved to be far from a trivial task. The average length of human mRNA is estimated to be 2.5 kb (Strachan & Read, 1999) and the average mammalian mRNA is 2.1 kb (2004). In comparison, NR2 subunits open reading frame (ORF) is relatively large ranging from approximately 3.7 kb to 4.4 kb (table IV-2). In addition, NR2C and NR2D have high GC content (table IV-2) and expression of NMDA receptors mRNA is relatively low in the optic nerve, compared to the brain (Salter & Fern, 2005). Another complication arises from the amount of RNA extracted from the rat optic nerve. A typical RNA extraction from brain tissue yields more than 100 µg from a fraction of the total brain. In contrast, 20 optic nerves yield 10 µg of total RNA. As a consequence, a smaller amount of optic nerve RNA is available for protocol optimization and scaling-up of

reactions is also hindered. For these reasons, PCR amplifications and clonings were initially optimized using brain cDNA and modified, where appropriate, to amplify NMDA receptors mRNA from the optic nerve. It should be noted that different PCR strategies/protocols were applied for the amplification of the NR2 subunits. These strategies are detailed on chapter II.

Table IV-2 - Molecular properties of rat NR2 subunits mRNA

Numbering of initiation and termination codon was done in relation to the first nucleotide of mRNA sequence as appears in the NCBI database. The corresponding accession numbers are also listed. GC content analysis was performed using the tool **geecee** at the website [Mobylye@Pasteur \(http://mobylye.pasteur.fr/cgi-bin/portal.py\)](http://mobylye@Pasteur).

Subunit	mRNA length	Initiation	Termination	ORF	GC content (%)	Accession Number
NR2A	6369	89	4481	4392	52	NM_012573.2
NR2B	5259	350	4796	4446	53	NM_012574.1
NR2C	4673	522	4272	3750	62	NM_012575.2
NR2D	5246	739	4708	3969	66	NM_022797.1

In spite of all optimizations, NR2A and NR2D were cloned from the rat brain but not the optic nerve. This could be due to two factors: (1) the RT reaction is not efficient enough to transcribe sufficient full-length mRNAs of such long (NR2A) or GC-rich (NR2D) transcripts, a problem exacerbated using optic nerve RNA as input for the reaction; and/or (2) NMDA receptor expression in white matter is relatively low and it is likely that NR2A and NR2D are not major components of white matter NMDA receptors (Karadottir *et al*, 2005; Salter & Fern, 2005). Also, at the developmental age at which animals were used (P10) NR2A expression levels have not yet peaked (Monyer *et al*, 1994). Although NR2C had GC content comparable to that of NR2D (table IV-2), it has higher expression in white matter and this might have facilitated PCR amplification and cloning (Karadottir *et al*, 2005; Salter & Fern, 2005).

IV.3.2 Novel NR2B splice variants

NR2B splice variants previously reported were found in mouse brain (Klein *et al*, 1998; Tabish & Ticku, 2004). The proto-typical NR2B mRNA has 3 non-coding exons at the 5'UTR and the ATG is located in exon 4. The variants are the result of the alternative exclusion of exon 2 alone or in combination with different length deletions of exon 1 (Klein *et al*, 1998; Tabish & Ticku, 2004). The remaining 2 variants result from the use of alternative acceptor sites in exon 2 and the exclusion of exon 3 (Tabish & Ticku, 2004). These variants are the result of alternative splicing in the 5'UTR of *Grin2b*. Here, I report for the first time the cDNA sequence of NR2B splice variants with altered coding regions. The three splice variants identified (figure IV-3) have deletions that change the mRNA reading frame, leading to the appearance of PTCs. In NR2B cl#26 and NR2B cl#46, exon 10 is skipped (cassette exon), one of the most common mechanisms of alternative splicing (Black, 2003; Matlin *et al*, 2005). Although NR2B cl#46 has an additional 30 nt deletion this does not change the reading frame of the mRNA raising the possibility that a NR2B variant containing only this 30 nt variation might also be expressed.

A common marker of cassette exons is the presence of weaker splice sites than those of constitutive exons, although several other factors such as the presence and density of exonic and intronic splicing enhancers and silencers, influence alternative splicing (Black, 2003; Garg & Green, 2007). To determine the strength of splice sites one has to resort to algorithms which calculate an arbitrary value in relation to the “perfect” canonical splice site. The NR2B exon 10 acceptor site score, a measure of how confident one can be of this being a true splice site, is higher than that of exon 11 using the tools NNSPLICE and EuSplice (Bhasi *et al*, 2007; Reese *et al*, 1997) (table IV-3). However, analyzing the splice site in a different tool, NetGene2 (Brunak *et al*, 1991), the outcome is that exon 11 acceptor site is stronger than exon 10 (0.92 vs 0.96, respectively). A weaker acceptor site in exon 10, comparatively to exon 11 may explain exon 10 as a cassette exon. The different results obtained with these tools

underline the importance of obtaining transcripts through an experimental approach rather than a computational prediction.

Table IV-3: Splice site analyses for *Grin2B*

Analysis of splice site strength performed with the tool NNSPLICE (Reese *et al*, 1997). *Grin2B* which codes for NR2D transcripts has 12 exons. According to NNSPLICE prediction, exon 10 splice sites are strong. Splice site are bolded and exonic sequences are underlined.

Splice junction (intron)	Donor 5' splice site	Acceptor 5' splice site	Donor site score	Acceptor site score
1	<u>AAG</u> GT AGGG	CCTTCTCTTTTC AG <u>A</u>	0.97	0.99
2	<u>AAG</u> GT AAAA	TTTTTCTTGAAA AG <u>G</u>	0.95	0.28
3	<u>TAG</u> GT GAGT	TTTTATCGTTGC AG <u>G</u>	0.98	0.98
4	<u>AGG</u> GT AGGA	TTCTCTCTGCG CA <u>GG</u>	0.2	0.98
5	<u>TGAG</u> T ATGA	CTTTAACTGGG TAG <u>G</u>	0.02	0.15
6	<u>GAG</u> GT CAGT	GTCTTTCTCTCC AG <u>G</u>	0.95	1.00
7	<u>TAG</u> GT TAAAT	TGCTTTCCTTTC AG <u>A</u>	0.96	0.99
8	<u>GAG</u> GT AAGT	TTGTATCACTCC AG <u>A</u>	1.00	0.77
9	<u>AAG</u> GT AAGA	CTTTCTCTCTCC AG <u>T</u>	0.99	0.99
10	<u>AGG</u> GT AAGA	TGTTTCTTGTGC AG <u>G</u>	1.00	0.97
11	<u>ATG</u> GT GAGT	TGTCCTCCTTCT AG <u>G</u>	0.97	0.99
12	<u>AG</u> GT AAGT	CTATGTCCCTT CA <u>GG</u>	0.99	0.93

NR2B_{Δ635} is generated in a non-canonical splice site and the resulting polypeptide is a C-terminally truncated NR2B isoform containing the membrane and ligand-binding domains (figure IV-3). Other functional truncated glutamate receptors have been identified. AMPA receptor, GluR4, has a splice variant, GluR4c, possibly resulting from an intron retention. This results in a shorter isoform with a different C-terminus downstream of M4. Despite having a different, shorter, C-terminal, GluR4c generates functional homomeric receptors after transient transfection in *Xenopus* (Gallo *et al*, 1992). There are also reports of truncated

NR2B created by recombinant DNA technology. Co-expression of C-terminal truncated NR2B with NR1 generated functional channels with reduced peak open probability and a reduced mean open time (Mohrmann *et al*, 2002). Mice expressing these truncated NR2B subunits die perinatally possibly due to impaired synaptic targeting of NMDA receptors at nascent synapses (Mohrmann *et al*, 2002; Sprengel *et al*, 1998). This indicates that although the C-terminal domain plays a fundamental role in the developmental role of NMDA receptors it is not essential for functional channel assembly.

Having found a naturally occurring NR2B with a truncated C-terminal, NR2B $_{\Delta 635}$, it was interesting to investigate its physiological properties. In cells transfected with NR1-CFP and NR2B $_{\Delta 635}$ -YFP, YFP fluorescence was not detected, indicating absence of NR2B $_{\Delta 635}$ protein expression. Furthermore, challenging these cells with glutamate did not elicit any changes in $[Ca^{2+}]_i$ (figure IV-4). The lack of YFP fluorescence is not the result of an error in constructing the chimeric protein as confirmed by sequencing of the plasmid coding for NR2B $_{\Delta 635}$ -YFP. This indicates NR2B $_{\Delta 635}$ is either a transcript targeted for degradation or it might perform some unknown role in regulation of gene expression.

It is emerging that cells commonly produce a substantial fraction of transcripts which are degraded before translation in a functional or regulated manner (Chang *et al*, 1999; Sreaton *et al*, 1997). Roughly a third of reliably deduced alternative splicing events in humans result in mRNA isoforms that contain a PTC. These transcripts are predicted to be degraded by the non-sense mediated decay (NMD) pathway (Maquat, 2004). It appears that cells routinely link alternative splicing and NMD to regulate the abundance of mRNA transcripts. This mechanism, termed “Regulated Unproductive Splicing and Translation” (RUST), has been experimentally shown to regulate the expression of a wide variety of genes in many organisms from yeast to humans (Lareau *et al*, 2007). This process may provide an additional level of genetic regulation to help the cell achieve the proper level of expression for a given protein. The cell could change the level of productive mRNA after transcription by diverting some

fraction of the already-transcribed pre-mRNA into an unproductive splice form and thence to the decay pathway (Lareau *et al*, 2007).

NR2B_{Δ635} mRNA contains a PTC downstream of the deleted sequence that generated the splice variants (figure IV-3). The presence of PTC 50-55 nucleotides upstream of an intron is usually an indication that this mRNA is targeted for degradation (Maquat, 2004). Another indication is the distance between the PTC and the polyA tail, which is the case in NR2B_{Δ635} transcripts (Buhler *et al*, 2006). In NR2B_{Δ635} the alternative deletion occurs intraexonically in the last exon, with a resulting frameshift and the coding for a termination codon ~720 nt before the polyA tail. I propose that targeting of NR2B_{Δ635} to degradation by NMD is the most likely explanation for the lack of protein expression in cells transfected with this variant. Whether NR2B_{Δ635} is a candidate for RUST remains to be addressed.

IV.3.3 NR2C splice variants

NR2C is believed to be a major component of NMDA receptors in whiter matter (Karadottir *et al*, 2005; Micu *et al*, 2006; Salter & Fern, 2005). In search for NR2C molecular features particular to the white matter a novel NR2C splice variant was cloned. Three NR2C splice variants containing PTCs before the final membrane domain have been described (Rafiki *et al*, 2000). These variants lack the final membrane domain and ligand-binding domain S2. The NR2C variants were detected in native tissue with expression levels lower than prototypical NR2C. However, when one of the variants was recombinantly coexpressed with NR1 in Hek293 cells, it did not form a functional channel (only one was tested) (Rafiki *et al*, 2000). Here I cloned a variant, NR2C cl#29, which has an intraexonic deletion in alternative non-canonical donor and acceptor sites (figure IV-5). The predicted translation of this variant lack important NMDA receptor domains. It thus seems unlikely that it generates a functional protein, or one that might assemble in functional NMDA receptor complexes. It is possible, as previously mentioned for NR2B, that these variants containing PTCs are expressed

either as mRNA as a mean of regulating protein expression, or are expressed as a protein with an unknown function (Lareau *et al*, 2007).

IV.3.4 NR2D splice variants: artefacts or overlooked?

The DNA databases contain mRNA sequences that correspond to 3 proposed NR2D splice variants (Ishii *et al*, 1993; Monyer *et al*, 1994). One of the variants, NR2D-1, contains an 82 nucleotide deletion in the corresponding C-terminus of the protein, was cloned by two labs and also reported here (Ishii *et al*, 1993; Monyer *et al*, 1994). It has been proposed that NR2D-1 is a cloning artefact due to high GC-content of this region in the NR2D gene (Monyer *et al*, 1994). This reasoning is based on: (1) the deletion occurs in non-consensus intron-exon junctions; (2) the gene region where it occurs has high GC content which may impair either the polymerase or the reverse-transcriptase; and (3) expression of NR2D-1 was not detected in the CNS (Monyer *et al*, 1994; Wenzel *et al*, 1996).

Finding NR2D-1 again approximately 15 years after the first report does beg the question if it is indeed a cloning artefact. The strategy employed here is different and used improved enzymes that were not available at the time of the original clonings. It has also been established that alternative splicing can occur in non-canonical splice sites and still give rise to fully functional proteins (Brackenridge *et al*, 2003; Gillespie *et al*, 1995; Hiller & Platzer, 2008). In addition, the splicing boundaries are 100% homologous across species (figure IV-7), suggesting that the conserved sequence is required for alternative splicing. Whether NR2D-1 is an artefact or an expressed NR2D variant is still an open question, not addressed here since it fell outside the scope of this work. The physiological properties of NR2D cl#51 and NR2D cl#56 were also not addressed. These variants are predicted to retain the ligand-binding domains and the four membrane domains (figure IV-7). Interestingly, although NR2D cl#56 and NR2D-1 do not share splice sites, they have same 90 amino acids at their C-terminals (figure IV-8) suggesting that NR2D alternative splicing of 3'UTR might be more complex

than previously expected and adding to the notion that NR2D-1 might be a *bona fide* transcript.

The NR2D cl#56 and NR2D-1 C-terminal is unique. The common 90 amino acids at their C-terminals do not share homology with other glutamate receptors and in a search for protein motifs, no putative conserved domains were detected. This unique C-terminal of NR2D-1 and NR2D cl#56 can have an impact in NR2D protein interactions. NMDA receptors C-terminus are important for regulation of activity by phosphorylation, cleavage by proteases, trafficking and clustering of the receptors at synapses (Bi *et al*, 1998; Groc *et al*, 2009; Guttman *et al*, 2002; Mohrmann *et al*, 2002; Salter & Kalia, 2004). NMDA receptor subtypes interact with the MAGUK family of proteins that regulate cell-surface expression of NMDA receptors in a subtype dependent manner (Cousins *et al*, 2008). For instance, PSD-95 interacts with NR2A and increases their surface expression. In contrast, NR2D also interacts with PSD-95 via the C-terminal domain but the interaction does not affect NR2D cell surface expression (Cousins *et al*, 2008; Kornau *et al*, 1995). The interaction between PSD-95 and NR2D is weaker than NR2A, providing an explanation for the relatively low presence of NR2D in synaptic complexes (Mi *et al*, 2004).

NR2D has a proline-rich region in the COOH-terminal domain immediately downstream from the M4 and extending approximately 200 amino acids. This proline-rich region contains sequences that are homologous to motifs known to bind to Src homology 3 (SH3) domains, which mediate protein-protein interactions with proline-rich target sequences (Ren *et al*, 1993). NR2D interacts specifically with tyrosine kinase Abl SH3 domain but not to the SH3 domains from kinases, and inhibits Abl auto-phosphorylation (Glover *et al*, 2000). The biological relevance of this interaction is still unknown, but the interaction with Abl will not occur with NR2D cl#51, because this variant lacks the proline-rich region. Modification of NR2D C-terminal domain can potentially affect these (and other) interactions and consequentially NR2D trafficking to synapses and neuronal activity.

In conclusion, novel splice variants of the NMDA receptors NR2 subunits were found to be expressed in the neonate rat optic nerve and in the brain. A variant of NR2B, NR2B_{Δ635}, when recombinantly expressed failed to produce detectable amounts of protein, suggesting that this variant might be targeted for degradation. Although NR2D splice variants physiology was not accessed, NR2D splice variants identified in the rat brain have interesting features that could affect NR2D trafficking and modulation by interacting partners. It would be worthwhile investigating its physiological properties and physiological role in the future.

Chapter V

Cloning and molecular characterization of novel NR3 splice variants

V.1 INTRODUCTION

V.1.1 Molecular properties of NR3 subunits

NR3 subunits were identified and cloned several years after the cloning of NR1. NR3A, also termed Chi-1 or NMDA receptor-like (NMDAR-L), was cloned in 1995 by two independent groups (Ciabarra *et al.*, 1995; Sucher *et al.*, 1995). Rat NR3A gene (*Grin3A*) has an open reading frame of 3345 nucleotides which codes for a polypeptide of 1115 amino acids. The protein has a predicted molecular weight of 125 kDa (Ciabarra *et al.*, 1995). The amino acid sequence of NR3A shares 27% identity with NR1 and 28% with the NR2 subunits (Ciabarra *et al.*, 1995). The human NR3A has 93% sequence identity with rat NR3A indicating that this variant is evolutionary conserved (Bendel, 2008).

In 2001 two independent groups reported the cloning of human and rat NR3B (Andersson *et al.*, 2001; Nishi *et al.*, 2001). The open reading frame of NR3B codes for a protein of 1003 amino acids with the predicted size of 109 kDa. Mouse and human NR3B sequences share 74.9% sequence identity. Most of the sequence divergence between the two species is attributable to a restricted gene region. The translated polypeptide sequence from exon 9 is only 37.8% homologous in human and mouse due to an extra 120 base pairs in human exon 9. Consequently, human NR3B is 40 amino acids longer (Andersson *et al.*, 2001; Bendel *et al.*, 2005; Matsuda *et al.*, 2002; Nishi *et al.*, 2001). Amongst the NMDA receptor subunits, NR3B is more closely related to NR3A, 47% sequence identity, than with NR1 or NR2 subunits with whom it shares only 17–21% sequence identity (Andersson *et al.*, 2001; Chatterton *et al.*, 2002; Matsuda *et al.*, 2002).

NR3 subunits contain many of the typical NMDA receptor structural features, in particular the motif SYTANLAA, conserved in all ionotropic glutamate receptors (Ishii *et al.*, 1993; Monyer *et al.*, 1992; Moriyoshi *et al.*, 1991). This motif appears to be important for the regulation of NMDA receptor channel gating (Chang & Kuo, 2008; Sobolevsky *et al.*, 2007). NR3 subunits also contain S1 and S2 domains responsible for determination of ligand-

binding specificity and the membrane domains are also conserved (Andersson *et al*, 2001; Chatterton *et al*, 2002; Matsuda *et al*, 2002; Yao & Mayer, 2006). One potentially critical difference between NR3 and the other NMDA receptor subunits is an alteration in the “Q/R/N” site, which is critical for high Ca²⁺ permeability of NMDA receptors. The “Q/R/N” site is located inside M2 (pore-forming region) and in NR3 subunits the asparagine is changed to glycine (Andersson *et al*, 2001; Dingleline *et al*, 1999; Matsuda *et al*, 2002). This asparagine and the adjacent amino acid (N+1 site), also an asparagine in NR1 and NR2s, are important for voltage-dependent Mg²⁺ block of the channel. However, in the NR3 subunits the asparagine at the N+1 is an arginine (Chatterton *et al*, 2002; Ciabarra *et al*, 1995; Matsuda *et al*, 2002; Nishi *et al*, 2001; Sucher *et al*, 1995). This shows that NR3 subunits have molecular features that could explain their functional properties and set them apart from NR1 and NR2 subunits.

V.1.2 NR3A splice variants

In rodents, two NR3A splice variants are expressed: NR3A-S (L34938) and NR3A-L (AF073379) (Sasaki *et al*, 2002a; Sun *et al*, 1998). The variants differ in the use of an alternative acceptor site of exon 9 with the consequent alternative inclusion of 60 nt. The resulting NR3A-L protein contains a 20 amino acids sequence inserted within the C-terminus which are absent from the NR3A-S. This sequence contains two threonine residues (T1009 and T1002) which are putative substrates for phosphorylation by Ca²⁺ calmodulin-dependent protein kinase-II (CamKII), protein kinase A (PKA) and/or protein kinase C (PKC) (Sasaki *et al*, 2002a; Sun *et al*, 1998). Although this putative phosphorylation site could influence NR3A activity, thus far no differences were found between NR3A-S and NR3A-L in electrophysiological studies (Sasaki *et al*, 2002). Alternative splicing in NR1 C-terminal affects the trafficking of this subunit. Whether this mechanism is also in place for NR3A is an open-ended question.

V.1.3 NR3 expression

V.1.3.1 NR3A

NR3A is expressed mostly during the embryonic stage. During this stage, NR3A mRNA is detected ubiquitously with the highest levels present in the spinal cord, brainstem, hypothalamus, thalamus, CA1 field of the hippocampus, and amygdala. Expression is detected as early as embryonic day 15 (E15) and peaks before birth until the first postnatal week. Between P7 and P14 levels of NR3A mRNA decrease sharply to low levels, although maintaining the regional expression patterns observed prenatally (Ciabarra *et al*, 1995; Sucher *et al*, 1995; Sun *et al*, 1998).

Expression of NR3A protein and mRNA broadly follow the same pattern both in terms of developmental and regional expression. A difference between NR3A mRNA and protein expression is that NR3A protein is expressed in cerebellar cortex, whereas only low levels of mRNA had previously been detected in that brain region (Al-Hallaq *et al*, 2002; Hon-Kit Wong, 2002; Sun *et al*, 1998). There are differences in NR3A expression between humans and rodents. In adult humans, the highest NR3A mRNA and protein levels are found in cerebrocortical regions and, contrary to rats, absent from the cerebellum (Hon-Kit Wong, 2002; Nilsson *et al*, 2007).

V.1.3.2 NR3A splice variants expression

NR3A-S is the major NR3A isoform and is predominant in early pre-natal and postnatal development (Sun *et al*, 1998). Nevertheless, both NR3A variants are expressed throughout the rat brain albeit with regional differences. NR3A-S expression is higher in the frontal and pyriform cortices as well as in the hippocampus and spinal cord, relative to NR3A-L. NR3A-L predominates in the occipital and entorhinal cortices, thalamus and cerebellum. Moreover, the NR3-S variant was barely detectable in the latter region (Sun *et al*, 1998). During post-natal

development these variants have similar patterns of expressions. Expression is high during the first post-natal week, decreasing sharply afterwards, reaching adult levels by P10 (Sun *et al*, 1998). Attempts were made to detect NR3A-L in the human brain, but it appears that NR3A-L is not expressed in this species (Bendel *et al*, 2005; Eriksson *et al*, 2001; Nilsson *et al*, 2007). The reason for species specific expression of NR3A-L is currently unknown.

V.1.3.3 NR3B

The most recent NMDA receptor to be identified, NR3B, was cloned from a mouse spinal cord cDNA library and initially reported to have restricted expression in the rodent spinal cord and brain stem (Chatterton *et al*, 2002; Nishi *et al*, 2001). However, it has now been established that NR3B mRNA expression is widespread in central nervous system. NR3B mRNA is expressed in the hippocampus, cerebral cortex, cerebellum, striatum, substantia nigra and spinal cord (Matsuda *et al*, 2002; Wee *et al*, 2008). NR3B expression is detected as early as E16 but at low levels, rising postnatally and maintaining relatively constant levels of expression during post-natal development (Chatterton *et al*, 2002; Fukaya *et al*, 2005; Matsuda *et al*, 2002; Nishi *et al*, 2001; Prithviraj & Inglis, 2008). NR3B mRNA and protein follow similar expression patterns (Wee *et al*, 2008).

The NR3B expression profile shares some similarities with NR1. Both are expressed in most cell types of the above mentioned brain regions and in the spinal cord. The two subunits have a similar developmental expression pattern. During development of the spinal cord there is an increase of NR1 and NR3B expression concomitant with a decrease of NR2A and NR3A, suggesting an increasing importance of NR3B in post-natal development (Fukaya *et al*, 2005; Matsuda *et al*, 2002; Moriyoshi *et al*, 1991). Indeed, NR3B may have a role in dendritic remodelling in the adult brain (Prithviraj & Inglis, 2008).

V.2 Results

NR3A is thought to be an important component of NMDA receptors complexes in white matter (Karadottir *et al*, 2005; Micu *et al*, 2006; Salter & Fern, 2005). However, little is known about the molecular features of white matter NR3 subunits. In this chapter I sought to confirm expression of NR3 subunits in white matter before cloning the full-length cDNAs in search for novel splice variants.

V.2.1 NR3A and NR3B expression

Expression of NR3A and NR3B in the neonatal brain and optic nerve was detected using real-time RT-PCR. The PCR reaction with specific primers for NR3A yielded only one band of the expected molecular size, ~140 bp as depicted in figure V-1A (table II-1). Unexpectedly NR3B amplification yielded 2 products. One of the expected size, ~100 bp, and one of ~280 bp (figure V-1, table II-1). To confirm the identity of these products, both were cloned and sequenced. Sequence search using Blast revealed that the 100 bp product corresponded to the expected amplified sequence of NR3B mRNA. The 280 bp product sequence aligned perfectly with NR3B gene sequence (*Grin3B*). Further analysis confirmed that this extra sequence corresponded to intron 6 retention (genomic organization of *Grin3B* is depicted in figure V-3).

Genomic DNA contamination can sometimes be mistaken with regulated intron retention in transcripts. This was unlikely in our experiments because all RNA samples were treated with “rigorous” DNase treatment to degrade any contaminating genomic DNA. Nevertheless, to exclude the hypothesis of DNA contamination, a “no-RT” RT-PCR reaction was set-up containing RNA as input instead of cDNA. As depicted in figure V-1C, no product was amplified using the same NR3B primers, demonstrating that the intron sequence was amplified from cDNA and not from contaminating genomic DNA. This finding suggested the presence of a previously unidentified NR3B splice variant, generated by intron

retention. To determine the precise molecular nature of NR3 subunits in the optic nerve and in particular that of the identified splice variant, the full-length cDNA of these subunits was PCR amplified and cloned (figure V-2).

V.2.1.1 NR3A cloning

Full-length PCR amplification of NR3A resulted in a single band of the expected size (~4 kb). This band was cloned and sequenced. Although NR3A exists in 2 forms, NR3A-S (L34938) and NR3A-L (AF073379), resultant from the alternative splicing of a 60 bp exon (Ciabarra *et al*, 1995; Sasaki *et al*, 2002a; Sucher *et al*, 1995), all 4 sequenced clones from either the brain or the optic nerve corresponded to the short NR3A variant, NR3A-S. Due to the coding of an extra amino acid sequence in the C-terminal with putative phosphorylation sites, it is speculated that NR3A-L may be involved in specific interactions with postsynaptic proteins different from those of NR3A-S (Sasaki *et al*, 2002a; Sun *et al*, 1998). Since NR3A appears to be an important subunit in white matter and may interact differently with regulatory proteins, expression of NR3A-L was investigated in neonatal rat optic nerve. To confirm the absence of NR3-L in the neonate optic nerve, primers that span across the spliced region were designed to amplify this region (figure V-1B). The amplification yielded only one product of the size expected for NR3A-S (figure V-1B). Although NR3A-L is expressed in the neonate rat brain, I was unable to detect it (Sun *et al*, 1998).

V.2.1.2 NR3B cloning reveals a wealth of novel splice variants

Given the appearance of more than one NR3B transcript in RT-PCR (figure V-1A), it was expected that amplification of full-length NR3B would yield more than one product. When the NR3B full-length cDNA was amplified (figure V-2), 3 bands were present in the gel: 3.5 Kb; 3 Kb; and 2.3 Kb. These bands were extracted and cloned separately. As the bands of low molecular size could correspond to NR3B transcripts with deleted sequences, several primer pairs were used to probe the bacterial colonies (clones) by PCR colony screening. This

strategy was adopted to avoid bias against splice variants which lacked the primer binding sites of one primer pair, during selection of positive clones and thus giving false negative results.

Several positive clones from each band were sequenced and Blast search confirmed that each band corresponded to more than one NR3B transcript. Among the sequenced clones, several corresponded to the NR3B variant whose sequence is deposited in databases (NM133308.1). This variant will be henceforth referred to as NR3B for the sake of brevity. A large number of novel splice variants from both the neonate rat brain and optic nerve were also identified. When describing these novel variants I will refer to deletions and insertions on those novel variants. Please note that these deletions are relative to the canonical NR3B since this is the best characterized transcript. A complete list of all splice variants with molecular and structural details can be found in table V-1 and figures V-3 and V-4.

In total, eight novel NR3B splice variants were found in the rat optic nerve, six in the whole brain and two splice variants are common to both tissues (figure V-3, figure V-4 and table V-1). Five introns are alternatively retained (2, 5, 6, 7, 8), and no event of intron retention for introns 1, 3 and 4 was detected. Introns 5 and 6 are retained in NR3B cl#1, creating a shift in the reading frame and coding for a PTC in intron 5 (figure V-3). These two introns are also retained in NR3B cl#16 alongside a 185 nt intraexonic deletion at a canonical GT-AG splice junction in exon 3 (figure V-3). Only one variant, NR3B cl#24, was found containing intron 3 retained (figure V-3). NR3B cl#24 is also the variant with more introns retained, four, and also has 2 deletions: 384 nt using alternative donor-acceptor sites (GT-TG) inside exon 1 and exon 2; and the tandem repeat CCT in exon 3 and exon 5, resulting in 1146 nt being alternatively deleted (figure V-3).

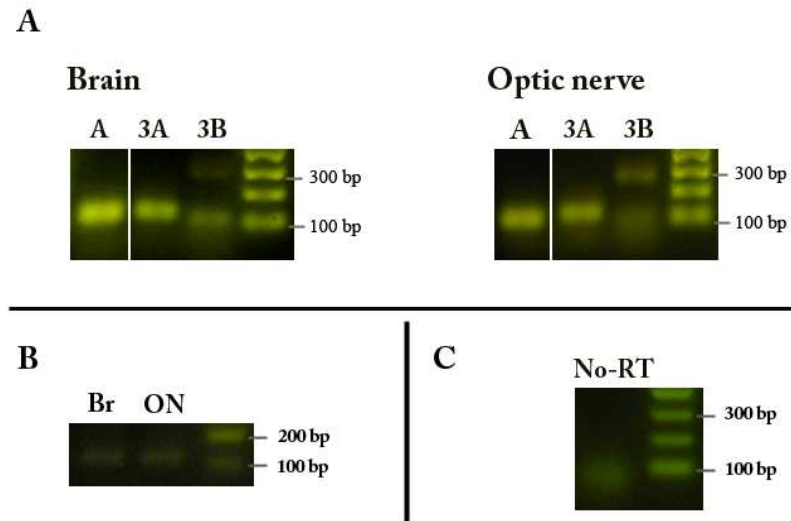


Figure V-1: Both NR3 subunits are expressed in the neonatal rat optic nerve

cDNA produced from neonate rat brain (panel A, left) and optic nerve mRNA (panel A, right), was PCR amplified using primers that amplify actin (A), PCR control, or the NR3 subunits: 3A, NR3A; 3B, NR3B. PCR products were separated in a 1.1% agarose gel, visualized with Sybr Safe dye, and the size of PCR products was estimated by comparison with a ladder (1 kb ladder, Invitrogen). Amplification products corresponding to the expected sizes were detected for each subunit. Expression of the two known NR3A splice variants was also tested (panel B). A primer pair was designed to anneal outside the spliced region to detect both variants, and used to amplify cDNA from the brain (Br) and optic nerve (ON). (C) A no-RT control was performed to exclude the possibility of genomic contamination in PCR reactions.

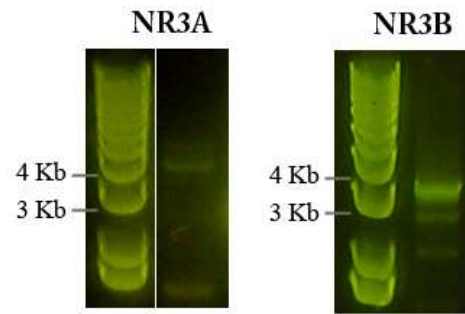


Figure V-2: Amplification of full-length NR3 cDNA from the RON

cDNA originating from neonate rat optic nerve mRNA was PCR amplified using primers annealing at the 5' and 3' UTR of NR3A and NR3B. PCR products were separated in a 1.1% agarose gel, visualized with Sybr Safe dye, and the bands sizes were estimated by comparison with a ladder (1 kb ladder, Invitrogen).

Four variants, NR3B cl#10, NR3B cl#12, NR3B cl#36 and NR3B cl#84, were found containing an 88 bp deletion. This deletion occurs intraexonically at +2379 nt using an alternative donor site inside exon 6 (GT) and exon 7 acceptor splice site (AG). The deletion causes a frame-shift resulting in a transcript without a termination codon (figure V-3). The 88 exon alternative deletion was the only variation in NR3B cl#84, but was accompanied by an 45 bp deletion in NR3B cl#12, using an alternative canonical splice site in exon 1 (1'', table V-2) and exon 2 acceptor site; a 161 bp deletion from nt +689 to +842 using the tandem repeat GGGGGAA as a splice junction in NR3B cl#10; in NR3B cl#36 in conjunction with a 335 bp deletion from nt +1390 to +1724 at the splice junction GT-TG. This 335 bp deletion in NR3B cl#36 leads to the coding of PTCs due to a frameshift (figure V-3). The alternative 45 bp deletion also generates NR3B Δ 45 (figure V-4 and V-5).

NR3B Δ 24 and NR3B cl#2 share a deletion of 24 bp that makes use of an alternative donor site in exon 1 (1', table V-2) and the acceptor site of exon 2 (figure V-3 and V-4). The alternative donor site 1', although canonical, appears to be weaker than the donor site used in NR3B (table V-2). There is a third alternative donor site in exon 1 used to generate NR3B Δ 45, 1'', which is relatively strong (table V-2 and figure V-5). NR3B cl#2 has two additional deletions of 161 nt and 630 nt with tandem repeats as splice sites: GGGGGAA and GGCC respectively. Although the 24 bp deletion does not change the NR3B cl#2 reading frame, the 162 deletion does, resulting in the coding of PTCs. The alternative donor site 1' is also used in conjunction with alternative donor sites (AG) inside intron 6 or intron 8, to generate NR3B cl#103 and NR3B cl#105 respectively (figure V-3). The deletions in these two variants are quite drastic and the predicted resulting polypeptides are less than a ¼ of the canonical NR3B protein.

Table V-1: NR3B splice variants

NR3B variants were found in the brain and in the rat optic nerve (RON). Alternative splicing can occur in one or more exons and or/ due to intron retention. The appearance of PTCs due to frame-shift of the reading frame is common to several variants.

Variant	Tissue	Intron retained	Number of deletions	ORF size (nt)	Predicted protein (a.a)	PTC +/-	Figure
NR3B _{Δ24}	brain		1 (24 nt at ex1)	2985	994	absent	V-4
NR3B _{Δ45}	brain/RON		1 (45 nt at ex1)	2964	987	absent	
NR3B _{Δ600}	RON		1 (600 nt at ex4-ex9)	2406	801	absent	
NR3B _{Δ1125}	RON		1 (1125 nt at ex3-ex9)	1884	627	absent	
NR3B cl#1	brain	5 and 6		3253	788	present	V-5
NR3B cl#2	brain		3 (24 nt at ex1; 155nt at ex2; 627nt at ex3)	2193	243	present	
NR3B cl#6	brain		1 (935 nt at ex1-ex3)	2066	105	present	
NR3B cl#10	brain		2 (155 nt at ex2; 88 nt at ex6-7)	2869	251	present	
NR3B cl#12	brain/RON		2 (45 nt at ex1; 88 nt at ex6-7)	2963 (including 3' UTR)	987	no stop codon	
NR3B cl#16	RON	5 and 6	1 (153 nt at ex3)	2253	371	present	
NR3B cl#24	RON	2; 6; 7; and 8	2 (384 nt at ex1-ex2; 1146 nt at ex3-5)	2089	135	present	
NR3B cl#36	brain		2 (326nt at ex3; 88 nt at ex6-7)	2695	522	present	
NR3B cl#75	RON		1 (901 nt at ex1-ex2)	2102	117	present	
NR3B cl#84	RON		1 (88 nt at ex6-7)	3008 (including 3'UTR)	1002	no stop codon	
NR3B cl#103	RON	6; 7; and 8		1271	186	present	
NR3B cl#105	RON		1 (entire ex2-ex7 sequence)	878	223	present	

Other variants were found containing extensive deletions. In NR3B cl#75 splicing at a tandem repeat, GGCCCGA, generates a transcript 907 nt shorter than NR3B. A transcript of only 937 nt, NR3B cl#6, was also found with an alternative deletions arising at the non-canonical splice junction GC-UG (figure V-3). Two variants were found that although containing extensive deletions retain the coding sequences of membrane domains, ligand-binding domains and part of the C-terminal domain. NR3B_{Δ600} has a 600 nt deletion due to the use of an alternative donor site at exon 4 and an alternative acceptor in exon 9, at the splice junction CG-UG (figure V-4). NR3B_{Δ1125} has an 1125 nt deletion due to the use of an alternative donor site at exon 3 and an alternative acceptor in exon 9, at the splice junction CU-GU (figure V-4).

V.2.1.3 Predicted structure of NR3B splice variants

The majority of the transcripts code for polypeptide chains lacking NMDA receptor membrane and ligand-binding domains (figure V-4). However, the four variants in which the reading frame remains unaltered retain some of typical NMDA receptors motifs (figure V-6). NR3B_{Δ24} and NR3B_{Δ45} lack 8 and 15 amino acids, respectively, in an overlapping region at the extracellular N-terminus and keep all membrane domains and the ligand-binding pocket (figure V-6; (Yao & Mayer, 2006). In NR3B_{Δ1125}, the deletion is predicted to lead to expression of a heavily truncated NR3B. Most of the protein sequence after M1 is missing (figure V-4 and V-6). Due to the extent of NR3B_{Δ600} and NR3B_{Δ1125} several putative phosphorylation and N-glycosylation sites are removed (figure V-6).

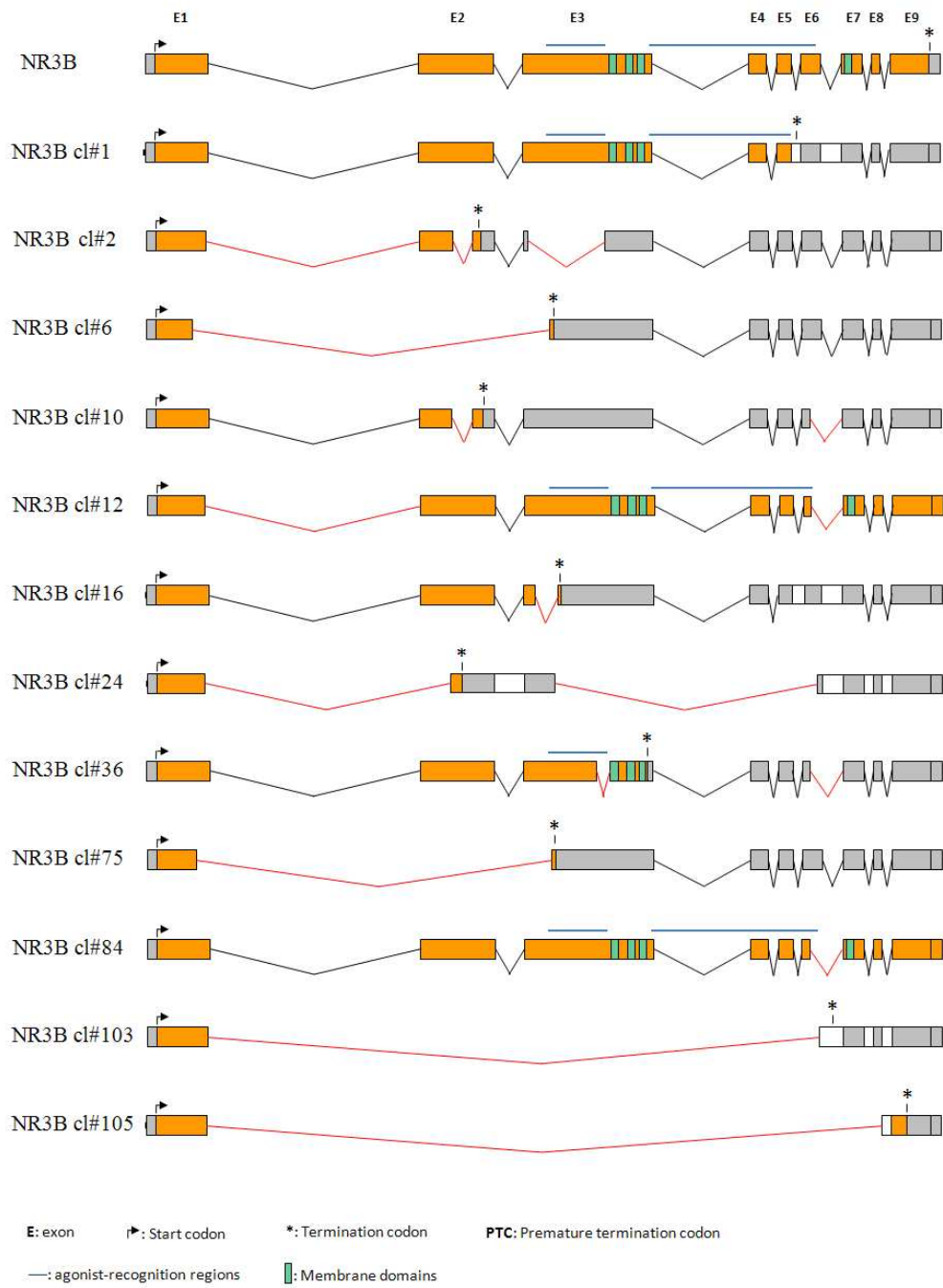


Figure V-3: Gene organization of *Grin3b* and NR3B splice variants predicted to be targeted for mRNA degradation pathways

Rat NR3B gene (*Grin2b*) has 9 exons and the coding region is represented by orange boxes. Non-coding regions are represented as gray boxes. Introns are excluded (black/red connecting lines) to give rise to the final mRNA molecule (accession# NM133308.2). In the newly identified variants a different pattern of intron exclusion occurs (red connecting lines) creating premature termination codons or absence of a stop codon in the transcript (NR3B cl#84). Exons and introns are drawn to scale. Variants here depicted were considered to be unlikely to be translated and thus its physiology was not assessed in chapter VI.

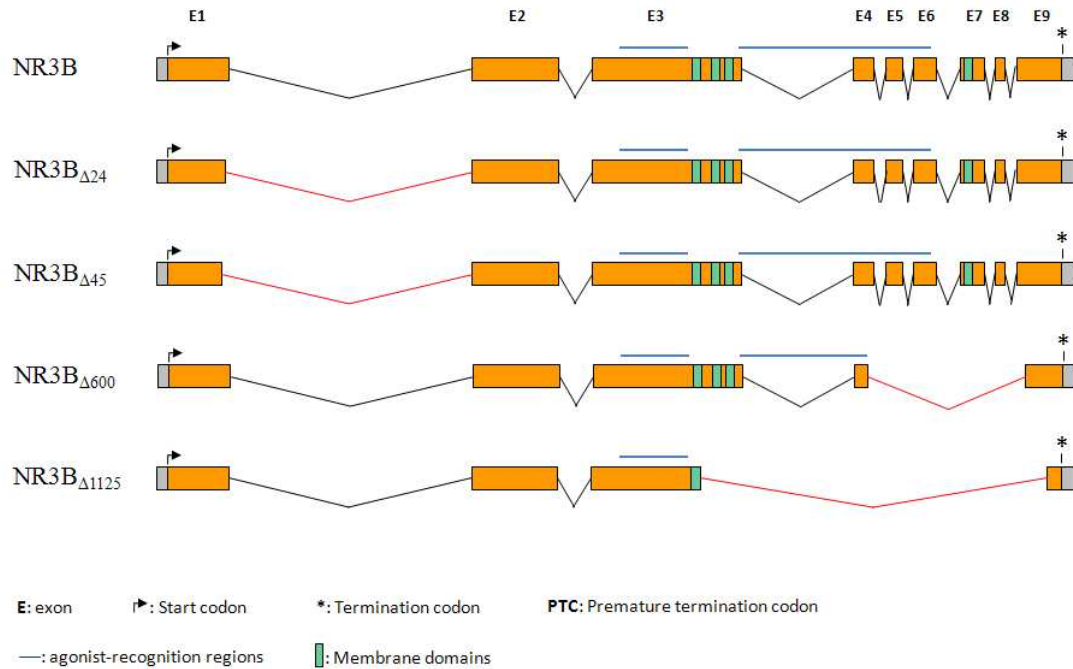


Figure V-4: NR3B splice variants that retain coding sequences for important NMDA receptor domains

Rat NR3B gene (*Grin2b*) has 9 exons and the coding region is represented by orange boxes. Non-coding regions are represented as gray boxes. Introns are excluded (black/red connecting lines) to give rise to the final mRNA molecule (accession# NM133308.2). In the newly identified variants NR3B_{Δ24}, NR3B_{Δ45}, NR3B_{Δ600} and NR3B_{Δ1125} a different pattern of intron exclusion occurs (red connecting lines). These variants retain important domains for NMDA receptor activity and share the same termination codon with the NR3B variant described in the literature. For this reason, they were chosen for recombinant expression in HEK293cells (chapter VI). Exons and introns are drawn to scale.

Table V-2: Splice site analyses of *Grin3B*

Analysis of splice site strength performed with the tool NNSPLICE. *Grin3B* has several exons with suboptimal splice sites. In conjunction with short introns, this leads to increased likelihood of intron retention (Lareau *et al*, 2004; Sakabe & de Souza, 2007; Stamm *et al*, 2000). Splice sites are bolded and exonic sequences are underlined. (1') 24 bp deletion: alternative donor in exon 1; (1'') 45 bp deletion: alternative donor in exon 1; (3') 1125 bp deletion: alternative donor in exon 3. A detailed scheme of splicing in exon 1 is depicted in figure V-5.

Splice junction (intron)	Donor 5' splice site	Acceptor 5' splice site	Donor site score	Acceptor site score
1	<u>CCG</u> GT ACGC	CCACCTCTT <u>CCC</u> AGA	0.95	0.40
2	<u>TCG</u> GT GAGT	TCTATATTCCAC AGG	0.99	0.98
3	<u>AAG</u> GT GAGG	TGTCT <u>CCCC</u> CAC AGC	1.00	0.46
4	<u>CAC</u> GT GAGT	GTCCTGCTCCAC AGG	0.99	0.92
5	<u>AGG</u> GT GAGT	CTCAATCTCCG CAGG	0.99	0.81
6	<u>GAG</u> GT GGGC	TTGACCATT <u>CGC</u> AGA	0.29	0.02
7	<u>CAG</u> GT GAGG	GTCTGTGCC <u>CTT</u> AGA	0.99	0.14
8	<u>CAG</u> GT GAGC	CTCCTCTGT <u>CCC</u> AGC	0.98	0.93
1'	<u>GAG</u> GT GCGC		0.35	
1''	<u>GTG</u> GT GAGC		0.87	
3'	<u>CCT</u> GT ACGA		0.07	

The 200 amino acids deletion in NR3B_{Δ600} may have an interesting structural consequence. The resultant polypeptide will lack M4 and part of the intracellular C-terminus (figure V-6). This means that the C-terminal, located intracellularly in NMDA receptors, will be extracellular in NR3B_{Δ600}. To confirm this prediction, the polypeptide sequences of NR3B and NR3B_{Δ600} were analyzed using an algorithm to detect putative membrane regions (figure V-7). As expected, NR3B has four predicted membrane domains, whereas NR3B_{Δ600} is lacking

M4 (figure V-6 and V-7). This indicates that NR3B_{Δ600} remaining C-terminus sequence is located extracellularly rather than intracellularly as it occurs in NR3B (figure V-7).

V.2.1.4 Addendum to annotated NR3B mRNA sequence

I should point out that while analysing the sequences in search of possible mutated amino acids, a recurrent amino acid differed from the annotated sequence: S186G. This is the result of a single nucleotide difference, A -> G (+558 bp), between our NR3B clones and the deposited sequence in the NCBI database (NM_133308.2). This is unlikely to be due to rat strains polymorphisms since it was found in clones from Wistar and lister hooded animals. We will upload this corrected sequence to NCBI nucleotide database.

```
NR3BΔ24 GCCGCCACAGAGACCCAGTGGTGAGCGTCCTGCGGAGGGAG-----  
NR3BΔ45 GCCGCCACAGAGACCCAGTG-----  
NR3B    GCCGCCACAGAGACCCAGTGGTGAGCGTCCTGCGGAGGGAGGTGCGCACGGCCCTCGGA
```

Figure V-5: Sequence alignment the splice junction of canonical NR3B, NR3B_{Δ24} and NR3B_{Δ45}

Splicing of NR3B_{Δ24}, NR3B_{Δ45} occurs intraexonically at the consensus 5' site GT. The variants differ in the location of the splice site by 24 nt. Regions where splicing occurs are delimited by red boxes. Traces represent non-homologous regions.

Chapter V – Cloning of novel NR3 splice variants

```

*      20      *      40      *      60      *      80      *      100
NR3B   MESVRTLWLSVALALAVGSRVVRGHPQPCRVPTRAGASVRLAALLPRAPAARARVLAALATPAPRLPHNLSLELVAVASPTRDPASLARGLCQVLPAPGV
NR3BΔ24 MESVRTLWLSVALALAVGSRVVRGHPQPCRVPTRAGASVRLAALLPRAPAARARVLAALATPAPRLPHNLSLELVAVASPTRDPASLARGLCQVLPAPGV
NR3BΔ45 MESVRTLWLSVALALAVGSRVVRGHPQPCRVPTRAGASVRLAALLPRAPAARARVLAALATPAPRLPHNLSLELVAVASPTRDPASLARGLCQVLPAPGV
NR3BΔ600 MESVRTLWLSVALALAVGSRVVRGHPQPCRVPTRAGASVRLAALLPRAPAARARVLAALATPAPRLPHNLSLELVAVASPTRDPASLARGLCQVLPAPGV
NR3BΔ1125 MESVRTLWLSVALALAVGSRVVRGHPQPCRVPTRAGASVRLAALLPRAPAARARVLAALATPAPRLPHNLSLELVAVASPTRDPASLARGLCQVLPAPGV

*      120     *      140     *      160     *      180     *      200
NR3B   VASIAFPEARPELRLQLAAATETPVVSVLRREVRTALGAPTPFHLQLDWASPLETILDVLSLVRAHAWEDIALVLCRVRDPGGLVTLWNTNHASQAPK
NR3BΔ24 VASIAFPEARPELRLQLAAATETPVVSVLRRE-----TPFHLQLDWASPLETILDVLSLVRAHAWEDIALVLCRVRDPGGLVTLWNTNHASQAPK
NR3BΔ45 VASIAFPEARPELRLQLAAATETPV-----TPFHLQLDWASPLETILDVLSLVRAHAWEDIALVLCRVRDPGGLVTLWNTNHASQAPK
NR3BΔ600 VASIAFPEARPELRLQLAAATETPVVSVLRREVRTALGAPTPFHLQLDWASPLETILDVLSLVRAHAWEDIALVLCRVRDPGGLVTLWNTNHASQAPK
NR3BΔ1125 VASIAFPEARPELRLQLAAATETPVVSVLRREVRTALGAPTPFHLQLDWASPLETILDVLSLVRAHAWEDIALVLCRVRDPGGLVTLWNTNHASQAPK

*      220     *      240     *      260     *      280     *      300
NR3B   FVLDIRLDSRNDLSRAGLALLGALEGGGTVPAAVLLGCSTARAHEVLEAAPPQPWLLGTPLPAEALPTTGLPPGVLAGGETEQHSLEAVVHDMVELV
NR3BΔ24 FVLDIRLDSRNDLSRAGLALLGALEGGGTVPAAVLLGCSTARAHEVLEAAPPQPWLLGTPLPAEALPTTGLPPGVLAGGETEQHSLEAVVHDMVELV
NR3BΔ45 FVLDIRLDSRNDLSRAGLALLGALEGGGTVPAAVLLGCSTARAHEVLEAAPPQPWLLGTPLPAEALPTTGLPPGVLAGGETEQHSLEAVVHDMVELV
NR3BΔ600 FVLDIRLDSRNDLSRAGLALLGALEGGGTVPAAVLLGCSTARAHEVLEAAPPQPWLLGTPLPAEALPTTGLPPGVLAGGETEQHSLEAVVHDMVELV
NR3BΔ1125 FVLDIRLDSRNDLSRAGLALLGALEGGGTVPAAVLLGCSTARAHEVLEAAPPQPWLLGTPLPAEALPTTGLPPGVLAGGETEQHSLEAVVHDMVELV

*      320     *      340     *      360     *      380     *      400
NR3B   AQALESMLVHPERALLPAVNVCDLKTGGSEATGRTLARFLGNTSFQGRGTGAVVVTGSSQVHVSRRHFVWMSLRRLDPLGAPAWATVGSWQDGLDFQPGA
NR3BΔ24 AQALESMLVHPERALLPAVNVCDLKTGGSEATGRTLARFLGNTSFQGRGTGAVVVTGSSQVHVSRRHFVWMSLRRLDPLGAPAWATVGSWQDGLDFQPGA
NR3BΔ45 AQALESMLVHPERALLPAVNVCDLKTGGSEATGRTLARFLGNTSFQGRGTGAVVVTGSSQVHVSRRHFVWMSLRRLDPLGAPAWATVGSWQDGLDFQPGA
NR3BΔ600 AQALESMLVHPERALLPAVNVCDLKTGGSEATGRTLARFLGNTSFQGRGTGAVVVTGSSQVHVSRRHFVWMSLRRLDPLGAPAWATVGSWQDGLDFQPGA
NR3BΔ1125 AQALESMLVHPERALLPAVNVCDLKTGGSEATGRTLARFLGNTSFQGRGTGAVVVTGSSQVHVSRRHFVWMSLRRLDPLGAPAWATVGSWQDGLDFQPGA

*      420     *      440     *      460     *      480     *      500
NR3B   AALRVPSPSGTQARPKLRVTVLVEHFFVFTRESDEDDGQCPAGQLCLDPGTNDSARLDALFAALVNGSVVPTLRRCYGYCIDLLERLAEDLAFDFELYIV
NR3BΔ24 AALRVPSPSGTQARPKLRVTVLVEHFFVFTRESDEDDGQCPAGQLCLDPGTNDSARLDALFAALVNGSVVPTLRRCYGYCIDLLERLAEDLAFDFELYIV
NR3BΔ45 AALRVPSPSGTQARPKLRVTVLVEHFFVFTRESDEDDGQCPAGQLCLDPGTNDSARLDALFAALVNGSVVPTLRRCYGYCIDLLERLAEDLAFDFELYIV
NR3BΔ600 AALRVPSPSGTQARPKLRVTVLVEHFFVFTRESDEDDGQCPAGQLCLDPGTNDSARLDALFAALVNGSVVPTLRRCYGYCIDLLERLAEDLAFDFELYIV
NR3BΔ1125 AALRVPSPSGTQARPKLRVTVLVEHFFVFTRESDEDDGQCPAGQLCLDPGTNDSARLDALFAALVNGSVVPTLRRCYGYCIDLLERLAEDLAFDFELYIV

*      520     *      540     *      560     *      580     *      600
NR3B   GDGKYGALRDGRWTGLVGDLLAGRAHMAVTSFINSARSQVVDFTSPPFFSTSLGIMVTRDTASPIGAFMPLHWSMWWGVFAALHLTALFLTYEWRSP
NR3BΔ24 GDGKYGALRDGRWTGLVGDLLAGRAHMAVTSFINSARSQVVDFTSPPFFSTSLGIMVTRDTASPIGAFMPLHWSMWWGVFAALHLTALFLTYEWRSP
NR3BΔ45 GDGKYGALRDGRWTGLVGDLLAGRAHMAVTSFINSARSQVVDFTSPPFFSTSLGIMVTRDTASPIGAFMPLHWSMWWGVFAALHLTALFLTYEWRSP
NR3BΔ600 GDGKYGALRDGRWTGLVGDLLAGRAHMAVTSFINSARSQVVDFTSPPFFSTSLGIMVTRDTASPIGAFMPLHWSMWWGVFAALHLTALFLTYEWRSP
NR3BΔ1125 GDGKYGALRDGRWTGLVGDLLAGRAHMAVTSFINSARSQVVDFTSPPFFSTSLGIMVTRDTASPIGAFMPLHWSMWWGVFAALHLTALFLTYEWRSP

*      620     *      640     *      660     *      680     *      700
NR3B   YGLTPRGRNRGTVFYSYSSALNLCYAILFGRTVSSKTPKCPTRFLMNLWAIFFCLLVLSYTYANLAAMVVGDKTFEELLSGIHDPKLLHHPSSQGFRTVWES
NR3BΔ24 YGLTPRGRNRGTVFYSYSSALNLCYAILFGRTVSSKTPKCPTRFLMNLWAIFFCLLVLSYTYANLAAMVVGDKTFEELLSGIHDPKLLHHPSSQGFRTVWES
NR3BΔ45 YGLTPRGRNRGTVFYSYSSALNLCYAILFGRTVSSKTPKCPTRFLMNLWAIFFCLLVLSYTYANLAAMVVGDKTFEELLSGIHDPKLLHHPSSQGFRTVWES
NR3BΔ600 YGLTPRGRNRGTVFYSYSSALNLCYAILFGRTVSSKTPKCPTRFLMNLWAIFFCLLVLSYTYANLAAMVVGDKTFEELLSGIHDPKLLHHPSSQGFRTVWES
NR3BΔ1125 -----

*      720     *      740     *      760     *      780     *      800
NR3B   SAEAYIKASFPEMHAHMRRHSAPTPHGVAMLTSDPPKLNAFIMDKSLLDVEVSDADCKLLTVGKPPFAIEGYGIGLPQNSPLTSLNLSSEFISRYKSSGFI
NR3BΔ24 SAEAYIKASFPEMHAHMRRHSAPTPHGVAMLTSDPPKLNAFIMDKSLLDVEVSDADCKLLTVGKPPFAIEGYGIGLPQNSPLTSLNLSSEFISRYKSSGFI
NR3BΔ45 SAEAYIKASFPEMHAHMRRHSAPTPHGVAMLTSDPPKLNAFIMDKSLLDVEVSDADCKLLTVGKPPFAIEGYGIGLPQNSPLTSLNLSSEFISRYKSSGFI
NR3BΔ600 SAEAYIKASFPEMHAHMRR-----
NR3BΔ1125 -----

*      820     *      840     *      860     *      880     *      900
NR3B   DLLHDKWYKMPVCGKRVFAVTETLQMGVYHFSGLFVLLCLGLGSALLTSLGHEVFYRLVLPRIIRRGKLNQYWLHTSQKIHRAALNTGPPPGQERAEQERS
NR3BΔ24 DLLHDKWYKMPVCGKRVFAVTETLQMGVYHFSGLFVLLCLGLGSALLTSLGHEVFYRLVLPRIIRRGKLNQYWLHTSQKIHRAALNTGPPPGQERAEQERS
NR3BΔ45 DLLHDKWYKMPVCGKRVFAVTETLQMGVYHFSGLFVLLCLGLGSALLTSLGHEVFYRLVLPRIIRRGKLNQYWLHTSQKIHRAALNTGPPPGQERAEQERS
NR3BΔ600 -----
NR3BΔ1125 -----

*      920     *      940     *      960     *      980     *      1000
NR3B   GPKDELPAIDGAGRWRVRRAVERERRVRFLEPGEAGGDRPWLCNSNGPGLQAELELELRIEAARERLRSALLRRGELRALLGDGTRLRPLRLLHAAPA
NR3BΔ24 GPKDELPAIDGAGRWRVRRAVERERRVRFLEPGEAGGDRPWLCNSNGPGLQAELELELRIEAARERLRSALLRRGELRALLGDGTRLRPLRLLHAAPA
NR3BΔ45 GPKDELPAIDGAGRWRVRRAVERERRVRFLEPGEAGGDRPWLCNSNGPGLQAELELELRIEAARERLRSALLRRGELRALLGDGTRLRPLRLLHAAPA
NR3BΔ600 -----AVERERRVRFLEPGEAGGDRPWLCNSNGPGLQAELELELRIEAARERLRSALLRRGELRALLGDGTRLRPLRLLHAAPA
NR3BΔ1125 -----RSALLRRGELRALLGDGTRLRPLRLLHAAPA

```

NR3B ES
NR3BΔ24 ES
NR3BΔ45 ES
NR3BΔ600 ES
NR3BΔ1125 ES

Figure V-6: Alignment of NR3B variants predicted polypeptide sequences

The deduce polypeptide sequence of NR3B and four novel splice variants that are predicted to form functional receptors was aligned using the software GeneDoc (<http://www.nrbsc.org/gfx/genedoc/>). Putative sites are shown for glycosylation (yellow boxes) and possible sites for protein kinase C (red boxes), Ca²⁺/calmodulin-dependent protein kinase II (green boxes), and tyrosine kinase (blue boxes) as analyzed by PROSITE. The putative phosphorylation sites were also assessed for strength using NetPhos2.0 (<http://www.cbs.dtu.dk/services/NetPhos/>). Only sites with high scores are listed. Bars show membrane-spanning regions (M1–M4) and ligand binding domains (S1 and S2).

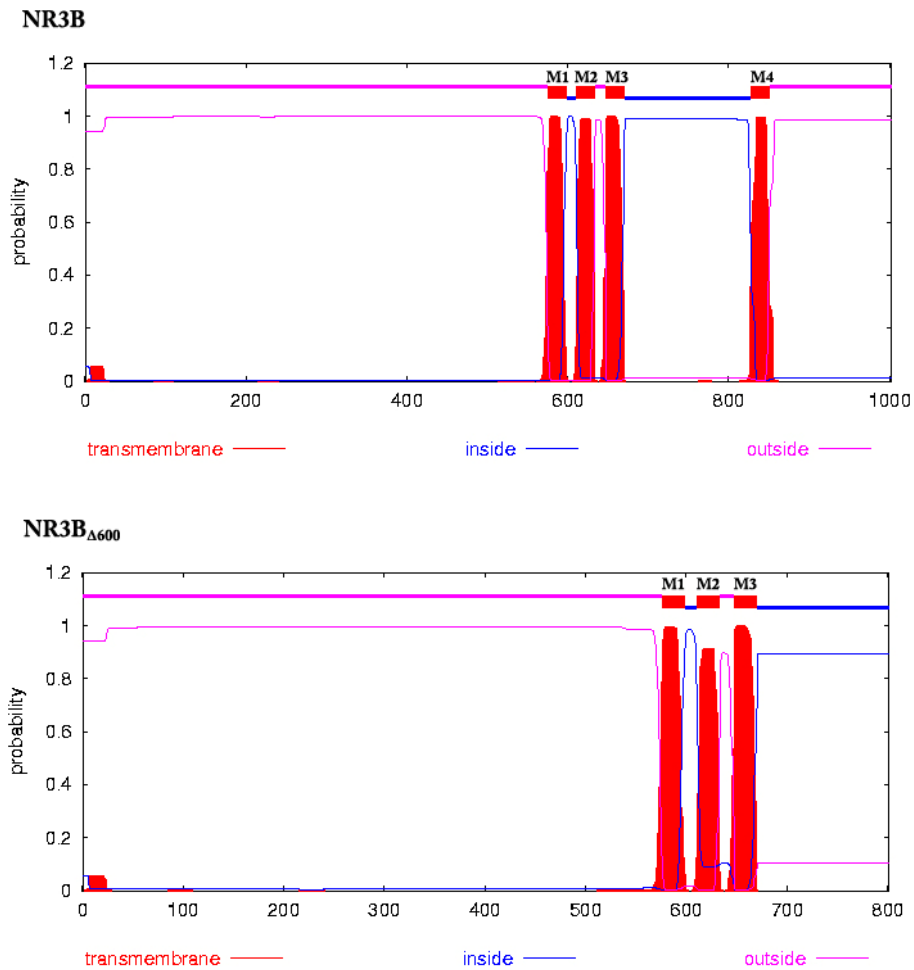


Figure V-7: Transmembrane domain prediction of NR3B and NR3B_{Δ600}

Transmembrane domains were predicted using the TMHMM analysis algorithm (version 2.0, <http://www.cbs.dtu.dk/services/TMHMM-2.0/>). Red regions indicated possible transmembrane domains with the relative probability of each indicated on the Y axis. Pink and blue regions denote predicted extracellular and intracellular domains, respectively. According to the algorithm NR3B has four membrane domains and NR3B_{Δ600} lacks M4. This algorithm is not able to predict membrane loops, and thus, although M2 is represented as a transmembrane domain, it is a membrane loop. Consequently, NR3B C-terminus is intracellular and NR3B_{Δ600} C-terminus extracellular (see figure V-4).

V.3 DISCUSSION

In this chapter I have found that both NR3 subunits are expressed in rat white and gray matter. Full-length transcripts of these subunits were cloned and sequenced, revealing that NR3B undergoes extensive alternative splicing whereas no splice variant for NR3A was detected. The molecular properties of NR3B variants were also investigated.

V.3.1 NR3 expression in white matter

In previous work two different molecular approaches were used to detect NR3-B expression in rodent white matter: (1) antibodies that do not select between NR3A and NR3B proteins (Micu *et al*, 2006), or (2) PCR amplification of mRNA with specific primers for the two subunits (Salter & Fern, 2005). Although NR3 expression was detected with antibodies, no conclusion could be made with regard to the identity of NR subunits expressed in white matter. On the other hand, PCR amplification of NR3A mRNA was achieved whereas NR3B mRNA was not detected (Micu *et al*, 2006; Salter & Fern, 2005). I was able to amplify and clone NR3A and NR3B from the neonate rat optic nerve. NR3B expression is not due to non-specific PCR amplification since sequencing confirmed the identity of amplified sequences. Thus, NR3B mRNA is expressed in rat white matter.

What could explain the failure to detect NR3B expression in the mouse optic nerve (Salter & Fern, 2005)? It could be either due to species differences in mRNA expression but *Grin3B* is highly conserved between these two species (>80% overall sequence identity and 92% identity at gene promoter regions). Another possibility is related to technical issues. RNA extraction from the mouse optic nerve yields less RNA than from the rat. Also, analysis of the primers used in previous work indicated that these might not be efficient enough for NR3B detection (Salter & Fern, 2005). Despite these considerations, the results here presented clearly show that both NR3A and NR3B are expressed in the developing white matter.

NR3A is expressed in two different forms due to alternative splicing: NR3A-L and NR3A-S. Their expression is somewhat different in that NR3A-S is more widely distributed in the brain and total NR3A-S mRNA levels are higher (Sasaki *et al*, 2002a; Sun *et al*, 1998). Expression of NR3A-L splice variant was not detected in the neonate optic nerve or brain (figure V-1B). Furthermore, cloning of full-length NR3A resulted in several NR3A-S clones but NR3A-L was not cloned. This is not particularly surprising as animal used were aged P10-14 and expression of both variants decreases sharply after P7. In addition, NR3A-L expression is more restricted than NR3A-S, possibly accounting for the lack of detection of NR3A-L (Sasaki *et al*, 2002a; Sun *et al*, 1998). In addition, novel NR3A splice variants were not identified although the approach used here was designed to thoroughly screen NMDA receptor transcripts. Given the expression profile of NR3A during development, I cannot exclude the possibility that other NR3A variants are expressed at earlier developmental stages.

V.3.2 Novel NR3B splice variants

V.3.2.1 Structural and functional consequences of NR3B splicing

In contrast to NR3A, for which only one transcript was identified, I have cloned a large number of novel NR3B splice variants from the optic nerve and the brain (table V-1, figures V-3 and V-4). Although the majority of these variants contain PTCs, four variants are originated by deletions that do not alter the reading frame: NR3B Δ 24; NR3B Δ 45; NR3B Δ 600 and NR3B Δ 1125 (table V-1, figure V-4 and V-6). NR3B Δ 24 and NR3B Δ 45 maintain all important NMDA receptor domains and no important residues appear to have been deleted (figure V-6). The deleted regions in these variants are located at the extracellular N-terminus, outside ligand-binding domains, and can possibly affect regulation NR3B activity by extracellular molecules (Yao & Mayer, 2006). These variations share some similarities with NR1 N1 insert (figure III-1). This insertion is relatively small in length (21 amino acids) and occurs outside the ligand binding-pockets. Nonetheless, N1 regulates NMDA receptor inhibition by

extracellular molecules (Hollmann *et al*, 1993; Traynelis *et al*, 1998). NR1 and NR3 also have in common glycine binding pockets (Hirai *et al*, 1996; Yao & Mayer, 2006). It is thus fair to speculate that the deletions, albeit minor in length, could modulate NMDA receptor pharmacological properties and/or affect protein folding and binding pocket accessibility.

NR3B_{Δ600} and NR3B_{Δ1125} suffer major changes as a result of the splicing (figure V-4 and V-6). NR3B_{Δ600} has a truncated S2 and lacks M4 entirely, resulting in a protein whose C-terminal domain is extracellular (figure V-4, V-6 and V-7). The truncation in the S2 is likely to affect glycine binding and receptor activity (Yao & Mayer, 2006). In NR3B_{Δ1125}, S2 is absent and only M1 is present. Despite the extent of these deletions, the remaining sequence is identical to that of NR3B and uses the same stop codon, indicating that these variants might be expressed and form functional receptors. Deletions at the C-terminal are likely to affect interaction with NR1 (or other NR3B-interacting proteins yet to be identified) and consequently trafficking of receptors to the membrane and receptor activity (Matsuda *et al*, 2003; Perez-Otano *et al*, 2006). NR3A C-terminal interactions with post-synaptic proteins is important for activity dependent endocytosis of NMDA receptors (Perez-Otano *et al*, 2006). This mechanism appears to be important for rapid local regulation of NMDA receptors and synapse formation during development (Das *et al*, 1998; Perez-Otano *et al*, 2006). It is possible that NR3B activity could be modulated by regulation of alternative splice variants expression that limits endocytosis (Prithviraj & Inglis, 2008).

V.3.2.2 Translation of splice variants

Due to the nature of NR3B_{Δ24} and NR3B_{Δ45} deletions, it is likely that these variants are translated and form functional channels in combination with NR1 and NR2 subunits. How about NR3B_{Δ600} and NR3B_{Δ1125}? On the one hand, the deletions do not alter the transcripts reading frame and nothing suggests in their molecular nature that these variants are targeted for degradation (Buhler *et al*, 2006; Maquat, 2004). On the other hand, their predicted structures lack important domains and NR3B_{Δ600} structure is somewhat at odds with a

“typical” NMDA receptor. This is not the first reported example of alternative spliced receptors that although lacking important functional domains are functional. For example, glycine receptor (GlyR) splice variant $\beta_{\Delta 7}$, despite lacking 2 out of 4 membrane domains, forms functional complexes with GlyR $\alpha 1$ (Oertel *et al*, 2007). This indicates that these new variants could be translated and form functional NMDA receptors.

Expression of NR1 with a NR2A mutant lacking the C-terminal tail produces functional channels, but the absence of the C-terminus alters the pharmacology of NR1/NR2A receptors (Puddifoot *et al*, 2009). C-terminal truncation increases NR1/NR2A glycine potency and alters Mg²⁺-block at low Mg²⁺ concentrations (Puddifoot *et al*, 2009). Also, truncation of NR2A M4 and C-terminal tail results in non-functional channels whose activity is partially restored by co-expression of the removed M4+C-terminal (Schorge & Colquhoun, 2003). Since NR3B is a modulatory NMDA receptor subunit, non-essential for the assembly of functional receptors, it is possible that NR3B $\Delta 600$ and NR3B $\Delta 1125$ can have modulatory roles in NMDA receptor activity.

Part of the splice variants here reported arise from a variety of molecular modifications which included alternative deletions, inclusions or a combination of both events (figure V-3-4 and table V-1). The inclusions found are a result of intron retention and regardless of the combinations, these events often lead to a change in the mRNA reading frame and the coding of PTCs (figure V-3 and table V-1). Some of NR3B variants found result from intraexonic splicing (Chikaev *et al*, 2005; Cox *et al*, 2001; van der Ven *et al*, 2006). These alternative intraexonic deletions can occur due to the presence of splice sites within the exon, or even in the absence of any known non-canonical splice sites, which seems to be the case for all the intraexonic deletions found (figure V-3) (Chikaev *et al*, 2005; Cox *et al*, 2001). GlyR $\alpha 1$ has several splice variants due to the use of alternative acceptor sites in exon 9. One the variants, GlyR $\alpha 1^{\text{del}}$, is originated in a non-canonical GT-CA. The resulting protein is truncated, generating a protein with a shortened loop between M3 and M4. Despite this truncation,

GlyR $\alpha 1^{\text{del}}$ forms functional glycinergic receptors with comparable properties to that of GlyR $\alpha 1$ (Inoue *et al.*, 2005).

Similarly to NR2 splice variants, one has to question whether these transcripts are biological products or cloning artefacts. Firstly, intron retention events are unlikely to be genomic contamination (figure V-1C). Secondly, it is now accepted that there is a variety of alternative splicing modes and non-canonical splice can originate functional splice variants (Brackenridge *et al.*, 2003; Gillespie *et al.*, 1995; Hiller & Platzner, 2008; Inoue *et al.*, 2005). If these variants were a mere PCR or RT artefacts one would expect deleted sequences and/or insertion of duplicated sequences (Chabot *et al.*, 2008; Roy & Irimia, 2008). However, intron retention events are unlikely to be genomic contamination (figure V-1 and materials and methods), excluding the possibility that these variants are artefacts.

V.3.2.3 Unsung NR3B splice variants

At the time this project started we were unaware of any reported NR3B splice variants. Indeed, there is no deposited NR3B splice variants sequence in NCBI repository. In the past months, it came to our attention that other groups have identified NR3B variants. A variant lacking M4 similarly to NR3B $_{\Delta 600}$, was cloned from the human spinal cord. This variant uses non-canonical splice sites (GC-GG) between exon 8 and exon 9 (O. Bendel personal communication and (Bendel, 2008)). After cloning, the authors did not investigate this variant further.

In a similar experiment to ours, when probing for NR3B gene expression, McRoberts and colleagues amplified a region of rat NR3B gene which yielded two products. One of the products was the result of a transcript containing intron 6 (figure V-1). Furthermore, this group designed a series of primers for NR3B mRNA and found multiple transcripts in adult rat dorsal root ganglia (DRG) primary sensory neurons due to intron retention between exons E4-E8 (McRoberts *et al.*, 2003) and JA James A. McRoberts, personal communication,

unpublished data). These results confirm our findings that multiple NR3B variants are expressed in gray and white matter. The occurrence of NR3B splicing in humans indicates that NR3B alternative splicing exists across mammalian species and is evolutionary conserved.

Table V-3: Sizes of rat NMDA receptors genes

Rat NMDA receptors genes are highly variably in length and number of exons. The number of exons appears to be conserved in the subclasses of NMDA receptors. NR3B is the smallest gene.

Gene	length (bp)	Exons
<i>Grin1</i>	26.592	22
<i>Grin2A</i>	417.141	13
<i>Grin2B</i>	461.293	13
<i>Grin2C</i>	17.998	15
<i>Grin2D</i>	38.384	13
<i>Grin3A</i>	195.684	9
<i>Grin3B</i>	6.324	9

A common outcome of intron retention is the insertion of premature stop codons in the mature transcript often leading to degradation by non-sense mediated decay (Galante *et al*, 2004; Lareau *et al*, 2004). This, however, is not the fate of all mRNAs with a retained intron. For example, an isoform of the mouse *tgif2* gene that retains an intron in the coding region was shown to have biological activity (Melhuish & Wotton, 2006). Even when intron retention marks a transcript for degradation, it can be biologically relevant (Lareau *et al*, 2004). Expression of the intron-retaining and intron-spliced isoforms varies along tissues, indicating that cellular factors are also involved in the control of intron retention (Stamm *et al*, 2000). In fact, decreasing the levels of mRNAs of a given gene can be a function of alternative splicing. Apolipoprotein (apo) E4 has an alternative spliced isoforms resultant from intron 3 retention (apoE-I3) (Xu *et al*, 2008). These transcripts are retained in the nucleus and are not translated in protein. Neuronal expression of apoE is controlled by transcription of apoE-I3

under normal conditions and by processing of apoE-I3 into mature apoE mRNA in response to injury (Xu *et al*, 2008). NR1 also has an mRNA isoform resulting from intron 11 retention that contains an in-frame stop codon (Campusano *et al*, 2005). The mRNA of this NR1 variant is expressed in various brain regions of the rat embryo but not in the adult. Interestingly, expression of the novel NR1 mRNA isoform is regulated by both BDNF and metabotropic receptors activity (Campusano *et al*, 2005). This establishes a precedent for regulated intron retention in NMDA receptors and suggests a role for this mechanism in regulation of glutamatergic neurotransmission in the developing central nervous system.

Intron retention is one of the major forms of alternative splicing and our results suggest that it is more prevalent in NR3B than in other NMDA receptor genes (Matlin *et al*, 2005). Before this work, only one splice variant resulting from intron retention in NR1 had been described (Campusano *et al*, 2005). Several mechanistic explanations have been put forward to explain intron retention. An intuitive explanation is that retained introns are flanked by weak splice sites that might not be properly recognized by the splicing machinery (Lareau *et al*, 2004; Sakabe & de Souza, 2007; Stamm *et al*, 2000). It has been reported that strengthening sub-optimal splice sites flanking retained introns caused an increase in their removal levels or completely abolished retention (Dirksen *et al*, 1995; Romano *et al*, 2001). Another observation is that retained introns tend to be shorter and to occur in genes with overall shorter introns (Sakabe & de Souza, 2007). This could provide an explanation for the extent of intron retention in NR3B. *Grin3B* is the NMDA receptor gene with the smallest length and has compact gene architecture in the 3' end (table V-3 and V-4; figure V-4). In addition, donor and acceptor splice sites of exons 6-8 are weak (table V-2). This genomic structure may put pressure on splicing machineries for intron recognition thus increasing likelihood of intron retention in NR3B (Sakabe & de Souza, 2007).

Table V-4: *Grin3B* intron-exon organization

NR3B gene organization (NC005106) is quite compact towards the 3' end of the gene. In this region relatively small exons are separated by small size introns and this organization may complicate intron-exon recognition by the splicing machinery leading to increased intron retention.

Exon	Start	End	Exon size	Intron size
Ex 1	5830	6323	493	1674
Ex 2	3561	4156	595	232
Ex 3	2298	3331	1033	765
Ex 4	1386	1534	148	81
Ex 5	1189	1305	116	75
Ex 6	962	1114	152	168
Ex 7	629	795	166	76
Ex 8	485	554	69	81
Ex 9	7	406	399	

V.3.3 *Grin3B* polymorphic nature may be the cause of extensive alternative splicing

Human *Grin3B* has a single nucleotide polymorphism per ~300 bp which is higher than the average gene (1 per ~1.400) (Altshuler *et al*, 2000; Niemann *et al*, 2008). Another frequent variation in human *Grin3B* is a small 4bp insertion in exon 3 that disrupts mRNA reading frame leading to non-functional protein (Niemann *et al*, 2008). Importantly, this null allele is present in ~10% of the human European-American population without any observable clinical or physiological consequence, consistent with the modulatory role of NR3B (Chatterton *et al*, 2002; Niemann *et al*, 2008; Nishi *et al*, 2001). In the adult brain, NR3B subunit may participate in activity-dependent reorganization of dendritic architecture and ablation of NR3B results in subtle behavioural changes (Niemann *et al*, 2007; Prithviraj & Inglis, 2008). Whether this role of NR3B is redundant and other proteins might compensate

for the absence of NR3B is still unknown. However, it seems unlikely that in the adult brain NR3A performs this compensatory role since its expression is low and restricted (Hon-Kit Wong, 2002).

Alternative splicing is a major source of functional diversity in animal proteins and may play a role in genome evolution by allowing new exons to evolve with less constraint (Boue *et al*, 2003). A possible way in which alternative splicing participates in evolution is by incorporation of new exons in a small number of transcripts. These minor transcripts would be free to “evolve”, that is, undergo selection for new function and improved fitness of the organism, while the original transcript form would still accomplish its function (Boue *et al*, 2003; Kondrashov & Koonin, 2003). Recently, it was demonstrated that genes implicated in various aspects of the nervous system show accelerated rates of evolution during human evolution and one of those genes could be NR3B (Dorus *et al*, 2004; Niemann *et al*, 2008). It is thought provoking to conceive that the NR3B variants herein described are part of this recent evolutionary process. Considering that NR3B is undergoing selective pressure, some of these variants could be gene products being tested for functionality. If functional and judging by the molecular structure of some that is likely, these variants could evolve to become major isoforms. That is, NR3B, unlike the other NMDA receptor subunits, is still evolving and the observed splice variants are part of that evolutionary process.

In conclusion, several novel NR3B splice variants were cloned. Of these, I proposed that four (NR3B Δ ₂₄; NR3B Δ ₄₅; NR3B Δ ₆₀₀ and NR3B Δ ₁₁₂₅) encode for functional receptor subunits with modified properties, thus increasing NMDA receptor functional diversity. This hypothesis was tested and the results are in the following chapter.

Chapter VI

Physiology of NR3 subunits

VI.1 INTRODUCTION

VI.1.1 NR3 modulatory properties

NR3 subunits are NMDA receptor modulatory subunits. NR3A and NR3B homomers, or NR1/NR3 and NR2/NR3 diheteromers, do not form functional glutamate channels (Ciabarra *et al*, 1995; Matsuda *et al*, 2002; Nishi *et al*, 2001; Sucher *et al*, 1995). When expressed in combination with NR1 and NR2, NR3 subunits are recruited to the receptor complex and modulate the channel properties. NR3A coexpression causes a reduction of NR1/NR2B and NR1/NR2D current amplitudes, unitary conductance, Mg^{2+} sensitivity, and increases the mean open time of these NR1/NR2 channels (Ciabarra *et al*, 1995; Sasaki *et al*, 2002a; Sucher *et al*, 1995). Similarly, coexpression of NR3B with NR1 and NR2A markedly depressed whole-cell current and Ca^{2+} permeability of the receptor (Matsuda *et al*, 2002; Nishi *et al*, 2001; Sasaki *et al*, 2002a). In contrast with NR3A, NR3B does not affect NR1/NR2A or NR1/NR2B voltage-dependent Mg^{2+} block, suggesting that although NR3 subunits have similar molecular and physiological properties, they are not functionally redundant (Nishi *et al*, 2001; Yamakura *et al*, 2005).

NR3 subunits cannot form functional glutamate receptors when assembled with NR1, possibly due to the lack of the pore-forming amino acids in their polypeptide sequence. The N and N+1 residues, which lie in the M2 domain of NR1 and NR2 subunits, control channel permeability in NR1 and voltage-dependent Mg^{2+} block in NR2 subunits (Dingledine *et al*, 1999). In the NR3A and NR3B polypeptide sequence, the corresponding residues are not conserved. It has thus been speculated that this difference is responsible for the lower Ca^{2+} permeability and Mg^{2+} insensitivity of NR3-containing NMDA receptors (Chatterton *et al*, 2002; Ciabarra *et al*, 1995; Matsuda *et al*, 2002; Nishi *et al*, 2001; Sucher *et al*, 1995). However, NR3A and NR3B do not relieve block by Mg^{2+} to the same extent. NR3A coexpression with NR1/NR2A relieves Mg^{2+} block of the receptor, whereas NR3B coexpression has no effect, indicating that changes in the N and N+1 site might not explain

NR3 modulatory properties. (Nishi *et al*, 2001; Sasaki *et al*, 2002a). This was confirmed by the observation that mutagenesis of NR3B aminoacids G629 and R630, to asparagines (N) as they occur in the NR1 pore, do not affect sensitivity to Mg^{2+} block (Yamakura *et al*, 2005). Furthermore, mutation of NR3A “N” site to asparagine does not alter NR3A dominant-negative effect in NR1/NR2B (Sucher *et al*, 1995). These results indicate that these residues alone are not responsible for the physiological properties of NR3 subunits.

VI.1.2 NR3 assembly and tracking

The stoichiometry of NMDA receptors has not yet been established definitely, but the consensus is that NMDA receptors are tetramers that most often incorporate two NR1 and two NR2 subunits of the same or different subtypes (Dingledine *et al*, 1999). It has also been proposed that in receptors containing NR1, NR2 and NR3 subunits, one NR3 subunit substitutes for one of the NR2 subunits. Thus, the stoichiometry of an NMDA receptor with NR3 should be $2xNR1+1xNR2+1xNR3$ (Kew & Kemp, 2005; Schuler *et al*, 2008). In the proposed model for NMDA receptor assembly by Schuler *et al* (2008), NR1 dimerizes separately with either an NR2 subunit or an NR3 subunit, and subsequently NR1/NR2 and NR1/NR3 dimers would assemble to form the final NMDA receptor complex. This model is predicted from the observation that neither the NR2 nor the NR3 subunits form oligomers in the absence of NR1 and that formation of NR1 dimers is not necessary for proper receptor assembly (Atlason *et al*, 2007; Meddows *et al*, 2001; Schuler *et al*, 2008). Under this model, NR2 and NR3 subunits would compete for assembly with NR1. Consistent with this model, coexpression of NR1, NR2A, and NR3A result in the appearance of a mixed population of functional NMDA receptor channels (NR1/NR2A and NR1-/NR2A/NR3A) (Perez-Otano *et al*, 2001). In addition to this *in vitro* work, complexes of NR1/NR2/NR3 subunits have also been found *in vivo* (Matsuda *et al*, 2003; Perez-Otano *et al*, 2001). This supports the idea that NR1 is the limiting subunit for the assembly of NMDA receptor complexes.

The association of NMDA receptor subunits occurs in the endoplasmic reticulum (ER). NR3A associates independently with both NR1 and NR2A in the ER, but only heteromeric complexes containing NR1 are targeted to the plasma membrane (Perez-Otano *et al*, 2001; Schuler *et al*, 2008). Indeed, coexpression of NR1 facilitates the surface expression of NR3A-containing receptors, reducing accumulation of NR3A subunits in the endoplasmic reticulum. Assembly of the NR3B subunit into receptors also occurs in the ER and surface expression of NR3B requires NR1 expression (Matsuda *et al*, 2003). Although NR3 subunits contain ER retention motifs, mutated subunits lacking the motifs are still retained in the ER, possibly because they lack forward trafficking signals (Matsuda *et al*, 2003; Perez-Otano *et al*, 2001). The C-terminal region of NR3B between amino acids 952 and 985 contains motifs that may mask the ER retention signal of the NR1 subunit, which then brings the NR3B subunit to the cell surface as a complex (Matsuda *et al*, 2003). Interestingly, although the C-terminal sequences of NR3B and NR3A do not share a high degree of homology, the region between positions 952 and 985 is relatively conserved amongst the two subunits (Matsuda *et al*, 2003). This suggests a common mechanism for NR3A and NR3B assembly and trafficking.

VI.1.3 NR3 (extra-)synaptic localization

Although NR3A can be found in synapses, it is localized predominantly in intracellular, peri- and extrasynaptic localizations in the dendritic spines of neurons (Perez-Otano *et al*, 2006). In oligodendrocytes, NR3A is predominately concentrated in cellular processes, in clusters with NR1 and NR2C, and less prominent in the soma (Karadottir *et al*, 2005; Salter & Fern, 2005). NR3B is preferentially localized in somata of neurons (Wee *et al*, 2008). NR3A targeting to the synapse appears to be regulated during development and by synaptic activity. NR3A interacts with PACSIN1, a protein involved in clathrin-mediated endocytosis that regulates NR3A cell-surface removal. Furthermore, NR3A endocytosis requires ongoing neuronal activity and is stimulated by NMDA receptor activation. This suggests that increased synaptic activity and maturation drives NR3A downregulation during development (Perez-

Otano *et al*, 2006). Whether such mechanism is in place for NR3B is still unknown. No NR3B interacting protein is known for NR3B, apart from NMDA receptors subunits. However, the apparent lack of NR3B in close proximity of synapses, contrary to NR3A, suggests non-redundant roles for these subunits in neuronal activity.

VI.1.4 Knockout mice and the neuroprotective role of NR3 subunits

The NR3A and NR3B knockout mouse are fertile and survive until adulthood without any noticeable abnormality, consistent with the proposed modulatory role for the NR3 subunits (Das *et al*, 1998; Niemann *et al*, 2007). Cell cultures using NR3A genetically modified mice also provided some clues about NR3A physiology. Whole-cell NMDA receptor currents in NR3A^{-/-} neuronal cortical cultures are unchanged, but current density is increased (Das *et al*, 1998). In NR3A^{-/-} retinal cells NMDA receptor mediated [Ca²⁺]_i rises were significantly higher than those in control cells (Sucher *et al*, 2003). Conversely, a population of neurons overexpressing NR3A has smaller conductance and show less Ca²⁺ permeability to NMDA-induced currents (Tong *et al*, 2008). In NR3A^{-/-}, NMDA receptor mediated synaptic transmission is also altered. NMDA receptor component of EPSCs is larger in knockout mice than that their wild-type littermates (Tong *et al*, 2008).

NR3A confers neuroprotection against several forms of excitotoxic insults. Cultured neurons prepared from NR3A^{-/-} mice display greater sensitivity to damage by NMDA than control neurons (Nakanishi *et al*, 2009). *In vivo*, adult wild-type mice and neonatal NR3A KO mice suffer more damage than neonatal mice, which contain NR3A, after hypoxia–ischaemia (Nakanishi *et al*, 2009). This data supports a neuroprotective role for NR3A.

NR3B ablation causes mild deficiencies in motor learning and coordination in mice. These mice also have higher social interactions in the cage, showing anxiety-like behaviour, suggesting a possibly link of NR3B with psychiatric disorders in humans (Niemann *et al*, 2007). The first reports of NR3B indicated that this subunit was predominately expressed in

motorneurons which was taken to indicate a role of NR3B in motorneuron diseases such as ALS (Chatterton *et al*, 2002; Nishi *et al*, 2001). However, and in contradiction with the putative neuroprotective role of NR3B, no motorneuron death was observed in knockout mice (Niemann *et al*, 2007). Consistently, approximately 10% of the human European-American population has a complete deficiency in NR3B which is not associated with ALS or with any obvious clinical problems (Niemann *et al*, 2008). In conjunction with reports showing a wider expression, a pathogenic role for NR3B in the context of motorneuron diseases can be excluded.

VI.2 RESULTS

The aim of this chapter was to study the modulatory properties of both known NR3 receptor subunits and novel splice variants. Expression of recombinant NMDA receptors in Hek293 has been used extensively with different aims. Hek293 cells do not express natively glutamate receptors and are easy to transfect and cultivate. The biophysical properties of native NMDA receptors and recombinant NMDA receptors expressed in Hek293 cells are similar (Lynch & Guttman, 2001). For my particular aim, the use of Hek293 cells also has another important advantage: Hek293 resting membrane potential (-40 mV) is similar to that of myelin-forming oligodendrocytes in the rat optic nerve (Bolton & Butt, 2006; Thomas & Smart, 2005). Thus, the results can be compared with the properties of oligodendrocytic NMDA receptors in the developing with matter. By using Ca^{2+} imaging I measured a physiological response to NMDA receptors activation in cells expressing various combinations of NR1/NR2 and NR3 subunits.

Following transfection with NMDA receptors subunits, Hek293 cells were loaded with fura-2, challenged with glutamate plus glycine and $[Ca^{2+}]_i$ rises were recorded. Unless stated otherwise, all recording were made in a Mg^{2+} -free solution. Cells expressing CFP and YFP (NR1/NR2x) or CFP, YFP and mCherry (NR1/NR2x/NR3x) were selected as regions of interest (ROI) for analysis. Stimulation of cells with increasing concentrations of glutamate (0.1; 1; 10; 100 and 1000 μ M) + 10 μ M glycine (gly) resulted in increased intracellular Ca^{2+} concentration ($[Ca^{2+}]_i$) as show by the representative traces of figure VI-1.

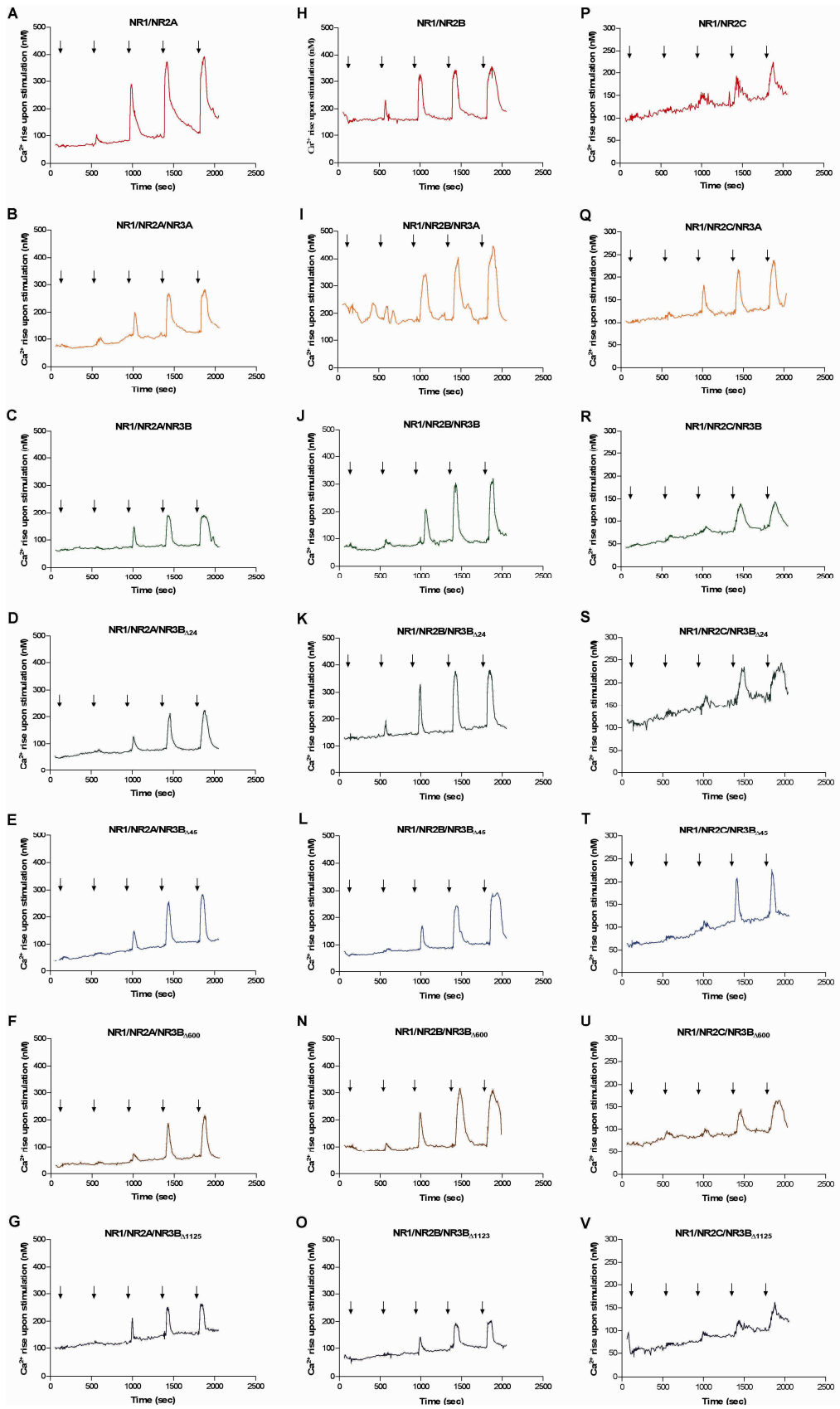


Figure VI-1: Representative traces of glutamate-evoked $[Ca^{2+}]_i$ in Hek293 cells transfected with NMDA receptors

Hek293 cells expressing NMDA receptors were loaded with fura-2 and stimulated for 15 sec with five different glutamate concentrations (0.1; 1; 10; 100 and 1000 μ M), in the presence of 10 μ M Glycine. Each trace represents recordings from a single representative cell. Arrows indicate the time point of stimulation.

VI.2.1 NR3 subunits modulate glutamate potency

Challenging transfected cells with increasing concentrations of glutamate (in the presence of 10 μ M glycine and absence of Mg^{2+}), resulted in $[Ca^{2+}]_i$ rises (figure VI-1). These $[Ca^{2+}]_i$ rises were plotted against the logarithmic values of the glutamate concentrations, as seen in figure VI-2, to calculate the half-maximal responses of NMDA receptors to glutamate. The calculated half maximal effective concentration (EC50) and the negative logarithm of the EC50 (pEC50) for glutamate are plotted in figure VI-3 and the results summarized in table VI-1.

VI.2.1.1 NR3A and NR3B

NR3A expression with NR1/NR2A or NR1/NR2B did not cause a significant change of the pEC50 (figure VI-3A and VI-3B). However, NR3A reduced glutamate potency for NR1/NR2C (pEC50=4.67 \pm 0.007 n=109 NR1/NR2C; pEC50=4.61 \pm 0.008 n=98 NR1/NR2C/NR3A; p<0.001, figure V-3C). Coexpression of NR3B with NR1/NR2A caused an increase in glutamate EC50 (pEC50=5.38 \pm 0.062, n=146 NR1/NR2A; pEC50=5.19 \pm 0.074, n=120 NR1/NR2A/3B; p<0.05, figure V-3A) and increased glutamate potency when expressed with NR1/NR2B (pEC50=5.30 \pm 0.041, n=185 NR1/NR2B; pEC50=5.56 \pm 0.071, n=150 NR1/NR2B/NR3B; p<0.05, figure V-3B) and NR1/NR2C (pEC50=4.67 \pm 0.007 n=109 NR1/NR2C; pEC50=4.99 \pm 0.007, n=66 NR1/NR2C/NR3B; p<0.001, figure V-3C).

VI.2.1.2 NR3B splice variants

The novel NR3B splice variants also caused changes in glutamate potency (figure VI-3). When expressed with NR1/NR2A (pEC50=5.38 \pm 0.062, n=146), NR3B Δ ₂₄ (pEC50=5.03 \pm 0.061, n=105, p<0.01), NR3B Δ ₄₅ (pEC50=4.96 \pm 0.042, n=145, p<0.001), NR3B Δ ₆₀₀ (pEC50=4.90 \pm 0.055, n=107, p<0.001) and NR3B Δ ₁₁₂₅ (pEC50=5.09 \pm 0.077,

n=159, $p < 0.05$) lead to an increase of the glutamate EC50. NR3B splice variants showed no significant differences in their influence on the glutamate potency for NR1/NR2A. NR3B Δ_{24} coexpression with NR1/NR2B decreased the glutamate EC50 ($pEC_{50} = 5.69 \pm 0.058$, n=147, $p < 0.001$). The other NR3B variants did not change significantly the glutamate EC50 of NR1/NR2B receptors (figure VI-3B). No significant difference was observed between the NR3B variants expressed in combination with NR1/NR2B (figure VI3.B). In combination with NR1/NR2C, NR3B variants have opposite effects in glutamate potency. NR1/NR2C/NR3B Δ_{600} increased EC50 for glutamate ($pEC_{50} = 4.87 \pm 0.105$, n=35) compared to NR1/NR2C alone ($pEC_{50} = 4.67 \pm 0.001$, n=109, $p < 0.001$), but this increase is smaller than that of NR1/NR2C/NR3B ($pEC_{50} = 4.99 \pm 0.001$, n=66 NR1/NR2C/NR3B; $p < 0.001$). In contrast, NR1/NR2C/NR3B Δ_{45} and NR1/NR2C/NR3B Δ_{1125} decreased the EC50 for glutamate of NR1/NR2C ($pEC_{50} = 4.56 \pm 0.148$, n=32 NR1/NR2C/NR3B Δ_{45} $p < 0.001$ compared to NR1/NR2C; $pEC_{50} = 4.48 \pm 0.121$, n=13 NR1/NR2C/NR3B Δ_{1125} ; $p < 0.001$ compared to NR1/NR2C, figure V-3C). NR3B Δ_{24} coexpression did not change NR1/NR2C glutamate EC50.

Table VI-1: Summary of NR3 effects on glutamate potency of NMDA receptors

Recombinant expression of NR3 subunits with NR1 and NR2 changes glutamate potency of NMDA receptors. These effects are dependent on NR2 identity. This is a qualitative summary of results plotted in figure VI-3. Variations are in comparison to NR1/NR2 expression without co-expression of NR3 subunits: (=) no changes observed; (+) increase in potency; (-) decrease in potency.

	NR1/NR2A	NR1/NR2B	NR1/NR2C
NR3A	=	=	---
NR3B	-	+	+++
NR3B Δ_{24}	--	+++	=
NR3B Δ_{45}	---	=	---
NR3B Δ_{600}	---	=	+++
NR3B Δ_{1125}	-	=	---

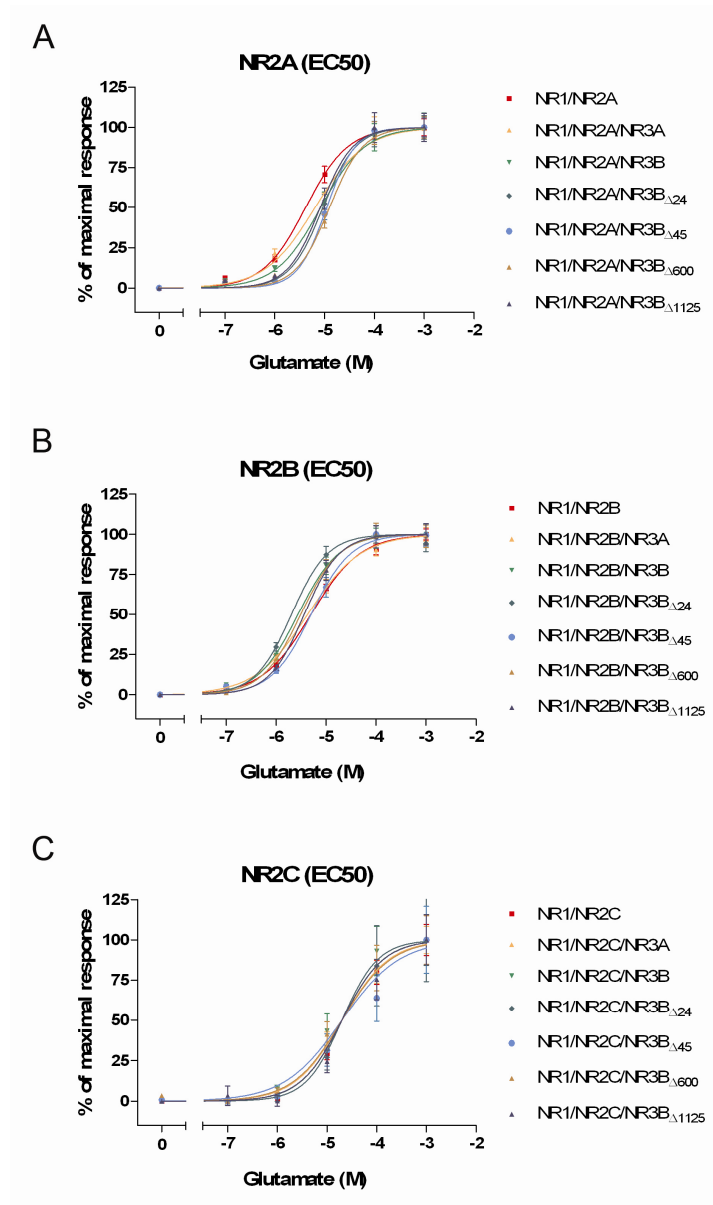


Figure VI-2: Glutamate dose-response curves of NMDA receptors

Glutamate dose-responses from individual cells transfected with NMDA receptors were plotted to calculate glutamate EC₅₀. Intracellular Ca²⁺ rises were normalized to the maximal responses (obtained with 1 mM glutamate). The calculated EC₅₀s can be shown on figure V-3. Data is represented as mean±sem. Each data point was obtained of at least 3 independent transfections. Number of cells per data point is 107-159 (A); 111-320 (B) and 13-126 (C).

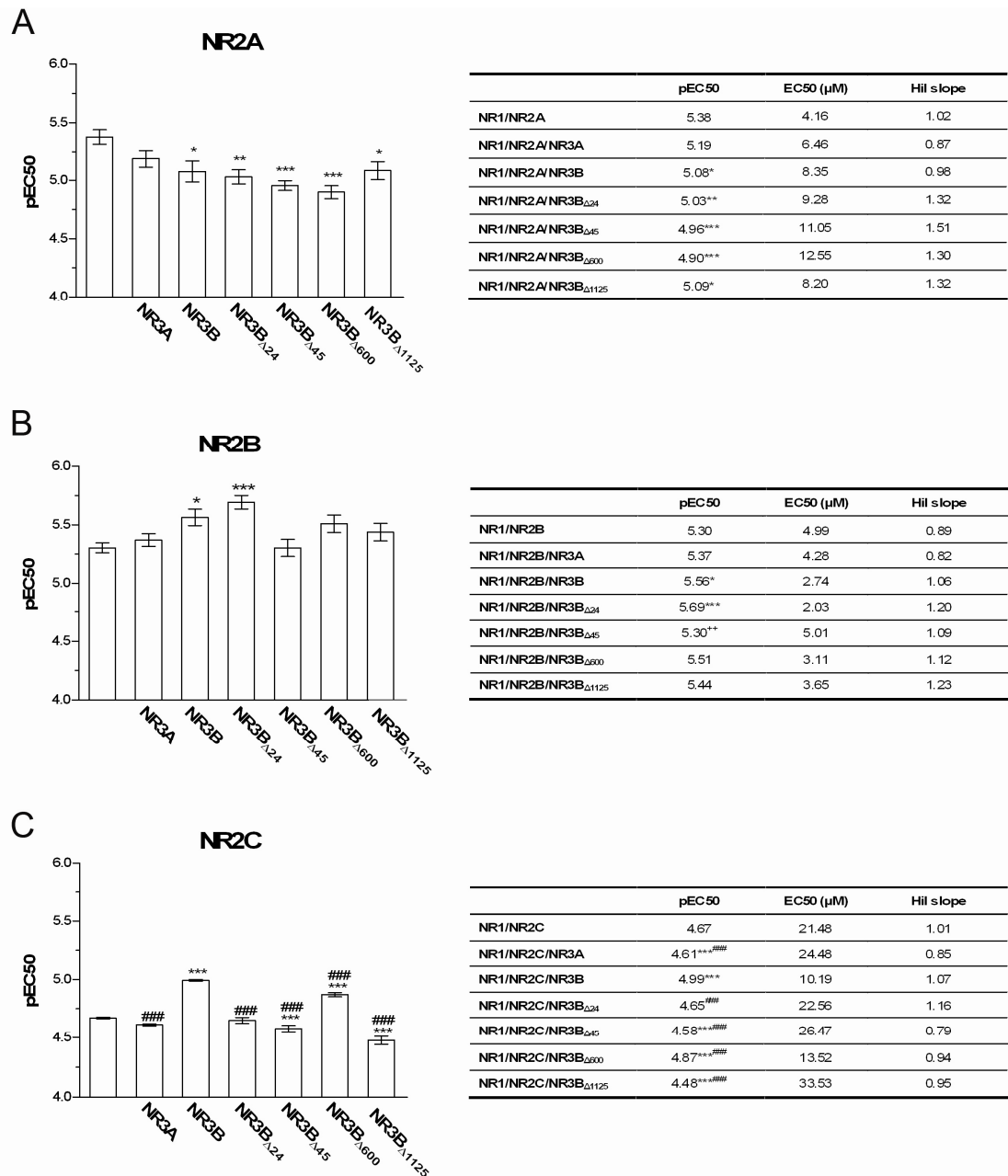


Figure VI-3: Estimates of glutamate potency (pEC50) for NMDA receptors

pEC50 values were estimated using glutamate dose-response curves (figure V-2) generated by single-cell Ca^{2+} imaging. Data is represented as mean \pm sem. Each data point was obtained of at least 3 independent transfections. Number of cells per data point is 107-159 (A); 111-320 (B) and 13-126 (C). *** $p < 0.001$ compared to the corresponding NR1/NR2 (A-C); ### $p < 0.001$ compared to NR1/NR2(A-B)/NR3B.

VI.2.2 NR3 modulation of glutamate-induced $[Ca^{2+}]_i$ rises

VI.2.2.1 NR3A and NR3B

$[Ca^{2+}]_i$ rises of NMDA receptors subtypes were different depending on the subunit combination (figure VI-4). $[Ca^{2+}]_i$ rises of NR1/NR2A expressing cells was 297.2 ± 12.70 nM, NR1/NR2B 196.1 ± 6.34 nM and NR1/NR2C 82.18 ± 7.21 nM. As expected NR1/NR2C $[Ca^{2+}]_i$ rises were modest compared to NR1/NR2A and NR1/NR2B. I also noticed that although a similar number of transfected cells was selected for analysis for these three subtypes, approximately 30 per coverslip, the percentage of cells with $[Ca^{2+}]_i$ rises above basal after stimulation was significantly smaller for NR1/NR2C, compared to NR2A and NR2B (figure VI-4 and VI-5). Furthermore, coexpression of NR3B variants with NR1/NR2C resulted in fewer cells responding above basal after stimulation (figure VI-4). This can be explained because NR1/NR2C channels have lower conductance, Ca^{2+} permeability and have a low open probability making the recordings more challenging (Burnashev *et al*, 1995; Dravid *et al*, 2008; Stern *et al*, 1992). Indeed there is only one paper where NR1/NR2C mediated single-cell $[Ca^{2+}]_i$ rises have been recorded. The method used in this work was confocal imaging of a non-ratiometric dye (Grant *et al*, 1998). In electrophysiological recordings, NR1/NR2C also shows small ion currents and is difficult to record electrophysiologically (Woodward JJ, personal communication and (Plested, 2008)).

Since fura-2 is a ratiometric dye, by inspection of the 340 and 380 nm readings, I could select for analysis cells that showed a true response to glutamate. Cells whose individual 340 and 380 individual fluorescence intensities did not change inversely were excluded. It is likely that a larger number of cells expressing NR1/NR2C respond to glutamate stimuli, but the increases are below our detection limit. Thus, $[Ca^{2+}]_i$ values in NR1/NR2C of expressing cells here presented reflect an overestimate, since only larger responses are detected.

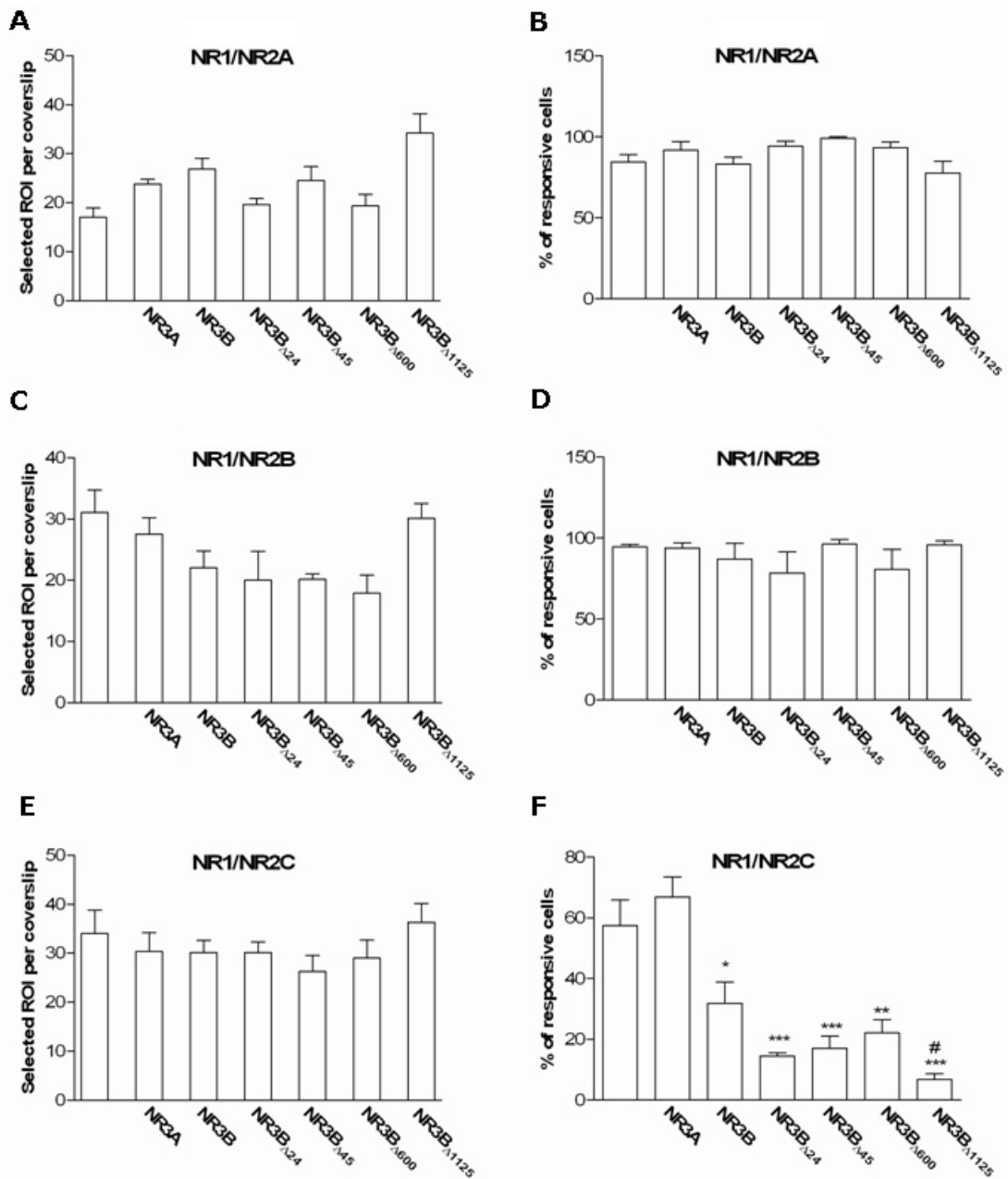


Figure VI-4: Quantification of transfected cells and responsive cells after stimulation with glutamate

Although a similar number of cells express each NMDA receptor subtype (A, C and E) the number of cells with $[Ca^{2+}]_i$ rises above basal is smaller in NR2C expressing cells. Coexpression of NR3B variants increases this effect (B, D and F). Data is represented as mean \pm sem. Number of cells per data point is 116-205 (A); 121-342 (B) and 174-218 (C) of at least 3 independent transfections. * $p < 0.05$ compared to NR1/NR2C; *** $p < 0.01$ compared to NR1/NR2C; *** $p < 0.001$ compared to NR1/NR2C; # $p < 0.05$ compared to NR1/NR2C/NR3B.

When stimulated at lower glutamate concentrations, 0.1 and 10 μM , the expression of NR3A reduced NR1/NR2A receptors mediated $[\text{Ca}^{2+}]_i$ rises by 43% and 33%, respectively (figure VI-5A). NR3B also reduced NR1/NR2A mediated $[\text{Ca}^{2+}]_i$ rises but the effect was more pronounced: it occurred in all concentrations tested, by 46%, 60%, 64%, 56%, 54%, respectively (figure VI-5B). NR1/NR2B $[\text{Ca}^{2+}]_i$ rises appear to be relatively unaffected by NR3 coexpression. NR3A coexpression with NR1/NR2B did not change glutamate induced $[\text{Ca}^{2+}]_i$ rises comparatively to NR1/NR2B, at any of the concentrations tested (figure VI-5C). Coexpression of NR3B lead to an increase in $[\text{Ca}^{2+}]_i$ rises of NR1/NR2B when cells were stimulated with 0.1 μM (36% increase vs NR1/NR2B) and 10 μM (21% increase vs NR1/NR2B, figure VI-5D). $[\text{Ca}^{2+}]_i$ rises of NR1/NR2C receptors increased significantly when NR3A was coexpressed with NR1/NR2C (figure VI-5E). This effect was observed in all glutamate concentrations tested except for 0.1 μM . Although NR3B coexpression had a similar effect at 1 μM , in all other concentrations tested, NR3B did not change NR1/NR2C mediated $[\text{Ca}^{2+}]_i$ rises (figure VI-5F).

VI.2.2.2 NR3B splice variants

The novel NR3B variants also affect $[\text{Ca}^{2+}]_i$ following stimulation with glutamate. These effects are dependent on the NR2 subunit and NR3B splice variant forming the receptor. Coexpression of NR3B variants with NR2A lead to a decrease in $[\text{Ca}^{2+}]_i$ compared to expression of NR1/NR2A as plotted in figure VI-6A. The extent of the decrease is similar for all variants at 0.1-10 μM , approximately 50-60%. However, stimulation with 100 μM and 1 mM, NR3B $_{\Delta 45}$ although diminishing $[\text{Ca}^{2+}]_i$, is less effective than the other NR3B variants (figure VI-6A). Coexpression of the variants with NR2B reveals no particular trend in terms of $[\text{Ca}^{2+}]_i$ following glutamate stimulation. NR3B $_{\Delta 1125}$ reduces $[\text{Ca}^{2+}]_i$ after stimulation with all glutamate concentrations except 0.1 μM (figure VI-6B). NR3B $_{\Delta 45}$ coexpression increases NR1/NR2B $[\text{Ca}^{2+}]_i$ rises induced with 1, 10 and 100 μM glutamate. A similar effect is observed in NR1/NR2B/NR3B $_{\Delta 600}$ expressing cells, but only after stimulation with 10 and

100 μM glutamate (figure VI-6B). Coexpression of the NR3B variants has no significant effect on NR1/NR2C (figure VI-6C).

Table VI-2: NR3 subunits modulate glutamate-induced $[\text{Ca}^{2+}]_i$ raise of NR1/NR2 receptors

Glutamate stimulation leads to $[\text{Ca}^{2+}]_i$ rises in NR1/NR2 expressing cells. Co-expression of NR3 variants modulate these glutamate-induced $[\text{Ca}^{2+}]_i$ rises. This is a qualitative summary of results plotted in figure VI-5 and VI-6. Variations are in comparison to NR1/NR2 expression without co-expression of NR3 subunits: (=) no changes observed; (+) increase in $[\text{Ca}^{2+}]_i$ rises; (-) decrease in $[\text{Ca}^{2+}]_i$ rises. When the effects were only observed in some of the glutamate concentrations tested, these are indicated.

	NR1/NR2A	NR1/NR2B	NR1/NR2C
NR3A	--- (1 and 10 μM)	=	++
NR3B	---	++(1 and 10 μM)	+ (1 μM)
NR3B $_{\Delta 24}$	---	+++ (1, 10 and 100 μM)	=
NR3B $_{\Delta 45}$	---	=	=
NR3B $_{\Delta 600}$	---	++(10 and 100 μM)	=
NR3B $_{\Delta 1125}$	---	---	=

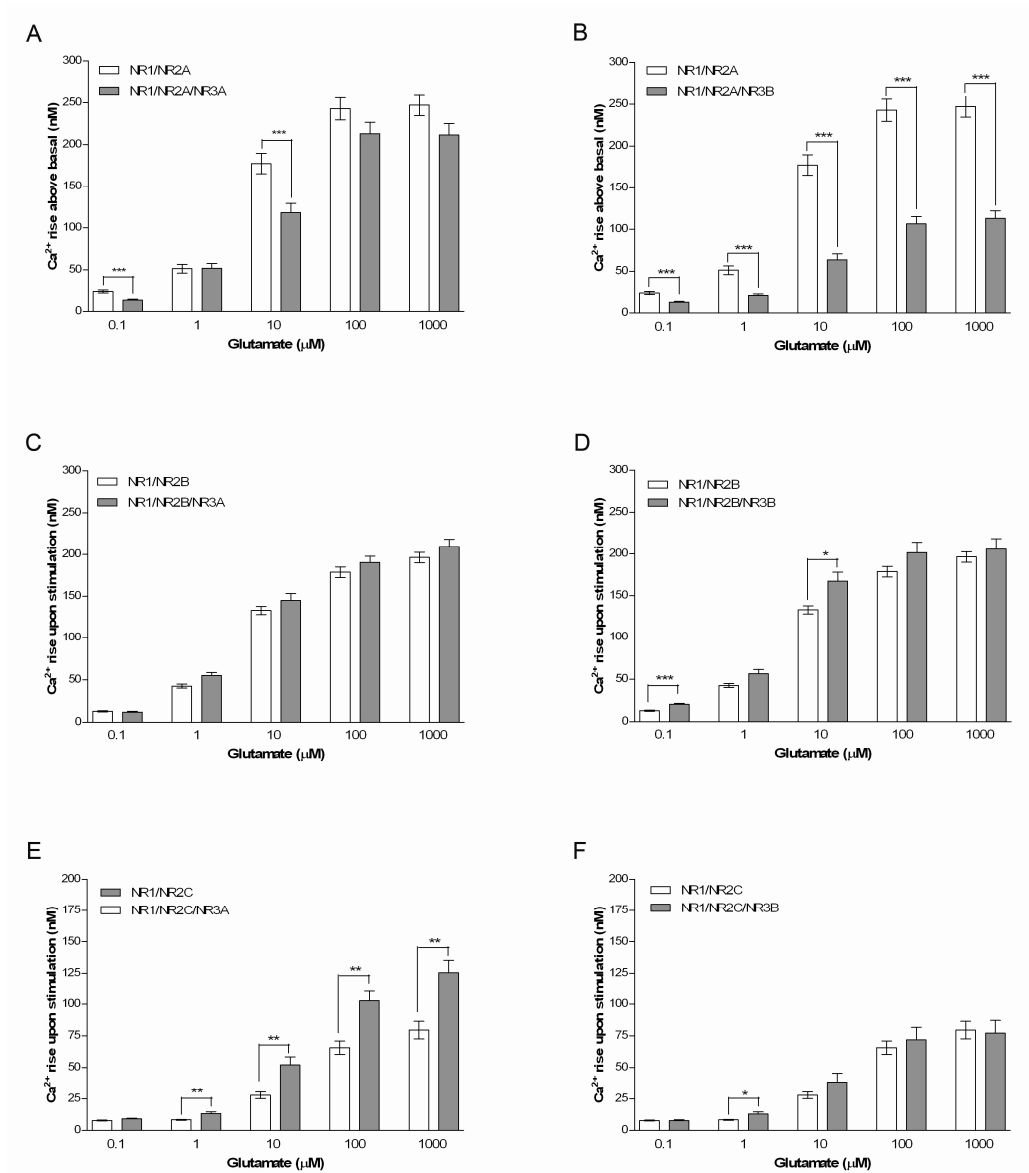


Figure VI-5: NR3A and NR3B subunits change Ca²⁺ influx through NMDA receptors in a NR2-dependent fashion

Single-cell [Ca²⁺]_i rises were recorded following stimulation with several glutamate concentrations in the presence of 10 μM glycine, figure V-5. Quantified of [Ca²⁺]_i rise for the various NMDA receptor compositions reveals that NR3A and NR3B effects dependent on the NR2 subunit expressed in the same cells. Data is represented as mean±sem. Each data point was obtained of at least 3 independent transfections. Number of cells per data point is 107-159 (A); 111-320 (B) and 13-126 (C). * p<0.05 compared to NR1/NR2B-C; ** p<0.01 compared to NR1/NR2C; *** p<0.001 compared to NR1/NR2A-B.

VI.2.3 Mg²⁺ sensitivity

Voltage-dependent Mg²⁺ block is one of most important aspects of NMDA receptor physiology (McBain & Mayer, 1994). To determine how NR3 subunits affect NMDA receptor Mg²⁺ block, transfected cells were exposed to 100 μM glutamate+10 μM glycine, followed by the same stimulus in the presence of 2 or 10 mM Mg²⁺ (figures VI-7 to VI-9). Values are expressed as arbitrary units relative to glutamate-induced [Ca²⁺]_i rise in the absence of Mg²⁺. The presence of both 2mM and 10 mM Mg²⁺ diminished [Ca²⁺]_i rises in cells expressing NR1/NR2A, NR1/NR2B and NR1/NR2C (figures VI-7 to VI-9). In cells expressing NR1/NR2A the [Ca²⁺]_i rises were 0.54±0.025 in the presence of 2 mM Mg²⁺, and 0.34±0.206 in presence of 10 mM Mg²⁺ (figure VI-7). Both Mg²⁺ concentrations had similar effect in NR1/NR2B: 2 mM Mg²⁺ lowered responses to 0.84±0.022 and 10 mM Mg²⁺ to 0.88±0.028 (figure VI-8). In the presence of 2 mM Mg²⁺, [Ca²⁺]_i of NR1/NR2C expressing cells was 0.60±0.058 and 0.29±0.027 in presence of 10 mM Mg²⁺ (figure VI-9).

VI.2.3.1 NR3 modulation of Mg²⁺-block

NR3A did not affect NR1/NR2A Mg²⁺ block (0.61±0.024, 2 mM Mg²⁺; 0.37±0.023, 10 mM Mg²⁺; figure VI-7). In contrast, all NR3B variants significantly increased Mg²⁺ block of NR1/NR2A (figure VI-7). NR3B reduced [Ca²⁺]_i rises to 0.33±0.022 in 2 mM Mg²⁺ (p<0.001 compared to NR1/NR2A) and 0.20±0.015 in 10 mM Mg²⁺ (p<0.001 compared to NR1/NR2A). Mg²⁺ had a similar effect in NR1/NR2A/NR3B_{Δ24} (0.28±0.018, 2 mM Mg²⁺; 0.14±0.017, 10 mM Mg²⁺; p<0.001 compared to NR1/NR2A in the same conditions), NR1/NR2A/NR3B_{Δ45} (0.37±0.019, 2 mM Mg²⁺; 0.16±0.013, 10 mM Mg²⁺; p<0.001 compared to NR1/NR2A in the same conditions), NR1/NR2A/NR3B_{Δ600} (0.30±0.018, 2 mM Mg²⁺; 0.13±0.010, 10 mM Mg²⁺; p<0.001 compared to NR1/NR2A in the same conditions) and NR1/NR2A/NR3B_{Δ1125} (0.27±0.016, 2 mM Mg²⁺; 0.23±0.017, 10 mM Mg²⁺; p<0.001 compared to NR1/NR2A in the same conditions).

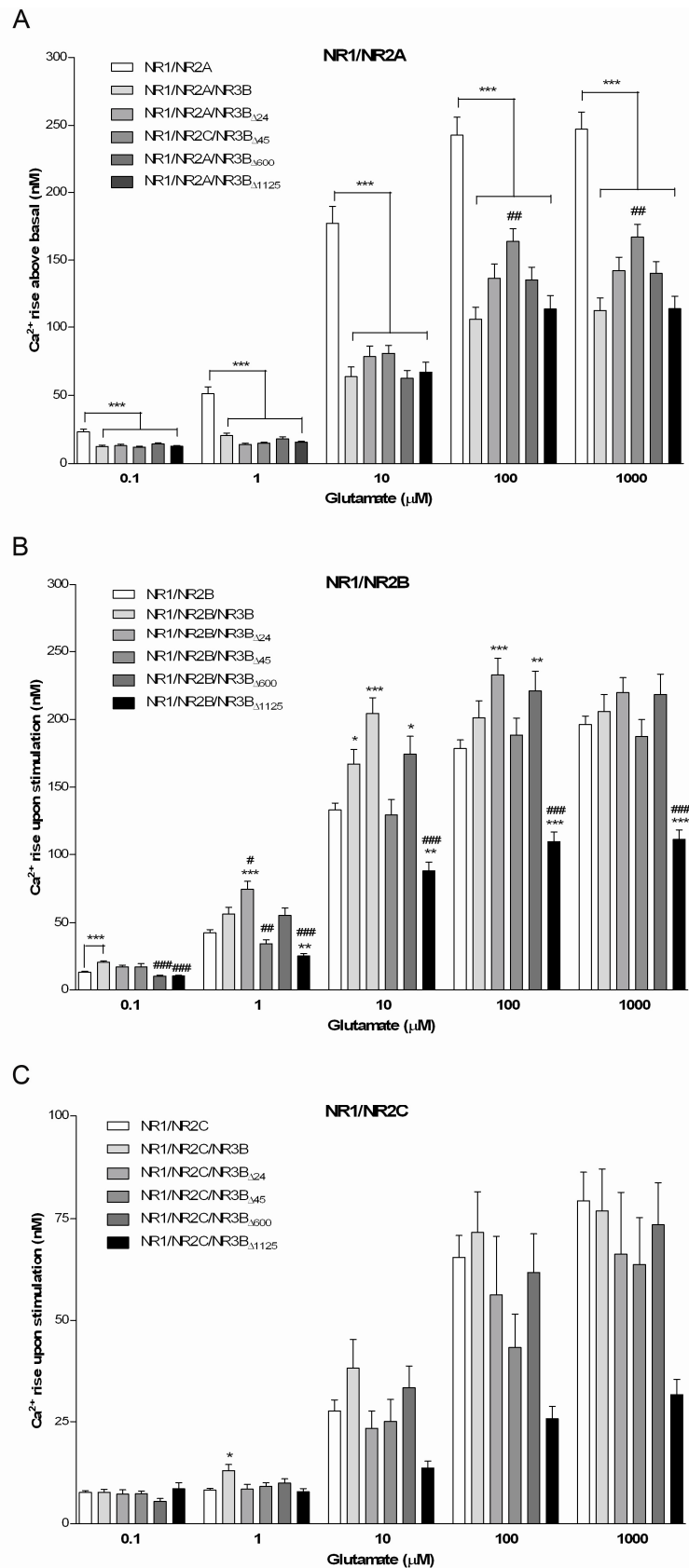


Figure VI-6: Effect of NR3B splice variants on $[Ca^{2+}]_i$ rises mediated by NMDA receptors

Single-cell $[Ca^{2+}]_i$ rises were recorded following stimulation with several glutamate concentrations in the presence of 10 μ M glycine, figure V-5. Quantification of $[Ca^{2+}]_i$ rises for the various NMDA receptor compositions reveals that NR3B splice variants differentially modify NMDA receptor mediated $[Ca^{2+}]_i$ rises. Data is represented as mean \pm sem. Each data point was obtained of at least 3 independent transfections. Number of cells per data point is 107-159 (A); 111-320 (B) and 13-126 (C). * $p < 0.05$ compared to NR1/NR2B-C; ** $p < 0.01$ compared to NR1/NR2B; *** $p < 0.001$ compared to NR1/NR2A-B. # $p < 0.05$ compared to NR1/NR2B/NR3B; ## $p < 0.01$ compared to NR1/NR2A-B/NR3-B; ### $p < 0.001$ compared to NR1/NR2B/NR3B.

Table VI-3: Modulation of NR1/NR2 Mg²⁺-block by NR3 subunits

Stimulation of NMDA receptors in the presence of extracellular Mg²⁺ results in reduced [Ca²⁺]_i rises. This block can be modulated by NR3 subunits. This table summarizes the effects that coexpression of NR3 subunits have on glutamate-induced [Ca²⁺]_i rises in cells expressing NR1/NR2A-C in the presence of 2 and 10 mM Mg²⁺. This is a qualitative summary of results plotted in figure VI-7, VI-8 and VI-9. Variations are in comparison to NR1/NR2 expression without co-expression of NR3 subunits stimulated in media containing equivalent amounts of Mg²⁺: (=) no changes observed; (+) increase in [Ca²⁺]_i rises; (-) decrease in [Ca²⁺]_i rises.

	NR1/NR2A		NR1/NR2B		NR1/NR2C	
	2 mM	10 mM	2 mM	10 mM	2 mM	10 mM
NR3A	=	=	---	---	=	=
NR3B	+++	+++	++	+++	=	=
NR3B_{Δ24}	+++	+++	=	+	=	=
NR3B_{Δ45}	+++	+++	=	+++	=	=
NR3B_{Δ600}	+++	+++	=	+++	=	=
NR3B_{Δ1125}	+++	+++	=	+++	=	=

NR3A expression relieved Mg²⁺ of NR1/NR2B in both concentrations (1.07±0.02, 2 mM Mg²⁺; 1.048±0.028, 10 mM Mg²⁺; p<0.001 compared to NR1/NR2B in the same conditions; figure VI-8). In the presence of 2 mM Mg²⁺, NR3B increased significantly Mg²⁺ block of NR1/NR2B (0.70±0.036, p<0.01) but none of the novel splice variants affected block by Mg²⁺ at this concentration (figure VI-8). In the presence of 10 mM Mg²⁺, NR1/NR2B/NR3B_{Δ24} increased Mg²⁺ block compared to NR1/NR2B (0.76±0.028, p<0.05) but to a lesser extent compared to NR1/NR2B/NR3B (p<0.001). The other three splice variants increased Mg²⁺ block, compared to NR1/NR2B (NR1/NR2B/NR3B_{Δ45} 0.62±0.030; NR1/NR2B/NR3B_{Δ600} 0.45±0.028; NR1/NR2B/NR3B_{Δ1125} 0.47±0.020; p<0.001).

In the presence of 2 and 10 mM Mg²⁺, [Ca²⁺]_i in NR1/NR2C expressing cells was 0.60±0.058 and 0.29±0.027, respectively (figure VI-9). Neither NR3A nor any of the NR3B splice variants had an effect in NR1/NR2C block by Mg²⁺ in both of the tested concentrations (figure VI-9).

VI.2.4 NR1/NR3 glycine receptors

NR3 subunits when expressed with NR1 form excitatory glycine receptors (Chatterton *et al*, 2002). The pharmacology of these receptors is quite different from “typical” NMDA receptors. NR1/NR3 receptors are activated by glycine alone and are unaffected by glutamate. These receptors are also insensitive to Mg²⁺ block and relatively impermeable to Ca²⁺ (Cavara *et al*, 2009; Chatterton *et al*, 2002). In mammalian cells, these glycinergic receptors are formed only when NR1 is expressed with both NR3A and NR3B (Smothers & Woodward, 2007). Since these receptor are poorly described in the literature I sought to express the novel NR3B variants and determine if they have effect on these receptors. NR3 glycine receptors have low permeability to Ca²⁺, but it is likely that they are permeable to Na²⁺ (Chatterton *et al*, 2002). Thus, I imaged [Na²⁺]_i with the dye SBFI. SBFI binds to Na²⁺ and has similar absorption and excitation properties as Fura-2 so it wasn't necessary to change microscopy or loading settings, and the same filters could be used.

Following loading with SBFI cells were challenged with 10 μM glycine, 100 μM and 100 μM glycine, and 100 μM glutamate. However, none of these stimulus evoked significant [Na²⁺]_i rises in cells expressing NR1/NR3A or NR1/NR3A/NR3B variants (figure VI-10). Replacing the canonical NR3B with the novel splice variants also failed to produced detectable changes in [Na²⁺]_i (figure VI-10). To exclude the possibility of some technical problem, cells expressing NR1/NR2B were challenged with 400 μM glutamate and 100 μM glycine. This stimulus evoked reproducible [Na²⁺]_i rises (figure VI-10).

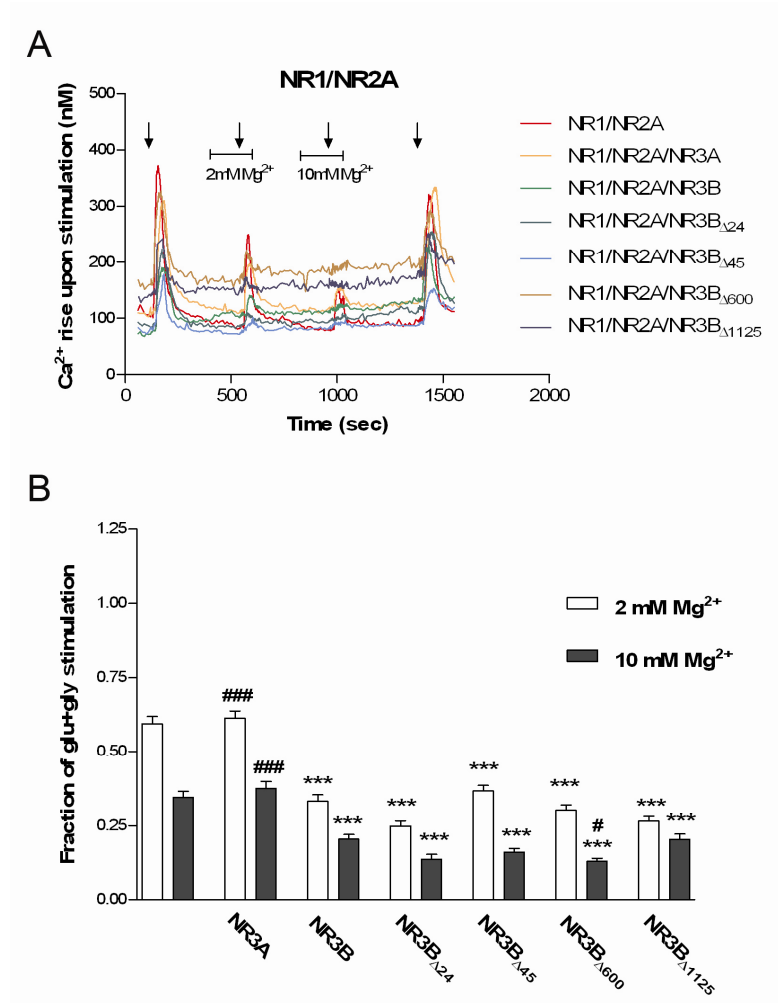


Figure VI-7: Sensitivity of NR1/NR2A to Mg²⁺ block in the presence of NR3 subunits

Representative traces of single-cell [Ca²⁺]_i responses to 100 μM glutamate + 10 μM glycine in the absence and presence and of 2 mM and 10 mM Mg²⁺. Arrows represent time of stimulation 100 μM glutamate+ μM glycine (15 seconds stimulus) and lines represent presence of Mg²⁺ in the solution. (B) Responses in the presence of Mg²⁺ are plotted as percentage of maximal response to glutamate in the absence of Mg²⁺. Data is represented as mean±sem. Each data point was obtained of at least 3 independent transfections. Number of cells per data point is 122-163. *** p<0.001 compared to NR1/NR2A; # p<0.05 compared to NR1/NR2A/NR3B; ### p<0.01 compared to NR1/NR2A/NR3B.

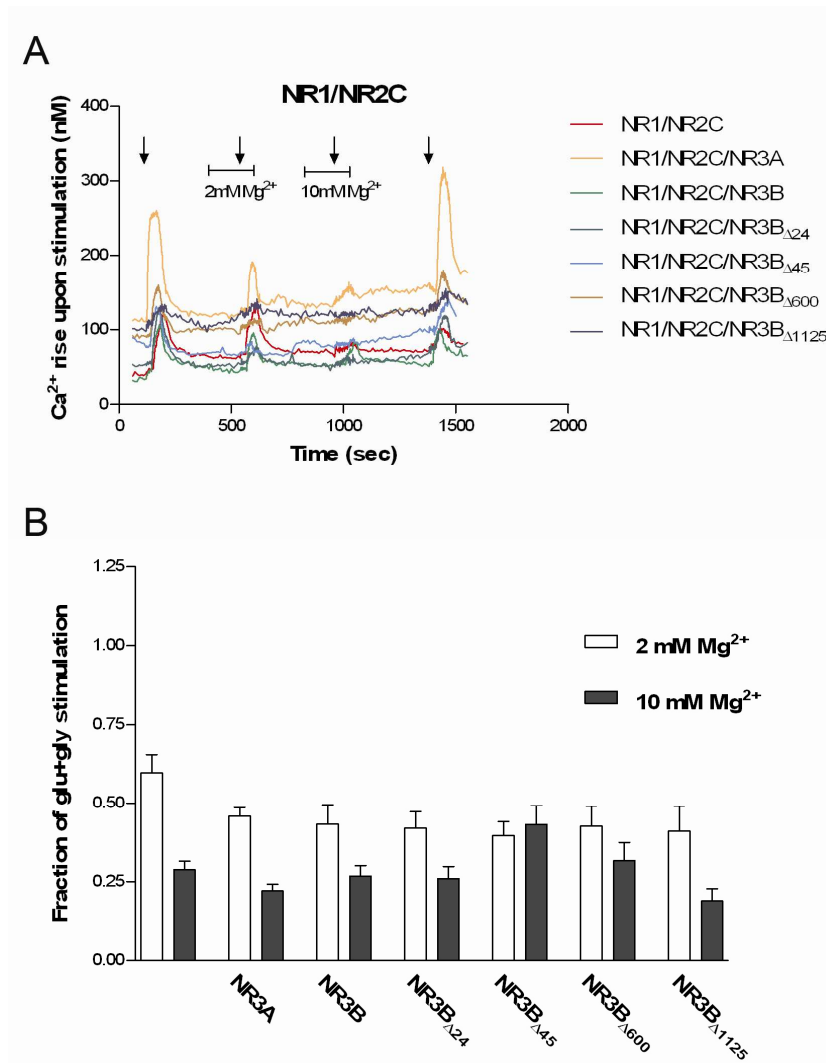


Figure VI-9: Sensitivity of NR1/NR2C to Mg²⁺ block in the presence of NR3 subunits.

(A) Representative traces of single-cell [Ca²⁺]_i responses to 100 μM glutamate + 10 μM glycine in the absence and presence and of 2 mM and 10 mM Mg²⁺. Arrows represent time of stimulation 100 μM glutamate+ μM glycine (15 seconds stimulus) and lines represent presence of Mg²⁺ in the solution. (B) Responses in the presence of Mg²⁺ are plotted as percentage of maximal response to glutamate in the absence of Mg²⁺. Data is represented as mean±sem. Each data point was obtained of at least 3 independent transfections. Number of cells per data point is 7-64.

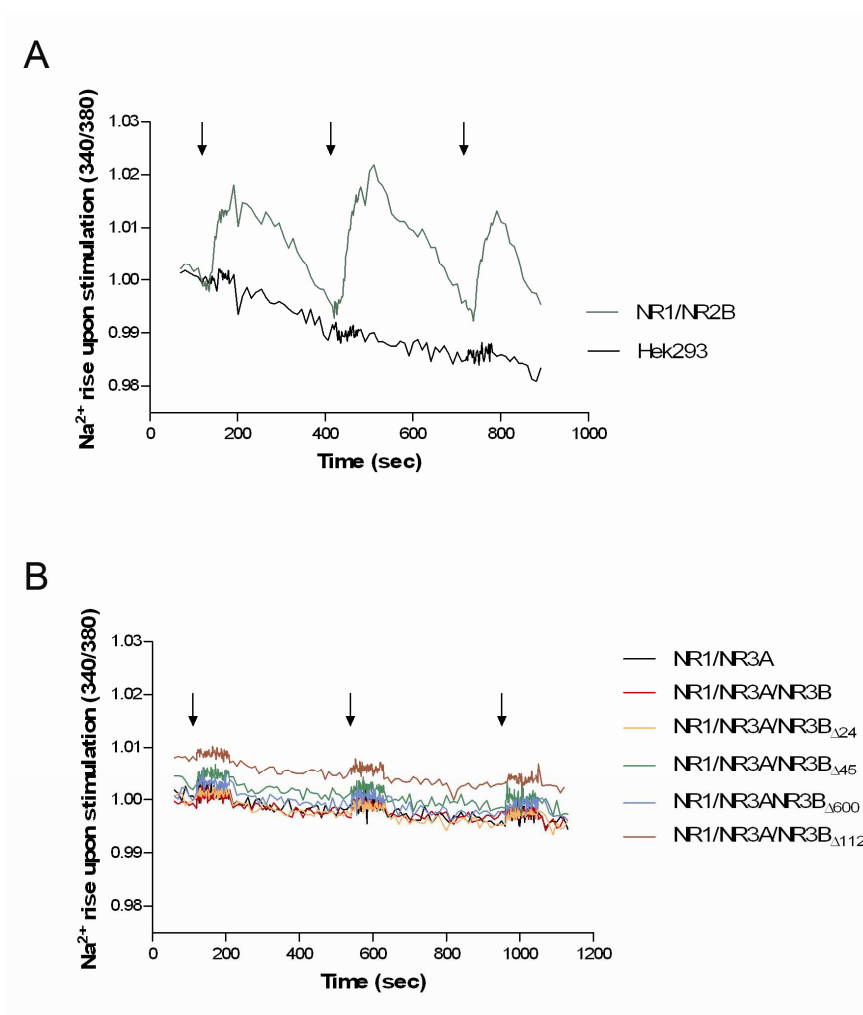


Figure VI-10: Representative traces of glutamate and/or glycine-evoked $[Na^+]_i$ rises in Hek293 cells transfected with NMDA receptors

Hek293 cells expressing NMDA receptors were loaded with SBF1 and stimulated for 15 sec with (A) 400 μ M glutamate and 100 μ M glycine which evoked responses in NR1/NR2B transfected cells, but not in Hek293 untransfected cells. (B) Cell expressing different combinations of NR1 and NR3 subunits were exposed sequentially to 10 μ M glycine, 100 μ M and 100 μ M glycine and 100 μ M glutamate. Stimulation did not evoke any response. Each trace represents recordings from a single representative cell. Arrows indicate the time point of stimulation. Values are expressed in arbitrary units.

VI.3 DISCUSSION

VI.3.1 Dominant-negative function of NR3s

VI.3.1.1 NR3A

The dominant-negative effect on NR1/NR2 currents and the relief of Mg²⁺ block is portrayed as the hallmark of NR3A and NR3B subunits. NR3A reduces the currents of both NR1/NR2A and NR1/NR2B, and Ca²⁺ permeability of NR1/NR2A (Ciabarra *et al.*, 1995; Perez-Otano *et al.*, 2001; Sucher *et al.*, 1995). Here I show that NR3A coexpression with NR1/NR2A results in decreased [Ca²⁺]_i rises, induced by lower glutamate concentrations (0.1 μM and 10 μM but not 1 μM, figure VI-5A). Coexpression of NR3A had no effect in glutamate-induced [Ca²⁺]_i rise of NR1/NR2B. I also report for the first time the effect of NR3A on NR1/NR2C glutamate-induced [Ca²⁺]_i rise. Contrasting with the expected dominant-negative effect of NR3A, coexpression of NR3A increased NR1/NR2C [Ca²⁺]_i rises by more than 30%. Considering that we are overestimating NR1/NR2C [Ca²⁺]_i rises following stimulation, this effect might be larger. This consistent upregulation of NR3A on NR1/NR2C indicates a new non-dominant-negative function for NR3A.

VI.3.1.2 NR3B

NR3B has distinctively opposite effects on NR1/NR2A and NR1/NR2B. When coexpressed with NR1/NR2A, NR3B decreases glutamate-induced [Ca²⁺]_i rises at all concentrations tested by about 50%. This is in accordance with previous studies which show that NR3B decreases NR1/NR2A currents and/or Ca²⁺ permeability (Matsuda *et al.*, 2002; Nishi *et al.*, 2001). In contrast, NR3B slightly increased NR1/NR2B-mediated [Ca²⁺]_i rise, although this effect was only observed at 0.1 and 10 μM. In the only study that tested this receptor subunit composition, NR3B reduced the current amplitude of NR1/NR2B (Yamakura *et al.*, 2005). However, this effect was dependent on the relative amount of plasmid

coding for NR3B used in the transfection. That is, as the amount of transfect NR3B increased (and NR1/NR2B decreased) so did the dominant effect of NR3B (Yamakura *et al*, 2005). Previously, Nishi and colleagues shown a similar NR3B transfection-dependent effect on NR1/NR2A which was not due a reduction in expression levels of either NR1 or NR2A (Nishi *et al*, 2001).

Existing data on NR3B effects on NR1/NR2 currents is not completely clear. In one study, it was found that coexpression of NR3B decreases NR1/NR2A glutamate induced currents (Nishi *et al*, 2001). In contrast, Matsuda and colleagues (Matsuda *et al*, 2003; Matsuda *et al*, 2002) reported that NR1/NR2A kinetics and voltage dependency currents where unaffected by expression of NR3B (Matsuda *et al*, 2003; Matsuda *et al*, 2002). Nonetheless, the estimated Ca^{2+} permeability in Hek293 cells coexpressing NR1/NR2A/NR3B is about 50% of cells coexpressing NR1/NR2A (Matsuda *et al*, 2002). Over-expression of NR3B in hippocampal neurons decrease Ca^{2+} permeability (about 30% of control neurons), but NMDA receptor current amplitude remains unchanged (Matsuda *et al*, 2003). Since these neurons express NR3B natively, the net results of NR3B overexpression might be masked, and the NR3B role underestimated. I also report that NR3B modifies glutamate potency of NR1/NR2A-C, whereas NR3A only increases glutamate EC50 of NR1/N2C. The results here presented cast even more doubts on the dominant-negative effect as a common feature of both NR3 subunits. NR3A and NR3B do not mimic each other, and importantly can modulate bidirectionally $[\text{Ca}^{2+}]_i$ rises and glutamate potency depending on NR2 subunit identity.

VI.3.2 Relief Mg block is not a common feature of NR3 receptors

The ability to reduce NMDA receptors sensitivity to Mg^{2+} is usually described as a common feature of NR3 subunits, however a close inspection of the literature argues against it. Coexpression of NR3A relieves Mg^{2+} block of NR1/NR2A and NR1/NR2B (Sasaki *et al*, 2002a) and in hippocampal neurons of transgenic mice overexpressing NR3A, the IC50 of

Mg²⁺ is increased compared to wild-type neurons (Tong *et al*, 2008). In contrast, Sucher and collaborators failed to see any differences in Mg²⁺ sensitivity of NR1/NR2B when coexpressed with NR3A, indicating that NR3A relieve of Mg²⁺-block is NR2 dependent (Sucher *et al*, 1995). Furthermore, the two studies that examined NR3B role in Mg²⁺-block of NMDA receptors, showed that NR3B coexpression with either NR1/NR2A or NR1/NR2B did not affect the sensitivity to Mg²⁺-block of these receptors (Nishi *et al*, 2001; Yamakura *et al*, 2005).

Here I show that NR3A does not affect NR1/NR2A Mg²⁺-block and reliefs slightly NR1/NR2B sensitivity to Mg²⁺ block. In contrast, NR3B increases sensitivity of both NR1/NR2A and NR1/NR2B to Mg²⁺ block. I am also reporting for the first time the effect of NR3 subunits on NR1/NR2C receptors. Neither NR3A nor NR3B affected the Mg²⁺ sensitivity of NR1/NR2C. This evidence indicates that NR3A and NR3B effect on NMDA receptor voltage-dependent Mg²⁺ block (1) is not similar for both subunits; and (2) needs to be reappraised to determine the reasons for discrepancies in the literature.

VI.3.3 Comparison with previous reports

2 mM Mg²⁺ produced 40% block of NR1/NR2A and NR1/NR2C receptors, and 20% block of NR1/NR2B; values ~2-3 fold lower than reported for recombinant receptors at -40 mV (Medina *et al*, 1995; Qian *et al*, 2005; Sasaki *et al*, 2002b). In our conditions cells will depolarize following receptor activation and low Mg²⁺-block is evident in HEK293 cells held at -30 mV (~50% in 1 mM Mg²⁺ for NR1/NR2A and ~30% for NR1/NR2B) (Jin *et al*, 2008; Renard *et al*, 1999). Similarly, in stably transfected L(tk-) cells, Mg²⁺ block measured by ⁴⁵Ca²⁺ influx was less effective than usually reported in electrophysiological measurements (Grimwood *et al*, 1996). These differences may be a reflection of different methodological approaches.

Some inconsistencies between my results and existing literature could be explained by the use of different expression systems and methodologies. I measured Ca²⁺ changes instead of

electrophysiological currents. Electrophysiological recordings do have the advantage of finer analysis of receptor currents. However, Ca^{2+} imaging measures directly a second messenger important for cellular responses following NMDA receptor activation (Schiller *et al*, 1998). Furthermore, using this system I was able to monitor routinely more than 100 cells per condition, in contrast with electrophysiological recordings, which usually report as low as four cells per condition tested. Hek293 cell membrane is relatively depolarized (-40 mV) which complicates comparative analysis with results obtained in either neurons (-80 mV) or Hek293 electrophysiological recording which are usually performed at more negative holding potentials (Thomas & Smart, 2005). Importantly, NMDA receptors were expressed in Hek293 cells that do not express natively glutamate receptors. This point seems to be largely overlooked in the literature. *Xenopus* express endogenous glutamate receptor subunits homologous to mammalian NR1 and NR2s that can mask or alter NMDA receptors currents (Schmidt & Hollmann, 2008; Soloviev *et al*, 1996).

VI.3.4 Novel splice variants properties

Four novel NR3B splice variants were expressed and their properties assessed. When expressed in combination with NR1 and NR2 subunits and challenged with glutamate the NR3B variants receptors generated robust $[\text{Ca}^{2+}]_i$ rises. A more in-depth analysis of their properties also shows that they modulate NMDA receptor physiology in a NR2-dependent manner and in some aspects, differently from the canonical NR3B. Thus, these variants are expressed and modulate NMDA receptor properties.

All variants, including the canonical NR3B, increase NR1/NR2A EC50 for glutamate to a similar extent. When expressed with NR1/NR2B, only NR3B, NR3B $_{\Delta 24}$ and NR3B $_{\Delta 45}$ altered the EC50 for glutamate. NR3B inclusion causes a 2-fold reduction in the NR1/NR2C glutamate EC50 and NR3B $_{\Delta 600}$ a similar, although smaller effect. In contrast, NR3B $_{\Delta 45}$ and NR3B $_{\Delta 1125}$ increase glutamate EC50 of NR1/NR2C. NR3B $_{\Delta 24}$ does not change NR1/NR2C EC50 for glutamate. Thus, NR1/NR2C seems to be the receptor more amenable to EC50

modulation by NR3B variants. One interesting aspect of NR3B modulation of NR2C is the reduction of cells with glutamate-induced $[Ca^{2+}]_i$ above basal. An important fraction of $[Ca^{2+}]_i$ following NR1/NR2C activation comes from the release of Ca^{2+} from intracellular stores (Grant *et al*, 1998). It is possible that NR3B variants modulate NR2C protein interactions that mediate this release and thus affect Ca^{2+} release. The reason for NR3B variant modulation of glutamate potency is unknown. It could be that deletions might be important for binding of proteins or co-factors that regulate glutamate sensitivity. Another hypothesis is that NR3B inclusion changes the receptor conformation and thus accessibility of glutamate binding pocket (Gielen *et al*, 2008; Mayer, 2006).

Ca^{2+} influx through NMDA receptor is modified differently by NR3 variants. NR3B $_{\Delta 1125}$ acted as a “dominant negative” variant in NR1/NR2A, diminishing influx to a similar extent as canonical NR3B. NR3B $_{\Delta 1125}$ is also the only NR3 that exerts any effect on NR1/NR2B mediated $[Ca^{2+}]_i$ rise. One possibility to explain this effect is that changes in trafficking of NR3B $_{\Delta 1125}$ could regulate the availability of NMDA receptors at the cell surface. However, NR3B $_{\Delta 1125}$ also changed NR1/NR2A and NR1/NR2B block by Mg^{2+} and the glutamate potency of NR1/NR2C. This is not consistent with fewer receptors at the membrane. If NR3B $_{\Delta 1125}$ reduced cell-surface expression of NR1/NR2 receptors one would expect that glutamate potency and Mg^{2+} -block would remain unchanged as measurement of these parameters is independent of the number of receptors at the membrane. However, this is not the case and NR3B $_{\Delta 1125}$ effects on NR2 receptor are more likely due to changes in receptor conformation, affinity to agonists or disruption of intracellular C-terminal protein interactions.

It is known that NR1 splice variant modulation of NMDA receptors is dependent on the identity of the NR2 subunit present in the complex. NR1 splice variants modulate Zn^{2+} and H^+ effects on NMDA receptor, but only when combined with certain NR2 subunits. The NR3B variants affect the glutamate sensitivity of the receptors, Mg^{2+} and $[Ca^{2+}]_i$ influx. Since all the physiological properties analysis was made with NR1-1a, it will be interesting to see

how and if NR1 and NR3B variants change each other modulatory properties. The study was also focused three of the most relevant properties of NMDA receptors: glutamate sensitivity, Ca^{2+} permeability and Mg^{2+} block. Other properties deserve attention such as glycine sensitivity and C-terminal protein interactions, in particular of NR3B $_{\Delta 600}$ and NR3B $_{\Delta 1125}$. The shortened C-terminal of these proteins predicts that some interactions with targeting proteins might be affected (Perez-Otano *et al*, 2006).

VI.3.5 NR1/NR3 glycine receptor

NR1/NR3A or NR1/NR3B glycine receptors have been identified in *Xenopus* and native expression of these receptors is still controversial (Chatterton *et al*, 2002; Tong *et al*, 2008). NR1/NR3 excitatory glycine receptors are impermeable to Ca^{2+} , unaffected by glutamate or NMDA, and inhibited by d-serine, a co-activator of conventional NMDA receptors (Chatterton *et al*, 2002). The original report of NR1/NR3 glycine receptors recorded currents in cerebrocortical neurons (Chatterton *et al*, 2002). In contrast, Tong *et al* (2008) failed to record glycine-evoked currents in hippocampal neurons over-expressing NR3A. The currents were recorded in NR3B-overexpressing cortical neurons, however, they were also present in NR1 $^{-/-}$ cortical neurons, inconsistent with the requirement of NR1 for the formation of this channel (Matsuda *et al*, 2003). A possible explanation for the elusiveness of these receptors *in vivo* could be regional or developmental regulated expression. The currents also desensitize quite quickly and make recording challenging (Chatterton *et al*, 2002; Tong *et al*, 2008). This difficulty in recording and identifying native NR1/NR3 glycine receptors raise unanswered questions about their physiological importance.

The molecular nature of NR1/NR3 glycine receptors is also controversial. They were initially identified following expression in *Xenopus* (Chatterton *et al*, 2002). In this system, either NR1/NR3A or NR1/NR3B expression was sufficient to generate inward glycine currents. However, this is not the case in mammalian cells. Expression of either NR1/NR3A or NR1/NR3B in Hek293, failed to generate functional glycine receptors which were detected

following expression of NR1/NR3A/NR3B (Smothers & Woodward, 2007). It should be noted that in *Xenopus*, NR1 subunits form homomeric channels. It has now been demonstrated that the homomeric NR1 receptors is actually a multimer of NR1 complexed with native *Xenopus* NMDA receptors (Schmidt & Hollmann, 2008; Soloviev *et al*, 1996). This could explain differences between the two different systems.

I failed to record Na^{2+} currents in NR1/NR3A/NR3B receptors. Glycine-induced currents of NR1/NR3 receptors are characterized by fast desensitization and our system might not be adequate to record such rapid changes (Smothers & Woodward, 2007; Tong *et al*, 2008). Another explanation could be that NR1/NR3 receptors have low Na^{2+} permeability that cannot be detected in our system or they might be indeed permeable to other ions other than sodium or Ca^{2+} . I decided to test Na^{2+} following the reasoning that NR1/NR3 glycine receptors are relatively impermeable to Ca^{2+} . As NMDA receptors are also permeable to Na^{2+} it seemed logical to test influx of this ion through NR1/NR3 receptors (Yu & Salter, 1998). The lack of $[\text{Na}^{2+}]_i$ suggest that NR1/NR3 glycine receptor may have low Na^{2+} permeability, or are permeable to other cations other than Na^{2+} and Ca^{2+} .

Chapter VII

Concluding remarks

In chapters IV and V, I described the cloning and molecular characterization of novel NMDA receptor splice variants. The logical sequence of this project was to (1) test if these variants are capable of forming functional glutamate receptors and (2) ascertain how they modulate NR1/NR2 receptors. To achieve these goals, NR3B splice variants were expressed in combination with NR1/NR2A-C subunits in Hek293 cells (devoid of native glutamate receptors) and $[Ca^{2+}]_i$ was measured following stimulation with glutamate and glycine. Using this method, three physiological parameters of NMDA receptors activity were tested: glutamate potency; $[Ca^{2+}]_i$ rises resulting from activation; and Mg^{2+} block.

I have also sought to perform a comprehensive study of the effects of full-length NR3A and NR3B on NR1/NR2 receptors. Although NR3 modulatory effects have been studied, the literature available lacks consistency in both methodological approaches and in the combination of subunits tested (reviewed in (Cavara & Hollmann, 2008)). Here I describe results obtained for the combination of NR1/NR2A-C with NR3A or NR3B using one experimental approach throughout the work and testing the same physiological parameters. This approach is also intended to provide insight into the complex modulation of NMDA receptors.

The finding that an NR3 subunit can increase NMDA receptor mediated Ca^{2+} influx is an interesting turnaround and defies the established dogma that NR3 subunits act only as dominant-negative subunits. Our results suggest that NR3A and NR3B, despite sharing high sequence homology and structural features, differ in the way they modulate NMDA receptors and that the modulation is dependent on the NR2 subunit present in the complex. For instance, NR3A coexpression causes a decrease in NR1/NR2A mediated $[Ca^{2+}]_i$ rises but increase NR1/NR2C $[Ca^{2+}]_i$ rises. The complex NMDA receptor pharmacology already known and exists at several levels: NR2s present in the receptor complex; NR1 splice variant; and post-translation modifications such as phosphorylation (Salter & Kalia, 2004). Our results point out to an extra level of complexity. Such complexity has implications in the development of NMDA receptor subtype tailored drugs. NMDA receptors mediate cell-

toxicity in a variety of neurological disorders and a great deal of attention has been devoted by pharmaceutical companies to the development of NMDA-targeted drugs. Most drugs selective towards NMDA receptor subtypes target NR2B receptors and only a handful of other compounds have been developed that target other NR2 subtypes, but with questionable selectivity (Berberich *et al*, 2005; Kemp & McKernan, 2002). The inclusion of NR3 subunits, and NR3B variants, in receptor complexes complicates even further the development of NMDA receptor subtype antagonists.

For some time it has been thought that the development of drugs that overactivate NR3-containing receptors would lead to increase neuroprotection, regardless of the NR2 subunit present in the complex. It makes sense in view of the portrayed generic role of NR3 subunits, but my data, and others, argue that NR3 receptors have diverse properties (Matsuda *et al*, 2002; Nishi *et al*, 2001; Sucher *et al*, 1995; Yamakura *et al*, 2005). Thus future drug development will have to take in consideration that activation of NR3A and NR3B will result in increased activity and possibly increased toxicity, rather than the expected neuroprotective effects (Nakanishi *et al*, 2009). But the development of NR3A and NR3B selective drugs is not without caveats. NR3A and NR3B sequences are homologous in the ligand-binding regions and form similar structural complexes with agonists (Yao *et al*, 2008). The practical implication is that ligand affinities of these subunits differ by ~four-fold, thus design of antagonists to discriminate between NR3A and NR3B will have to be targeted outside the ligand-domain (Yao *et al*, 2008).

VII.1 Is NR1/NR2C/NR3A the “oligodendrocytic NMDA receptor”?

Due to its high expression in oligodendrocytic processes NR3s are thought to have a major role in the physiology of oligodendrocytes and also in pathological events (Karadottir *et al*, 2005; Micu *et al*, 2006; Salter & Fern, 2005). Although initial evidence point out to an NMDA receptor complex composed of NR1/NR2C/NR3A, the precise identity of the NR3 subunit and the NR2 subunit that compose oligodendrocytic NMDA receptors is yet to be

determined. Analysis of $[Ca^{2+}]_i$ rises after application of glutamate and glycine reveals that the only subunit where there is a consistent increase in $[Ca^{2+}]_i$ rises with NR3 coexpression is NR1/NR2C (figure V-5 and V-6). Coexpression of NR3B with NR1/NR2B also leads to higher $[Ca^{2+}]_i$ but only when the receptors are stimulated with 1 or 10 μ M, whereas NR3A consistently increases NR1/NR2C mediated $[Ca^{2+}]_i$ influx at the several glutamate concentrations tested (with the exception of 0.1 μ M). This is consistent with NR1/NR2C/NR3A as the main NMDA receptor in oligodendrocytes and could be of particular importance for ischaemic damage to oligodendrocyte process.

The amount of glutamate available in periaxonal space to activate NMDA receptor present in oligodendrocytes processes facing axons, and preferentially targeted in ischaemic damage has not been determined (Salter & Fern, 2005). However, axonal glutamate release is possible in this space (Fields, 2008; Kukley *et al*, 2007; Ziskin *et al*, 2007). Clearance of glutamate in periaxonal space can be performed by oligodendrocytic and axonal glutamate transporters but it is unknown how efficient this process is (Arranz *et al*, 2008; Domercq *et al*, 1999). In the synaptic cleft astrocytes play a major role in clearing glutamate; however these cells are not present in the periaxonal space suggesting that control of extracellular glutamate concentration might be less efficient (Gross, 2006). It can be speculated that in the event of excessive glutamate release to the periaxonal space, and lack of efficient clearance, NMDA receptor in the myelin process will be overactivated and injury to oligodendrocytes will ensue.

In normal physiological concentrations, glutamate concentration in the brain extracellular fluid is in the low micromolar range and rises sharply following ischaemia (Uchiyama-Tsuyuki *et al*, 1994; Umemura *et al*, 1996). In glutamate concentrations higher than the physiological levels, NR3A increases NR1/NR2C $[Ca^{2+}]_i$ suggesting that activation of the latter would have a pathological effect following ischaemic events. Interestingly, NR1/NR2C has a smaller EC50 for glutamate than NR1/NR2C/NR3A. Inclusion of NR3A could be a double-edged sword: at physiological concentrations might help glial development as part of neuron-glia communication and the reduced sensitivity to glutamate works as “fail-safe” mechanism to

avoid overactivation of the receptor in higher, but still physiological, glutamate concentrations (Fields, 2008; Karadottir *et al*, 2008; Roberts *et al*, 2009). But in ischaemia, the increased $[Ca^{2+}]_i$ rises following activation will lead to deleterious consequences (Karadottir *et al*, 2005; Micu *et al*, 2006; Salter & Fern, 2005).

If the results on Ca^{2+} influx through NR1/NR2C/NR3A indicate that this is the NMDA receptor present on oligodendrocytes, the Mg^{2+} block results neither support nor deny this claim. In oligodendrocytes, 10 mM Mg^{2+} blocks NMDA-evoked current to 0.25-0.35 of the current in the absence of Mg^{2+} (Karadottir *et al*, 2005; Micu *et al*, 2006; Salter & Fern, 2005). In our system the same Mg^{2+} concentration caused a similar decrease in $[Ca^{2+}]_i$ rise for NR1/NR2C and inclusion of NR3A (or any other NR3 subunit) did not change the Mg^{2+} block on NR1/NR2C. This does not contradict the hypothesis that NR1/NR2C/NR3A is a major NMDA receptor complex in glia. Furthermore, not all glial cells express these “ Mg^{2+} -insensitive” NMDA receptors. In NG2-glia, the most prevalent cycling progenitor cell population in the adult CNS, NMDA receptors currents are sensitive to Mg^{2+} -block at resting membrane potential, indicating that glial NMDA receptors could be a mixed population of receptors (Dawson *et al*, 2003; Ziskin *et al*, 2007). Indeed, the co-existence of different NMDA receptor populations has been established for neurons and all NMDA receptor subtypes are expressed, albeit at different levels, in white matter (Al-Hallaq *et al*, 2002; Chazot *et al*, 1994; Dunah *et al*, 1998; Karadottir *et al*, 2005; Luo *et al*, 1997; Micu *et al*, 2006; Salter & Fern, 2005). I conclude that although NR1/NR2C/NR3A may play a major role in white matter, it is likely that other NMDA receptors are present ensuring physiological diversity to glutamate transmission.

VII.2 NR3B splice variants

VII.2.1 Expression in white and grey matter

The variants here reported were cloned from the whole brain and/or white matter (optic nerve). Although it would be tempting to associate some of the variants with either neurons or glia, it would not be correct to make such assumptions for two reasons: (1) variants cloned from only one of those tissues might still be expressed in the other. That is, failure to clone does not represent absence of expression. (2) White matter contains only glial mRNA but the whole brain is a mass of both neurons and glia. Thus, expression in the rat optic nerve represent faithful expression in glial cells (most likely oligodendrocytes) but expression in the brain does not necessarily mean expression in neurons. Further studies will be required to determine regional, cellular and developmental expression profiles of NR3B splice variants. At the moment I have designed probes for the detection of splice variant expression in native tissue by Northern blot and the work is currently undergoing in collaboration with Dr. Michael Salter (Leeds University).

VII.2.2 Future research on NR3B splice variants

With the cloning and functional characterization of novel NR3B splice variants a range of questions emerge. I have determined that NR3B splice variants modulate NR1/NR2 receptor properties, in particular glutamate potency and glutamate mediated $[Ca^{2+}]_i$. However, I did not probe for the structural reasons responsible for these effects. It is also quite clear that NR3B $_{\Delta 600}$ and NR3B $_{\Delta 1125}$ will probably differ substantially from the other variants in terms of protein interactions. Although no protein interactions have so far been described for NR3B (apart from interactions with NR1 and NR2s) it is rather unlikely that NR3B does not have interacting partners. The C-terminal of all other NMDA receptor subunits interacts with diverse proteins. For example, NR3A interacts with PACSIN1/syndapin1 which regulates the receptor endocytic removal from the dendritic plasma membrane thus affecting NMDA receptor mediated synaptic activity (Perez-Otano *et al*, 2006). Whether this is the case of NR3B, it remains to be investigated. Nonetheless, it will be likely that these variants will play a part in regulation of NR3B, and NMDA receptor trafficking and subcellular localization.

One way to investigate the role of NR3B variants in neurons and white matter, would be the use of primary cell cultures derived from NR3B^{-/-} (Bradley *et al*, 2006; Niemann *et al*, 2007). These cells are devoid of NR3B receptors, and recombinant expression of individual NR3B splice variants can be performed to reconstitute NR3B activity in these cells and analysis the differential outcomes in several parameters (Bradley *et al*, 2006). Using this strategy, it was determined that C-terminal NR1 variants have different roles in gene expression driven by NMDA receptor activity (Bradley *et al*, 2006). NR3B^{-/-} cell cultures, or organotypic brain slices, can also provide many clues about NR3B role in synaptic transmission and/or participation in toxic events. A similar approach has already been used for NR3A revealing the importance of NR3A for both synaptic development and neuroprotection (Das *et al*, 1998; Ishihama & Turman, 2006). Evaluating ultrastructurally white matter tracts, such as the optic nerve, could also proved clear evidence for the role of NR3A and NR3B in white matter development. NR3B knockout mice have only recently been created and thus these studies are yet to be performed.

Alternative splicing is a common mechanism in the CNS in particular to generate functional diversity neurotransmitter receptors (Grabowski & Black, 2001). The cloning of such a wealth of splice variants is uncommon in glutamate receptors and should warrant careful analysis. I find the idea that even predicted non-functional variants have a role in regulating the number of receptors available and thus cellular functions, intellectually challenging (Campusano *et al*, 2005; Lareau *et al*, 2007; Lareau *et al*, 2004). The possibility that NR3B is undergoing evolutionary pressure is also interesting and perhaps additional genetic association studies could provide further evident supporting or negating this view (Niemann *et al*, 2008).

The effect of NR3 subunits on NMDA receptors is more complex than previously thought. The scarce literature available indicates that NR3A and NR3B have some functional differences, and the cloning of functional NR3B splice variants in this study, argues that the differences maybe even deeper. NR3A and NR3B modulatory effects differ depending on the NR2 subunit present, and NR3B has functional splice variants that add an extra layer of complexity to this modulation. Reappraising and investigating the physiological and molecular properties of NR3 variants are required to the development of successful therapeutic strategies in the future.

Bibliography

Abeliovich A, Chen C, Goda Y, Silva AJ, Stevens CF, Tonegawa S (1993) Modified hippocampal long-term potentiation in PKC ϵ -mutant mice. *Cell* **75**(7): 1253-1262

Akazawa C, Shigemoto R, Bessho Y, Nakanishi S, Mizuno N (1994) Differential expression of five N-methyl-D-aspartate receptor subunit mRNAs in the cerebellum of developing and adult rats. *J Comp Neurol* **347**(1): 150-160

Al-Hallaq RA, Jarabek BR, Fu Z, Vicini S, Wolfe BB, Yasuda RP (2002) Association of NR3A with the N-Methyl-D-aspartate Receptor NR1 and NR2 Subunits. *Mol Pharmacol* **62**(5): 1119-1127

Alix JJP, Dolphin AC, Fern R (2008) Vesicular apparatus, including functional calcium channels, are present in developing rodent optic nerve axons and are required for normal node of Ranvier formation. *The Journal of Physiology* **586**(17): 4069-4089

Alix JP, Fern R (2009) Glutamate receptor-mediated ischemic injury of premyelinated central axons. *Annals of Neurology* **9999**(999A): *in press*

Altshuler D, Pollara VJ, Cowles CR, Van Etten WJ, Baldwin J, Linton L, Lander ES (2000) An SNP map of the human genome generated by reduced representation shotgun sequencing. *Nature* **407**(6803): 513-516

An P, Grabowski PJ (2007) Exon silencing by UAGG motifs in response to neuronal excitation. *PLoS Biol* **5**(2): e36

Anantharam V, Panchal RG, Wilson A, Kolchine VV, Treistman SN, Bayley H (1992) Combinatorial RNA splicing alters the surface charge on the NMDA receptor. *FEBS Letters* **305**(1): 27-30

Andersson O, Stenqvist A, Attersand A, von EG (2001) Nucleotide sequence, genomic organization, and chromosomal localization of genes encoding the human NMDA receptor subunits NR3A and NR3B. *Genomics* **78**(3): 178-184

Anegawa NJ, Lynch DR, Verdoorn TA, Pritchett DB (1995) Transfection of N-methyl-D-aspartate receptors in a nonneuronal cell line leads to cell death. *Journal of Neurochemistry* **64**(5): 2004-2012

Arranz AM, Hussein A, Alix JJ, Perez-Cerda F, Allcock N, Matute C, Fern R (2008) Functional glutamate transport in rodent optic nerve axons and glia. *Glia* **56**(12): 1353-1367

- Atlason PT, Garside ML, Meddows E, Whiting P, McIlhinney RAJ (2007) N-methyl-D-aspartate (NMDA) receptor subunit NR1 forms the substrate for oligomeric assembly of the NMDA receptor. *J Biol Chem*: M702778200
- Back SA, Gan X, Li Y, Rosenberg PA, Volpe JJ (1998) Maturation-dependent vulnerability of oligodendrocytes to oxidative stress-induced death caused by glutathione depletion. *J Neurosci* **18**(16): 6241-6253
- Back SA, Han BH, Luo NL, Chricton CA, Xanthoudakis S, Tam J, Arvin KL, Holtzman DM (2002) Selective vulnerability of late oligodendrocyte progenitors to hypoxia-ischemia. *The Journal Of Neuroscience: The Official Journal Of The Society For Neuroscience* **22**(2): 455-463
- Back SA, Luo NL, Borenstein NS, Levine JM, Volpe JJ, Kinney HC (2001) Late oligodendrocyte progenitors coincide with the developmental window of vulnerability for human perinatal white matter injury. *J Neurosci* **21**(4): 1302-1312
- Back SA, Volpe JJ (1997) Cellular and molecular pathogenesis of periventricular white matter injury. *Mental Retardation and Developmental Disabilities Research Reviews* **3**(1): 96-107
- Balestrino M, Somjen GG (1988) Concentration of carbon dioxide, interstitial pH and synaptic transmission in hippocampal formation of the rat. *The Journal of Physiology* **396**(1): 247-266
- Baumann N, Pham-Dinh D (2001) Biology of Oligodendrocyte and Myelin in the Mammalian Central Nervous System. *Physiological Reviews* **81**(2): 871-927
- Ben-Dov C, Hartmann B, Lundgren J, Valcarcel J (2008) Genome-wide Analysis of Alternative Pre-mRNA Splicing. *J Biol Chem* **283**(3): 1229-1233
- Bendel O (2008) NMDA receptors in neurodegeneration : Studies on NMDA receptor subunit expression preceding ischemia-induced delayed nerve cell death PhD Thesis, Department of Clinical Neuroscience, Karolinska Institute, Stockholm
- Bendel O, Meijer B, Hurd Y, von EG (2005) Cloning and expression of the human NMDA receptor subunit NR3B in the adult human hippocampus. *NeurosciLett* **377**(1): 31-36
- Berberich S, Punnakkal P, Jensen V, Pawlak V, Seeburg PH, Hvalby O, Kohr G (2005) Lack of NMDA Receptor Subtype Selectivity for Hippocampal Long-Term Potentiation. *J Neurosci* **25**(29): 6907-6910

- Bergles DE, Roberts JD, Somogyi P, Jahr CE (2000) Glutamatergic synapses on oligodendrocyte precursor cells in the hippocampus. *Nature* **405**(6783): 187-191
- Bettler B, Boulter J, Hermans-Borgmeyer I, O'Shea-Greenfield A, Deneris ES, Moll C, Borgmeyer U, Hollmann M, Heinemann S (1990) Cloning of a novel glutamate receptor subunit, GluR5: Expression in the nervous system during development. *Neuron* **5**(5): 583-595
- Bettler B, Mulle C (1995) Neurotransmitter receptors II. AMPA and kainate receptors. *Neuropharmacology* **34**(2): 123-139
- Bharadwaj R, Kolodkin AL (2006) Descrambling DSCAM Diversity. *Cell* **125**(3): 421-424
- Bhasi A, Pandey RV, Utharasamy SP, Senapathy P (2007) EuSplice: a unified resource for the analysis of splice signals and alternative splicing in eukaryotic genes. *Bioinformatics* **23**(14): 1815-1823
- Bi X, Rong Y, Chen J, Dang S, Wang Z, Baudry M (1998) Calpain-mediated regulation of NMDA receptor structure and function. *Brain Research* **790**(1-2): 245-253
- Black DL (2003) Mechanisms of alternative pre-messenger RNA splicing. *Annual Review of Biochemistry* **72**(1): 291-336
- Blencowe BJ (2006) Alternative Splicing: New Insights from Global Analyses. *Cell* **126**(1): 37-47
- Bolton S, Butt AM (2006) Cyclic AMP-mediated regulation of the resting membrane potential in myelin-forming oligodendrocytes in the isolated intact rat optic nerve. *Experimental Neurology* **202**(1): 36-43
- Bonetta L (2005) The inside scoop - evaluating gene delivery methods. *Nat Meth* **2**(11): 875-883
- Boue S, Letunic I, Bork P (2003) Alternative splicing and evolution. *BioEssays* **25**(11): 1031-1034
- Brackenridge S, Wilkie AO, Sreaton GR (2003) Efficient use of a 'dead-end' GA 5' splice site in the human fibroblast growth factor receptor genes. *EMBO J* **22**(7): 1620-1631
- Bradley J, Carter SR, Rao VR, Wang J, Finkbeiner S (2006) Splice Variants of the NR1 Subunit Differentially Induce NMDA Receptor-Dependent Gene Expression. *J Neurosci* **26**(4): 1065-1076

Brickley SG, Misra C, Mok MHS, Mishina M, Cull-Candy SG (2003) NR2B and NR2D Subunits Coassemble in Cerebellar Golgi Cells to Form a Distinct NMDA Receptor Subtype Restricted to Extrasynaptic Sites. *J Neurosci* **23**(12): 4958-4966

Brothwell SLC, Barber JL, Monaghan DT, Jane DE, Gibb AJ, Jones S (2008) NR2B- and NR2D-containing synaptic NMDA receptors in developing rat substantia nigra pars compacta dopaminergic neurones. *The Journal of Physiology* **586**(3): 739-750

Brunak S, Engelbrecht J, Knudsen S (1991) Prediction of human mRNA donor and acceptor sites from the DNA sequence. *Journal of Molecular Biology* **220**(1): 49-65

Brusa R, Zimmermann F, Koh DS, Feldmeyer D, Gass P, Seeburg PH, Sprengel R, Sakmann B (1995) Early-onset epilepsy and postnatal lethality associated with an editing-deficient GluR-B allele in mice. *Science* **270**(5242): 1677-1680

Buhler M, Steiner S, Mohn F, Paillusson A, Muhlemann O (2006) EJC-independent degradation of nonsense immunoglobulin- μ mRNA depends on 3[prime] UTR length. *Nat Struct Mol Biol* **13**(5): 462-464

Buller AL, Larson HC, Schneider BE, Beaton JA, Morrisett RA, Monaghan DT (1994) The molecular basis of NMDA receptor subtypes: Native receptor diversity is predicted by subunit composition. *Journal of Neuroscience* **14**(9): 5471-5484

Burnashev N, Monyer H, Seeburg PH, Sakmann B (1992) Divalent ion permeability of AMPA receptor channels is dominated by the edited form of a single subunit. *Neuron* **8**(1): 189-198

Burnashev N, Zhou Z, Neher E, Sakmann B (1995) Fractional calcium currents through recombinant GluR channels of the NMDA, AMPA and kainate receptor subtypes. *Journal of Physiology* **485**(2): 403-418

Burne JF, Staple JK, Raff MC (1996) Glial cells are increased proportionally in transgenic optic nerves with increased numbers of axons. *J Neurosci* **16**(6): 2064-2073

Butt AM, Pugh M, Hubbard P, James G (2004) Functions of optic nerve glia: axoglial signalling in physiology and pathology. *Eye* **18**(11): 1110-1121

Butt AM, Ransom BR (1993) Morphology of astrocytes and oligodendrocytes during development in the intact rat optic nerve. *J Comp Neurol* **338**(1): 141-158

- Campusano JM, Andres ME, Magendzo K, Abarca J, Tapia-Arancibia L, Bustos G (2005) Novel alternative splicing predicts a truncated isoform of the NMDA receptor subunit 1 (NR1) in embryonic rat brain. *Neurochem Res* **30**(4): 567-576
- Cavara N, Hollmann M (2008) Shuffling the Deck Anew: How NR3 Tweaks NMDA Receptor Function. *Molecular Neurobiology* **38**(1): 16-26
- Cavara N, Orth A, Hollmann M (2009) Effects of NR1 splicing on NR1/NR3B-type excitatory glycine receptors. *BMC Neuroscience* **10**(1): 32
- Cawley SL, Pachter L (2003) HMM sampling and applications to gene finding and alternative splicing. *Bioinformatics* **19**(suppl_2): ii36-41
- Chabot B, Elela SA, Zhuo D (2008) Comment on "When good transcripts go bad: artifactual RT-PCR 'splicing' and genome analysis". *BioEssays* **30**(11-12): 1256; author reply 1257-1258
- Chang ACY, Sohlberg B, Trinkle-Mulcahy L, Claverie-Martin F, Cohen P, Cohen SN (1999) Alternative splicing regulates the production of ARD-1 endoribonuclease and NIPP-1, an inhibitor of protein phosphatase-1, as isoforms encoded by the same gene. *Gene* **240**(1): 45-55
- Chang H-R, Kuo C-C (2008) The Activation Gate and Gating Mechanism of the NMDA Receptor. *J Neurosci* **28**(7): 1546-1556
- Chatterton JE, Awobuluyi M, Premkumar LS, Takahashi H, Talantova M, Shin Y, Cui J, Tu S, Sevarino KA, Nakanishi N *et al* (2002) Excitatory glycine receptors containing the NR3 family of NMDA receptor subunits. *Nature* **415**(6873): 793-798
- Chazot PL, Coleman SK, Cik M, Stephenson FA (1994) Molecular characterization of N-methyl-D-aspartate receptors expressed in mammalian cells yields evidence for the coexistence of three subunit types within a discrete receptor molecule. *Journal of Biological Chemistry* **269**(39): 24403-24409
- Chazot PL, Stephenson FA (1997) Molecular dissection of native mammalian forebrain NMDA receptors containing the NR1 C2 exon: direct demonstration of NMDA receptors comprising NR1, NR2A, and NR2B subunits within the same complex. *J Neurochem* **69**(5): 2138-2144
- Chen BE, Kondo M, Garnier A, Watson FL, Püettmann-Holgado R, Lamar DR, Schmucker D (2006) The Molecular Diversity of Dscam Is Functionally Required for Neuronal Wiring Specificity in *Drosophila*. *Cell* **125**(3): 607-620

- Chen N, Moshaver A, Raymond LA (1997) Differential Sensitivity of Recombinant N-Methyl-D-Aspartate Receptor Subtypes to Zinc Inhibition. *Mol Pharmacol* **51**(6): 1015-1023
- Chikaev NA, Bykova EA, Najakshin AM, Mechetina LV, Volkova OY, Peklo MM, Shevelev AY, Vlasik TN, Roesch A, Vogt T *et al* (2005) Cloning and characterization of the human FCRL2 gene. *Genomics* **85**(2): 264-272
- Choi DW (1995) Calcium: still center-stage in hypoxic-ischemic neuronal death. *Trends in Neurosciences* **18**(2): 58-60
- Choi DW, Rothman SM (1990) The role of glutamate neurotoxicity in hypoxic-ischemic neuronal death. *Annual Review of Neuroscience* **13**: 171-182
- Chong A, Zhang G, Bajic VB (2004) Information for the Coordinates of Exons (ICE): a human splice sites database. *Genomics* **84**(4): 762-766
- Ciabarra AM, Sullivan JM, Gahn LG, Pecht G, Heinemann S, Sevarino KA (1995) Cloning and characterization of Chi-1: A developmentally regulated member of a novel class of the ionotropic glutamate receptor family. *Journal of Neuroscience* **15**(10): 6498-6508
- Conti F, DeBiasi S, Minelli A, Melone M (1996) Expression of NR1 and NR2A/B subunits of the NMDA receptor in cortical astrocytes. *Glia* **17**(3): 254-258
- Cousins SL, Papadakis M, Rutter AR, Stephenson FA (2008) Differential interaction of NMDA receptor subtypes with the post-synaptic density-95 family of membrane associated guanylate kinase proteins. *Journal of Neurochemistry* **104**(4): 903-913
- Coward E, Haas SA, Vingron M (2002) SpliceNest: visualizing gene structure and alternative splicing based on EST clusters. *Trends in Genetics* **18**(1): 53-55
- Cox PR, Siddique T, Zoghbi HY (2001) Genomic organization of Tropomodulins 2 and 4 and unusual intergenic and intraexonic splicing of YL-1 and Tropomodulin 4. *BMC Genomics* **2**(1): 7
- Daggett LP, Johnson EC, Varney MA, Lin FF, Hess SD, Deal CR, Jachec C, Lu CC, Kerner JA, Landwehrmeyer GB *et al* (1998) The Human N-Methyl-d-Aspartate Receptor 2C Subunit: Genomic Analysis, Distribution in Human Brain, and Functional Expression. *Journal of Neurochemistry* **71**(5): 1953-1968
- Dalby B, Cates S, Harris A, Ohki EC, Tilkins ML, Price PJ, Ciccarone VC (2004) Advanced transfection with Lipofectamine 2000 reagent: primary neurons, siRNA, and high-throughput applications. *Methods* **33**(2): 95-103

- Danbolt NC (2001) Glutamate uptake. *Progress in Neurobiology* **65**(1): 1-105
- Das S, Sasaki YF, Rothe T, Premkumar LS, Takasu M, Crandall JE, Dikkes P, Conner DA, Rayudu PV, Cheung W *et al* (1998) Increased NMDA current and spine density in mice lacking the NMDA receptor subunit NR3A. *Nature* **393**(6683): 377-381
- Dawson MRL, Polito A, Levine JM, Reynolds R (2003) NG2-expressing glial progenitor cells: an abundant and widespread population of cycling cells in the adult rat CNS. *Molecular and Cellular Neuroscience* **24**(2): 476-488
- Dewar D, Underhill SM, Goldberg MP (2003) Oligodendrocytes and Ischemic Brain Injury. *J Cereb Blood Flow Metab* **23**(3): 263-274
- Dingledine R, Borges K, Bowie D, Traynelis SF (1999) The glutamate receptor ion channels. *Pharmacological Reviews* **51**(1): 7-61
- Dirksen WP, Sun Q, Rottman FM (1995) Multiple Splicing Signals Control Alternative Intron Retention of Bovine Growth Hormone Pre-mRNA. *Journal of Biological Chemistry* **270**(10): 5346-5352
- Doble A (1999) The Role of Excitotoxicity in Neurodegenerative Disease: Implications for Therapy. *Pharmacology & Therapeutics* **81**(3): 163-221
- Dokka S, Toledo D, Shi X, Ye J, Rojanasakul Y (2000) High-efficiency gene transfection of macrophages by lipoplexes. *International Journal of Pharmaceutics* **206**(1-2): 97-104
- Domercq M, Sanchez-Gomez MV, Areso P, Matute C (1999) Expression of glutamate transporters in rat optic nerve oligodendrocytes. *European Journal of Neuroscience* **11**(7): 2226-2236
- Dorus S, Vallender EJ, Evans PD, Anderson JR, Gilbert SL, Mahowald M, Wyckoff GJ, Malcom CM, Lahn BT (2004) Accelerated Evolution of Nervous System Genes in the Origin of Homo sapiens. **119**(7): 1027-1040
- Dravid SM, Prakash A, Traynelis SF (2008) Activation of recombinant NR1/NR2C NMDA receptors. *J Physiol* **586**(18): 4425-4439
- Dror G, Sorek R, Shamir R (2005) Accurate identification of alternatively spliced exons using support vector machine. *Bioinformatics* **21**(7): 897-901

Dunah AW, Luo J, Wang Y-H, Yasuda RP, Wolfe BB (1998) Subunit Composition of N-Methyl-D-aspartate Receptors in the Central Nervous System that Contain the NR2D Subunit. *Mol Pharmacol* **53**(3): 429-437

Durand GM, Bennett MVL, Zukin RS (1993) Splice variants of the N-methyl-D-aspartate receptor NR1 identify domains involved in regulation by polyamines and protein kinase C. *Proceedings of the National Academy of Sciences of the United States of America* **90**(14): 6731-6735

Durand GM, Gregor P, Zheng X, Bennett MVL, Uhl GR, Zukin RS (1992) Cloning of an apparent splice variant of the rat N-methyl-D-aspartate receptor NMDAR1 with altered sensitivity to polyamines and activators of protein kinase C. *Proceedings of the National Academy of Sciences of the United States of America* **89**(19): 9359-9363

Ebralidze AK, Rossi DJ, Tonegawa S, Slater NT (1996) Modification of NMDA receptor channels and synaptic transmission by targeted disruption of the NR2C gene. *Journal of Neuroscience* **16**(16): 5014-5025

Egebjerg J, Bettler B, Hermans-Borgmeyer I, Heinemann S (1991) Cloning of a cDNA for a glutamate receptor subunit activated by kainate but not AMPA. *Nature* **351**(6329): 745-748

Ehlers MD, Fung ET, O'Brien RJ, Huganir RL (1998) Splice variant-specific interaction of the NMDA receptor subunit NR1 with neuronal intermediate filaments. *J Neurosci* **18**(2): 720-730

Ehlers MD, Tingley WG, Huganir RL (1995) Regulated subcellular distribution of the NR1 subunit of the NMDA receptor. *Science* **269**(5231): 1734-1737

Eriksson M, Nilsson A, Froelich-Fabre S, Åkesson E, Dunker J, Seiger Å, Folkesson R, Benedikz E, Sundström E (2001) Cloning and expression of the human N-methyl--aspartate receptor subunit NR3A. *Neuroscience Letters* **321**(3): 177-181

Felgner PL, Gadek TR, Holm M, Roman R, Chan HW, Wenz M, Northrop JP, Ringold GM, Danielsen M (1987) Lipofection: a highly efficient, lipid-mediated DNA-transfection procedure. *Proc Natl Acad Sci U S A* **84**(21): 7413-7417

Feliciello A, Cardone L, Garbi C, Ginsberg MD, Varrone S, Rubin CS, Avvedimento EV, Gottesman ME (1999) Yotiao protein, a ligand for the NMDA receptor, binds and targets cAMP-dependent protein kinase II(1). *FEBS Lett* **464**(3): 174-178

Fern R, Muller T (2000) Rapid ischemic cell death in immature oligodendrocytes: A fatal glutamate release feedback loop. *Journal of Neuroscience* **20**(1): 34-42

- Fields RD (2008) Oligodendrocytes Changing the Rules: Action Potentials in Glia and Oligodendrocytes Controlling Action Potentials. *Neuroscientist* **14**(6): 540-543
- Forrest D, Yuzaki M, Soares HD, Ng L, Luk DC, Sheng M, Stewart CL, Morgan JI, Connor JA, Curran T (1994) Targeted disruption of NMDA receptor 1 gene abolishes NMDA response and results in neonatal death. *Neuron* **13**(2): 325-338
- Foster RE, Connors BW, Waxman SG (1982) Rat optic nerve: electrophysiological, pharmacological and anatomical studies during development. *Brain Res* **255**(3): 371-386
- Frank M, Schaeren-Wiemers N, Schneider R, Schwab ME (1999) Developmental expression pattern of the myelin proteolipid MAL indicates different functions of MAL for immature Schwann cells and in a late step of CNS myelination. *J Neurochem* **73**(2): 587-597
- Fukaya M, Hayashi Y, Watanabe M (2005) NR2 to NR3B subunit switchover of NMDA receptors in early postnatal motoneurons. *Eur J Neurosci* **21**(5): 1432-1436
- Furukawa H, Singh SK, Mancusso R, Gouaux E (2005) Subunit arrangement and function in NMDA receptors. *Nature* **438**(7065): 185-192
- Galante PAF, Sakabe NJ, Kirschbaum-Slager N, De Souza SJ (2004) Detection and evaluation of intron retention events in the human transcriptome. *RNA* **10**(5): 757-765
- Gallo V, Upson LM, Hayes WP, Vyklicky L, Jr., Winters CA, Buonanno A (1992) Molecular cloning and development analysis of a new glutamate receptor subunit isoform in cerebellum. *J Neurosci* **12**(3): 1010-1023
- Garg K, Green P (2007) Differing patterns of selection in alternative and constitutive splice sites. *Genome Research* **17**(7): 1015-1022
- Gielen M, Le Goff A, Stroebel D, Johnson JW, Neyton J, Paoletti P (2008) Structural Rearrangements of NR1/NR2A NMDA Receptors during Allosteric Inhibition. *Neuron* **57**(1): 80-93
- Gillespie LL, Chen G, Paterno GD (1995) Cloning of a Fibroblast Growth Factor Receptor 1 Splice Variant from *Xenopus* Embryos That Lacks a Protein Kinase C Site Important for the Regulation of Receptor Activity. *J Biol Chem* **270**(39): 22758-22763
- Glover RT, Angiolieri M, Kelly S, Monaghan DT, Wang JYJ, Smithgall TE, Buller AL (2000) Interaction of the N-Methyl-D-Aspartic Acid Receptor NR2D Subunit with the c-Abl Tyrosine Kinase. *J Biol Chem* **275**(17): 12725-12729

- Goldberg MP, Choi DW (1993) Combined oxygen and glucose deprivation in cortical cell culture: calcium-dependent and calcium-independent mechanisms of neuronal injury. *Journal of Neuroscience* **13**(8): 3510-3524
- Goldberg MP, Ransom BR (2003) New Light on White Matter. *Stroke* **34**(2): 330-332
- Grabowski PJ (1998) Splicing Regulation in Neurons: Tinkering with Cell-Specific Control. *Cell* **92**(6): 709-712
- Grabowski PJ, Black DL (2001) Alternative RNA splicing in the nervous system. *Progress in Neurobiology* **65**(3): 289-308
- Graham FL, Smiley J, Russell WC, Nairn R (1977) Characteristics of a Human Cell Line Transformed by DNA from Human Adenovirus Type 5. *J Gen Virol* **36**(1): 59-72
- Graham FL, van der Eb AJ (1973) Transformation of rat cells by DNA of human adenovirus 5. *Virology* **54**(2): 536-539
- Grant ER, Bacskai BJ, Anegawa NJ, Pleasure DE, Lynch DR (1998) Opposing contributions of NR1 and NR2 to protein kinase C modulation of NMDA receptors. *J Neurochem* **71**(4): 1471-1481
- Green D, Kroemer G (1998) The central executioners of apoptosis: caspases or mitochondria? *Trends in Cell Biology* **8**(7): 267-271
- Gregor P, O'Hara BF, Yang X, Uhl GR (1993) Expression and novel subunit isoforms of glutamate receptor genes GluR5 and GluR6. *Neuroreport* **4**(12): 1343-1346
- Grimwood S, Gilbert E, Ragan CI, Hutson PH (1996) Modulation of $^{45}\text{Ca}^{2+}$ influx into cells stably expressing recombinant human NMDA receptors by ligands acting at distinct recognition sites. *Journal of Neurochemistry* **66**(6): 2589-2595
- Groc L, Bard L, Choquet D (2009) Surface trafficking of N-methyl-d-aspartate receptors: Physiological and pathological perspectives. *Neuroscience* **158**(1): 4-18
- Gross L (2006) "Supporting" Players Take the Lead in Protecting the Overstimulated Brain. *PLoS Biol* **4**(11): e371
- Grynkiewicz G, Poenie M, Tsien RY (1985) A new generation of Ca^{2+} indicators with greatly improved fluorescence properties. *J Biol Chem* **260**(6): 3440-3450

- Guttmann RP, Sokol S, Baker DL, Simpkins KL, Dong Y, Lynch DR (2002) Proteolysis of the N-Methyl-D-Aspartate Receptor by Calpain in Situ. *J Pharmacol Exp Ther* **302**(3): 1023-1030
- Hafez IM, Maurer N, Cullis PR (2001) On the mechanism whereby cationic lipids promote intracellular delivery of polynucleic acids. *Gene Ther* **8**(15): 1188-1196
- Hamilton N, Vayro S, Kirchhoff F, Verkhratsky A, Robbins J, Gorecki DC, Butt AM (2008) Mechanisms of ATP- and glutamate-mediated calcium signaling in white matter astrocytes. *Glia* **56**(7): 734-749
- Hardingham GE, Fukunaga Y, Bading H (2002) Extrasynaptic NMDARs oppose synaptic NMDARs by triggering CREB shut-off and cell death pathways. *Nat Neurosci* **5**(5): 405-414
- Hatton CJ, Paoletti P (2005) Modulation of Triheteromeric NMDA Receptors by N-Terminal Domain Ligands. *Neuron* **46**(2): 261-274
- Herb A, Burnashev N, Werner P, Sakmann B, Wisden W, Seeburg PH (1992) The KA-2 subunit of excitatory amino acid receptors shows widespread expression in brain and forms ion channels with distantly related subunits. *Neuron* **8**(4): 775-785
- Hiller M, Platzer M (2008) Widespread and subtle: alternative splicing at short-distance tandem sites. *Trends in Genetics* **24**(5): 246-255
- Hirai H, Kirsch J, Laube B, Betz H, Kuhse J (1996) The glycine binding site of the N-methyl-D-aspartate receptor subunit NR1: Identification of novel determinants of co-agonist potentiation in the extracellular M3-M4 loop region. *Proceedings of the National Academy of Sciences of the United States of America* **93**(12): 6031-6036
- Hollmann M, Boulter J, Maron C, Beasley L, Sullivan J, Pecht G, Heinemann S (1993) Zinc potentiates agonist-induced currents at certain splice variants of the NMDA receptor. *Neuron* **10**(5): 943-954
- Hollmann M, Heinemann S (1994) Cloned glutamate receptors. *Annu Rev Neurosci* **17**: 31-108
- Hollmann M, O'Shea-Greenfield A, Rogers SW, Heinemann S (1989) Cloning by functional expression of a member of the glutamate receptor family. *Nature* **342**(6250): 643-648
- Hon-Kit Wong X-BLMFMSFCIP-OMBJCNNJSTEGJSA (2002) Temporal and regional expression of NMDA receptor subunit NR3A in the mammalian brain. *The Journal of Comparative Neurology* **450**(4): 303-317

- Hoopengardner B (2006) Adenosine-to-inosine RNA editing: perspectives and predictions. *Mini Rev Med Chem* **6**(11): 1213-1216
- Human Genome Sequencing C (2004) Finishing the euchromatic sequence of the human genome. *Nature* **431**(7011): 931-945
- Hume RI, Dingledine R, Heinemann SF (1991) Identification of a site in glutamate receptor subunits that controls calcium permeability. *Science* **253**(5023): 1028-1031
- Ikeda K, Araki K, Takayama C, Inoue Y, Yagi T, Aizawa S, Mishina M (1995) Reduced spontaneous activity of mice defective in the epsilon4 subunit of the NMDA receptor channel. *Molecular Brain Research* **33**(1): 61-71
- Ikeda K, Nagasawa M, Mori H, Araki K, Sakimura K, Watanabe M, Inoue Y, Mishina M (1992) Cloning and expression of the epsilon 4 subunit of the NMDA receptor channel. *FEBS Letters* **313**(1): 34-38
- Ilona O, Richard LB, Scott PG, Cindy MR, Lindsay AL, Alexis WA, William AT, Karen KS (2009) Differential Effects of Chronic Ethanol Consumption and Withdrawal on Homer/Glutamate Receptor Expression in Subregions of the Accumbens and Amygdala of P Rats. *Alcoholism: Clinical and Experimental Research* **9999**(9999)
- Inoue K, Ueno S, Yamada J, Fukuda A (2005) Characterization of newly cloned variant of rat glycine receptor [alpha]1 subunit. *Biochemical and Biophysical Research Communications* **327**(1): 300-305
- Ishihama K, Turman JE, Jr. (2006) NR3 protein expression in trigeminal neurons during postnatal development. *Brain Res* **1095**(1): 12-16
- Ishii T, Moriyoshi K, Sugihara H, Sakurada K, Kadotani H, Yokoi M, Akazawa C, Shigemoto R, Mizuno N, Masu M *et al* (1993) Molecular characterization of the family of the N-methyl-D-aspartate receptor subunits. *Journal of Biological Chemistry* **268**(4): 2836-2843
- Jin C, Smothers CT, Woodward JJ (2008) Enhanced ethanol inhibition of recombinant N-methyl-D-aspartate receptors by magnesium: role of NR3A subunits. *Alcohol Clin Exp Res* **32**(6): 1059-1066
- Johnson MB, Kawasawa YI, Mason CE, Krsnik Z, Coppola G, Bogdanovic D, Geschwind DH, Mane SM, State MW, Sestan N (2009) Functional and Evolutionary Insights into Human Brain Development through Global Transcriptome Analysis. *Neuron* **62**(4): 494-509

- Jones S, Gibb AJ (2005) Functional NR2B- and NR2D-containing NMDA receptor channels in rat substantia nigra dopaminergic neurones. *The Journal of Physiology* **569**(1): 209-221
- Kadotani H, Hirano T, Masugi M, Nakamura K, Nakao K, Katsuki M, Nakanishi S (1996) Motor discoordination results from combined gene disruption of the NMDA receptor NR2A and NR2C subunits, but not from single disruption of the NR2A or NR2C subunit. *Journal of Neuroscience* **16**(24): 7859-7867
- Kampa D, Cheng J, Kapranov P, Yamanaka M, Brubaker S, Cawley S, Drenkow J, Piccolboni A, Bekiranov S, Helt G *et al* (2004) Novel RNAs Identified From an In-Depth Analysis of the Transcriptome of Human Chromosomes 21 and 22. *Genome Research* **14**(3): 331-342
- Karadottir R, Cavalier P, Bergersen LH, Attwell D (2005) NMDA receptors are expressed in oligodendrocytes and activated in ischaemia. *Nature* **438**(7071): 1162-1166
- Karadottir R, Hamilton NB, Bakiri Y, Attwell D (2008) Spiking and nonspiking classes of oligodendrocyte precursor glia in CNS white matter. *Nat Neurosci* **11**(4): 450-456
- Keinanen K, Wisden W, Sommer B, Werner P, Herb A, Verdoorn TA, Sakmann B, Seeburg PH (1990) A family of AMPA-selective glutamate receptors. *Science* **249**(4968): 556-560
- Kemp JA, McKernan RM (2002) NMDA receptor pathways as drug targets. *Nat Neurosci*
- Kettenmann H, Ransom B (1995) *Neuroglia*, New York: Oxford University Press.
- Kew JN, Kemp JA (2005) Ionotropic and metabotropic glutamate receptor structure and pharmacology. *Psychopharmacology (Berl)* **179**(1): 4-29
- Kim E, Cho KO, Rothschild A, Sheng M (1996) Heteromultimerization and NMDA receptor-clustering activity of Chapsyn-110, a member of the PSD-95 family of proteins. *Neuron* **17**(1): 103-113
- Kinney HC, Back SA (1998) Human oligodendroglial development: Relationship to periventricular leukomalacia. *Seminars in Pediatric Neurology* **5**(3): 180-189
- Klein M, Pieri I, Uhlmann F, Pfizenmaier K, Eisel U (1998) Cloning and characterization of promoter and 5'-UTR of the NMDA receptor subunit [epsilon]2: evidence for alternative splicing of 5'-non-coding exon. *Gene* **208**(2): 259-269
- Kohr G, Eckardt S, Luddens H, Monyer H, Seeburg PH (1994) NMDA receptor channels: subunit-specific potentiation by reducing agents. *Neuron* **12**(5): 1031-1040

- Kondrashov FA, Koonin EV (2003) Evolution of alternative splicing: deletions, insertions and origin of functional parts of proteins from intron sequences. *Trends in Genetics* **19**(3): 115-119
- Kornau HC, Schenker LT, Kennedy MB, Seeburg PH (1995) Domain interaction between NMDA receptor subunits and the postsynaptic density protein PSD-95. *Science* **269**(5231): 1737-1740
- Kotewicz ML, Sampson CM, D'Alessio JM, Gerard GF (1988) Isolation of cloned Moloney murine leukemia virus reverse transcriptase lacking ribonuclease H activity. *Nucl Acids Res* **16**(1): 265-277
- Krebs C, Fernandes HB, Sheldon C, Raymond LA, Baimbridge KG (2003) Functional NMDA Receptor Subtype 2B Is Expressed in Astrocytes after Ischemia In Vivo and Anoxia In Vitro. *J Neurosci* **23**(8): 3364-3372
- Kreutz MR, Bockers TM, Bockmann J, Seidenbecher CI, Kracht B, Vorwerk CK, Weise J, Sabel BA (1998) Axonal Injury Alters Alternative Splicing of the Retinal NR1 Receptor: the Preferential Expression of the NR1b Isoforms Is Crucial for Retinal Ganglion Cell Survival. *J Neurosci* **18**(20): 8278-8291
- Kukley M, Capetillo-Zarate E, Dietrich D (2007) Vesicular glutamate release from axons in white matter. *Nat Neurosci* **10**(3): 311-320
- Kutsuwada T, Kashiwabuchi N, Mori H, Sakimura K, Kushiya E, Araki K, Meguro H, Masaki H, Kumanishi T, Arakawa M *et al* (1992) Molecular diversity of the NMDA receptor channel. *Nature* **358**(6381): 36-41
- Kutsuwada T, Sakimura K, Manabe T, Takayama C, Katakura N, Kushiya E, Natsume R, Watanabe M, Inoue Y, Yagi T *et al* (1996) Impairment of suckling response, trigeminal neuronal pattern formation, and hippocampal LTD in NMDA receptor epsilon2 subunit mutant mice. *Neuron* **16**(2): 333-344
- Kwak S, Kawahara Y (2005) Deficient RNA editing of GluR2 and neuronal death in amyotrophic lateral sclerosis. *Journal of Molecular Medicine* **83**(2): 110-120
- Lalo U, Pankratov Y, Kirchhoff F, North RA, Verkhratsky A (2006) NMDA receptors mediate neuron-to-glia signaling in mouse cortical astrocytes. *Journal of Neuroscience* **26**(10): 2673-2683

- Lamas M, Lee-Rivera I, Lopez-Colome AM (2005) Cell-specific Expression of N-Methyl-D-Aspartate Receptor Subunits in Muller Glia and Neurons from the Chick Retina. *Invest Ophthalmol Vis Sci* **46**(10): 3570-3577
- Lander ES, Linton LM, Birren B, Nusbaum C, Zody MC, Baldwin J, Devon K, Dewar K, Doyle M, FitzHugh W *et al* (2001) Initial sequencing and analysis of the human genome. *Nature* **409**(6822): 860-921
- Lareau LF, Brooks AN, Soergel DAW, Meng Q, Brenner SE (2007) The Coupling of Alternative Splicing and Nonsense-Mediated mRNA Decay. In *Alternative Splicing in the Postgenomic Era*, Blencowe BJ, Graveley BR (eds), pp 190-211. Austin, USA: Landes Bioscience
- Lareau LF, Green RE, Bhatnagar RS, Brenner SE (2004) The evolving roles of alternative splicing. *Current Opinion in Structural Biology* **14**(3): 273-282
- Lau L-F, Mammen A, Ehlers MD, Kindler S, Chung WJ, Garner CC, Huganir RL (1996) Interaction of the N-Methyl--aspartate Receptor Complex with a Novel Synapse-associated Protein, SAP102. *J Biol Chem* **271**(35): 21622-21628
- Laube B, Hirai H, Sturgess M, Betz H, Kuhse J (1997) Molecular determinants of agonist discrimination by NMDA receptor subunits: Analysis of the glutamate binding site on the NR2B subunit. *Neuron* **18**(3): 493-503
- Laube B, Kuhse J, Betz H (1998) Evidence for a Tetrameric Structure of Recombinant NMDA Receptors. *J Neurosci* **18**(8): 2954-2961
- Laurie DJ, Putzke J, Zieglansberger W, Seeburg PH, Tolle TR (1995) The distribution of splice variants of the NMDAR1 subunit mRNA in adult rat brain. *Molecular Brain Research* **32**(1): 94-108
- Laurie DJ, Seeburg PH (1994) Ligand affinities at recombinant N-methyl-D-aspartate receptors depend on subunit composition. *European Journal of Pharmacology - Molecular Pharmacology Section* **268**(3): 335-345
- Lee JA, Xing Y, Nguyen D, Xie J, Lee CJ, Black DL (2007) Depolarization and CaM kinase IV modulate NMDA receptor splicing through two essential RNA elements. *PLoS Biol* **5**(2): e40
- Lester RAJ, Clements JD, Westbrook GL, Jahr CE (1990) Channel kinetics determine the time course of NMDA receptor-mediated synaptic currents. *Nature* **346**(6284): 565-567

Lewin B (2004) *Genes VIII*: Pearson Prentice Hall, Pearson Education, Inc.

Li S, Mealing GA, Morley P, Stys PK (1999) Novel injury mechanism in anoxia and trauma of spinal cord white matter: glutamate release via reverse Na⁺-dependent glutamate transport. *The Journal of neuroscience : the official journal of the Society for Neuroscience* **19**(14)

Li Y, Erzurumlu RS, Chen C, Jhaveri S, Tonegawa S (1994) Whisker-related neuronal patterns fail to develop in the trigeminal brainstem nuclei of NMDAR1 knockout mice. *Cell* **76**(3): 427-437

Lin JW, Wyszynski M, Madhavan R, Sealock R, Kim JU, Sheng M (1998) Yotiao, a novel protein of neuromuscular junction and brain that interacts with specific splice variants of NMDA receptor subunit NR1. *J Neurosci* **18**(6): 2017-2027

Lomeli H, Mosbacher J, Melcher T, Hoyer T, Geiger JRP, Kuner T, Monyer H, Higuchi M, Bach A, Seeburg PH (1994) Control of kinetic properties of AMPA receptor channels by nuclear RNA editing. *Science* **266**(5191): 1709-1713

Lomeli H, Wisden W, Kohler M, Keinänen K, Sommer B, Seeburg PH (1992) High-affinity kainate and domoate receptors in rat brain. *FEBS Letters* **307**(2): 139-143

Luo J, Wang Y, Yasuda RP, Dunah AW, Wolfe BB (1997) The Majority of N-Methyl-D-Aspartate Receptor Complexes in Adult Rat Cerebral Cortex Contain at Least Three Different Subunits (NR1/NR2A/NR2B). *Mol Pharmacol* **51**(1): 79-86

Luo JH, Fu ZY, Losi G, Kim BG, Prybylowski K, Vissel B, Vicini S (2002) Functional expression of distinct NMDA channel subunits tagged with green fluorescent protein in hippocampal neurons in culture. *Neuropharmacology* **42**(3): 306-318

Luque JM, Richards JG (1995) Expression of NMDA 2B receptor subunit mRNA in Bergmann glia. *Glia* **13**(3): 228-232

Lynch DR, Anegawa NJ, Verdoorn T, Pritchett DB (1994) N-methyl-D-aspartate receptors: Different subunit requirements for binding of glutamate antagonists, glycine antagonists, and channel-blocking agents. *Molecular Pharmacology* **45**(3): 540-545

Lynch DR, Guttman RP (2001) NMDA receptor pharmacology: perspectives from molecular biology. *Curr Drug Targets* **2**(3): 215-231

Lynch DR, Guttman RP (2002) Excitotoxicity: Perspectives Based on N-Methyl-D-Aspartate Receptor Subtypes. *J Pharmacol Exp Ther* **300**(3): 717-723

- Lyons SA, Kettenmann H (1998) Oligodendrocytes and microglia are selectively vulnerable to combined hypoxia and hypoglycemia injury in vitro. *Journal of Cerebral Blood Flow and Metabolism* **18**(5): 521-530
- MacDermott AB, Mayer ML, Westbrook GL (1986) NMDA-receptor activation increases cytoplasmic calcium concentration in cultured spinal cord neurones. *Nature* **321**(6069): 519-522
- Maquat LE (2004) Nonsense-mediated mRNA decay: splicing, translation and mRNP dynamics. *Nat Rev Mol Cell Biol* **5**(2): 89-99
- Marshall J, Molloy R, Moss GWJ, Howe JR, Hughes TE (1995) The jellyfish green fluorescent protein: A new tool for studying ion channel expression and function. *Neuron* **14**(2): 211-215
- Matlin AJ, Clark F, Smith CWJ (2005) Understanding alternative splicing: towards a cellular code. *Nat Rev Mol Cell Biol* **6**(5): 386-398
- Matsuda K, Fletcher M, Kamiya Y, Yuzaki M (2003) Specific assembly with the NMDA receptor 3B subunit controls surface expression and calcium permeability of NMDA receptors. *J Neurosci* **23**(31): 10064-10073
- Matsuda K, Kamiya Y, Matsuda S, Yuzaki M (2002) Cloning and characterization of a novel NMDA receptor subunit NR3B: a dominant subunit that reduces calcium permeability. *Brain Res Mol Brain Res* **100**(1-2): 43-52
- Matute C (2006) Oligodendrocyte NMDA receptors: a novel therapeutic target. *Trends in Molecular Medicine* **12**(7): 289-292
- Matute C, Alberdi E, Domercq M, rez C, rez S, nchez G (2001) The link between excitotoxic oligodendroglial death and demyelinating diseases. *Trends in Neurosciences* **24**(4): 224-230
- Matute C, Alberdi E, Ibarretxe G, Sanchez-Gomez MV (2002) Excitotoxicity in glial cells. *European Journal of Pharmacology* **447**(2-3): 239-246
- Matute C, Domercq M, Fogarty DJ, Pascual de Zulueta M, nchez G (1999) On how altered glutamate homeostasis may contribute to demyelinating diseases of the CNS. *The Function of Glial Cells in Health and Disease: Dialogue Between Glia and Neurons*: 97-108
- Matute C, nchez G, nez M, Miledi R (1997) Glutamate receptor-mediated toxicity in optic nerve oligodendrocytes. *Proceedings of the National Academy of Sciences of the United States of America* **94**(16): 8830-8835

- Mayer ML (2006) Glutamate receptors at atomic resolution. *Nature* **440**(7083): 456-462
- Mayer ML, Westbrook GL (1987) Permeation and block of N-methyl-D-aspartic acid receptor channels by divalent cations in mouse cultured central neurones. *Journal of Physiology* **394**: 501-527
- Mayer ML, Westbrook GL, Buthrie PB (1984) Voltage-dependent block by Mg²⁺ of NMDA responses in spinal cord neurones. *Nature* **309**(5965): 261-263
- McBain CJ, Mayer ML (1994) N-methyl-D-aspartic acid receptor structure and function. *Physiological Reviews* **74**(3): 723-760
- McCulloch RM, Johnston GA, Game CJ, Curtis DR (1974) The differential sensitivity of spinal interneurons and Renshaw cells to Kainate and N-methyl-D-aspartate. *Exp Brain Res* **21**(5): 515-518
- McCutchan JH, Pagano JS (1968) Enhancement of the infectivity of simian virus 40 deoxyribonucleic acid with diethylaminoethyl-dextran. *J Natl Cancer Inst* **41**(2): 351-357
- McDonald JW, Althomsons SP, Hyrc KL, Choi DW, Goldberg MP (1998) Oligodendrocytes from forebrain are highly vulnerable to AMPA/kainate receptor-mediated excitotoxicity. *Nat Med* **4**(3): 291-297
- McRoberts JA, Ennes HS, Li J, Slice L, Mayer EA (2003) Rat DRG neurons express NR3 NMDA receptor subunits and excitatory glycine receptors. *Gastroenterology* **124**(4, Supplement 1): A468-A468
- Meddows E, Le B, Grimwood S, Wafford K, Sandhu S, Whiting P, McIlhinney RAJ (2001) Identification of Molecular Determinants That Are Important in the Assembly of N-Methyl-D-aspartate Receptors. *Journal of Biological Chemistry* **276**(22): 18795-18803
- Medina I, Filippova N, Charton G, Rougeole S, Ben-Ari Y, Khrestchatisky M, Bregestovski P (1995) Calcium-dependent inactivation of heteromeric NMDA receptor-channels expressed in human embryonic kidney cells. *J Physiol* **482** (Pt 3): 567-573
- Meguro H, Mori H, Araki K, Kushiya E, Kutsuwada T, Yamazaki M, Kumanishi T, Arakawa M, Sakimura K, Mishina M (1992) Functional characterization of a heteromeric NMDA receptor channel expressed from cloned cDNAs. *Nature* **357**(6373): 70-74

- Mei Q, Maharaj KT (2005) Role of AP-1 in ethanol-induced *N*-methyl-d-aspartate receptor 2B subunit gene up-regulation in mouse cortical neurons. *Journal of Neurochemistry* **95**(5): 1332-1341
- Melhuish T, Wotton D (2006) The *Tgif2* gene contains a retained intron within the coding sequence. *BMC Molecular Biology* **7**(1): 2
- Mi R, Sia G-M, Rosen K, Tang X, Moghekar A, Black JL, McEnery M, Haganir RL, O'Brien RJ (2004) AMPA Receptor-Dependent Clustering of Synaptic NMDA Receptors Is Mediated by Stargazin and NR2A/B in Spinal Neurons and Hippocampal Interneurons. *Neuron* **44**(2): 335-349
- Micu I, Jiang Q, Coderre E, Ridsdale A, Zhang L, Woulfe J, Yin X, Trapp BD, McRory JE, Rehak R *et al* (2006) NMDA receptors mediate calcium accumulation in myelin during chemical ischaemia. *Nature* **439**(7079): 988-992
- Misra C, Brickley SG, Farrant M, Cull-Candy SG (2000) Identification of subunits contributing to synaptic and extrasynaptic NMDA receptors in Golgi cells of the rat cerebellum. *The Journal of Physiology* **524**(1): 147-162
- Miyamoto Y, Yamada K, Noda Y, Mori H, Mishina M, Nabeshima T (2002) Lower Sensitivity to Stress and Altered Monoaminergic Neuronal Function in Mice Lacking the NMDA Receptor epsilon 4 Subunit. *J Neurosci* **22**(6): 2335-2342
- Modrek B, Resch A, Grasso C, Lee C (2001) Genome-wide detection of alternative splicing in expressed sequences of human genes. *Nucl Acids Res* **29**(13): 2850-2859
- Mohrmann R, Köhr G, Hatt H, Sprengel R, Gottmann K (2002) Deletion of the C-terminal domain of the NR2B subunit alters channel properties and synaptic targeting of N-methyl-D-aspartate receptors in nascent neocortical synapses. *Journal of Neuroscience Research* **68**(3): 265-275
- Monaghan DT, Bridges RJ, Cotman CW (1989) The Excitatory Amino Acid Receptors: Their Classes, Pharmacology, and Distinct Properties in the Function of the Central Nervous System. *Annual Review of Pharmacology and Toxicology* **29**(1): 365-402
- Monyer H, Burnashev N, Laurie DJ, Sakmann B, Seeburg PH (1994) Developmental and regional expression in the rat brain and functional properties of four NMDA receptors. *Neuron* **12**(3): 529-540

Monyer H, Sprengel R, Schoepfer R, Herb A, Higuchi M, Lomeli H, Burnashev N, Sakmann B, Seeburg PH (1992) Heteromeric NMDA receptors: Molecular and functional distinction of subtypes. *Science* **256**(5060): 1217-1221

Morgan KG (1993) Ca²⁺i versus [Ca²⁺]_i. *Biophys J* **65**(2): 561-562

Mori H, Mishina M (1995) Neurotransmitter receptors VIII. Structure and function of the NMDA receptor channel. *Neuropharmacology* **34**(10): 1219-1237

Moriyoshi K, Masu M, Ishii T, Shigemoto R, Mizuno N, Nakanishi S (1991) Molecular cloning and characterization of the rat NMDA receptor. *Nature* **353**(6348): 31-37

Mu Y, Otsuka T, Horton AC, Scott DB, Ehlers MD (2003) Activity-Dependent mRNA Splicing Controls ER Export and Synaptic Delivery of NMDA Receptors. *Neuron* **40**(3): 581-594

Müller BM, Kistner U, Kindler S, Chung WJ, Kuhlendahl S, Fenster SD, Lau L-F, Veh RW, Haganir RL, Gundelfinger ED *et al* (1996) SAP102, a Novel Postsynaptic Protein That Interacts with NMDA Receptor Complexes In Vivo. *Neuron* **17**(2): 255-265

Nakanishi N, Axel R, Shneider NA (1992) Alternative splicing generates functionally distinct N-methyl-D-aspartate receptors. *Proc Natl Acad Sci USA* **89**(18): 8552-8556

Nakanishi N, Tu S, Shin Y, Cui J, Kurokawa T, Zhang D, Chen HSV, Tong G, Lipton SA (2009) Neuroprotection by the NR3A Subunit of the NMDA Receptor. *J Neurosci* **29**(16): 5260-5265

Nakanishi S (1992) Molecular diversity of glutamate receptors and implications for brain function. *Science* **258**(5082): 597-603

Nam DK, Lee S, Zhou G, Cao X, Wang C, Clark T, Chen J, Rowley JD, Wang SM (2002) Oligo(dT) primer generates a high frequency of truncated cDNAs through internal poly(A) priming during reverse transcription. *Proc Natl Acad Sci U S A* **99**(9): 6152-6156

Negulescu PA, Machen TE (1990) Intracellular ion activities and membrane transport in parietal cells measured with fluorescent dyes. *Methods Enzymol* **192**: 38-81

Nicotera P, Lipton SA (1999) Excitotoxins in neuronal apoptosis and necrosis. *Journal of Cerebral Blood Flow and Metabolism* **19**(6): 583-591

Niemann S, Kanki H, Fukui Y, Takao K, Fukaya M, Hynynen MN, Churchill MJ, Shefner JM, Bronson RT, Brown RH, Jr. *et al* (2007) Genetic ablation of NMDA receptor subunit

NR3B in mouse reveals motoneuronal and nonmotoneuronal phenotypes. *Eur J Neurosci* **26**(6): 1407-1420

Niemann S, Landers JE, Churchill MJ, Hosler B, Sapp P, Speed WC, Lahn BT, Kidd KK, Brown RH, Jr., Hayashi Y (2008) Motoneuron-specific NR3B gene: No association with ALS and evidence for a common null allele. *Neurology* **70**(9): 666-676

Niethammer M, Kim E, Sheng M (1996) Interaction between the C terminus of NMDA receptor subunits and multiple members of the PSD-95 family of membrane-associated guanylate kinases. *Journal of Neuroscience* **16**(7): 2157-2163

Nilsson A, Eriksson M, Muly EC, Akesson E, Samuelsson EB, Bogdanovic N, Benedikz E, Sundstrom E (2007) Analysis of NR3A receptor subunits in human native NMDA receptors. *Brain Res* **1186**: 102-112

Nishi M, Hinds H, Lu HP, Kawata M, Hayashi Y (2001) Motoneuron-specific expression of NR3B, a novel NMDA-type glutamate receptor subunit that works in a dominant-negative manner. *J Neurosci* **21**(23): RC185

Noseworthy JH (1999) Progress in determining the causes and treatment of multiple sclerosis. *Nature* **399**(6738 Suppl): A40-A47

Nowak L, Bregestovski P, Ascher P (1984) Magnesium gates glutamate-activated channels in mouse central neurones. *Nature* **307**(5950): 462-465

O'Brien JS, Sampson EL (1965) Lipid composition of the normal human brain: gray matter, white matter, and myelin. *J Lipid Res* **6**(4): 537-544

Obrenovitch TP, Scheller D, Matsumoto T, Tegtmeier F, Holler M, Symon L (1990) A rapid redistribution of hydrogen ions is associated with depolarization and repolarization subsequent to cerebral ischemia reperfusion. *J Neurophysiol* **64**(4): 1125-1133

Oertel J, Villmann C, Kettenmann H, Kirchhoff F, Becker C-M (2007) A Novel Glycine Receptor beta Subunit Splice Variant Predicts an Unorthodox Transmembrane Topology: ASSEMBLY INTO HETEROMERIC RECEPTOR COMPLEXES. *J Biol Chem* **282**(5): 2798-2807

Okabe S, Miwa A, Okado H (1999) Alternative Splicing of the C-Terminal Domain Regulates Cell Surface Expression of the NMDA Receptor NR1 Subunit. *J Neurosci* **19**(18): 7781-7792

- Ozawa S, Kamiya H, Tsuzuki K (1998) Glutamate receptors in the mammalian central nervous system. *Progress in Neurobiology* **54**(5): 581-618
- Pantoni L, Garcia JH, Gutierrez JA, Rosenblum WI (1996) Cerebral White Matter Is Highly Vulnerable to Ischemia. *Stroke* **27**(9): 1641-1647
- Paoletti P, Ascher P, Neyton J (1997) High-Affinity Zinc Inhibition of NMDA NR1-NR2A Receptors. *J Neurosci* **17**(15): 5711-5725
- Payam R, Andrew D (2002) Periventricular leukomalacia, inflammation and white matter lesions within the developing nervous system. *Neuropathology* **22**(3): 106-132
- Perez-Otano I, Lujan R, Tavalin SJ, Plomann M, Modregger J, Liu X-B, Jones EG, Heinemann SF, Lo DC, Ehlers MD (2006) Endocytosis and synaptic removal of NR3A-containing NMDA receptors by PACSIN1/syndapin1. *Nat Neurosci* **9**(5): 611-621
- Perez-Otano I, Schulteis CT, Contractor A, Lipton SA, Trimmer JS, Sucher NJ, Heinemann SF (2001) Assembly with the NR1 Subunit Is Required for Surface Expression of NR3A-Containing NMDA Receptors. *J Neurosci* **21**(4): 1228-1237
- Petito CK, Olarte JP, Roberts B, Nowak TS, Jr., Pulsinelli WA (1998) Selective glial vulnerability following transient global ischemia in rat brain. *J NeuropatholExpNeurol* **57**(3): 231-238
- Petralia RS, Yokotani N, Wenthold RJ (1994) Light and electron microscope distribution of the NMDA receptor subunit NMDAR1 in the rat nervous system using a selective anti-peptide antibody. *Journal of Neuroscience* **14**(2): 667-696
- Pitt D, Werner P, Raine CS (2000) Glutamate excitotoxicity in a model of multiple sclerosis. *NatMed* **6**(1): 67-70
- Plested AJR (2008) How 2C a channel that's (almost) not there. *The Journal of Physiology* **586**(18): 4339-4340
- Poliak S, Peles E (2003) The local differentiation of myelinated axons at nodes of Ranvier. *Nat Rev Neurosci* **4**(12): 968-980
- Polumuri SK, Ruknudin A, Schulze DH (2002) RNase H and its effects on PCR. *Biotechniques* **32**(6): 1224-1225

- Prithviraj R, Inglis FM (2008) Expression of the N-methyl-d-aspartate receptor subunit NR3B regulates dendrite morphogenesis in spinal motor neurons. *Neuroscience* **155**(1): 145-153
- Prybylowski K, Rumbaugh G, Wolfe BB, Vicini S (2000) Increased exon 5 expression alters extrasynaptic NMDA receptors in cerebellar neurons. *J Neurochem* **75**(3): 1140-1146
- Prybylowski KL, Grossman SD, Wrathall JR, Wolfe BB (2001) Expression of splice variants of the NR1 subunit of the N-methyl-D-aspartate receptor in the normal and injured rat spinal cord. *J Neurochem* **76**(3): 797-805
- Prybylowski KL, Wolfe BB (2000) Developmental differences in alternative splicing of the NR1 protein in rat cortex and cerebellum. *Developmental Brain Research* **123**(2): 143-150
- Puddifoot CA, Chen PE, Schoepfer R, Wyllie DJA (2009) Pharmacological characterization of recombinant NR1/NR2A NMDA receptors with truncated and deleted carboxy termini expressed in *Xenopus laevis* oocytes. *British Journal of Pharmacology* **156**(3): 509-518
- Qian A, Buller AL, Johnson JW (2005) NR2 subunit-dependence of NMDA receptor channel block by external Mg²⁺. *J Physiol* **562**(Pt 2): 319-331
- Qiu S, Hua Y-l, Yang F, Chen Y-z, Luo J-h (2005) Subunit Assembly of N-Methyl-D-aspartate Receptors Analyzed by Fluorescence Resonance Energy Transfer. *J Biol Chem* **280**(26): 24923-24930
- Rafiki A, Bernard A, Medina I, Gozlan H, Khrestchatsky M (2000) Characterization in cultured cerebellar granule cells and in the developing rat brain of mRNA variants for the NMDA receptor 2C subunit. *J Neurochem* **74**(5): 1798-1808
- Rameau GA, Akaneya Y, Chiu L-Y, Ziff EB (2000) Role of NMDA receptor functional domains in excitatory cell death. *Neuropharmacology* **39**(12): 2255-2266
- Rani CSS, Qiang M, Ticku MK (2005) Potential Role of cAMP Response Element-Binding Protein in Ethanol-Induced N-Methyl-D-aspartate Receptor 2B Subunit Gene Transcription in Fetal Mouse Cortical Cells. *Mol Pharmacol* **67**(6): 2126-2136
- Reese MG, Eeckman FH, Kulp D, Haussler D (1997) Improved splice site detection in Genie. *J Comput Biol* **4**(3): 311-323
- Ren R, Mayer BJ, Cicchetti P, Baltimore D (1993) Identification of a ten-amino acid proline-rich SH3 binding site. *Science* **259**(5098): 1157-1161

- Renard S, Drouet-Pétre C, Partiseti M, Langer SZ, Graham D, Besnard F (1999) Development of an inducible NMDA receptor stable cell line with an intracellular Ca²⁺ reporter. *European Journal of Pharmacology* **366**(2-3): 319-328
- Riedel G, Platt B, Micheau J (2003) Glutamate receptor function in learning and memory. *BehavBrain Res* **140**(1-2): 1-47
- Roberts AC, Díez-García J, Rodriguiz RM, López IP, Luján R, Martínez-Turrillas R, Picó E, Henson MA, Bernardo DR, Jarrett TM *et al* (2009) Downregulation of NR3A-Containing NMDARs Is Required for Synapse Maturation and Memory Consolidation. *Neuron* **63**(3): 342-356
- Romano M, Marcucci R, Baralle FE (2001) Splicing of constitutive upstream introns is essential for the recognition of intra-exonic suboptimal splice sites in the thrombopoietin gene. *Nucl Acids Res* **29**(4): 886-894
- Roy SW, Irimia M (2008) When good transcripts go bad: artifactual RT-PCR 'splicing' and genome analysis. *BioEssays* **30**(6): 601-605
- Rueter SM, Burns CM, Coode SA, Mookherjee P, Emeson RB (1995) Glutamate receptor RNA editing in vitro by enzymatic conversion of adenosine to inosine. *Science* **267**(5203): 1491-1494
- Rumbaugh G, Prybylowski K, Wang JF, Vicini S (2000) Exon 5 and spermine regulate deactivation of NMDA receptor subtypes. *Journal of Neurophysiology* **83**(3): 1300-1306
- Ryan T, Emes R, Grant S, Komiyama N (2008) Evolution of NMDA receptor cytoplasmic interaction domains: implications for organisation of synaptic signalling complexes. *BMC Neuroscience* **9**(1): 6
- Sakabe N, de Souza S (2007) Sequence features responsible for intron retention in human. *BMC Genomics* **8**(1): 59
- Sakimura K, Kutsuwada T, Ito I, Manabe T, Takayama C, Kushiya E, Yagi T, Aizawa S, Inoue Y, Sugiyama H *et al* (1995) Reduced hippocampal LTP and spatial learning in mice lacking NMDA receptor epsilon 1 subunit. *Nature* **373**(6510): 151-155
- Salter MG, Fern R (2005) NMDA receptors are expressed in developing oligodendrocyte processes and mediate injury. *Nature* **438**(7071): 1167-1171
- Salter MW, Kalia LV (2004) Src kinases: a hub for NMDA receptor regulation. *Nat Rev Neurosci* **5**(4): 317-328

Sans N, Petralia RS, Wang Y-X, Blahos J, II, Hell JW, Wenthold RJ (2000) A Developmental Change in NMDA Receptor-Associated Proteins at Hippocampal Synapses. *J Neurosci* **20**(3): 1260-1271

Sans N, Prybylowski K, Petralia RS, Chang K, Wang Y-X, Racca C, Vicini S, Wenthold RJ (2003) NMDA receptor trafficking through an interaction between PDZ proteins and the exocyst complex. *Nat Cell Biol* **5**(6): 520-530

Sasaki YF, Rothe T, Premkumar LS, Das S, Cui J, Talantova MV, Wong HK, Gong X, Chan SF, Zhang D *et al* (2002a) Characterization and comparison of the NR3A subunit of the NMDA receptor in recombinant systems and primary cortical neurons. *Journal of Neurophysiology* **87**(4): 2052-2063

Sasaki YF, Rothe T, Premkumar LS, Das S, Cui J, Talantova MV, Wong HK, Gong X, Chan SF, Zhang D *et al* (2002b) Characterization and comparison of the NR3A subunit of the NMDA receptor in recombinant systems and primary cortical neurons. *J Neurophysiol* **87**(4): 2052-2063

Sasner M, Buonanno A (1996) Distinct N-Methyl--aspartate Receptor 2B Subunit Gene Sequences Confer Neural and Developmental Specific Expression. *J Biol Chem* **271**(35): 21316-21322

Schiffer HH, Swanson GT, Heinemann SF (1997) Rat GluR7 and a Carboxy-Terminal Splice Variant, GluR7b, Are Functional Kainate Receptor Subunits with a Low Sensitivity to Glutamate. *Neuron* **19**(5): 1141-1146

Schiller J, Schiller Y, Clapham DE (1998) NMDA receptors amplify calcium influx into dendritic spines during associative pre- and postsynaptic activation. *Nat Neurosci* **1**(2): 114-118

Schipke CG, Ohlemeyer C, Matyash M, Nolte C, Kettenmann H, Kirchhoff F (2001) Astrocytes of the mouse neocortex express functional N-methyl-D-aspartate receptors. *FASEB J*: 00-0439fje

Schmidt C, Hollmann M (2008) Apparent Homomeric NR1 Currents Observed in *Xenopus* Oocytes are Caused by an Endogenous NR2 Subunit. *Journal of Molecular Biology* **376**(3): 658-670

Schmidt C, Werner M, Hollmann M (2006) Revisiting the Postulated "Unitary Glutamate Receptor": Electrophysiological and Pharmacological Analysis in Two Heterologous Expression Systems Fails to Detect Evidence for Its Existence. *Mol Pharmacol* **69**(1): 119-129

- Schorge S, Colquhoun D (2003) Studies of NMDA Receptor Function and Stoichiometry with Truncated and Tandem Subunits. *Journal of Neuroscience* **23**(4): 1151-1158
- Schuler T, Mesic I, Madry C, Bartholomaeus I, Laube B (2008) Formation of NR1/NR2 and NR1/NR3 Heterodimers Constitutes the Initial Step in N-Methyl-D-aspartate Receptor Assembly. *J Biol Chem* **283**(1): 37-46
- Scott DB, Blanpied TA, Swanson GT, Zhang C, Ehlers MD (2001) An NMDA Receptor ER Retention Signal Regulated by Phosphorylation and Alternative Splicing. *J Neurosci* **21**(9): 3063-3072
- Screaton GR, Xu X-N, Olsen AL, Cowper AE, Tan R, McMichael AJ, Bell JI (1997) LARD: A new lymphoid-specific death domain containing receptor regulated by alternative pre-mRNA splicing. *Proceedings of the National Academy of Sciences of the United States of America* **94**(9): 4615-4619
- Sheng M (2001) Molecular organization of the postsynaptic specialization. *Proceedings of the National Academy of Sciences of the United States of America* **98**(13): 7058-7061
- Sheng M, Cummings J, Roldan LA, Jan YN, Jan LY (1994) Changing subunit composition of heteromeric NMDA receptors during development of rat cortex. *Nature* **368**(6467): 144-147
- Shigeri Y, Seal RP, Shimamoto K (2004) Molecular pharmacology of glutamate transporters, EAATs and VGLUTs. *Brain Research Reviews* **45**(3): 250-265
- Skoff RP (1990) Gliogenesis in rat optic nerve: Astrocytes are generated in a single wave before oligodendrocytes. *Developmental Biology* **139**(1): 149-168
- Sladeczek F, Pin JP, Recasens M, Bockaert J, Weiss S (1985) Glutamate stimulates inositol phosphate formation in striatal neurones. *Nature* **317**(6039): 717-719
- Smith T, Groom A, Zhu B, Tukski L (2000) Autoimmune encephalomyelitis ameliorated by AMPA antagonists. *Nature Medicine* **6**(1): 62-66
- Smothers CT, Woodward JJ (2003) Effect of the NR3 subunit on ethanol inhibition of recombinant NMDA receptors. *Brain Research* **987**(1): 117-121
- Smothers CT, Woodward JJ (2007) Pharmacological Characterization of Glycine-Activated Currents in HEK 293 Cells Expressing N-Methyl-D-aspartate NR1 and NR3 Subunits. *J Pharmacol Exp Ther* **322**(2): 739-748

- Sobolevsky AI, Prodromou ML, Yelshansky MV, Wollmuth LP (2007) Subunit-specific Contribution of Pore-forming Domains to NMDA Receptor Channel Structure and Gating. *J Gen Physiol* **129**(6): 509-525
- Soloviev MM, Brierley MJ, Shao ZY, Mellor IR, Volkova TM, Kamboj R, Ishimaru H, Sudan H, Harris J, Foldes RL *et al* (1996) Functional expression of a recombinant unitary glutamate receptor from *Xenopus*, which contains N-methyl-D-aspartate (NMDA) and non-NMDA receptor subunits. *Journal of Biological Chemistry* **271**(51): 32572-32579
- Sommer B, Burnashev N, Verdoorn TA, Keinänen K, Sakmann B, Seeburg PH (1992) A glutamate receptor channel with high affinity for domoate and kainate. *EMBO Journal* **11**(4): 1651-1656
- Sommer B, Keinänen K, Verdoorn TA, Wisden W, Burnashev N, Herb A, Kohler M, Takagi T, Sakmann B, Seeburg PH (1990) Flip and flop: A cell-specific functional switch in glutamate-operated channels of the CNS. *Science* **249**(4976): 1580-1585
- Sprengel R, Suchanek B, Amico C, Brusa R, Burnashev N, Rozov A, Hvalby Ø, Jensen V, Paulsen O, Andersen P *et al* (1998) Importance of the Intracellular Domain of NR2 Subunits for NMDA Receptor Function In Vivo. *Cell* **92**(2): 279-289
- Stamm S, Zhu J, Nakai K, Stoilov P, Stoss O, Zhang MQ (2000) An Alternative-Exon Database and Its Statistical Analysis. *DNA and Cell Biology* **19**(12): 739-756
- Standley S, Roche KW, McCallum J, Sans N, Wenthold RJ (2000) PDZ domain suppression of an ER retention signal in NMDA receptor NR1 splice variants. *Neuron* **28**(3): 887-898
- Stern P, Behe P, Schoepfer R, Colquhoun D (1992) Single-channel conductances of NMDA receptors expressed from cloned cDNAs: Comparison with native receptors. *Proceedings of the Royal Society of London - B Biological Sciences* **250**(1329): 271-277
- Stocca G, Vicini S (1998) Increased contribution of NR2A subunit to synaptic NMDA receptors in developing rat cortical neurons. *J Physiol* **507** (Pt 1): 13-24
- Strachan T, Read AP (1999) *Human Molecular Genetics*, 2nd edn.: BIOS Scientific Publishers Ltd.
- Stys PK (2004) White matter injury mechanisms. *Current Molecular Medicine* **4**(2): 113-130
- Stys PK, Lipton SA (2007) White matter NMDA receptors: an unexpected new therapeutic target? *Trends in Pharmacological Sciences* **28**(11): 561-566

- Suchanek B, Seeburg PH, Sprengel R (1995) Gene structure of the murine N-methyl D-aspartate receptor subunit NR2C. *Journal of Biological Chemistry* **270**(1): 41-44
- Sucher NJ, Akbarian S, Chi CL, Leclerc CL, Awobuluyi M, Deitcher DL, Wu MK, Yuan JP, Jones EG, Lipton SA (1995) Developmental and regional expression pattern of a novel NMDA receptor- like subunit (NMDAR-L) in the rodent brain. *Journal of Neuroscience* **15**(10): 6509-6520
- Sucher NJ, Awobufuyi M, Choi YB, Lipton SA (1996) NMDA receptors: From genes to channels. *Trends in Pharmacological Sciences* **17**(10): 348-355
- Sucher NJ, Kohler K, Tenneti L, Wong H-k, Grunder T, Fauser S, Wheeler-Schilling T, Nakanishi N, Lipton SA, Guenther E (2003) N-Methyl-D-Aspartate Receptor Subunit NR3A in the Retina: Developmental Expression, Cellular Localization, and Functional Aspects. *Invest Ophthalmol Vis Sci* **44**(10): 4451-4456
- Sugihara H, Moriyoshi K, Ishii T, Masu M, Nakanishi S (1992) Structures and properties of seven isoforms of the NMDA receptor generated by alternative splicing. *Biochemical and Biophysical Research Communications* **185**(3): 826-832
- Sullivan JM, Traynelis SF, Chen HSV, Escobar W, Heinemann SF, Lipton SA (1994) Identification of two cysteine residues that are required for redox modulation of the NMDA subtype of glutamate receptor. *Neuron* **13**(4): 929-936
- Sun L, Margolis FL, Shipley MT, Lidow MS (1998) Identification of a long variant of mRNA encoding the NR3 subunit of the NMDA receptor: its regional distribution and developmental expression in the rat brain. *FEBS Letters* **441**(3): 392-396
- Sydow S, Kopke AKE, Blank T, Spiess J (1996) Overexpression of a functional NMDA receptor subunit (NMDAR1) in baculovirus-infected *Trichoplusia ni* insect cells. *Molecular Brain Research* **41**: 228-240
- Szafranski K, Schindler S, Taudien S, Hiller M, Huse K, Jahn N, Schreiber S, Backofen R, Platzer M (2007) Violating the splicing rules: TG dinucleotides function as alternative 3' splice sites in U2-dependent introns. *Genome Biology* **8**(8): R154
- Tabish M, Ticku MK (2004) Alternate splice variants of mouse NR2B gene. *Neurochemistry International* **44**(5): 339-343
- Tang CM, Dichter M, Morad M (1990) Modulation of the N-methyl-D-aspartate channel by extracellular H⁺. *Proc Natl Acad Sci U S A* **87**(16): 6445-6449

- Tazi J, Bakkour N, Stamm S (2009) Alternative splicing and disease. *Biochimica et Biophysica Acta (BBA) - Molecular Basis of Disease* **1792**(1): 14-26
- Thomas P, Smart TG (2005) HEK293 cell line: A vehicle for the expression of recombinant proteins. *Journal of Pharmacological and Toxicological Methods* **51**(3): 187-200
- Tong G, Takahashi H, Tu S, Shin Y, Talantova M, Zago W, Xia P, Nie Z, Goetz T, Zhang D *et al* (2008) Modulation of NMDA Receptor Properties and Synaptic Transmission by the NR3A Subunit in Mouse Hippocampal and Cerebrocortical Neurons. *J Neurophysiol* **99**(1): 122-132
- Tovar KR, Westbrook GL (1999) The Incorporation of NMDA Receptors with a Distinct Subunit Composition at Nascent Hippocampal Synapses In Vitro. *J Neurosci* **19**(10): 4180-4188
- Traynelis SF, Burgess MF, Zheng F, Lyuboslavsky P, Powers JL (1998) Control of voltage-independent Zinc inhibition of NMDA receptors by the NR1 subunit. *Journal of Neuroscience* **18**(16): 6163-6175
- Traynelis SF, Cull-Candy SG (1990) Proton inhibition of N-methyl-D-aspartate receptors in cerebellar neurons. *Nature* **345**(6273): 347-350
- Traynelis SF, Hartley M, Heinemann SF (1995) Control of proton sensitivity of the NMDA receptor by RNA splicing and polyamines. *Science* **268**(5212): 873-876
- Tsien R, Pozzan T (1989) Measurement of cytosolic free Ca²⁺ with quin2. *Methods Enzymol* **172**: 230-262
- Uchiyama-Tsuyuki Y, Araki H, Yae T, Otomo S (1994) Changes in the extracellular concentrations of amino acids in the rat striatum during transient focal cerebral ischemia. *J Neurochem* **62**(3): 1074-1078
- Umemura K, Gemba T, Mizuno A, Nakashima M (1996) Inhibitory effect of MS-153 on elevated brain glutamate level induced by rat middle cerebral artery occlusion. *Stroke* **27**(9): 1624-1628
- Vallano ML, Beaman-Hall CM, Benmansour S (1999) Ca²⁺ and pH modulate alternative splicing of exon 5 in NMDA receptor subunit 1. *Neuroreport* **10**(17): 3659-3664
- Vallano ML, Lambolez B, Audinat E, Rossier J (1996) Neuronal activity differentially regulates NMDA receptor subunit expression in cerebellar granule cells. *J Neurosci* **16**(2): 631-639

- van der Ven PFM, Ehler E, Vakeel P, Eulitz S, Schenk JA, Milting H, Micheel B, Furst DO (2006) Unusual splicing events result in distinct Xin isoforms that associate differentially with filamin c and Mena/VASP. *Experimental Cell Research* **312**(11): 2154-2167
- Verdoorn TA, Burnashev N, Monyer H, Seeburg PH, Sakmann B (1991) Structural determinants of ion flow through recombinant glutamate receptor channels. *Science* **252**(5013): 1715-1718
- Verkhatsky A, Kettenmann H (1996) Calcium signalling in glial cells. *Trends in Neurosciences* **19**(8): 346-352
- Verkhatsky A, Orkand RK, Kettenmann H (1998) Glial calcium: Homeostasis and signaling function. *Physiological Reviews* **78**(1): 99-141
- Vicini S, Wang JF, Li JH, Zhu WJ, Wang YH, Luo JH, Wolfe BB, Grayson DR (1998) Functional and pharmacological differences between recombinant N- methyl-D-aspartate receptors. *Journal of Neurophysiology* **79**(2): 555-566
- Volpe JJ (2001) Neurobiology of periventricular leukomalacia in the premature infant. *Pediatric Research* **50**(5): 553-562
- Von Boyen GBT, Steinkamp M, Adler G, Kirsch J (2006) Glutamate Receptor Subunit Expression in Primary Enteric Glia Cultures. *Journal of Receptors and Signal Transduction* **26**(4): 329-336
- Vyklicky L, Jr., Vlachova V, Krusek J (1990) The effect of external pH changes on responses to excitatory amino acids in mouse hippocampal neurones. *J Physiol* **430**: 497-517
- Wafford KA, Bain CJ, Le BB, Whiting PJ, Kemp JA (1993) Preferential co-assembly of recombinant NMDA receptors composed of three different subunits. *Neuroreport* **4**(12): 1347-1349
- Wang M, Marín A (2006) Characterization and prediction of alternative splice sites. *Gene* **366**(2): 219-227
- Watanabe M, Mishina M, Inoue Y (1994) Distinct spatiotemporal expressions of five NMDA receptor channel subunit mRNAs in the cerebellum. *J Comp Neurol* **343**(4): 513-519
- Watkins JC, Jane DE (2006) The glutamate story. *BrJPharmacol* **147 Suppl 1**: S100-S108

- Waxman EA, Lynch DR (2005) N-methyl-D-aspartate Receptor Subtypes: Multiple Roles in Excitotoxicity and Neurological Disease. *Neuroscientist* **11**(1): 37-49
- Wee KS, Zhang Y, Khanna S, Low CM (2008) Immunolocalization of NMDA receptor subunit NR3B in selected structures in the rat forebrain, cerebellum, and lumbar spinal cord. *J Comp Neurol* **509**(1): 118-135
- Wenzel A, Fritschy JM, Mohler H (1997) NMDA Receptor Heterogeneity During Postnatal Development of the Rat Brain: Differential Expression of the NR2A, NR2B, and NR2C Subunit Proteins. *Journal of Neurochemistry* **68**(2): 469-478
- Wenzel A, Villa M, Mohler H (1996) Developmental and Regional Expression of NMDA Receptor Subtypes Containing the NR2D Subunit in Rat Brain. *Journal of Neurochemistry* **66**(3): 1240-1248
- Werner P, Voigt M, Keinänen K, Wisden W, Seeburg PH (1991) Cloning of a putative high-affinity kainate receptor expressed predominantly in hippocampal CA3 cells. *Nature* **351**(6329): 742-744
- Westphal RS, Tavalin SJ, Lin JW, Alto NM, Fraser ID, nbsp, C, Langeberg LK, Sheng M, Scott JD (1999) Regulation of NMDA Receptors by an Associated Phosphatase-Kinase Signaling Complex. *Science* **285**(5424): 93-96
- Williams K (1996) Separating dual effects of zinc at recombinant N-methyl--aspartate receptors. *Neuroscience Letters* **215**(1): 9-12
- Williams K, Zappia AM, Pritchett DB, Shen YM, Molinoff PB (1994) Sensitivity of the N-methyl-D-aspartate receptor to polyamines is controlled by NR2 subunits. *Molecular Pharmacology* **45**(5): 803-809
- Wollmuth LP, Sobolevsky AI (2004) Structure and gating of the glutamate receptor ion channel. *Trends in Neurosciences* **27**(6): 321-328
- Wrighton DC, Baker EJ, Chen PE, Wyllie DJA (2008) Mg²⁺ and memantine block of rat recombinant NMDA receptors containing chimeric NR2A/2D subunits expressed in *Xenopus laevis* oocytes. *The Journal of Physiology* **586**(1): 211-225
- Wyllie DJA, Behe P, Nassar M, Schoepfer R, Colquhoun D (1996) Single-channel currents from recombinant NMDA NR1a/NR2D receptors expressed in *xenopus* oocytes. *Proceedings of the Royal Society - Biological Sciences (Series B)* **263**(1373): 1079-1086

- Xu Q, Walker D, Bernardo A, Brodbeck J, Balestra ME, Huang Y (2008) Intron-3 Retention/Splicing Controls Neuronal Expression of Apolipoprotein E in the CNS. *J Neurosci* **28**(6): 1452-1459
- Yamakura T, Askalany AR, Petrenko AB, Kohno T, Baba H, Sakimura K (2005) The NR3B subunit does not alter the anesthetic sensitivities of recombinant N-methyl-D-aspartate receptors. *AnesthAnalg* **100**(6): 1687-1692
- Yamazaki M, Mori H, Araki K, Mori KJ, Mishina M (1992) Cloning, expression and modulation of a mouse NMDA receptor subunit. *FEBS Letters* **300**(1): 39-45
- Yao Y, Harrison CB, Freddolino PL, Schulten K, Mayer ML (2008) Molecular mechanism of ligand recognition by NR3 subtype glutamate receptors. *EMBO J* **27**(15): 2158-2170
- Yao Y, Mayer ML (2006) Characterization of a Soluble Ligand Binding Domain of the NMDA Receptor Regulatory Subunit NR3A. *Journal of Neuroscience* **26**(17): 4559-4566
- Yoshioka A, Bacskai B, Pleasure D (1996) Pathophysiology of oligodendroglial excitotoxicity. *JNeurosciRes* **46**(4): 427-437
- Yu X-M, Salter MW (1998) Gain control of NMDA-receptor currents by intracellular sodium. *Nature* **396**(6710): 469-474
- Yu Y, Maroney PA, Denker JA, Zhang XHF, Dybkov O, Lührmann R, Jankowsky E, Chasin LA, Nilsen TW (2008) Dynamic Regulation of Alternative Splicing by Silencers that Modulate 5' Splice Site Competition. *Cell* **135**(7): 1224-1236
- Zhong J, Carrozza DP, Williams K, Pritchett DB, Molinoff PB (1995) Expression of mRNAs encoding subunits of the NMDA receptor in developing rat brain. *J Neurochem* **64**(2): 531-539
- Zimmer M, Fink TM, Franke Y, Lichter P, Spiess J (1995) Cloning and structure of the gene encoding the human N-methyl--aspartate receptor (NMDAR1). *Gene* **159**(2): 219-223
- Ziskin JL, Nishiyama A, Rubio M, Fukaya M, Bergles DE (2007) Vesicular release of glutamate from unmyelinated axons in white matter. *Nat Neurosci* **10**(3): 321-330
- Zukin RS, Bennett MV (1995) Alternatively spliced isoforms of the NMDARI receptor subunit. *Trends Neurosci* **18**(7): 306-313

"Every answer harbours a multitude of new questions"